SECRET

LIMITED DISTRIBUTION

25X1A

[redacted]-1-65
15 October 1965

ADVANCE COPY

AVSAS S-7-2
copy 1 of 6 copies

ADVANCED VEHICLE SYSTEMS ANALYSIS STUDY

VOL. II - APPENDIX

by

[redacted]

25X1A

[redacted]

25X1A

GROUP - 1
EXCLUDED FROM AUTOMATIC DOWNGRADING
AND DECLASSIFICATION

SECRET

LIMITED DISTRIBUTION

ADVANCED VEHICLE SYSTEMS ANALYSIS STUDY

TABLE OF CONTENTS

APPENDIX A

LAUNCH SYSTEM ANALYSIS

APPENDIX A

LAUNCH SYSTEM ANALYSIS

1. Air Launch Techniques

Several air launch techniques were considered for application to this problem. Among these were the following:

a. The Skybolt type, horizontal attitude air drop of the missile with induced aircraft horizontal velocity followed by a missile ignition and pull-up to a near vertical trajectory using movable aerodynamic surfaces on the missile.

b. A vertical expulsion through the top of the carrier aircraft.

c. A horizontal attitude air drop with subsequent pull-up to the vertical attitude prior to ignition by use of a parawing or similar deployable aerodynamic surface.

d. Aircraft pull-up and subsequent missile release (lofting techniques).

e. Missile as an external wing store released with deployable decelerator with ignition following an attitude correction to near vertical as a result of a stabilizing deceleration in a descent trajectory.

f. Missile ejected from the rear of the aircraft with a rearward velocity relative to the aircraft, followed by a stable vertical descent prior to ignition.

g. Missile extracted from the rear of the aircraft using a deployable decelerator, followed by a stable vertical descent prior to ignition.

Eleven criteria were established for evaluating the air launch methods considered as candidates. They are:

a. Capability for limiting the shock load factors to less than 20 g's peak.

b. Capability for limiting sustained load factors to less than 10 g's.

c. Minimization of aircraft payload weight, volume, and complexity penalties.

d. Stable pre-ignition attitude of the missile; i.e., minimization of oscillations prior to vehicle ignition.

e. Rapid attitude change if launched horizontally (0°) to a near vertical (80°) attitude angle.

f. Minimization of post air launch, altitude loss.

g. Minimization of descent velocity at the time of rocket ignition.

h. The use of proven state-of-the-art techniques; (i.e., special weighing is given to proven or tested methods and reliable existing equipments as opposed to proposed or theoretically feasible techniques).

i. Minimization of system costs.

j. Rapid response capability for system build-up and checkout.

k. Compatibility of air launch requirements with other system requirements.

An analysis of the alternate system performance was made by ranking of the candidate systems in each of the eleven evaluation criterion categories. The rankings were as follows:

+2 - Superior performance

+1 - Acceptable or favorable performance

0 - Nil or no known effect or median performance

-1 - Uncertain performance or some recognized penalty

-2 - Serious penalty probable

A weighing of the 11 criteria was also used. The weighings assigned to the performance requirements were as follows:

Unity - Reasonable performance acceptable
2 Multiple - Important to successful operation
3 Multiple - Near critical importance

The results of this ranking analysis are shown in Table A-1. The table clearly shows a dominance of the weighted scores of the two systems #5 and #7 over all other systems. These are the wing store and rear extraction with deployable decelerators. It is noted that these two

TABLE A-1

	REQUIREMENT										
Wt. factors	3	3	1	2	1	1	2	3	3	2	
Air Launch Method	(1) Peak Shock Loads	(2) Sustained Loads	(3) Min. Wt. Vol.	(4) Stabil.	(5) Alt. Loss	(6&7) Vel. & Att. at Ignition	(8) Reli.	(9) $	(10) Response	(11) Compat.	Total Wt. Score
1	1	1	-1	1	+1	+1	+1	-2	-1	+1	4
2	-1	1	-2	1	+2	+2	-2	-1	-1	-1	-8
3	+1	1	-1	-1	+1	+1	-1	0	-1	+1	2
4	+1	1	+1	0	+1	+1	-2	+1	-1	-1	3
5	+1	+1	+1	+1	-1	-1	+1	+1	+1	+1	17
6	+1	+1	-1	+1	-1	-1	+1	0	-1	+1	6
7	+1	+1	+1	+1	-1	-1	+1	+1	+1	+1	17

methods can be considered roughly equivalent, with the choice of a wing store or internal store and decelerator extraction made primarily on the basis of the missile-to-aircraft size considerations and convenience of design adaptations. On the basis of these results it was considered worthwhile to investigate the characteristic performance of the deployable extraction decelerator more thoroughly.

The first consideration is that several drag devices such as cones, rotochutes, paravanes, parachutes and similar devices could be considered as candidates for decelerators. Consistant with our system criteria for low cost reliable and available systems, however, we will consider the implications of the use of a parachute system as our extraction decelerator in the light of its proven status. Characteristic of parachute systems however, is the inherent tendency to impart two forms of shock loading to the suspended payload. The first of these loads is the snatch load which occurs prior to canopy inflation at the instant of complete extension of suspension lines or static lines. Although snatch load factors can attain very large magnitudes in undamped systems the state of the art of snatch load damping is well known and could easily be applied to the ALIAS air launch problem. Thus we may relegate this to the category of a design consideration in which bag deployment, skirt hesitation, vesiolastic suspension lines, packing methods and/or sequencing may be employed to control the snatch load factors.

A second shock loading occurs at the instant of full canopy inflation, and is known as the opening shock force. This force, like the snatch load can be controlled to some degree by canopy selection, by reefing or by staging of parachutes. It is obvious, however, that such techniques provide the undesirable effect of delaying deceleration sequence thus extending the time for attitude correction and resulting in a greater altitude loss. It would therefore be desirable to have a system in which shock loading due to opening shock would be inherently low. To analyze the requirements of such a system the relationships between the primary parameters which contribute to opening shock loads were investigated, they are: parachute diameter, suspended weight, launch velocity and launch altitude. Figures A-1, A-2 and A-3 were prepared to graphically present the trade-offs in these parameters. An empirically derived relationship between the $F_p/q_o\ S_o$ and $\frac{\rho D_o^3}{M}$, appearing in Figure A-1, was obtained from Reference (1), and is based on data from 15% extended skirt parachutes. These parachutes areused extensively and primarily for both air drop and for aerospace vehicle recovery purposes as noted in Reference (2) of this appendix. It is thus considered a typical candidate type for ALIAS launch extraction and descent trajectory.

The second empirical relationship presented in Figure A-3 was established by Reference (3) and relates the approximate weight of the canopy to the opening shock load for 32 different types of parachutes, representative of applications to missile and space vehicle recovery, aerial delivery, and aircraft landing brake use. Weight of risers must be added to these values to obtain total drag system weights.

Nomenclature for the Figures is as follows:

D_o = Parachute constructed diameter, ft.

S_o = $\frac{\pi D_o^2}{4}$ = chute reference drag area, ft^2.

W = Weight of attached load, lb

M = Mass of attached load, slug

F_p = Peak shock load, lb

q_o = dynamic pressure at instant of canopy inflation lb/ft^2

V_o = Inflation velocity = launch velocity, fps

L.F. = Shock load factor, "g" s

Pw = Parachute weight, lbs

SECRET LIMITED DISTRIBUTION

FIG 1

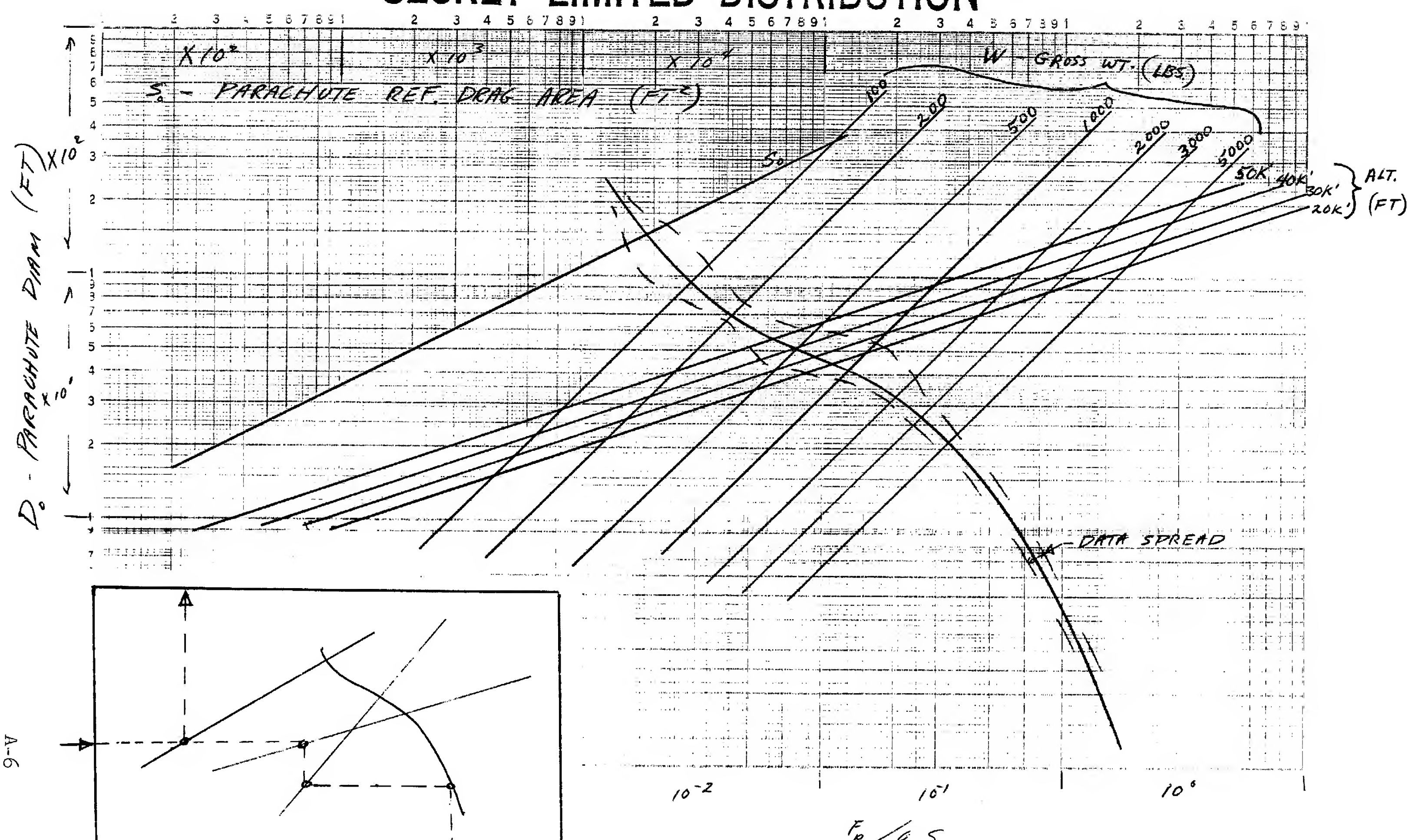

A-6

SECRET LIMITED DISTRIBUTION

6 Aug 65

SECRET LIMITED DISTRIBUTION

FIG 2

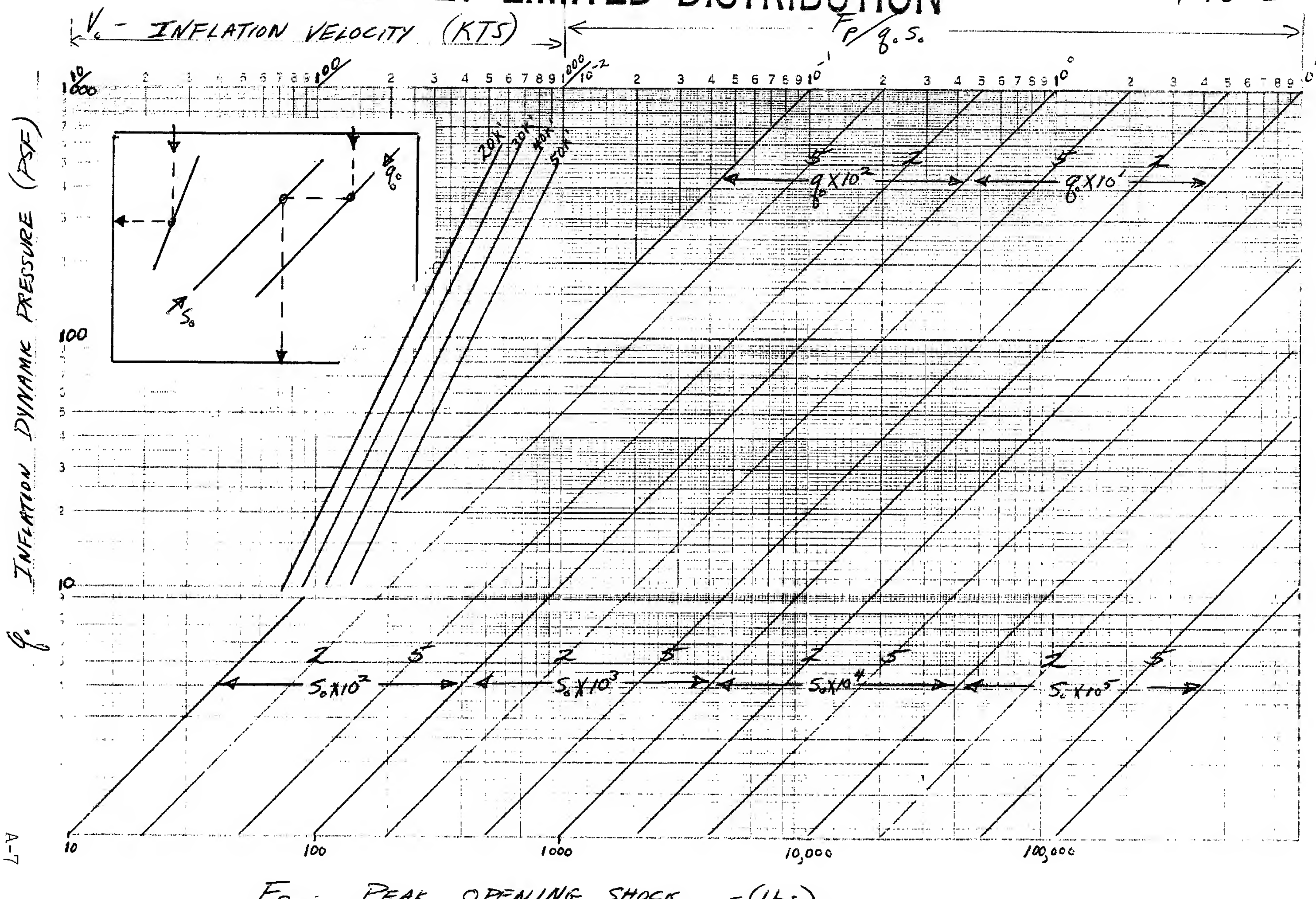

SECRET LIMITED DISTRIBUTION

FIGURE A-2

TM 6 Aug 65

SECRET LIMITED DISTRIBUTION

FIG 3

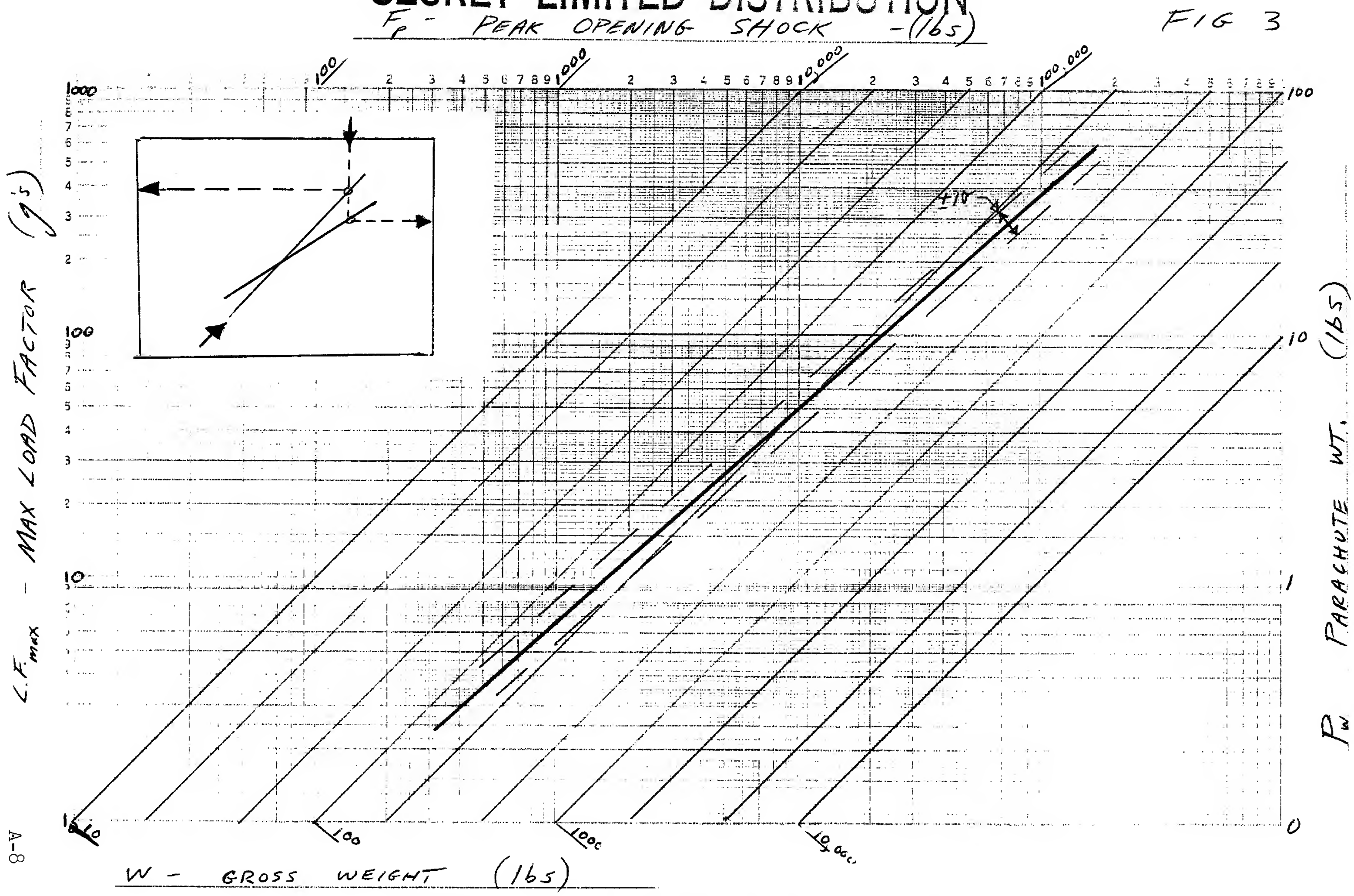

SECRET LIMITED DISTRIBUTION

FIGURE A3

TM 6 Aug 65

2. Carrier Aircraft Implications

Considering the sources and approximate magnitudes of the parametric values which contribute to opening shock load it was seen that little control could be exercised over the launch weight since that is set primarily by the missile size, which in turn depends upon the specific trajectory requirements. Parachute diameter is determined to a large degree by the descent velocity requirement. Launch altitude and launch airspeed are seen to be determined by the characteristics of candidate ALIAS carrier aircraft. Thus it was considered pertinent to investigate the implications of the capabilities of two candidate carrier aircraft on the opening shock loads of the parachute extraction - descent air launch scheme. The candidate aircraft which represent two relatively widespread capability differences were the C-130 and the C-135.

For purposes of comparison the following sample problem was assumed.

launch load = 2500 lb
parachute = 50 ft. diameter single stage, non-reefed 15% extended skirt type
aircraft mission radius = 1000 n. mi.
aircraft total prelaunch payload less fuel = 15,000 lb
launch altitude = aircraft service ceiling (rate of climb = 100 fpm)
launch speed = 1.2 times true velocity of aircraft stall ($1.2\ V_{stall}$) at service ceiling

The latter two criteria of the sample problem were based on the assumption that the maximum aircraft altitude capability should be utilized and that a minimum speed sufficient to maintain aircraft stability and control would be used for launch. The first two charts of Figure A-4, derived from data of References (4) and (5) for the C-130 and C-135 aircraft respectively establish the launch conditions at:

C-130: altitude = 37,500 ft, air speed = 201 kts
C-135: altitude = 47,500 ft, airspeed = 275 kts

The resultant shock load factors imparted by these conditions are:

C-130 launch: Max. load factor = 17.6
C-135 launch: Max. load factor = 29.2

Thus the load factor for the C-135 exceeds the limit criteria previously established for the air launch system.

A second example was used to compare the peak load factors for both aircraft for launches from the same altitude. The results of this comparison are shown in Figure A-5 over a wide range of altitudes. Here we note that the peak load factors for the same altitude launches are on

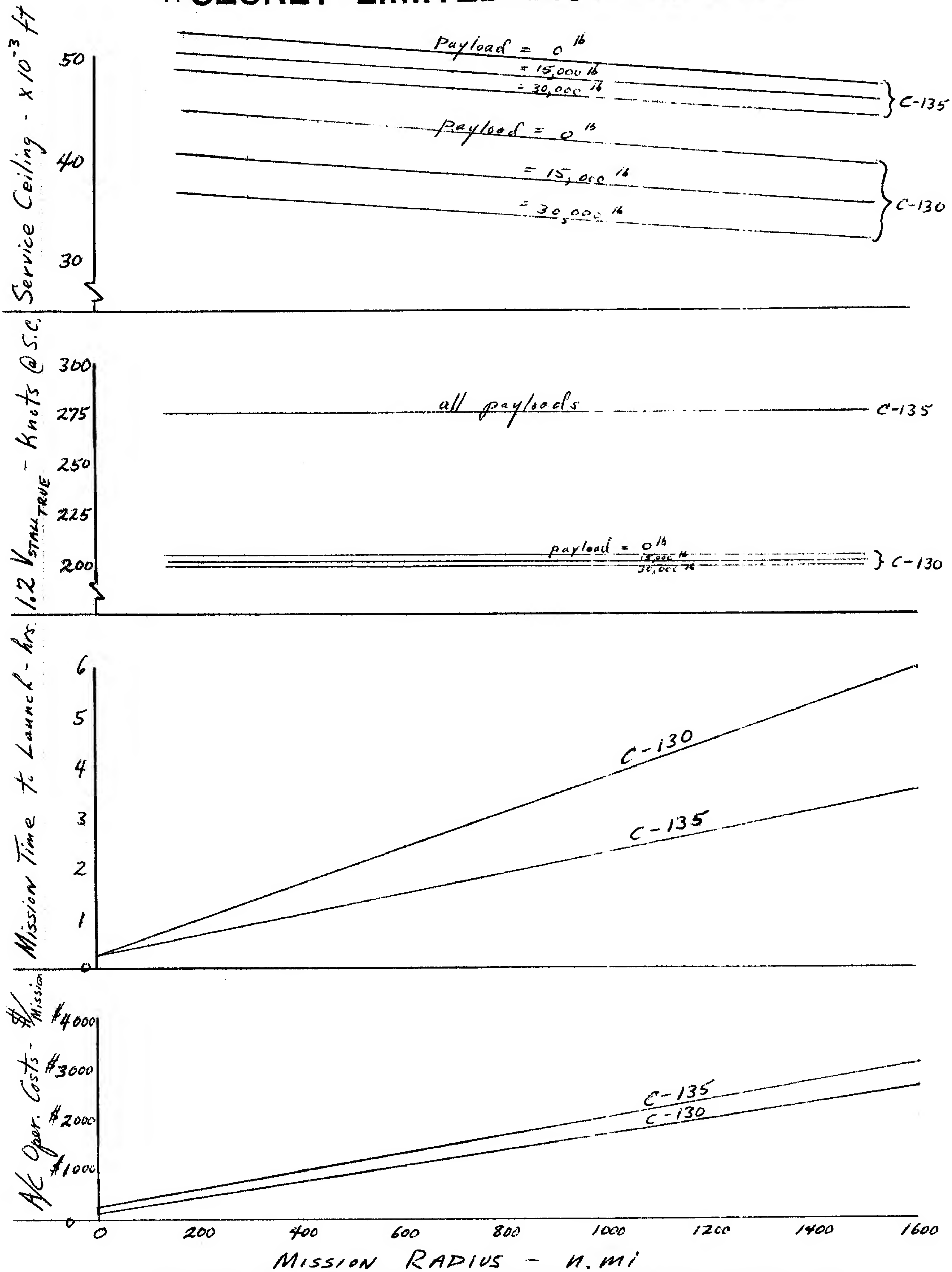

A-4

JAn 24 Aug 65

LAUNCH SPEED & DECELERATOR'S OPENING SHOCK LOAD FACTOR VS. LAUNCH ALTITUDE FOR TWO AIRCRAFT

Conditions: 50' Diam 15% Extended Skirt Parachute
2500 lb launched weight
700 nmi radius A/C mission
15,000 lb A/C payload

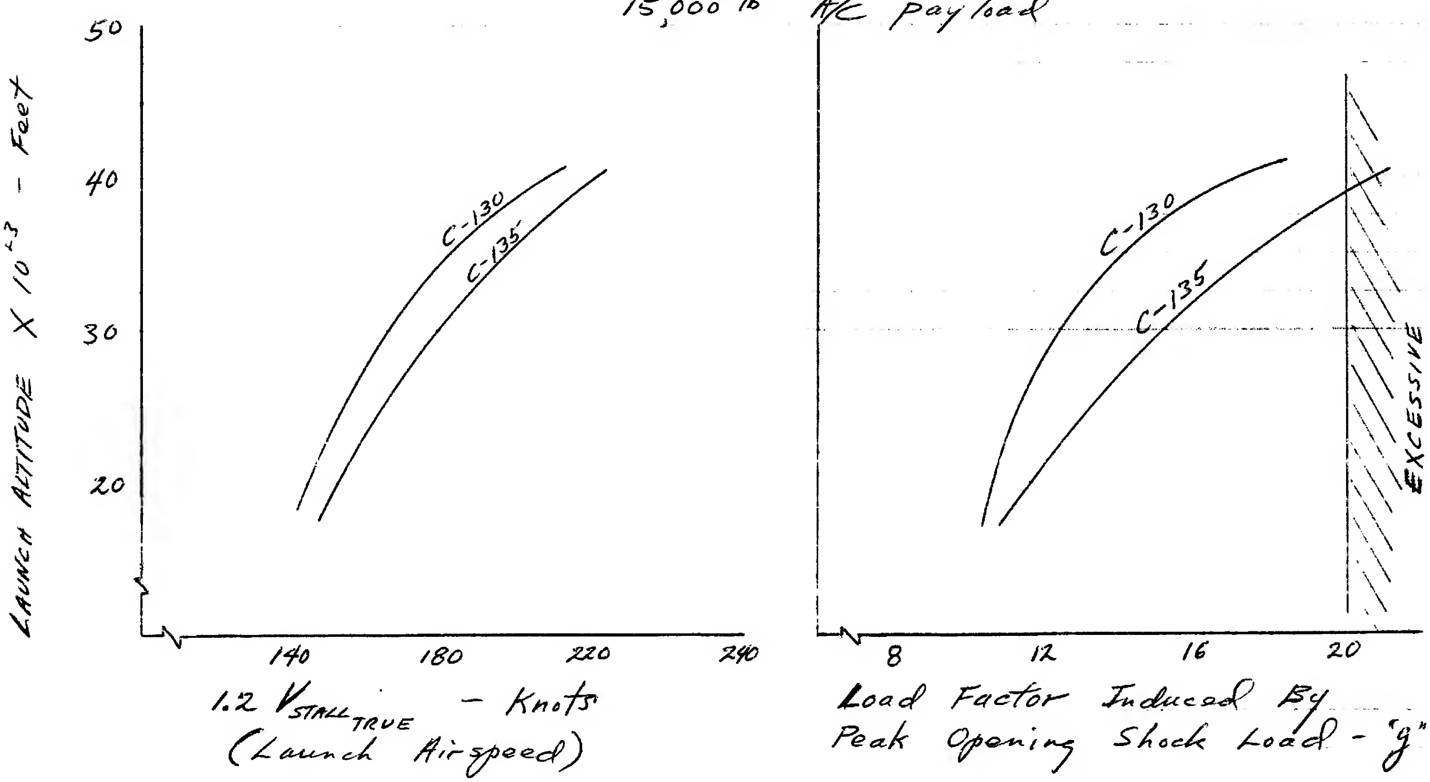

FIGURE A-5

TM 24 Aug 65

the order of 15 to 25% higher for the C-135 as apposed to the C-130 and that this increment is essentially proportional to the square of the allowable launch speed differential. Further, since:

$$V_{\substack{stall \\ TRUE}} = \sqrt{\frac{2W}{C_{L_{max}} \rho S}} = K \sqrt{\frac{1}{\rho}}$$

where $C_{L_{max}}$ = maximum lift coefficient for the particular aircraft, it is seen that the stall speed as a function of altitude is determined by the constant term which is an essential by-product of the aircraft design. Thus the higher wing loading (W/S) of the C-135 type aircraft compared to the C-130 imposes an inherently higher shock load condition on the deployable decelerator regardless of altitude. It is noted, however, that below 38,000 ft. altitude assuming a standard atmosphere condition, that either aircraft is an acceptable launch platform within the selected limits of maximum load factor, since parameter values chosen for the examples are considered typical for the ALIAS system. We may thus conclude that snatch loads and opening shock as well as carrier aircraft selection do not present significant barriers to a feasible ALIAS system design.

A second major factor in the selection of a carrier aircraft is the extent of the aircraft modifications required to accomplish the ALIAS vehicle air launch extraction. Assuming an internal transport of ALIAS, it is readily seen from a comparison of aircraft configurations between the C-130 and C-135 aircraft that a C-130 modification would be much less extensive. The cargo floor of a C-135 is located at approximately one half of the height of the fuselage diameter. The horizontal tail is located immediately aft of the cargo compartment. The lower half of the fuselage contains a series of fuel bays. Thus it is seen that a rearward horizontal extraction from the cargo floor would intercept the empennage. A lower positioning of the ALIAS below the cargo floor level would require removal of the aft fuel cells thus upsetting the capability for fuel transfer for aircraft center of gravity control. In either case extraction ports would be required to cut through primary structure thus requiring extensive redesign & testing to insure the flight safety of the modification.

The C-130 aircraft on the other hand features a low positioning of the cargo floor within the fuselage combined with a high tail and aft opening cargo doors. The doors are designed to allow their opening in flight and thus are not primary structure. From the standpoint of crew comfort it is desirable not to open these doors at the ALIAS launch altitude of 35,000 feet. Thus an extraction port provision could be provided through the closed cargo door with only a minor aircraft modification. A sketch of this scheme using the cargo floor of the C-130 to mount a guide rail is shown in Figure A-6.

SECRET LIMITED DISTRIBUTION

C-130 AIRCRAFT WITH ALIAS AIR LAUNCH MODIFICATION

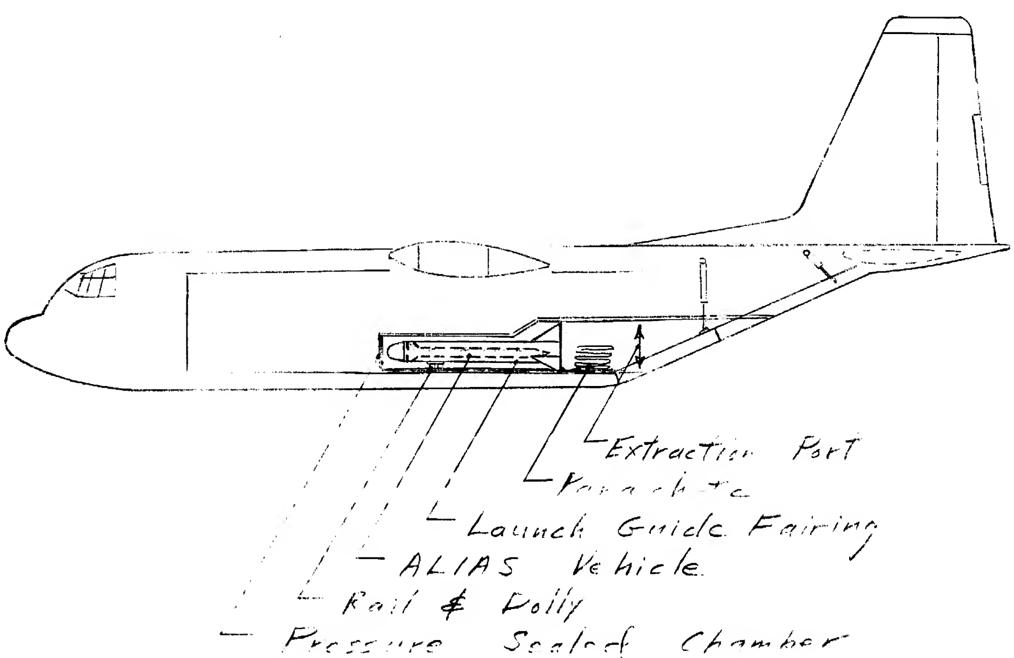

FIGURE A-6

SECRET LIMITED DISTRIBUTION

3. Deployable Decelerator Descent Trajectory

The interactions of selected parachutes and launch conditions on the trajectory factors; i.e., altitude loss, descent velocity and attitude change as a function of time after deployment were considered. Again using a sample problem and parameter values similar to the previous example; a determination of the trajectory histories of the descending ALIAS system was made for both candidate aircraft for a 35,000 ft altitude launch. The following additional assumptions were also established;

1. The launch was made in a zero wind condition

2. The ALIAS system attitude immediately following extraction from the aircraft is 0^{o} relative to the horizon.

3. A ribbed guide surface canopy configuration was chosen as the parachute type, to take advantage of its inherent high stability, low opening shock factor, high drag coefficient (.95), reliability and uniform operational history.

Thus for the 50 foot canopy, the trajectory history was determined and is shown in Figures A-7 and A-8. We see by this example that the required attitude change occurs within approximately 5.0 to 5.3 seconds with a loss of 200 and 220 feet altitude for the C-130 and C-135 aircraft launches respectively. For the ribbed guide surface parachute, the average angle of oscillation is less tha $\pm$ 2 degrees when a vertical descent velocity of 50 ft/sec is obtained as in the example.

It should be cautioned, of course, that these values are for a no-wind condition. Figure A-9 presents the "Sissenwine" wind profile chart which represents a 3 sigma distribution of wind velocities over the northeastern U.S. Assuming this profile as representative of the ALIAS launch environment it is noted that the winds are maximum at the assumed launch altitude of 35,000 ft. Hence a higher descent velocity than 50 fps may be desirable in the presence of wind to insure that the relative wind vector experienced by the parachute is near vertical. It is also recognized that changes in the wind velocity and direction during descent could significantly perturb the stability of the descent trajectory. If further analysis suggests that parachute oscillation magnitudes induced by varying winds are excessive for the missile launch, a geodetic suspension system could be utilized to transmit external loads on the parachute in a plane intercepting the center of mass of the suspenced load. Thus the turning moment and hence the oscillations of the missile in its launch tube would be substantially decreased.

From the previous discussion we conclude that an air launch system utilizing an extraction technique for the C-130 aircraft which uses a parachute for purposes of stability, attitude control and deceleration of the air laucnhed ALIAS system is feasible.

Parachute Trajectory
pg 1 of 2

Altitude: 35,000'
Para Diam 50'
Launched wt. 2500 lb

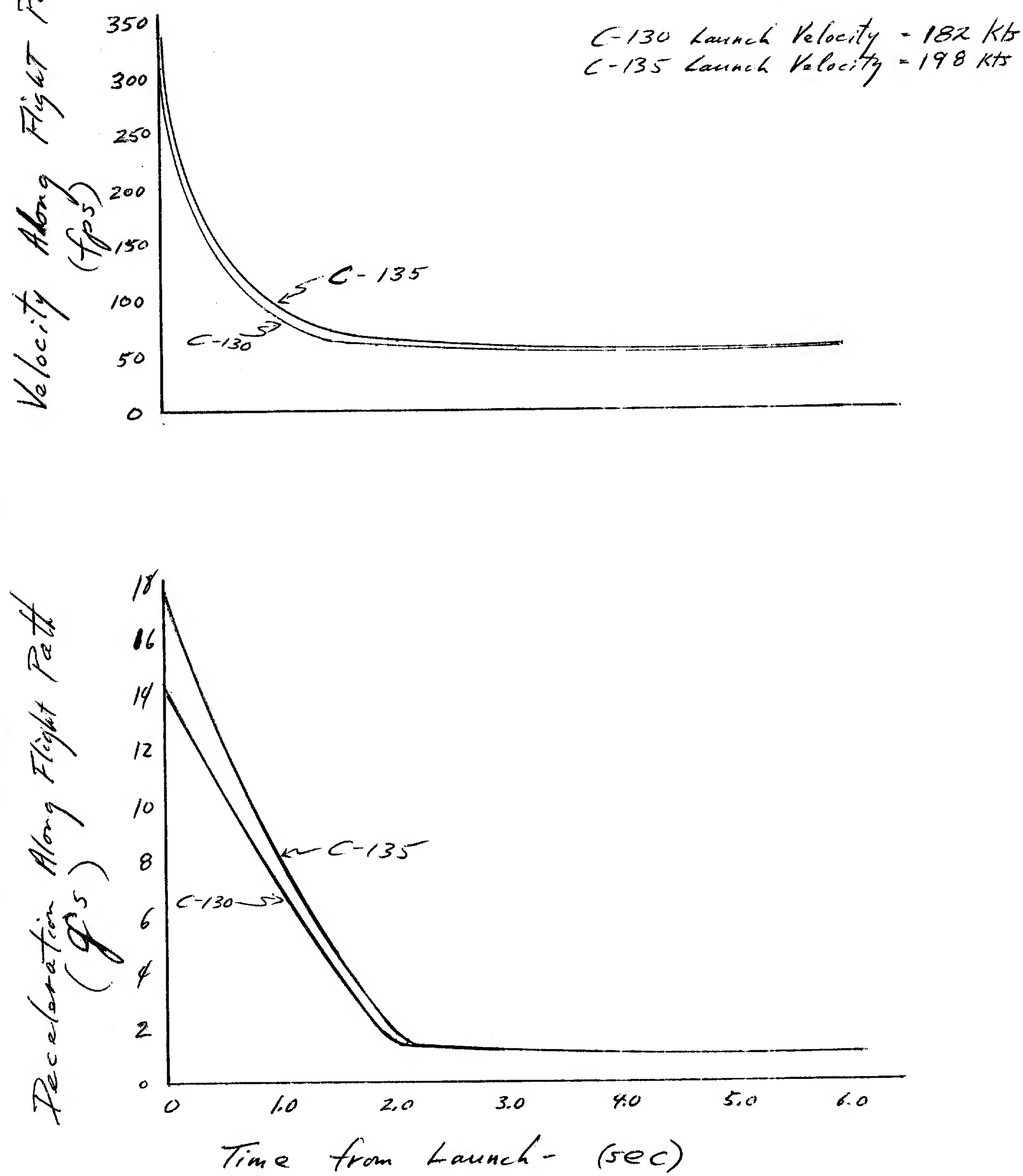

FIGURE A-

27 Aug 65

Parachute Trajectory
Page 2 of 2

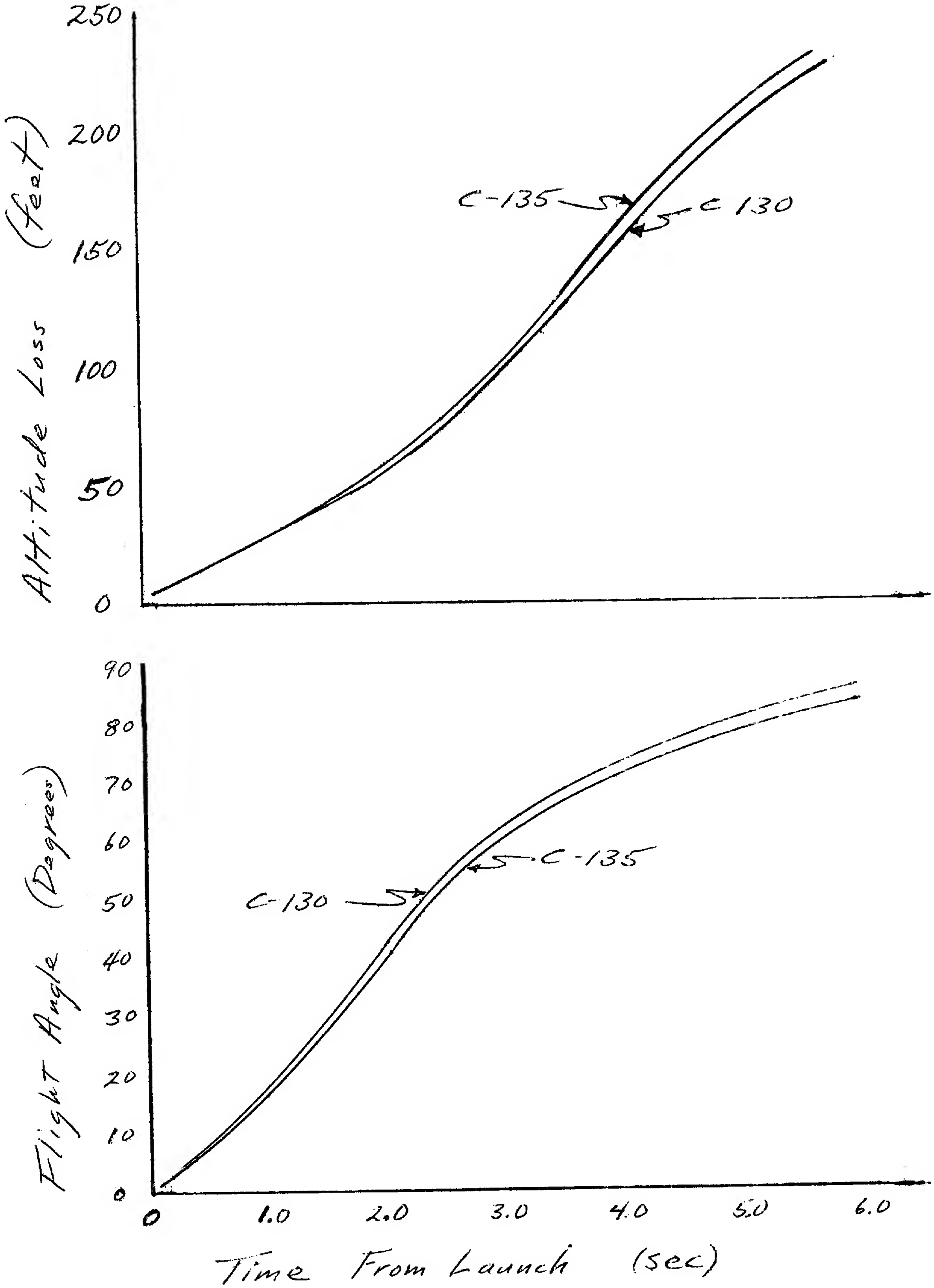

"Sissenwine" Wind Profile

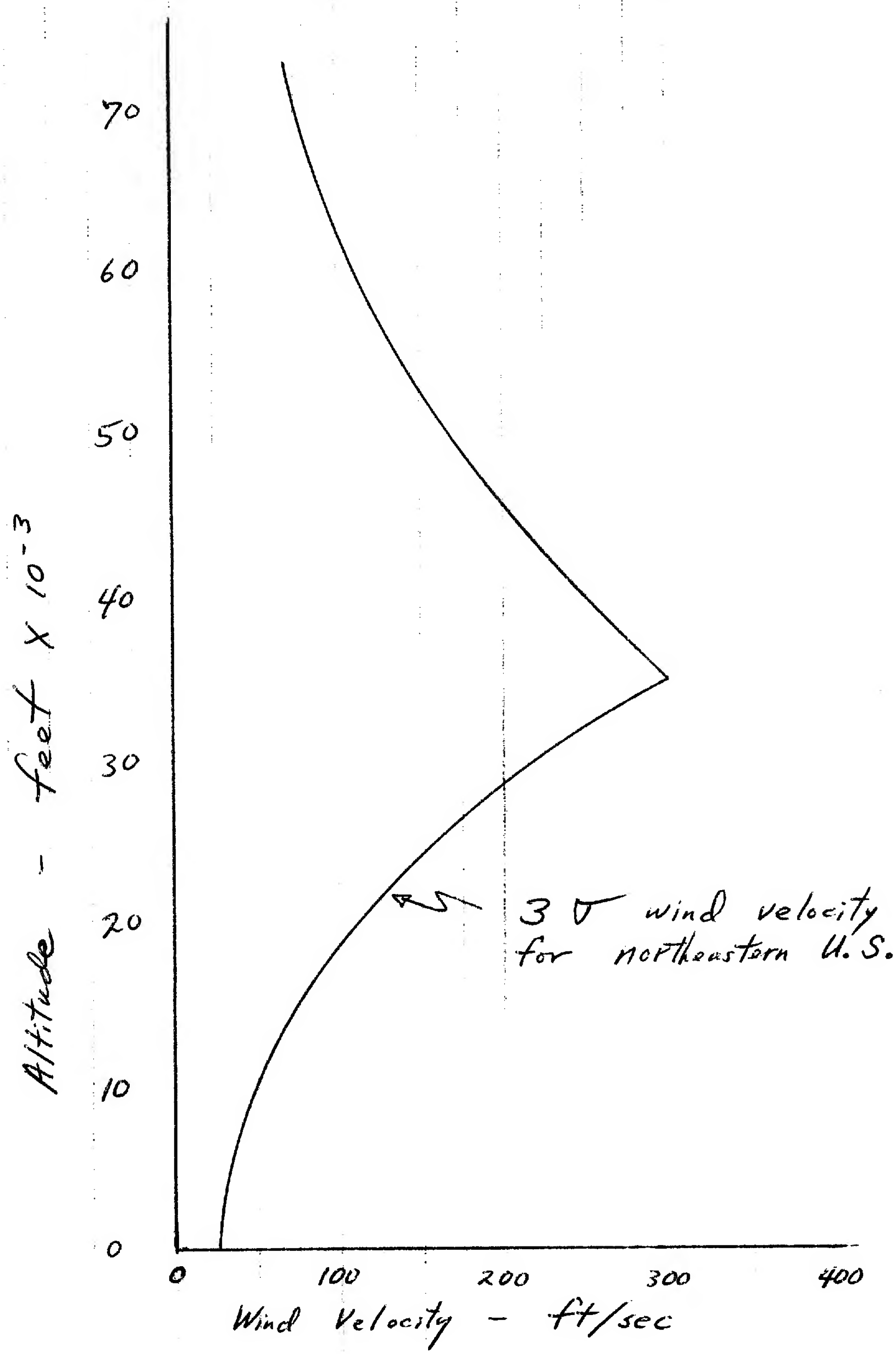

FIGURE A-9

4. Postscript and Selected ALIAS Concept

It is noted that the preceding sections of this Appendix were prepared at an early stage in the development of the ALIAS feasibility study without the benefit of a detailed estimate of the ALIAS air-launch weight. A conservative estimate of 2500 lbs was thus used throughout the preceding analysis. The subsequent detailed sizing analysis for the total vehicle (Appendix E) determined a selected ALIAS concept vehicle gross weight of 1153 lb. Allowing for the weights of an extraction parachute and a launch guide fairing we may expect that the total launch weight is closer to a 1500 lb figure. This difference in launch weight thus required a re-evaluation of the previous analysis. The results of this check indicated that the conclusions previously determined were not significantly affected thus the feasibility of using a parachute deployment for an ALIAS air-launch remains valid as do the relative advantages stated for the C-130 type aircraft over the C-135 in this scheme.

In order to further develop the details of a selected ALIAS concept the following were assumed:

Launch aircraft	C-130
Launch altitude	35,000 ft.
Average mission radius	700 n.mi.
Aircraft payload weight	15,000 lb
ALIAS air-launch weight	1,500 lb
Aircraft launch speed	182 kts
Parachute drag coefficient	0.80
ALIAS pre-ignition descent velocity at 35,000	60 kts

Analysis based on these assumptions yields:

Parachute surface area required	1360 ft^2
Single parachute diameter	41.5 ft
Single stage opening shock load factor	14.0 "g"
Parachute weight	23.0 lb

One innovation to the basic parachute extraction and deceleration scheme for ALIAS is considered necessary to insure that the powered ALIAS vehicle will clear the parachute during its initial ascent. A cluster of three parachutes sized to the same effective drag as the single parachute used in the previous analysis is suggested as a substitute configuration. Typically the airflow spill-over interference effect of such a cluster maintains a relatively wide separation of the individual chutes on the order of two parachute diameters. Thus the area above the suspended ALIAS vehicle is clear to allow its travel through

the cluster, without interference. The equivalent diameter of the individual parachutes of a three parachute cluster for the selected ALIAS concept is 23.0 feet each including an allowance factor of 0.85 for the effect of drag coefficient decrease due to clustering flow interference. A sketch of the ALIAS vehicle launch from the parachute suspended launch guide fairing is shown in Figure A-10. It is noted that the launch guide fairing is vented to preclude a closed breech effect at rocket ignition causing a relatively large reaction load on the parachute. Such a load would create a short period high descent rate forcing the chutes to move closer together in the cluster.

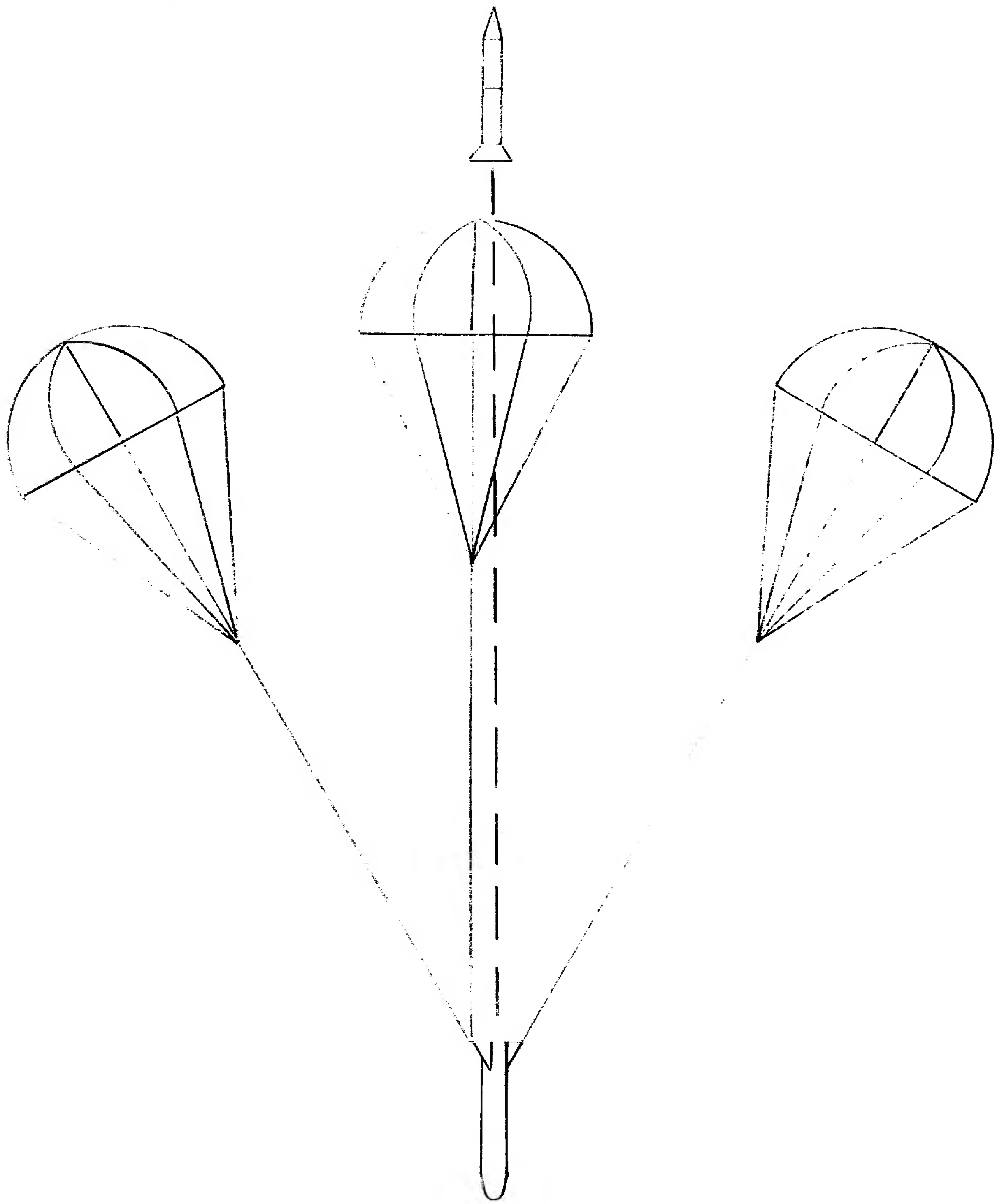

ALIAS VEHICLE LAUNCH

FIGURE A-10

SECRET LIMITED DISTRIBUTION
Approved For Release 2003/12/09 : CIA-RDP75B00157R000100110001-0

REFERENCES

1. K.E. French, "Model Law for Parachute Opening Shock", American Institute of Aeronautics and Astronautics Journal, December 1964

2. "Performance of and Design Criteria for Deployable Aerodynamic Decelerators" Aeronautical Systems Division, ASD-TR-61-579, Wright Paterson Air Force Base, December 1963

3. K. E. French, "Drogue Parachute Weight", Astronautics and Aerospace Engineering, June 1963

4. Personal Correspondence from Lockheed - Georgia Co., Div. of Lockheed Aircraft Corp. July 1965

5. Air Force Guide 2, Vol. 2 July - August 1962

APPENDIX B

GUIDANCE SYSTEM ANALYSIS

APPENDIX B

GUIDANCE SYSTEM ANALYSIS

1. Alternate Guidance Concepts

The function to be performed by the Air Launched Intelligence Acquisition System (ALIAS) guidance system is the positioning of the payload at the offset distance from the satellite trajectory which is compatible with the chosen sensor capabilities. For a desired 1 inch resolution capability, 5401 film, a 1 percent image motion compensation error, and a 7.5" diameter, 40" focal length optical system, the desired offset distance is 3000 ft and the allowable one sigma guidance error is 1500 ft.

The selection of the intercept region along the satellite trajectory will be based on ephemeris data. The quality of the ephemeris data which should be assumed to be available prior to choosing this initial intercept point depends on the time since the satellite was launched and the inclination of the orbit. The ground rule for the study was a spherical ephemeris error volume of 10 n.m. in diameter. A more realistic assessment of probable ephemeris errors during the operational time period of ALIAS can be obtained from Columbia University, Electronics Research Laboratory Final Report F-196. The capability of an updated ephemeris net referred to as SPADATS 66 (II) is shown in Figure B-1. The data shown in this figure are three sigma errors along the satellite trajectory after 24 hrs of observation and 72 hrs of observation. The cross track errors, or more correctly the three sigma error ellipsoid diameters, are, for low altitude orbits, approximately in the ratio of 5 to 1 smaller than the along track errors shown in the figure. The prediction error grows at the rate of 7 n.m. per day after 24 hrs of observation and 2 n.m. per day after 72 hrs of observation. The velocity error is expected to be within the 0.1% value desired for ALIAS and trajectory plane orientation is anticipated to be known to better than 5 minutes of arc.

An additional error source is present for low altitude (100 n.m.) low ballistic coefficient (5 to 50 lbs/ft^2) satellites. This is caused by either a variable satellite ballistic coefficient or an incorrect measurement of satellite ballistic coefficients. For a 10 lbs/ft^2 ballistic coefficient satellite, and with an error of 10 lbs/ft^2 in the ballistic coefficient measurement, prediction errors grow at the rate of 10 n.m. in the first hour and 50 n.m. in the second hour for a 116 n.m. altitude circular orbit.

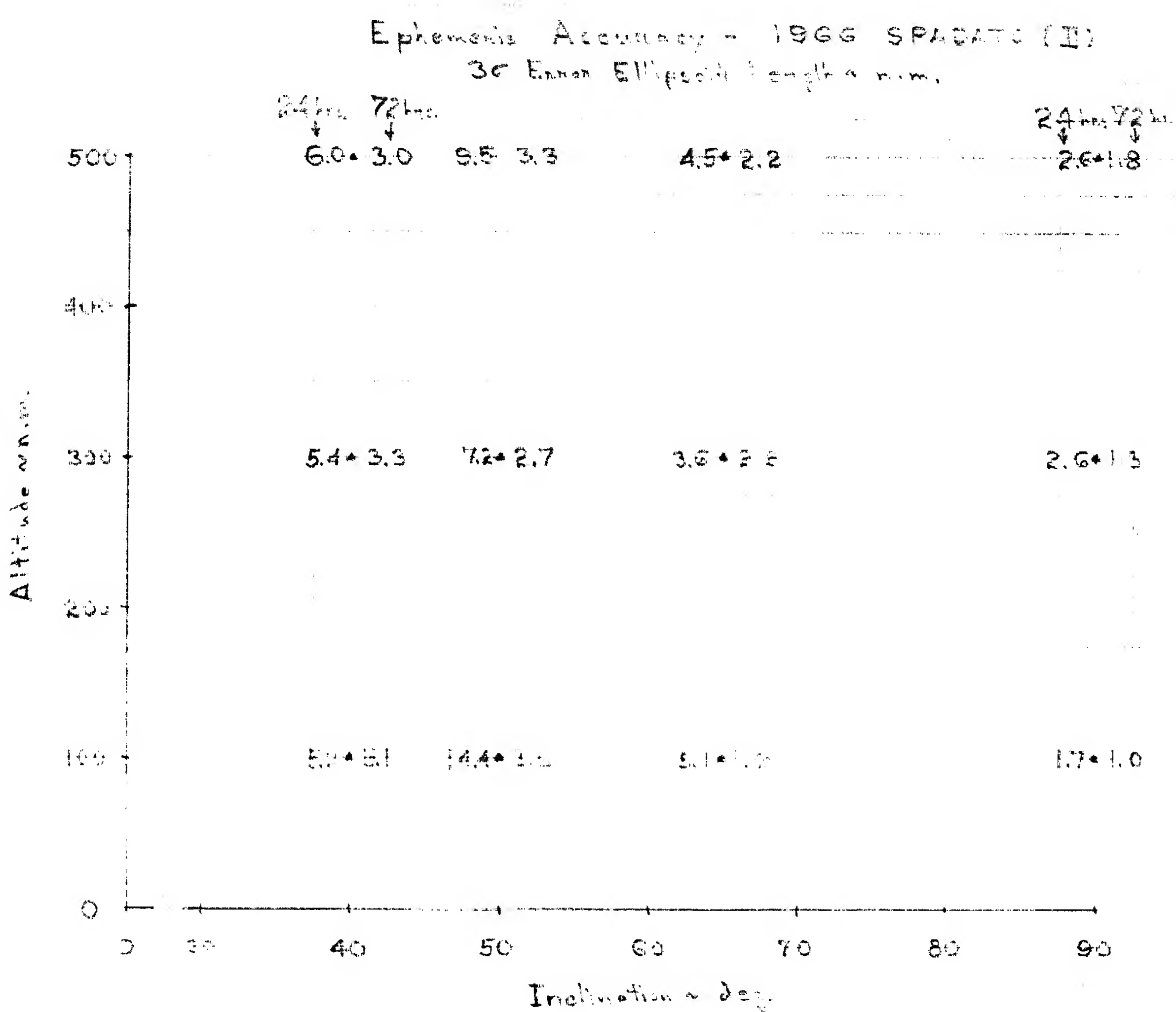

Figure B-1

SECRET LIMITED DISTRIBUTION

Approved For Release 2003/12/09 : CIA-RDP75B00157R000100110001-0

a. All-Inertial Guidance. The 10 n.m. diameter sphere of uncertainty is pessimistic in terms of the cross track errors of the ephemeris data after 24 hrs of observation; however, the ephemeris errors are still large enough to preclude achieving the desired missile guidance errors by purely inertial means even after 72 hrs of observation. For intercept attempts prior to 24 hrs after launch, the ephemeris accuracy is dependent on the particular trajectory to be intercepted, the launch point, and the lag time between receiving the latest ephemeris data and the launch of the missile. The inherent capability of the recommended ALIAS system is a correction capability of 77 n.m. in error ellipsoid length and 10 n.m. in diameter. This capability is consistent with intercepts much less than 24 hrs after launch and, if a radio link is available between the launch aircraft and the satellite tracking net, this will allow launches on the latest possible ephemeris data which will further reduce ALIAS reaction time, for satellites of interest.

b. Command Guidance. As shown above, inertial guidance of the ALIAS missile cannot achieve the desired guidance error. On the other hand, the use of command guidance to achieve the desired guidance errors could be accomplished; however, it would require the development of airborne radars which do not now exist. The required radars would be heavy, expensive, and present significant problems in terms of aircraft compatibility. The 1500 foot errors at 200 n.m. range represent an angular error of about 1 milliradian which is difficult to achieve even in ground based systems. A single phased array radar aboard the aircraft tracking both the satellite and the ALIAS missile would be the most promising candidate for this concept. While the use of command guidance is feasible and perhaps within the current state-of-the-art it is not a promising technique for ALIAS.

c. Inertial, Plus On-Board Sensing for Final Correction. An alternate approach is to guide the ALIAS missile to within the ephemeris uncertainty volume by inertial means and then use an on-board sensor to make a final guidance correction. This guidance approach has been studied within the context of numerous non-nuclear anti-satellite systems. Alternate means like command guidance, radio guidance, and inertial guidance have been suggested to position the terminal stage in the vicinity of the satellite trajectory and radar, IR, and optical (visible spectrum) sensors have been studied for making the final guidance correction.

(1) On-Board Radar - A radar system carried aboard the ALIAS terminal stage offers the capability of correcting for satellite along track errors although its capability for positioning the ALIAS missile at the proper offset distance from the satellite trajectory plane is limited for large initial ephemeris errors. In order to correct a

5 n.m. cross track error with the 1000 ft/sec correction capability inherent in the recommended ALIAS vehicle, the guidance correction has to be made at 35 seconds to go. A 1500 ft lateral error is equivalent to about 1.5 mr. which is not within the envisioned on-board radar capability. An X-band radar with the required 170 n.m. range capability on a one-square-meter target has an average power of 700 watts and weighs 250 lbs. The 250 lbs is a severe weight penalty to the ALIAS system and this approach is thus not recommended.

(2) On-Board IR Sensors - An IR sensor requires that along track errors must be sensed by supplementary sensors. The IR sensor does have the required angular resolution of 1.5 mr. and as with the radar, there are no acquisition problems associated with the star background. An IR sensor compatible with ALIAS requirements weighs less than 50 lbs. The IR sensor optics have to be cooled to very low temperatures, however, and there are significant developmental problems associated with this approach.

(3) On-Board Visual Sensor - The third alternate for the ALIAS system is an optical tracker operating in the visible range. It has the primary advantage that it can share the optics which are already necessary for the ALIAS photographic sensor. The additional weights for the angle tracking sensor are thus minimal. The optical tracker can acquire all targets at the desired range of 170 n.m. except for very small reflectivity objects at very unfavorable sun, to satellite, to ALIAS vehicle phase angles. The target can be discriminated from the star background by angular motion detection as discussed in paragraph 4 below. The optical tracker has angle rate and angle measurement capability consistent with the error correction capability of the ALIAS vehicle. The optical sensor does, however, also need a separate measurement of satellite along-track errors to be most effective.

(4) Along-track Ephemeris Data Updating - An optical sensor is attractive for the ALIAS terminal stage for many reasons, including availability within current state-of-the-art. Separate means to measure satellite position along the satellite trajectory were thus considered. Two approaches to updating the ephemeris data along the trajectory are readily feasible. The use of U.S. Navy developed airborne early warning radars aboard the ALIAS launch aircraft is feasible, although certain modifications, such as beam collapsing or spotlighting are necessary to extend the range capability to the desired 250 n.m. against a one-square-meter target. The other approach is to modify the Nortronics Airborne-Lightweight Optics Tracking System (ALOTS) to meet the ALIAS requirements. Higher sensitivity, greater sky-background rejection and a more accurate inertial reference for the optical angle data are required. The ALOTS system is potentially less costly but it restricts ALIAS system operation to near sun shadow line crossing. This in turn complicates the payload recovery aspects of the ALIAS system. A third, back-up, degraded accuracy range measuring technique will also be discussed in Sub-section 6, below.

d. Booster Guidance Concept. Reviewing the guidance options available for positioning the ALIAS vehicle to within the ephemeris errors, it becomes apparent that the use of an inertial guidance system is most appropriate. The optical tracker must be supplied with a fairly accurate inertial reference to operate properly and radar systems which can compete with inertial systems in accuracy for the flight regime of the ALIAS vehicle are large and expensive.

The use of inertial guidance for the first stage of the ALIAS vehicle of course requires that the initial position, the velocity, and an inertial reference frame be available aboard the launch aircraft. Further, in order to minimize the thrust requirements of the ALIAS booster, launch position control is necessary. Current airborne stellar inertial navigation systems more than satisfy the guidance requirements.

2. Launch Platform Navigation. Inherent to the ALIAS concept is the use of an airborne platform for launching the missile. The location of potential intercept points is chosen based on ephemeris data. The aircraft is flown to the area, and when it is below the chosen intercept point, the missile is released. In order to accomplish these functions an accurate navigation capability must be presumed for this launch platform. Current state-of-the-art all inertial navigation systems have a minimum drift rate of .5 n.m. to 1. n.m. per hour. Since intercept points for an ALIAS system may well be more than 6 hours away from the base, the 3 n.m. to 6 n.m. navigation accuracy must be corrected by the ALIAS terminal vehicle. Such an error make up capability is a serious constraint for the terminal vehicle and since the attitude reference of the inertial platform would have drifted more than is acceptable, a stellar-inertial navigation system is recommended. A Litton stellar inertial navigation system designated AN/ASN-59 has a CEP of 2400 feet and inertial reference misalignment of about $\frac{1}{2}$ minute of arc. About one hour is required for the complete navigation cycle. This system is to be available in June of 1966 at a cost of about $200,000 per unit. Nortronics has demonstrated a comparable capability during their C-131 Precision Navigation System flight test program. The position error of 2400 ft and the platform misalignment of .5 min of arc are completely acceptable for the ALIAS system.

In addition to the astronertial instrument and platform, a ballistic computer, portable chronometer, and prelaunch computer are required to provide a display for the pilot of time-to-go, heading, and range-to-go to ALIAS vehicle launch. The integration of the above components to perform the functions very similar to those required for ALIAS has been demonstrated by Nortronics in their C-131 flight test program.

3. Along-Track Ephemeris Data Correction

As discussed in paragraph 1 above, two approaches are feasible for measuring the satellite position along its trajectory: 1) by use of a modified ALOTS system, and, 2) by use of a modified airborne early warning radar such as the AN/APS-96. The modified ALOTS system is limited by inability to acquire low luminance targets and inability to operate with a high background sky luminance. The radar is limited by insufficient range capability for targets of low radar cross-section.

The desired accuracy capability of these sensors is best defined in terms of satellite arrival time errors. For an expected ALIAS terminal vehicle velocity of about 3000 ft/sec near closest approach to the satellite and an allowable one sigma error 1500 ft, the one sigma arrival time error must be 0.5 seconds. This means that satellite position must be known to within about 2 miles along its trajectory if all other error contributions were negligible. A 1 n.m. along-track satellite position error will allow flexibility in the constraints on the other sources of guidance error.

For a 100 n.m. orbit the 1 n.m. error must be achievable at a range of 200 n.m. The range information must be transmitted to the ALIAS terminal stage before 35 seconds-to-go if a 5 n.m. lateral correction is to be achieved.

a. ALOTS Performance Requirements. Within this context it is instructive to look at ALOTS system capability in more detail. At a range to target of 200 n.m., an object with a diameter of 10 ft subtends an angle of 1/120 mr. For a state-of-the-art vidicon sensor having 525 lines across its face and subtending a 6.00° field of view the minimum resolution element has an angular size of 1/5 mr. This means that the intensity of a focused image must be 576 times the intensity of the background in order to equal the observed intensity of the background in the vidicon resolution element. If a signal to noise ratio of about 3.7 to 1 is to be achieved, the initial background to satellite luminance intensities must be in the ratio of 2130 to 1.

The minimum vidicon faceplate illumination criteria must also be satisfied. Faceplate illumination (H_o) must be on the order of .05 foot candles for a Westinghouse 7290 vidicon.

$$H_o = \frac{\delta_1 H_{eff}}{4 (\Delta \theta)^2 (F)^2}$$

H_o = Faceplate illumination

δ_1 = optical efficiency

H_{eff} = target irradiance at entrance aperture

$\Delta\theta$ = resolution element angular dimension

F = relative aperture of the optical system

For $\rho A_t = 1m^2$, spherical diffuse reflecting target, a range of 200 n.m., sun-phase angle of 90°, and an S-20 photo cathode, $H_{eff} = 2.2 \times 10^{-14}$ watts/cm^2. For a $\Delta\theta = .2$ mr, and $F = 5.35$, a δ_1 = .7 and $H_{eff} = 2.2 \times 10^{-14}$ watts/cm^2

$$H_o = 10^{-8} \text{ watts/cm}^2$$

$$6.32 \times 10^5 \frac{\text{foot-candles}}{\text{watts/cm}^2} \quad \text{at } 555\ m\mu \qquad H_o = 6.75 \times 10^{-3} \text{ foot-candles}$$

The data reported in STL report 8424-6017-RS000 on the signal current verses faceplate illumination for the Westinghouse 7290 vidicon does not include a description of the light source employed for this calibration. If near monochromatic light at 550 mμ was used for the vidicon calibration the above calculations for faceplate illumination in terms of foot-candles is correct. The point to be made is that in terms of the vidicon sensitivity the calculated faceplate illumination is too low by an order of magnitude. This conclusion should be re-evaluated for other vidicons, smaller resolution elements, and smaller relative aperatures. The faceplate illumination could certainly be increased to an acceptable value if the penalty of reduced field of view can be tolerated. This reduced field of view necessitates either a search pattern along the trajectory, or acquisition and centering of the target by external means. Conceptually an image orthicon tube could be used for the initial acquisition phase and be employed only to center the image for a vidicon tracker with a smaller field of view. The sky background would be the limiting factor for the orthicon approach, and the 2000 to 1 background to target luminance ratio criteria derived above for a 10 ft diameter target at 200 nautical miles may well have to be increased.

A large number of sky background to target luminance ratios are calculated in Appendix C Itek report SHC 64-8435-492. Figures B-2 and B-3 give representive values and show that for low sun elevation angles it is possible to track the satellite of the size and reflective properties assumed by Itek. (For high sun elevation angles it is not). (At 60,000 ft., Itek has assumed a 6 ft dia x 7.5 ft long right circular cylinder with reflectivity of 1.0). In going from 60,000 ft to 35,000 ft, (ALIAS operating altitude), the sky radiance for low sun elevation angles is further increased by a factor of four.

(1) <u>Target Acquisition</u> - If satellite acquisition by the modified ALOTS must be accomplished externally by a human observer, the operational limitations of the ALIAS system become extremely severe, (due to the restricted field of view). A human observer looking through an eight power telescope can track 7th magnitude objects in a star background if the solar depression angle is near 13.5 degrees or near sunset for a 100 n.m. orbit. Fourth magnitude objects can be tracked with solar depression angles of near 5°. Such a satellite acquisition system would definitely be restricted to operations near the sun shadow line crossing. This not only restricts the flexibility of the system but also severely hampers the payload recovery operations.

Satellite and Sky Luminance at Twilight

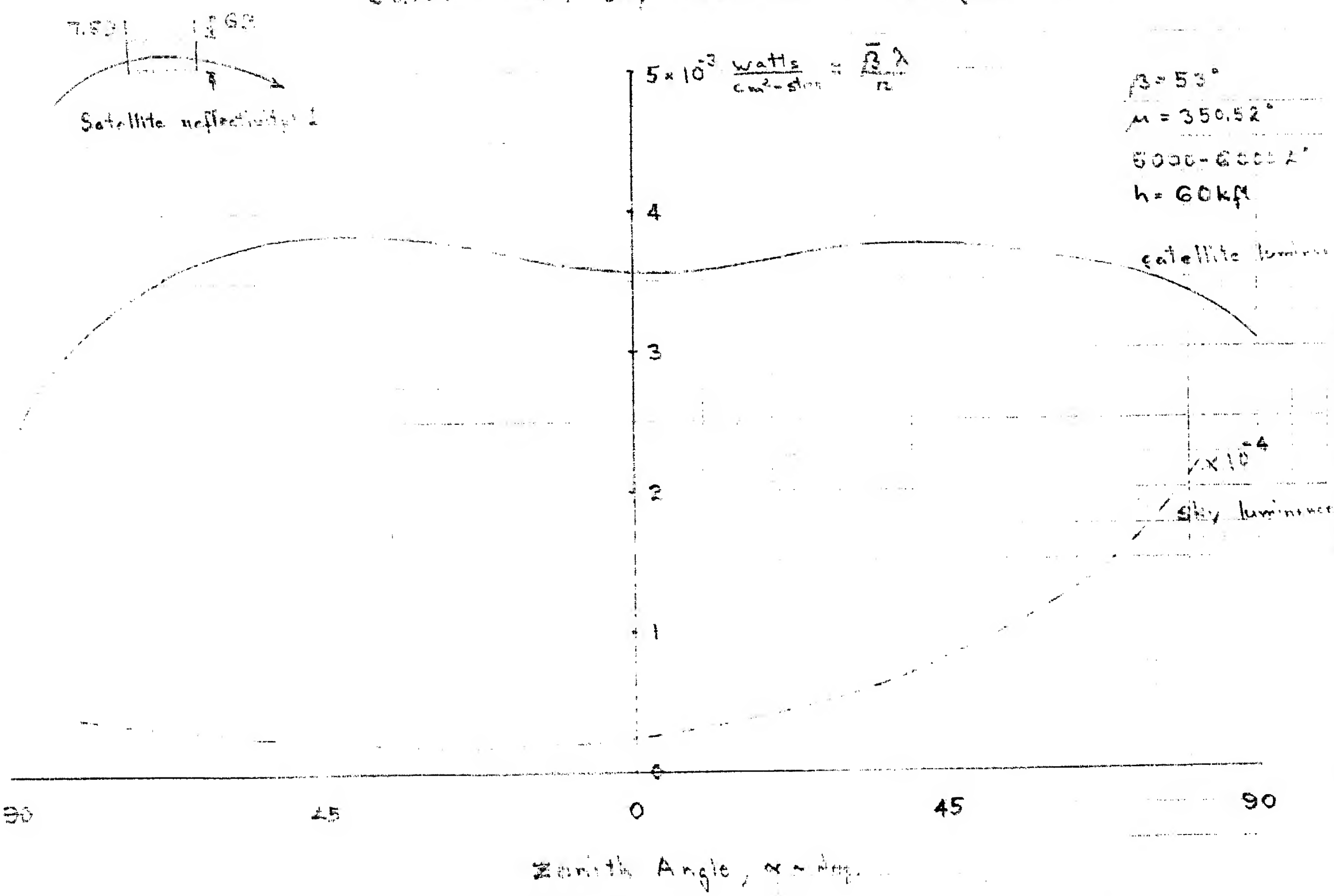

Figure B-2

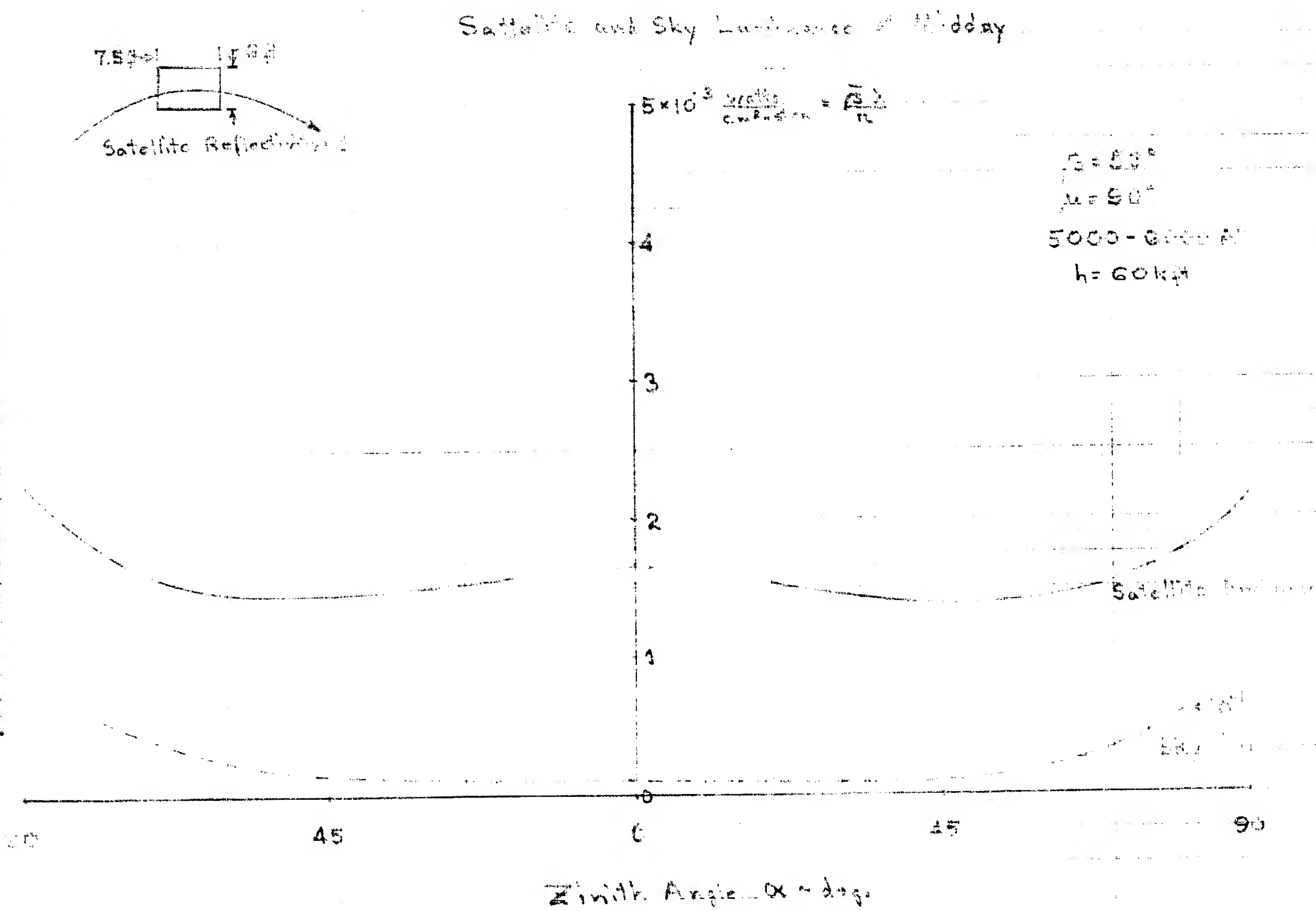

Figure B-3

SECRET LIMITED DISTRIBUTION

Approved For Release 2003/12/09 : CIA-RDP75B00157R000100110001-0

Objects of 1.5 m. in major dimension do have stellar magnitudes of about 1 to 3 for the twilight condition referred to above. At 40,000 ft the background becomes bright enough to prevent acquisition by the observer with the eight power telescope over all elevation angles when the sun is about 30° above the horizon. This means that such a system would have an acquisition capability only at positions less than 2 to 3 hours from the satellite sun shadow line crossing.

An alternate approach would be to go through a programmed search of the ephemeris uncertainty volume with the necessarily restricted field of view tracking system. Such a technique would possibly extend the capability to 4 hours from satellite shadow line crossing. An exact definition of the maximum sky luminance under which tracking is possible with a modified ALOTS optical tracker is not possible without considering the detailed design choices that could be made.

Northrop Nortronics Div. estimates that a $\rho A_t = 1.2 m^2$ target with a sun phase angle of 60° could be acquired at 700 n.m. with a maximum sky luminance of 650 ft-lamberts. Such a modified system is a fairly sophisticated system with a very small angular field of view, large optics and uses nine vidicons. At 40,000 ft and a sun elevation of 35°, the modified ALOTS system could track objects in 50% of the sky, (Figure B-4). About 10 seconds will be required to search a $3/4^{\circ}$ angular field. The required field of view for a 5 n.m. radial error, a 5 second arrival time error, a range of 200 miles and a look up angle of 30° from the horizontal is about 6° which means that 640 seconds will be required to search the satellite position uncertainty volume. A 640 second search time is of course inconceivable. For targets of higher intensity the search time for $3/4^{\circ}$ field of view is about 2 seconds which still means that 120 seconds will be required for search. Thus, while the modified ALOTS system is feasible and has a capability for acquiring targets when the sun is near the horizon, it has obvious limitations.

(2) Target Tracking - Once the satellite has been acquired, ALOTS tracking accuracies are quite acceptable. The .2 mr resolution element of the modified ALOTS system in conjunction with a similar capability aboard the ALIAS vehicle terminal stage, constrain range errors to about 600 ft. This means that a 2.5 mr misalignment of the ALOTS system inertial reference is acceptable for the 1 n.m. accuracy range estimate. Less than 2.5 mr. misalighment with the inertial frame is readily achievable with the Nortronics NIP-107 inertial platform, acceleration matched to the master inertial platform aboard the aircraft and with the vidicon sensor in turn referenced to the nearby NIP 107 inertial platform.

b. Airborne Early Warning Radar Performance Requirements

The existing airborne early warning and tracking radars of most interest to ALIAS are the APS-70, 70A, APS-96 and APS-111. The APS-96 Airborne Early Warning (AEW) radar has the desired performance capability and appears to be most readily available. The characteristics of APS-96 are as follows:

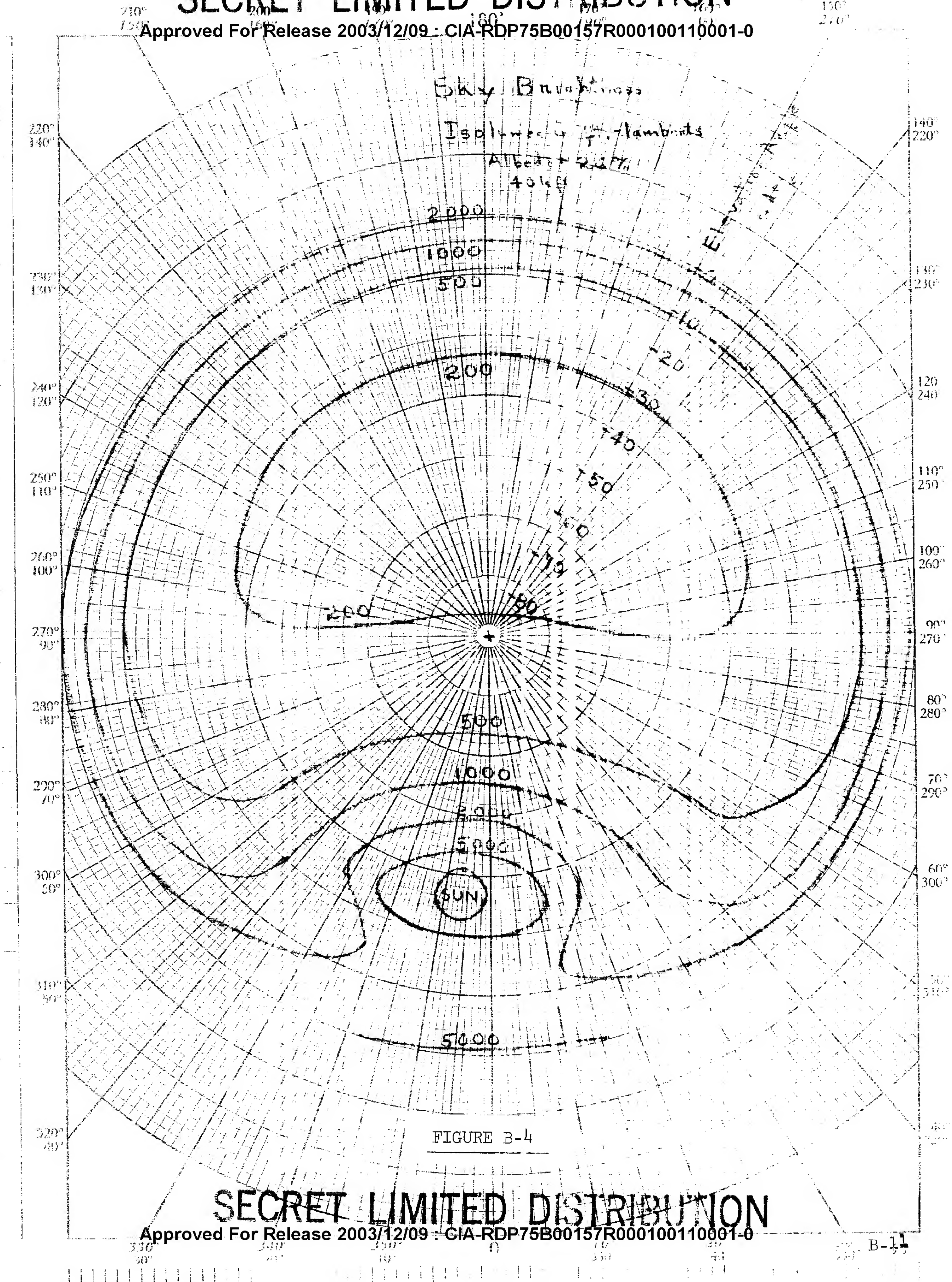
Sky Brightness
Isolines in ft-lamberts
Albedo
2000
1000
500
200
500
1000
2000
5000
SUN
5000
10
20
30
40
50
60
70
80
Elevation Angle
200

FIGURE B-4

Antenna	24-foot rotodome
Frequency	400 - 450 mc
Power-peak	1 megawatt
Power-average	3800 watts
Pulse length	12.8 μ sec (compressed to .2μ sec)
Pulse repetition frequency	300 pps
Noise Figure	6 db.
Antenna Gain	22 db
Elevation beamwidth	26°
Azimuth beamwidth	6.5°
Radar Range Accuracy	1.1 n.m.

The acquisition range performance of this radar in the scanning mode is given in Figure B-5. The APS-96 acquisition range for a 10 m^2 target is 90% probability of detection at about 200 n.m. if the search is restricted to a particular azimuth. The Cosmos class satellite radar cross section has been observed to range from 1 to 600 m^2 at UHF frequencies. The additional gains in APS-96 radar range performance which could be realized for high altitude targets arriving from a defined azimuth are as follows:

No scan losses	= 2 db
No MTI required	= 3 db
Longer integration times	= 5.5 to 7 db
total	= 10.5 to 12 db

The 10.5 to 12 db increase in signal strength represents an increase in detection range by a factor of 1.85 to 2. or a reduction in the radar cross section of the satellite by a factor of about 10. A field degradation of 5 db has been assumed throughout this brief radar performance analysis. For a carefully controlled flight program, as envisioned for ALIAS, something less than the 5 db loss may be realized.

The major APS-96 modifications which would be required to make this AEW radar compatible with the ALIAS mission are first the tilting of the antenna to acquire satellites 90-150 n.m. in altitude at a slant range

SECRET LIMITED DISTRIBUTION

BLIP/SCAN RATIO VS RANGE FOR APS - 96 RADAR - THREE TARGET AREAS (5 - DB FIELD DEGRADATION)

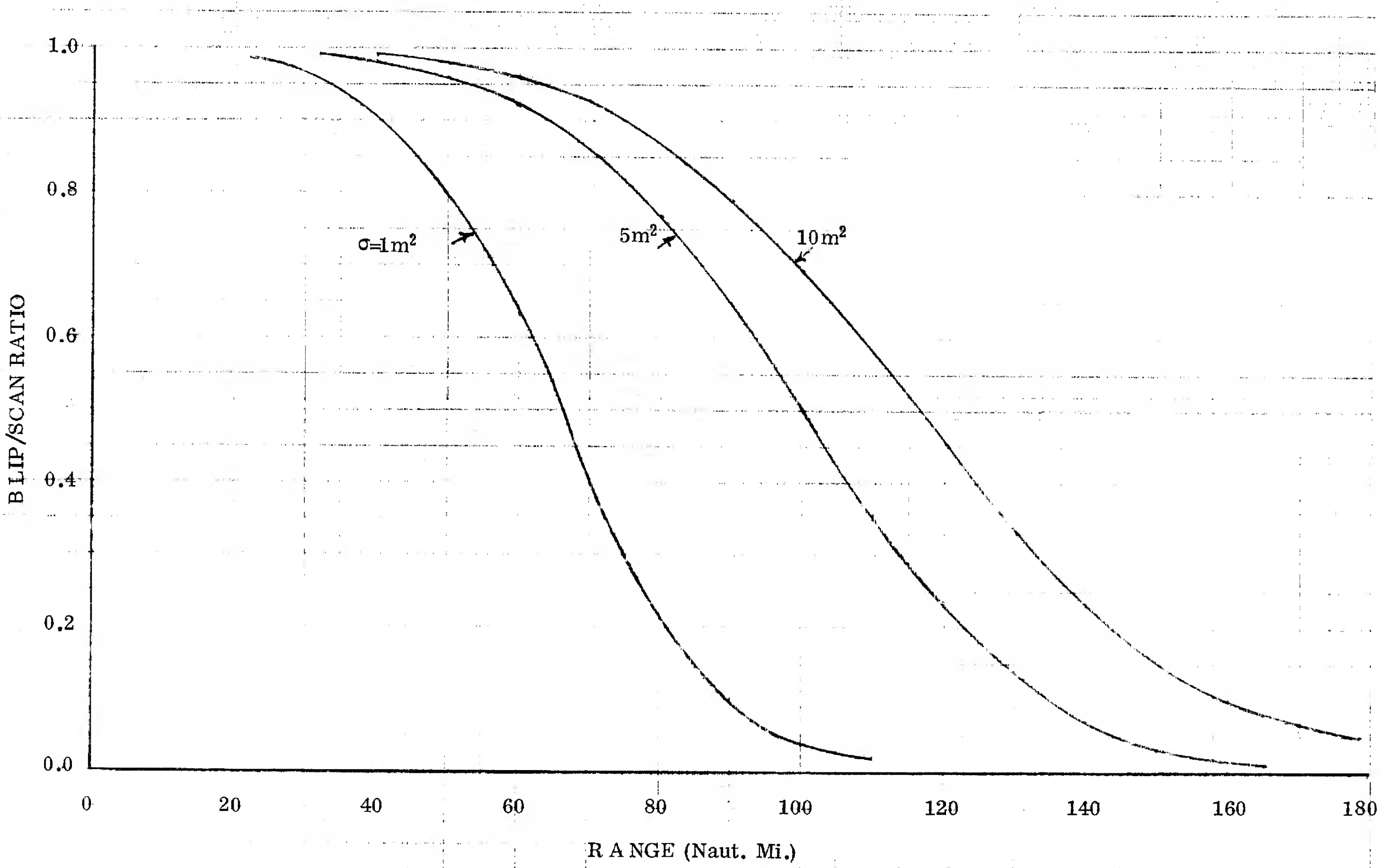

Figure B-5

SECRET LIMITED DISTRIBUTION

of about 200 n.m. and, second, the modification of the radar receiver to accept target closing velocities on the order of 4.0 n.m. per second. As the target azimuth will be known from ephemeris data and the airplane azimuth can be changed to accommodate the radar, a non-scanning radar mount is acceptable. This also allows the possibility of a side looking radar which eases the airplane, antenna compatability problem.

4. Booster Guidance

The ALIAS first stage is controlled by an inertial guidance system. The important parameters of this flight phase are initial platform errors, prelaunch calculations, ignition criteria, guidance equations, thrust terminations, and the overall error contributions to the system.

a. Initial Platform Errors. The stellar inertial navigation system aboard the launch aircraft supplies the missile guidance computer with the initial position, initial velocity, a predicted intercept point, time to go, and latest ephemeris data. The missile stable platform is aligned with the aircraft inertial reference by acceleration matching. Since the missile will be stored inside the aircraft, the possibility of direct optical platform alignment also exists.

b. Prelaunch Calculations. The prelaunch solution input into the missile guidance computer is based on a nominal ejection and stabilization sequence. During the actual ejection the on-board inertial measurement unit detects variations from the nominal and updates the prelaunch solution based on stored nominal missile characteristics.

c. Ignition Criteria. The ignition criteria are: 1) less than 10° attitude difference between missile centerline and the vertical, 2) an acceptable angular rate based on attitude control system limitations, and 3) the existance of a valid prelaunch solution. The ALIAS first stage attitude is controlled by a reaction control system which will be functioning during the stabilization phase. The ejection and stabilization sequence is discussed in Appendix A.

d. Guidance Equations. The recommended guidance equations for the ALIAS systems are very similar to those incorporated in the Minuteman Wing VI airborne digital computer. These equations are referred to as constant time of flight (CTOF) guidance equations and affect interception at a time and position selected by the Pre-launch computer. The only modification for ALIAS would be use of both downrange and vertical velocities for the control system gain criteria, rather than just the downrange velocity. STL simulations using this guidance for intercept of satellites at ranges of over 500 n.m. indicate that time of arrival errors will be less than .3 seconds. The ALIAS airborne digital computer is adequate in size to accommodate these guidance equations and the arrival time errors should be considerably less for the shorter intercept ranges of interest to ALIAS.

A possible further modification of the constant time of flight guidance equations, to limit ALIAS velocity at intercept, is desirable. The terminal velocity, however is best controlled during the pre-launch phase by choosing the launch time to permit long times of flight to intercept altitude which assures low velocities at intercept and minimizes the effect of time to intercept prediction errors.

e. Thrust Termination. From considerations of system handling ease, cost, and safety, only solid propellant rocket motors have been considered candidates for the ALIAS booster mission. Ideally, the ALIAS solid propellant rocket motors should also have thrust cut-off capability. The only thrust termination capabilities that have been incorporated into solid rocket motors to date, however, have been applied to rockets of much greater total impulse than are required for the ALIAS trajectory. The development of a new rocket providing thrust termination and designed for the ALIAS mission or the possible modification of an existing solid rocket to provide thrust cut-off does not appear warranted from the standpoint of time and cost. Thus, a means of short duration thrust reversal, separation, and immediate ALIAS booster tumble is recommended. For the thrust level of the candidate ALIAS rockets, six or seven small, lightweight, high thrust, short duration rockets placed on the main rocket forward dome would reverse thrust, cause separation, and with the aid of a minute tumble motor effectively end terminal stage thrusting. The ignition command for these six to seven little rockets is provided by the constant time of flight guidance equation.

f. Overall Error Contributions. The position error contribution of ALIAS first stage guidance system to the final intercept error should be evaluated in terms of the ephemeris error in the cross-range direction and the 1 n.m. error of the range measuring system along the satellite trajectory. The velocity and attitude reference errors of the inertial guidance system have a more direct effect on the accuracy of the terminal guidance correction. Significant errors are 25 ft/sec and 5 minutes of arc for the velocity vector and azimuth alignment respectively. The effect of these errors will be discussed in Paragraph 5 below.

The probable errors of the ALIAS inertial guidance systems can be approximated from the figures in Table B-1. This table presents the results of a Nortronics study for the Large Payload Test Vehicle Program (NORT 65-25) and is representative of the capability of an inertial measurement unit somewhat inferior to the one selected for the ALIAS system. The trajectory to which these guidance errors correspond is approximately twice as severe as the 150 n.m. altitude ALIAS trajectory. The flight time of 510 seconds and burnout velocity of 16,000 ft/sec are twice the ALIAS values and thus the predicted guidance errors are also approximately twice as great as those anticipated for ALIAS. The accelerator null bias for ALIAS guidance is expected to be 10^{-5} g's as opposed to 10^{-3} g's which has been assumed in the Nortronics error analysis and thus the initial platform misalignment for ALIAS would also be materially reduced.

Table B-1 represents errors in guidance system computation of ALIAS booster flight parameters and does not represent errors resulting from lack of accurate booster thrust cut-off capability. The magnitude of the thrust cut-off errors and their effect on terminal correction motor performance requirements is examined in Appendix E.

Table B-1

TABLE B-1

ERROR SUMMARY

Guidance Parameters	Velocity Errors (ft/sec)			Position Errors (Ft)			Angular Errors (deg)		
Sources	ΔV_x	ΔV_y	ΔV_z	ΔP_x	ΔP_y	ΔP_z	ϕ_x	ϕ_y	ϕ_z
Accelerometer Scale Factor	1.76	0	0.42	300	0	576	-	-	-
Initial Misalignment	0.88	6.1	18.0	1000	1000	520	0.06	0.06	0.02
Accelerometer Null	0	0	8.2	0	0	4180	-	-	-
Gyro Random Drift Rate	0.39	0.88	0.80	482	545	244	0.014	0.014	0.014
Gyro Mass Unbalance Drift Rate	4.62	9.2	11.6	68	115	104	0.074	0.074	0.0036
Total Error RMS (One Sigma)	5.0	11.0	23.0	1150	1140	4260	0.09	0.09	0.025

Accelerometer null bias	10^{-3} g's
Accelerometer scale factor	.1%
Gyro Random Drift Rate	.1 deg/hr
Gyro Mass Unbalance Drift Rate	.5 deg/hr/g
Initial Level Misalignment	.06 deg
Initial Azimuth Misalignment	.06 deg

SECRET LIMITED DISTRIBUTION

Approved For Release 2003/12/09 : CIA-RDP75B00157R000100110001-0

5. Terminal Guidance Correction

The ALIAS terminal guidance correction will be computed on the basis of a corrected along-track satellite position transmitted from the launch aircraft, and the direction and magnitude of the angular rotation of the line of sight to the satellite away from the computed relative velocity vector, as observed by the on-board optical sensor. In order to make up a cross track error of 30,000 ft with 1000 ft/sec correction capability the guidance signal must be available at 35 seconds to go. The capability of: 1) acquiring the target prior to 35 seconds to go with the optical sensor, and 2) measuring the angle with sufficient accuracy to satisfy the 1500 ft one sigma off-set error at 35 seconds to go, pose the severest constraints on the ALIAS terminal stage optical sensor.

a. Target Acquisition. The acquisition problem is that of having sufficient sensitivity to detect the target and also being able to discriminate the target from the star backgound. A vidicon and an image orthicon are discussed below as two possible sensors for the ALIAS mission. The vidicons are preferable, since they are more rugged, small, and readily available.

Before making an estimate of sensor capability the satellite effective irradiance at the entrance aperture must be specified. Figure B-6 gives the effective irradiance of different reflectivity (ρ) and area (A_T) objects for a silicon and an S-20 detector at various ranges, and for a sun phase angle of 90°. Sun phase angle is measured at the satellite, between the line of sight to the sun and the line of sight to the observer. Figure B-7 provides the correction factor for a range of sun phase angles from 0° to 180° and a diffuse reflecting spherical target.

The sensitivity of the vidicon is described by the following equation:

$$\frac{\rho A_t}{\Omega} = \frac{S}{N} \; \frac{8\,(\Delta\theta)\,(F)^2}{K_1\,K_2\,\pi\,S_1} \left(\frac{KTG}{\alpha T_f}\right)^{\frac{1}{2}}$$

Where

ρ = Target Reflectivity

A_T = Target Effective Area

Ω = Field of view

F = Focal ratio

$\Delta\theta$ = Angular size of resolution element

T_f = Frame time

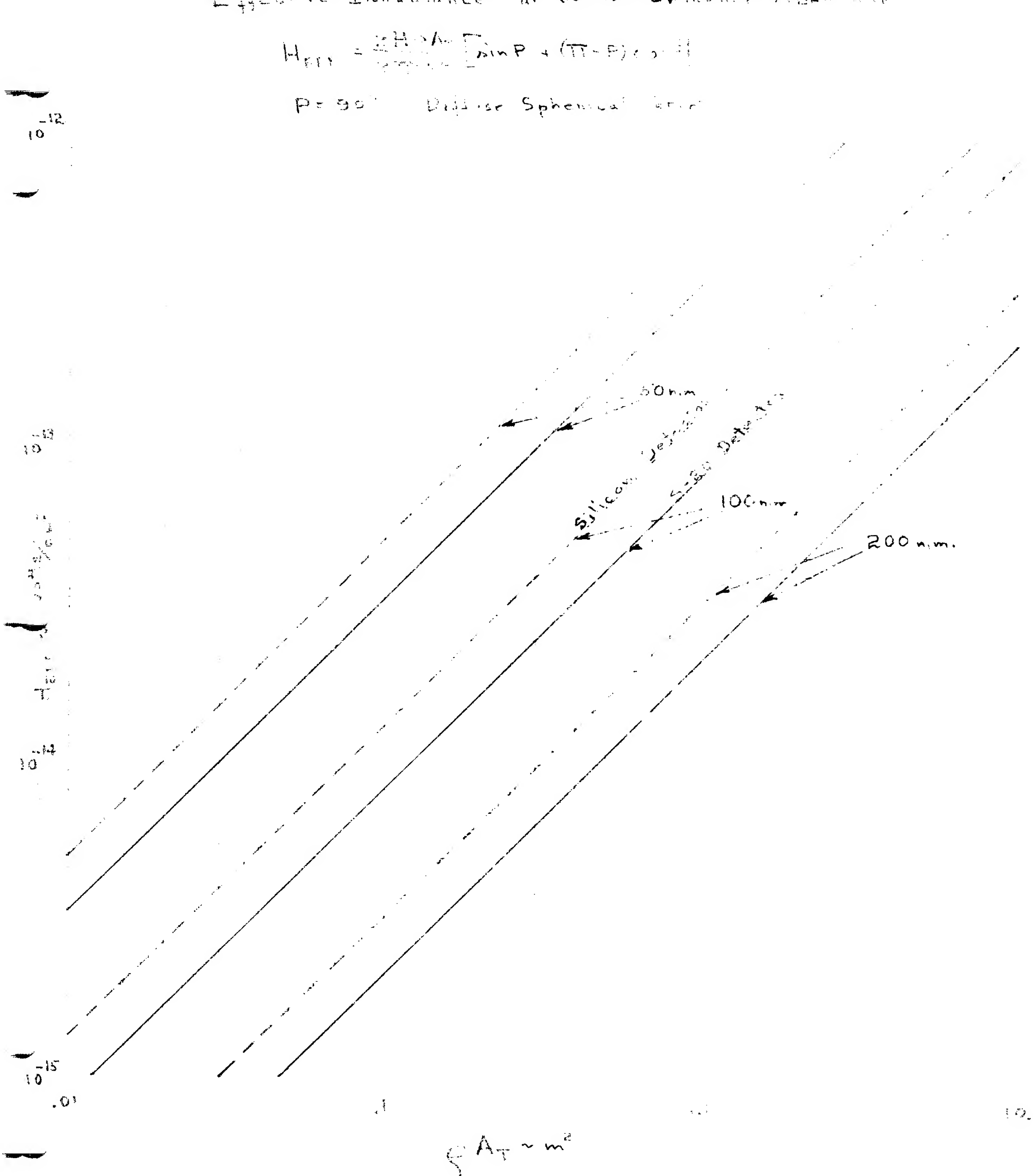
Diffuse Spherical
10^{-12}
10^{-13}
10^{-14}
10^{-15}
50 n.m.
Silicon Detector
S-20 Detector
100 n.m.
200 n.m.
.01
.1
10.
A_T ~ m^2

Figure B-6

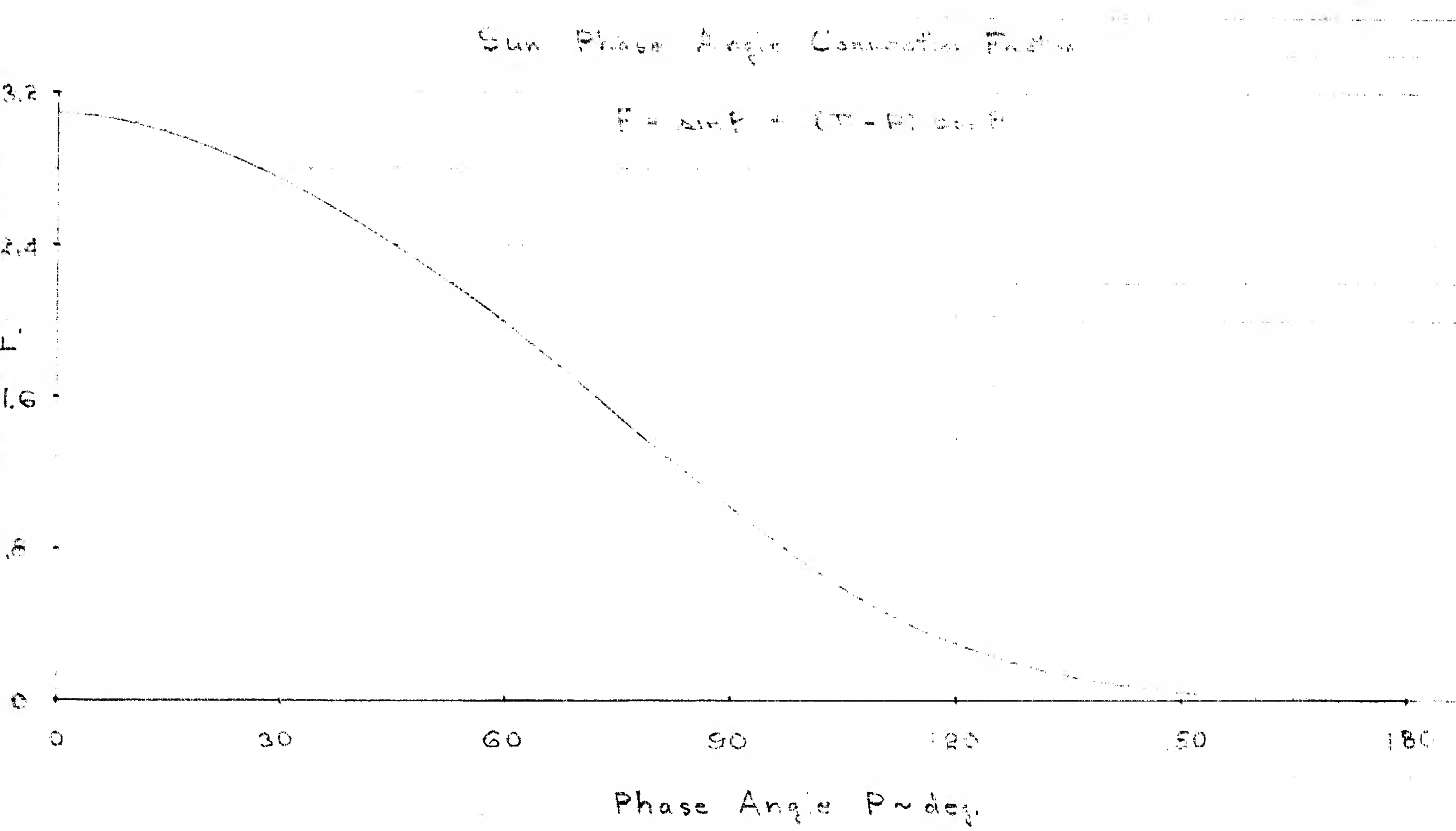

Figure B-7

SECRET LIMITED DISTRIBUTION

Approved For Release 2003/12/09 : CIA-RDP75B00157R000100110001-0

α = Fraction of frame time spent scanning the target

K_1 = Constant, relating faceplate illumination to signal current

K_2 = Constant, relating target size to effective target irradiance at the entrance aperture (contains inverse range-squared factor)

ξ_1 = Optical efficiency

k = Boltzman's constant

T = Load resistor temperature of vidicon

G = Conductance of the load resistor of the vidicon

S/N = Signal to noise ratio

The sensitivity of the image orthicon is described by the following equation:

$$\frac{[illegible]\, A_t}{\Omega} = \left(\frac{S}{N}\right)^2 (F)^2 R^2 \left(\frac{1+\gamma^2}{\gamma d^2}\right) \left(\frac{12\,\pi\, e\, [illegible]}{\xi_1\, T_2\, S\, [illegible]}\right)$$

R = range to target

γ = raster width to height ratio

d = diagonal of photocathrode

β = constant related to tube performance

P = sun phase angle

e = electron charge

S = photoelectric constant of tube

H = S-20 response

STL has analyzed the capabilities of a Westinghouse 7290 vidicon and an RCA C74081 image orthicon in a space environment using the following additional parameters:

S/N = 5.7 (.95 prob. of det. (10^{-4} false alarm)

T_f = 1/30 second

F = 2

$\Delta\theta$ = .8 mrad. for orthicon, (.6 mrad. for vidicon)

ϕ = 140 deg.

R = 100 n.m. for orthicon, (50 n.m. for the vidicon)

The relationships between field of veiw and required effective target are given in Figure B-8. It is interesting to note that the image orthicon S/N varies inversely with range while the vidicon S/N varies inversely with range-squared.

From Figure B-8, it is obvious that the orthicon is much more sensitive. Reducing the vidicon frame rate in the acquisition mode to 5 frames per second, however, and choosing a more favorable sun phase angle of about 60° increases the range capability of the vidicon by over a factor of 3 and decreases the required target size to $1m^2$. Thus, while the orthicon definitely has a greater range of applicability, it is not clear that the vidicon will not function adequately for ALIAS. Certainly there are no vidicon sensitivity problems associated with an error make-up of 18,000 ft. One hundred percent of the available light should be used for acquisition. Five percent of the light is sufficient during the picture taking phase. (A 100% mirror and a 5% beamsplitter is in the optical path with removal of the 100% mirror at 4 seconds-to-go to provide the required capability).

The second major consideration in evaluating the satellite acquisition range of the ALIAS terminal vehicle is the capability for discrimination from the star background. The desired field of view of the ALIAS optical system is less than 3° in radius or less than 8.65×10^{-3} steradians. If a $\rho A_t = 1m^2$ spherical diffuse reflecting target is to be acquired at 170 n.m. or about 40 seconds to go, stars with an effective irradiance of 2.8×10^{-14} watts/cm^2 for an S-20 detector must be accepted when the sun phase angle is 90°. The star population in 4π steradians having greater than this light level is 420 as shown in Figure B-9. The expected number of stars in the field of view brighter than the target is thus .3. Even for a sun phase angle of 140 degrees, the expected number of stars brighter than the satellite in the field of view is 6. This discrimination task poses no problems either in terms of computer space or delays in acquiring the target. The satellite will be discriminated from the star background by angular motion discrimination. The minimum angular rate which is available for this discrimination technique is .5 mr/sec. If angular rates of .5 mr/sec are not

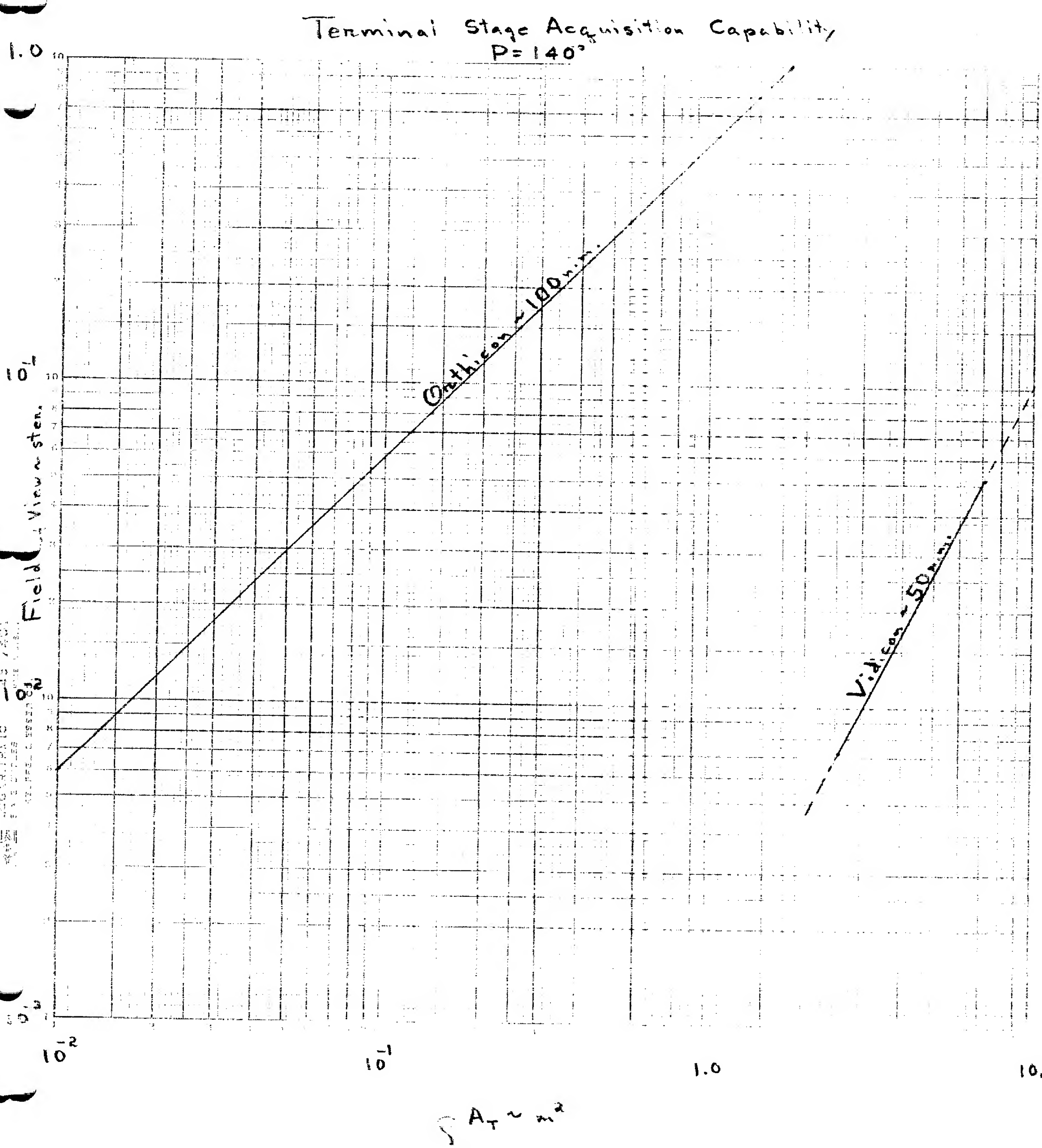
Terminal Stage Acquisition Capability
P = 140°
1.0
10^{-1}
10^{-2}
10^{-3}
Field of View ~ ster.
10^{-2}
10^{-1}
1.0
10.
A_T ~ m^2
Orthicon ~ 100 n.m.
Vidicon ~ 50 n.m.

Figure B-8

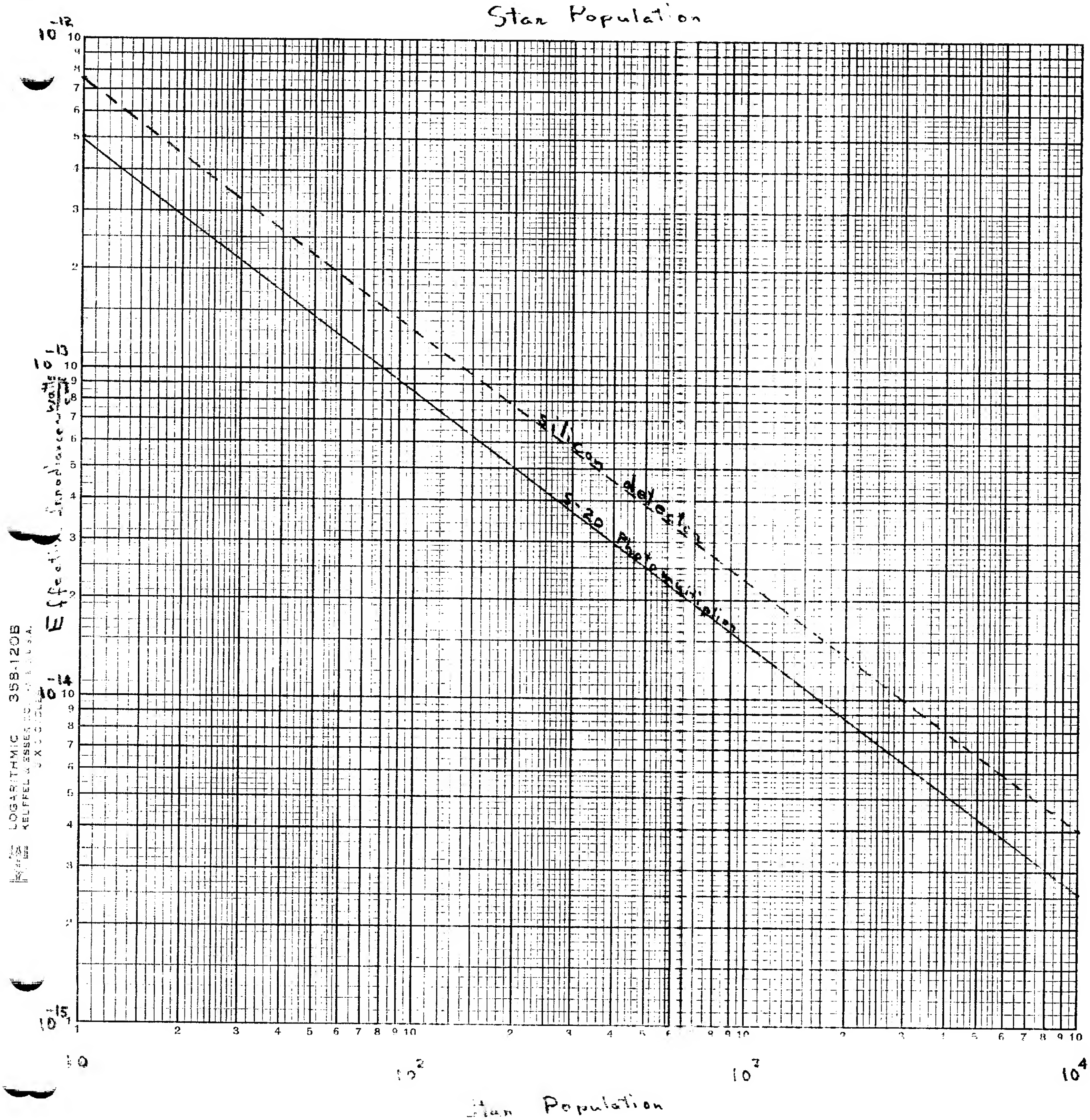
Star Population
Effective Irradiance watts
Silicon detector
S-20 Photomultiplier
Star Population
LOGARITHMIC 358-120B
KEUFFEL & ESSER CO.

Figure B-9

observed by 14 seconds to go the correction thrust will be used to bias the terminal vehicle trajectory .5 n.m. to the sun side of the satellite trajectory plane so that, by definition, a satellite line of sight rate greater than .5 mr/sec will be available.

Before evaluating the accuracy of the guidance correction which is available from the ALIAS terminal stage optical sensor, it is instructive to note the magnitude of the angles and angular rates that are consistent with various terminal vehicle offset distances and times to go from closest approach. Figure B-10 shows the angle between the computed relative velocity vector and observed line of sight. Figure B-11 shows the observed rate of rotation of the line of sight for the range of probable ALIAS initial offset errors. The time at which the guidance correction must be available to correct the given error with a 1000 ft/sec, 5-g motor is also shown. The guidance correction must be made by 14 seconds to go if final tracking and image motion compensation is to be initiated at 4 seconds to go. An allowance of 2 seconds is made for attitude positioning the terminal stage both before, and after, terminal stage motor firing. Figures B-10, B-11 also show Gemini Retro Motor Capability.

b. Tracking Accuracy. The accuracy of the ALIAS optical sensor can be approximated as follows:

The quantization error is estimated to be the dominant noise error for the vidicon. If the vidicon is quantized at increments of $\Delta\theta$. The rms quantization error, σ, is

$$\sigma = \frac{\Delta\theta}{2\sqrt{3}}$$

The angular rate error is

$$\sigma_w = \sqrt{\frac{N_o}{T^3}} \qquad N_o = \frac{T_f\ (\Delta\theta)^2}{12} \qquad \frac{\text{milliradians}^2}{\text{cps}}$$

T = Total time lag of filter

T_f = frame time

For a total field of view of 6^o and 525 lines across the face of the vidicon, the tracking system has a quantification error of .2 milliradians. The 6^o field of view is adequate for 10 n.m. diameter ephemeris errors at ranges where the guidance correction must be made and the 525 line is consistent with the Westinghouse 7290 vidicon. If T_f = .2 seconds, T = 2 seconds, and $\Delta\theta$ = .2 milliradians, σ = .06 milliradians and σ_w = .01 milliradians/sec. As will be discussed in para. 6 below, the quantization

SECRET LIMITED DISTRIBUTION

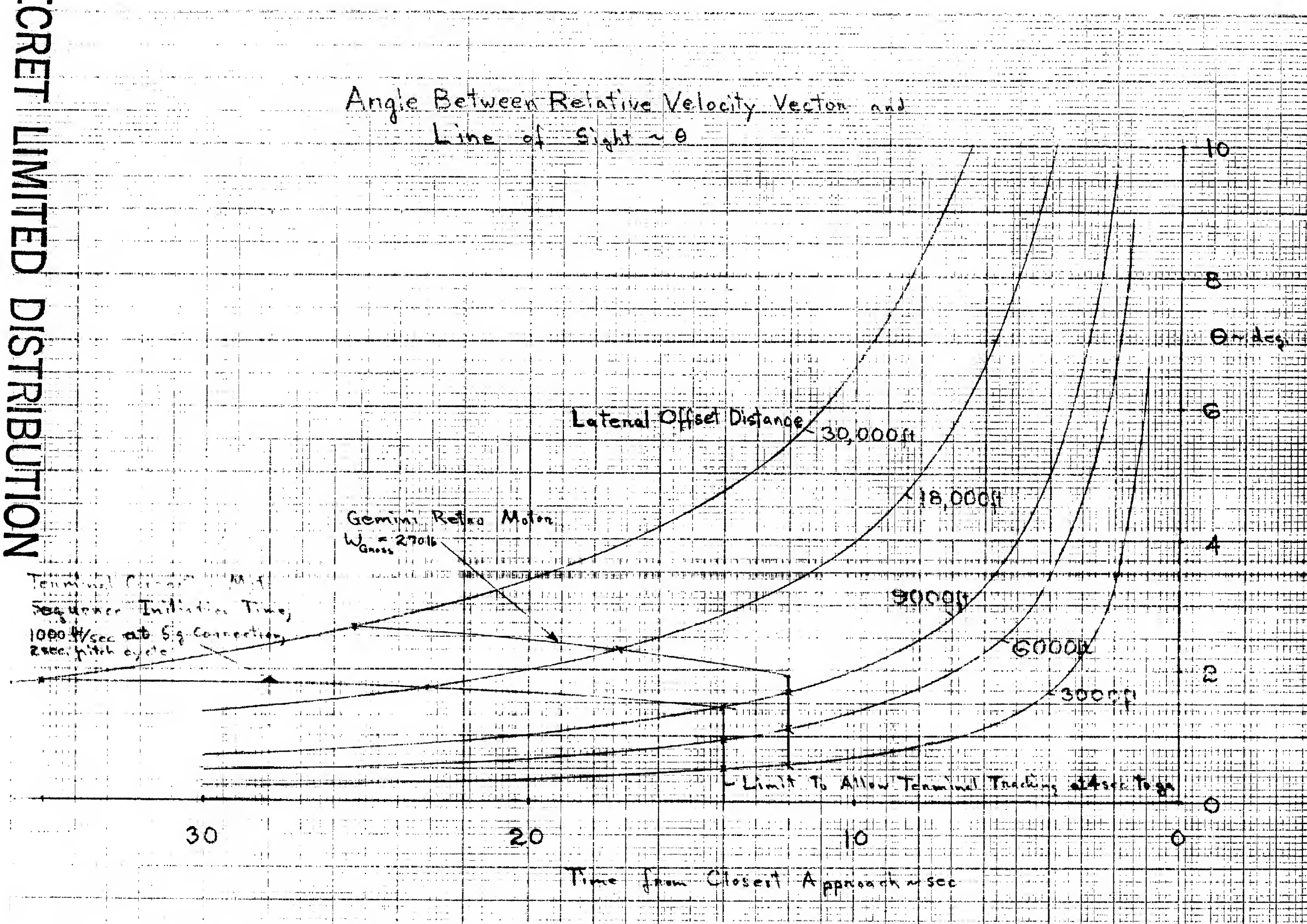

SECRET LIMITED DISTRIBUTION

Figure B-10

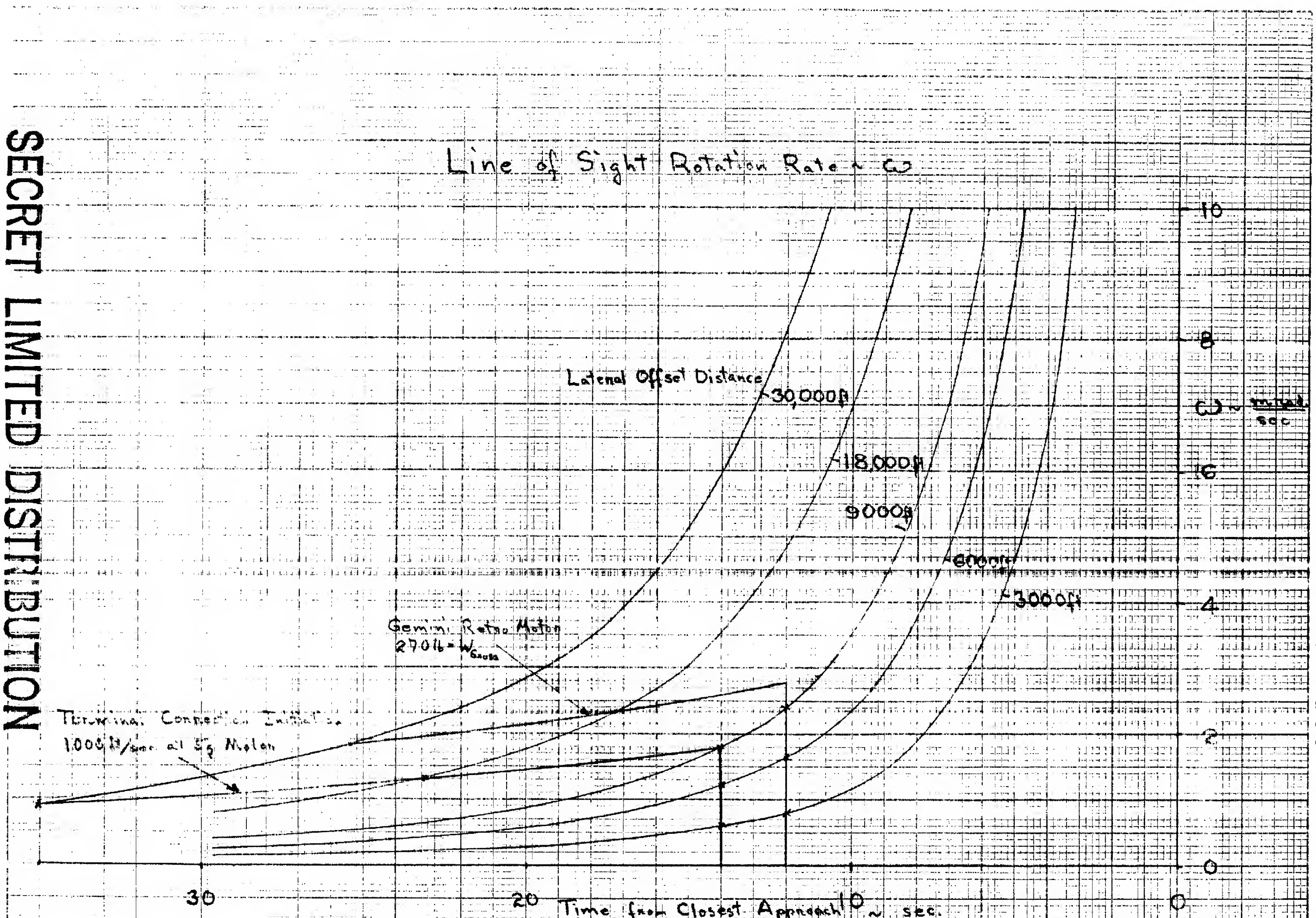

Figure B-11

Approved For Release 2003/12/09 : CIA-RDP75B00157R000100110001-0

error is much smaller, than the bias errors resulting from platform drift which are seen to be on the order of 1.5 mr. The angular rates change at the rate of between .05 mr/sec^2 to .2 mr/sec^2 at the time to go when guidance corrections must be made thus there is bias error in the smoothed angular velocity data, (σ_w) which must be corrected by predicting the line of sight angular acceleration.

6. System Accuracy and Back-up Guidance Mode

The errors that must be corrected by the ALIAS terminal stage consist primarily of the ephemeris errors. The inertial guidance error accrued during ALIAS booster guidance and launch platform navigation are minor compared to ephemeris errors. The accuracy to which the terminal correction can be made depends on the accuracy of the guidance computations and the tolerances on the terminal stage propulsion system. The accuracy of the guidance computation limits ALIAS system guidance accuracy. The primary sources of terminal guidance computation error are misalignment of the on-board reference frame, ALIAS to satellite slant range uncertainty, and relative velocity vector computation error.

a. Reference Frame Errors. The misalignment of the ALIAS terminal stage reference frame is caused by the following:

(1) Misalignment of Aircraft Master Reference with inertial frame	= .5 min of arc
(2) Errors in Acceleration Matching ALIAS Stable platform to Aircraft platform	= 1 ÷ 2 min of arc
(3) Drift of ALIAS platform during ejection phase and booster flight	= 3 min of arc
Total	$= \sqrt{3^2+1^2+.5^2} = 3.2$ min of arc

b. Slant Range Errors. ALIAS to satellite slant range is in error due to:

(1) Aircraft to Satellite Range Measurement	= 1 n.m.
(2) ALIAS booster inertial navigation error in down range direction	= .25 n.m.
Total	= 1.032 n.m.

c. Velocity Vector Errors. Relative Velocity vector errors are due to:

(1) Error of Satellite Velocity Computed by SPADATS 66 (normal to relative velocity vector direction)	= 30 ft/sec
(2) ALIAS booster inertial navigation error	= 30 ft/sec
Total	= 42.5 ft/sec
Relative Velocity Vector direction	= 5.6 arc min
Relative Velocity Vector Magnitude	= .17%

d. Overall Errors. The measured angle between the relative velocity vector and line of sight to the satellite is thus in error by $\sqrt{3.2^2 + 5.6^2} = 6.5$ min of arc. The arrival time error is .25 seconds. Thus, if the guidance correction is made at 35 seconds to go or for the case of a 30000 ft lateral offset and 3000 ft/sec ALIAS crossing velocity the guidance correction will have a one sigma error about 1800 ft. For an 18,000 ft offset, the guidance correction will have a one sigma error of about 1250 ft. The errors in the desired offset distance due to non-nominal performance of the correction motor can readily be made small compared to the errors due to the guidance computation.

e. Alternate Guidance Mode. An alternate, although degraded, guidance mode is possible with the envisioned ALIAS concept. This mode of operation depends on deriving time of arrival at closest approach data from the angle and angle rate information available on the ALIAS terminal stage. The required angle rate measurement accuracy depends on the range to the satellite and the offset distance. The time to closest approach is given by the following equation:

$$\frac{V_R \text{ Sin } \theta}{V_R T_1 \cos \theta} = \omega \qquad t_{ca} = T_1 - T_1 \sin^2 \theta \qquad t_{ca} \approx \frac{\theta}{\omega} \text{ (for small values of } \theta)$$

θ = angle between the line of sight and the relative velocity vector

ω = rotation rate of the line of sight

t_{ca} = time to closest approach

V_R = Relative velocity vector magnitude

APPENDIX C

SENSOR SYSTEM ANALYSIS

APPENDIX C

SENSOR SYSTEM ANALYSIS

The sensor discussions in this appendix apply to the intelligence gathering and storage functions of the Air Launched Intelligence Acquisition System (ALIAS) and do not pertain directly to the sensing functions required for target tracking and vehicle guidance. Some commonality of functions has led to dual use of common system elements, such as the recommended use of the primary payload optics for both target tracking and intelligence sensing functions. Such overlapping functions are treated later in this appendix as design interface details. The parametric analyses are based solely on the acquisition of imagery for intelligence purposes.

1. Sensing Techniques

A survey by North American Aviation, Inc, (NAA) of properties which might yield usable intelligence information[1] has been reviewed for potential application to the ALIAS mission concept. The NAA report categorized ground target observable properties as follows:

Electrical Fields
Magnetic Fields
Gravity Fields
Temperature
Chemical Concentrations
Nuclear Radiation
Ultraviolet Radiation
Visible Radiation
Infrared Radiation
Microwave, Radio, and Low-Frequency Radiations
Mechanical and Acoustic Vibrations

Several of these properties might be exploited for acquiring additional technical information by a co-orbital satellite inspector operating in a stabilized position quite near the target; however, only UV radiation and visible radiation afford the remote sensing information capacity required for the high speed crossing trajectory envisioned for the ALIAS mission.

[1] Survey of Sensors and Techniques Applicable to Arms Control Inspection and Verification, Vol. III Sensors and Sensing Techniques, North American Aviation, Inc., Space and Information Systems Division, Report No. SID-64-536-3, 13 July 1964 (SECRET)

Within the visible UV and IR spectrum, a variety of solid state detectors are available based on photovoltaic, photoconductive, photoelectromagnetic, photodiffusion and quantum-measuring techniques. The size of photodetector elements and the complexity and weight of data processing elements preclude the use of such systems as imaging devices for the terminal stage of the system currently under consideration.

The remaining techniques for acquisition of intelligence information in the form of imagery are television, (including image converters and image intensifier devices), and photographic film, or combinations of both. Television image forming systems can exceed photographic techniques in sensitivity, but they cannot as yet achieve the detailed resolution that is currently possible with photographic film. The information storage capacity of TV systems would place severe constraints on resolution, field-of-view, dynamic range, and picture-taking rate of the ALIAS mission as presently conceived. If there is a high confidence that the ALIAS payload can be successfully recovered, then the utilization of film does provide the required sensitivities, resolution and storage capacity. In the event that payload recovery were not considered practical, then combinations of photographic and TV techniques could provide (at some increase on payload weight), a reasonable capability for high resolution imagery to be processed and transmitted via radio link for readout by the ALIAS aircraft. The total information capacity of such a combined system would, however, be considerably reduced from that of the photographic system with physical data recovery.

Within the ultraviolet spectrum, the portion between 3000 and 4000 Angstroms is within the sensitivity region of photographic film. Tests by Texas Instruments Inc. in 1964 reportedly showed some unique imaging characteristics applicable to both low altitude ground target sensing and to space-borne surveillance of missiles and other space targets.1/ During our preliminary study we have treated this limited UV spectral region merely as an extension of the visual spectrum under consideration.

2. Sensor Selection

a. Resolution. The primary criterion for selection of sensor elements has been the ultimate system resolution capability. As a design goal we have set one-inch resolution of high contrast target details as sufficient to obtain a high percentage of the target technical intelligence information available to remote imaging techniques. At this resolution it is possible to detect point detail of about 2-inch diameter, and under proper conditions to measure significant target elements

of 5-6 inch dimensions to an accuracy of about 20%. We have assumed that analysis of the received imagery will include electro-optical readout and image reconstruction to present target detail not normally detectable by the human eye. Within the kinematic constraints of the ALIAS mission, we have considered those parameters necessary to obtain one-inch resolution and have selected an approach which should obtain a large quantity of photographs with reasonable resolution, and under ideal conditions should approach the one-inch resolution capability for several photographs on each flight.

b. Sensitivity. In order to obtain this high resolution under the kinematic constraints imposed, it is necessary to utilize high sensitivity recording media and extremely short exposure times. Our preliminary survey has revealed that photographic film is the only currently available method of obtaining the necessary combination of high resolution and high sensitivity. The sensitivity of current television-type imaging devices exceeds that of film, but the resolution limit (roughly 40 line pairs per mm) is several times less than that of current films which have sufficient sensitivity to meet ALIAS objectives. It is interesting to note that a 25 mm diameter state-of-the-art image intensifier is now limited to a peak of about 25 line pairs per mm. New developments in microchannel-array-electron-multiplication image intensifiers are expected to yield upwards of 40 lines/mm with light gains of about 10^5.[2] Although linear resolution limits would constrain field of view and other system design parameters, the extreme sensitivities could provide very short exposure times for close-in photography at high crossing rates. This concept has not been explored, however, because of the uncertain availability of the microchannel arrays and because of our findings which show the feasibility of using conventional photographic techniques.

c. Information Storage Capacity. In order to obtain the maximum amount of usable information, we have considered that a high cycling rate during the picture taking sequence will enhance the probability of obtaining optimum coverage at those times when the various system degrading factors are minimized. This approach requires a large data storage capacity and high rates of storage. The total information storage capacity of film far exceeds that of any other current imaging technique. For the ALIAS terminal stage

---

[2] Warfare Vision II, Night Vision Program of the U.S. Army Mobility Command, USAERDL, 1964 (CONFIDENTIAL), and discussions with ERDL research personnel.

sequence which we presently consider most desirable, the rate of information gathering capability during the picture taking sequence may exceed 5×10^{10} bits-per-second, of which the actual target image information would average about 5×10^{6} bits-per-second.3/ Substitution of TV sensors would result in total capacity of 10^{8} bits/second of which roughly 6×10^{5} would contain target information.4/ The TV estimate is based on accepting reduced resolution and reducing the field-of-view, and does not consider the losses incurred by readout and data transmission.

3. Sensor System Concept

a. Alternative Approaches. A review of the target intercept problem indicates several alternative approaches to the ALIAS mission:

(1) A co-orbit or velocity-match trajectory could provide for close-up stabilized photography or use of other close-range sensory techniques; however, the ALIAS concept for low-cost light-weight propulsion and guidance systems precludes this sophisticated intercept method.

(2) A minimum velocity orbit-path crossing intercept could allow for a series of photographs to be taken along the orbit path as the target approached. This would eliminate high angular crossing rates, at the expense of high closing velocity with attendant probability of forbidden collision with the target. This concept would require excessively large optics in order to safely provide useful photo coverage, and would further restrict coverage to the direct approaching or departing aspect.

3/ (Assuming full-frame 35mm film, 100 frames-per-second, and grey scale density resolution of 32 steps).

4/ (Assuming 500 line pairs resolution, 100 frames-per-second, and grey-scale density resolution of 15 steps).

(3) A direct (or small miss-distance) intercept increases the probability of a forbidden collision; and in addition, poses problems because of the extremely high target closing and crossing rates. Although the use of high gain image intensifiers could provide for extremely short exposure times; the problem of tracking with a small field-of-view at extreme angular rates, coupled with the probability of collision, has discouraged further investigation of this concept at this time.

(4) A low missile velocity crossing intercept, deliberately biased for an offset distance well within missile CEP, should provide intercept vectors within reasonable photographic ranges and within practical angular tracking rates. This is the concept which we have analyzed as having the greatest potential for a feasible system using existing hardware techniques.

b. Selected Sensor Concept. We have selected an offset crossing intercept at low missile velocity as the most practical concept to meet the ALIAS objectives. By selection of appropriate state-of-the-art optical and tracking parameters, we find that excellent photo coverage should be possible at reasonable ranges that fall within the limits of practical angular tracking rates. We estimate that photographic resolution of two-inches or better can be obtained within a sector of about 75 to 45 degrees to the position of the intercept vector at closest approach. Continuous photographic coverage would be programmed for about 1.8 seconds each, on the approaching and departing sectors. Photographic ranges would vary between the limits of about 8 n.m. to 1 n.m. at line-of-sight rates of less than 2 radian-per-second. The analysis has centered on photographic design parameters for providing adequate field-of-view, a means of centering the target at high angular crossing rates, short exposure times for reducing effects of image motion, and angular resolution capability.

(1) Field-of-View. Inasmuch as target tracking must be quite precise in order to provide adequate image motion compensation, a field-of-view of roughly 6 degrees is considered sufficient for initial target acquisition by the tracker subsystem, which will use a negative field lens to encompass 6 degrees across the vidicon face. A 2 degree photographic field will be used during the picture-taking sequence to provide for full photographic framing of the target at minimum photographic range. Full-frame 35 mm film (24 x 36 mm) has been

large moment-of-inertia of the payload, and the complexity of a dual-control system is expected to negate any advantages of this approach.

TRACKING MIRROR CONCEPTS

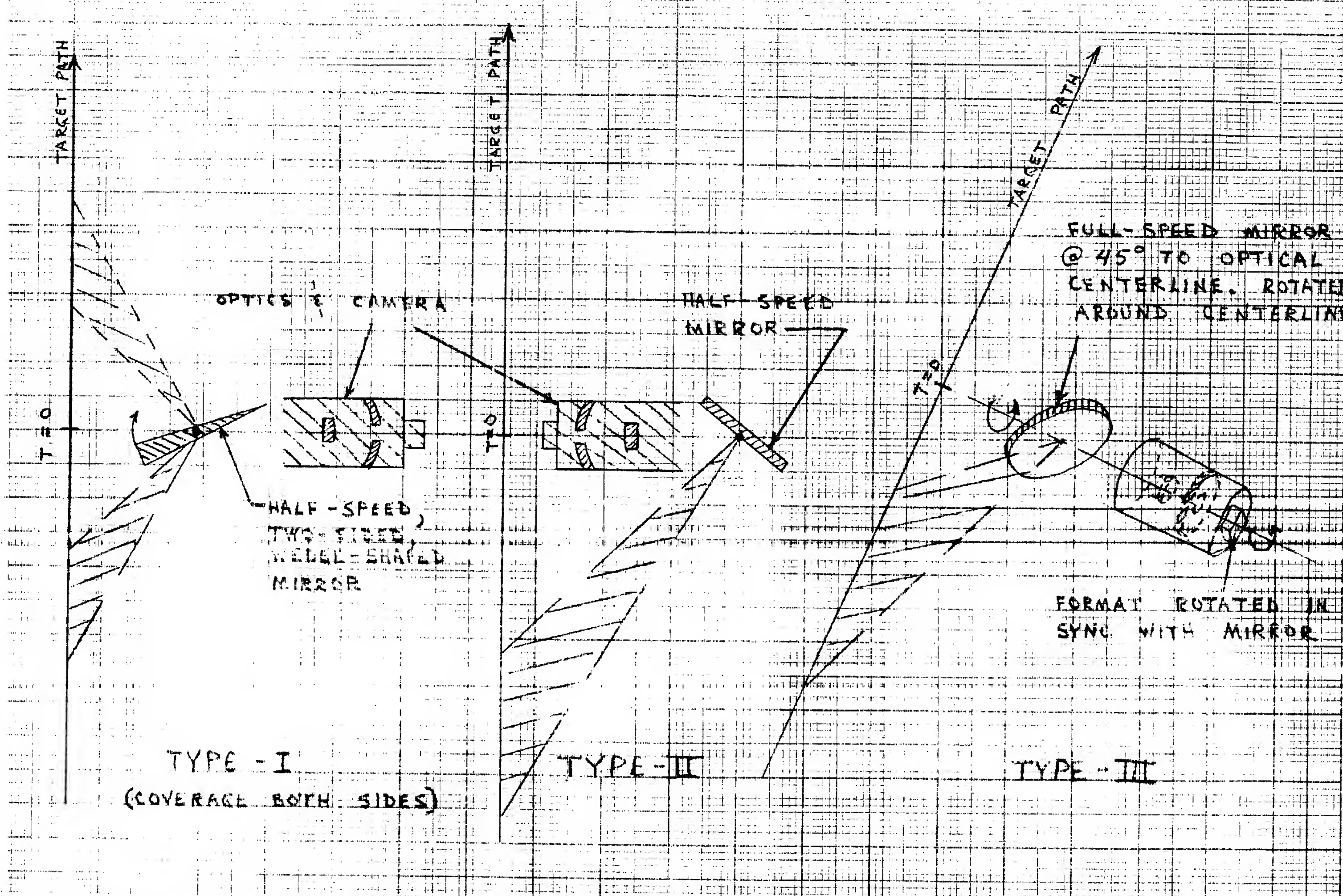

FIGURE C-1

The second method would have a similar mirror rotation, but with the entire camera reversed so that mirror size could be less than 1.4 times the lens diameter. This concept would require rotation of the ALIAS vehicle for optimum operation on the approaching sector. Angular rotation at half the line-of-sight rate would be utilized, but the system as now conceived could not be mechanized for both approach and departure coverage.

The third method would rotate the mirror around the optical centerline. Mounting would be somewhat simplified and mirror size would be 1.4 times the lens diameter. This technique requires mirror rotation at the same angular rate as the line-of-sight. The system probably could not be mechanized for both approach and departure coverage. This system also results in rotation of the image around the optical centerline, necessitating use of either a fairly large dove prism (derotation prism) or synchronized rotation of the film format and tracking detector assembly.

If a small primary aperture is eventually selected, the first mirror system appears most desirable. If large optics are found to be necessary, one of the latter two techniques may be more desirable.

(3) Image Motion - The most significant photographic system tradeoffs are concerned with compromises between the resolution effects of distance from target versus angular motion limitations. The missile CEP at closest approach determines the acceptable offset trajectory bias. The probable trajectory offset distances are then assessed for limitations on optical angular tracking rates. For a missile crossing velocity of 3000 fps and various offset distances the angular target movement rates as a function of time from closest approach are shown in Figure C-2.

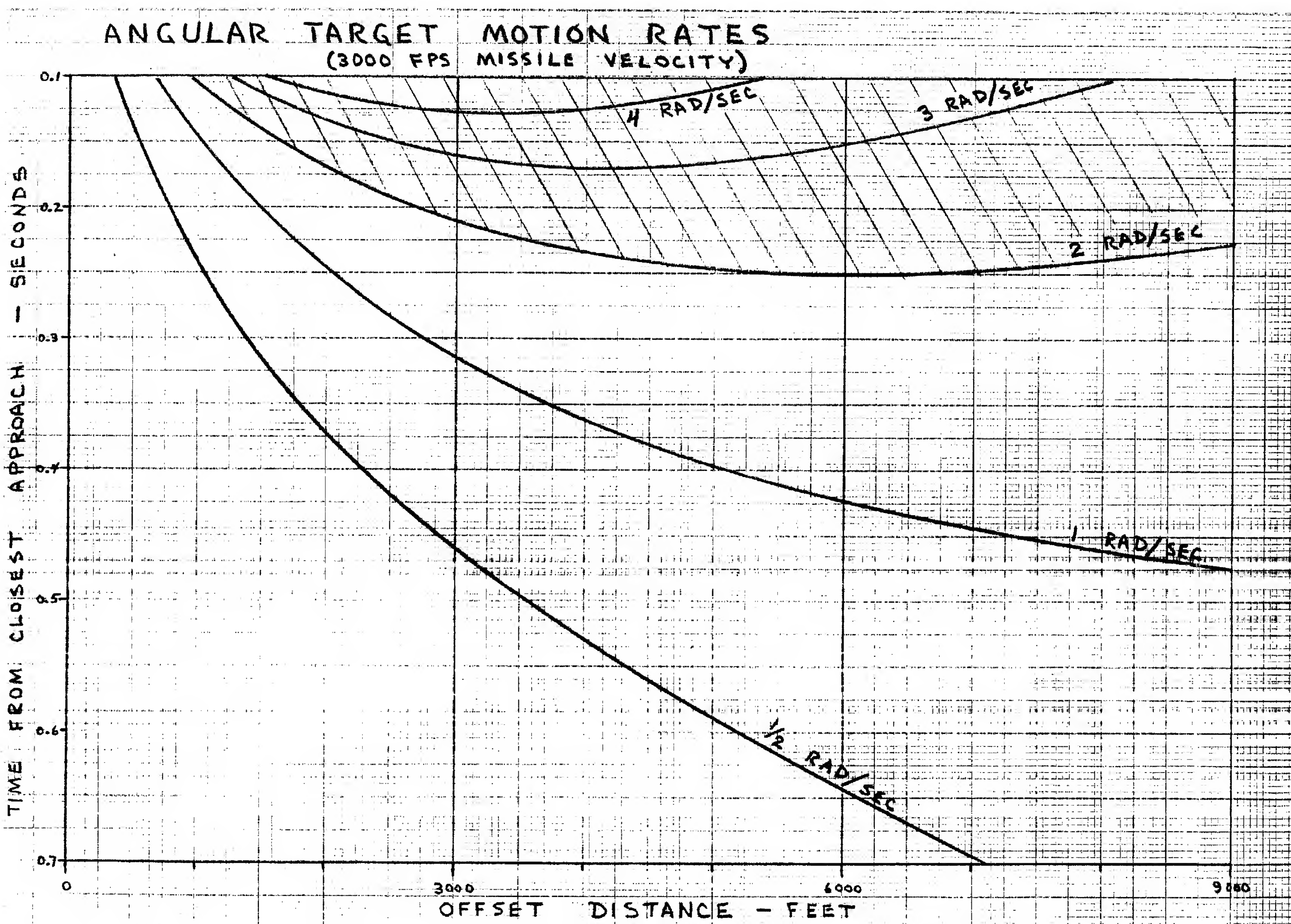

FIGURE C-2

SECRET LIMITED DISTRIBUTION

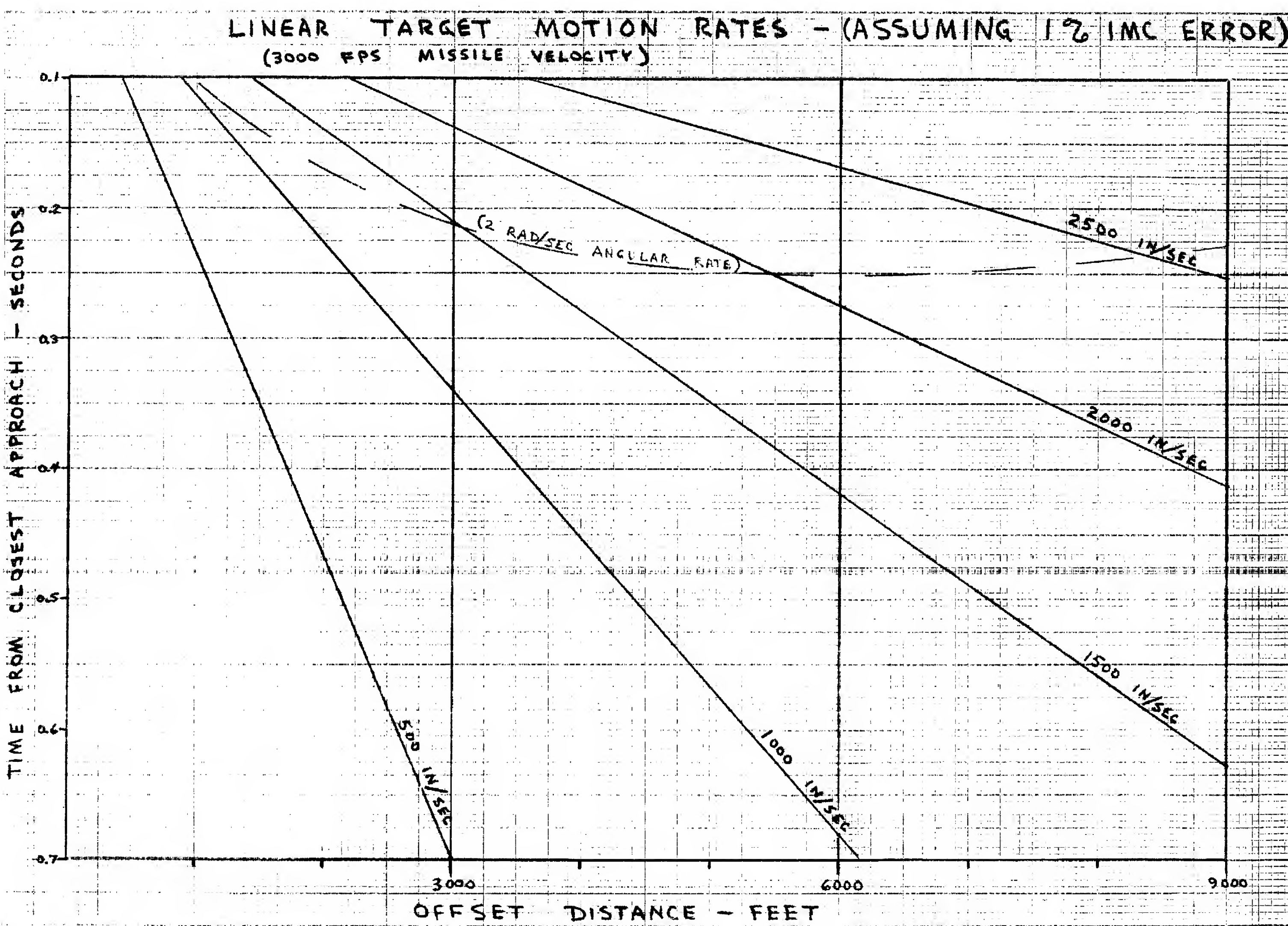

LINEAR TARGET MOTION RATES - (ASSUMING 1% IMC ERROR)
(3000 FPS MISSILE VELOCITY)
TIME FROM CLOSEST APPROACH - SECONDS
0.1
0.2
0.3
0.4
0.5
0.6
0.7
(2 RAD/SEC ANGULAR RATE)
2500 IN/SEC
2000 IN/SEC
1500 IN/SEC
1000 IN/SEC
500 IN/SEC
3000
6000
9000
OFFSET DISTANCE - FEET

FIGURE C-3

From a component design standpoint we consider 2 radians/sec to be the practical maximum tracking rate where line-of-sight angular acceleration can be accurately matched by mirror torquing commands. For purposes of initial selection of camera system parameters we consider that tracking accuracy (image motion compensation) of 1 percent or better is practical for the AIIAS system during the photographic sequence. The 1% image motion compensation (IMC) value is assumed for the initial analyses presented in Figures C-3 through C-11. After initial selection of system angular resolution criteria, the assessment of tracking stability in terms of angular resolution and exposure time is more appropriate. This is discussed for selected system parameters in paragraphs c and d, below. The related rate of target linear motion under these conditions is presented in Figure C-3, as a function of time from closest approach.

With 1% tracking accuracy (Image Motion Compensation), and assuming unlimited tracking rate capability, the shutter speed required to reduce image motion to 1/2 inch (approx. 1 inch resolution) would be about 1/6200 second at time of closest approach. At 3000 ft offset this would represent an angular rate of 8.6 radians/second which also represents an angular acceleration of over 36 radians/sec/sec; a figure perhaps beyond the limitations of 1% rate accuracy mechanical tracking loops. From the standpoint of image motion only, the maximum number of high resolution photographs will be obtained if the missile offset (and CEP) is kept small, and photography is accomplished at those larger look angles where the angular tracking rates are below 2 radians/second.

A logical compromise of missile CEP, reasonable photographic range, acceptable range of look angles, and target tracking parameters; would

ANGULAR RESOLUTION REQUIRED TO RESOLVE ONE-INCH

(DISCOUNTING IMAGE MOTION)

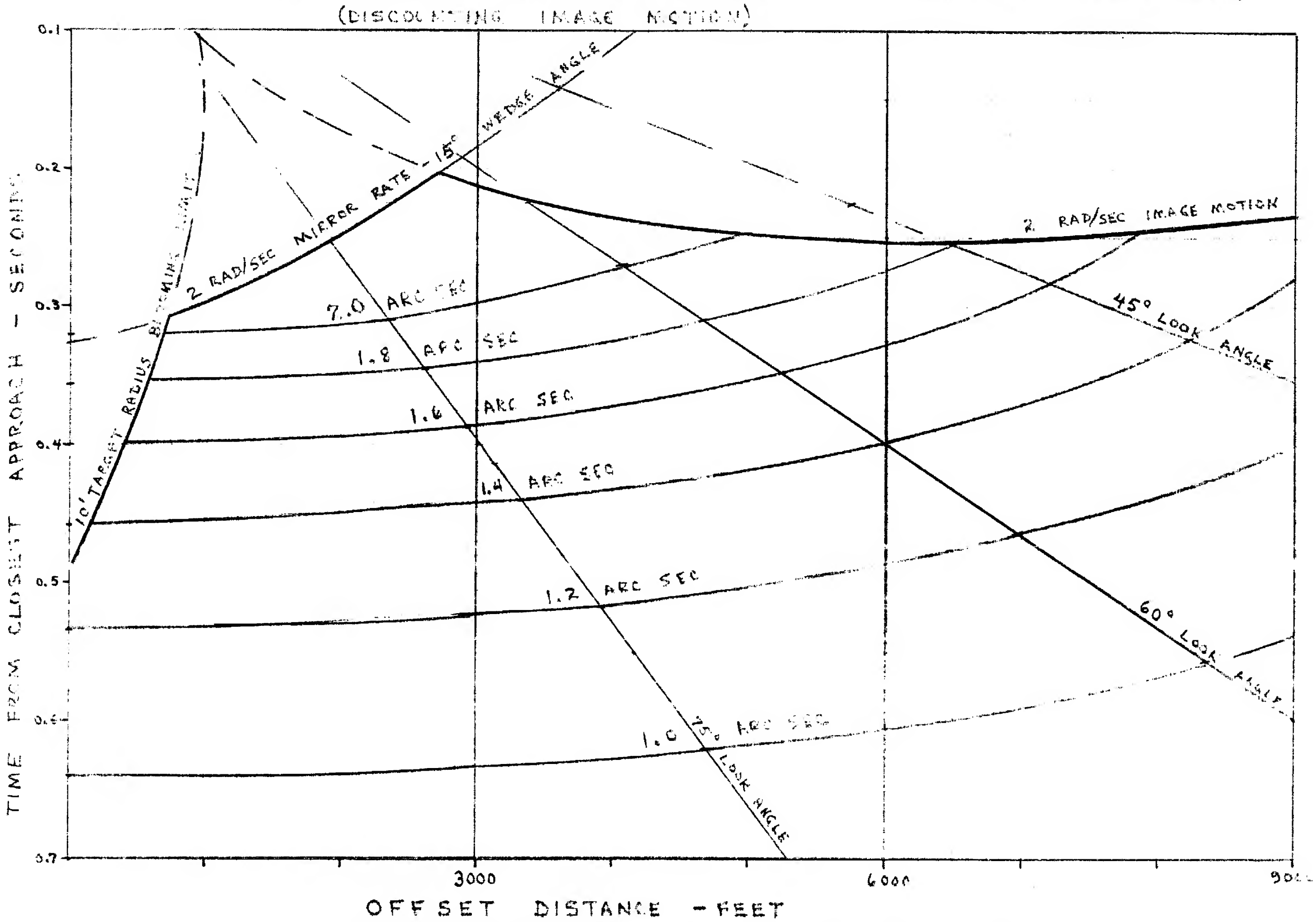

FIGURE C-4

ANGULAR RESOLUTION AS A FUNCTION OF FOCAL LENGTH AND FILM RESOLUTION

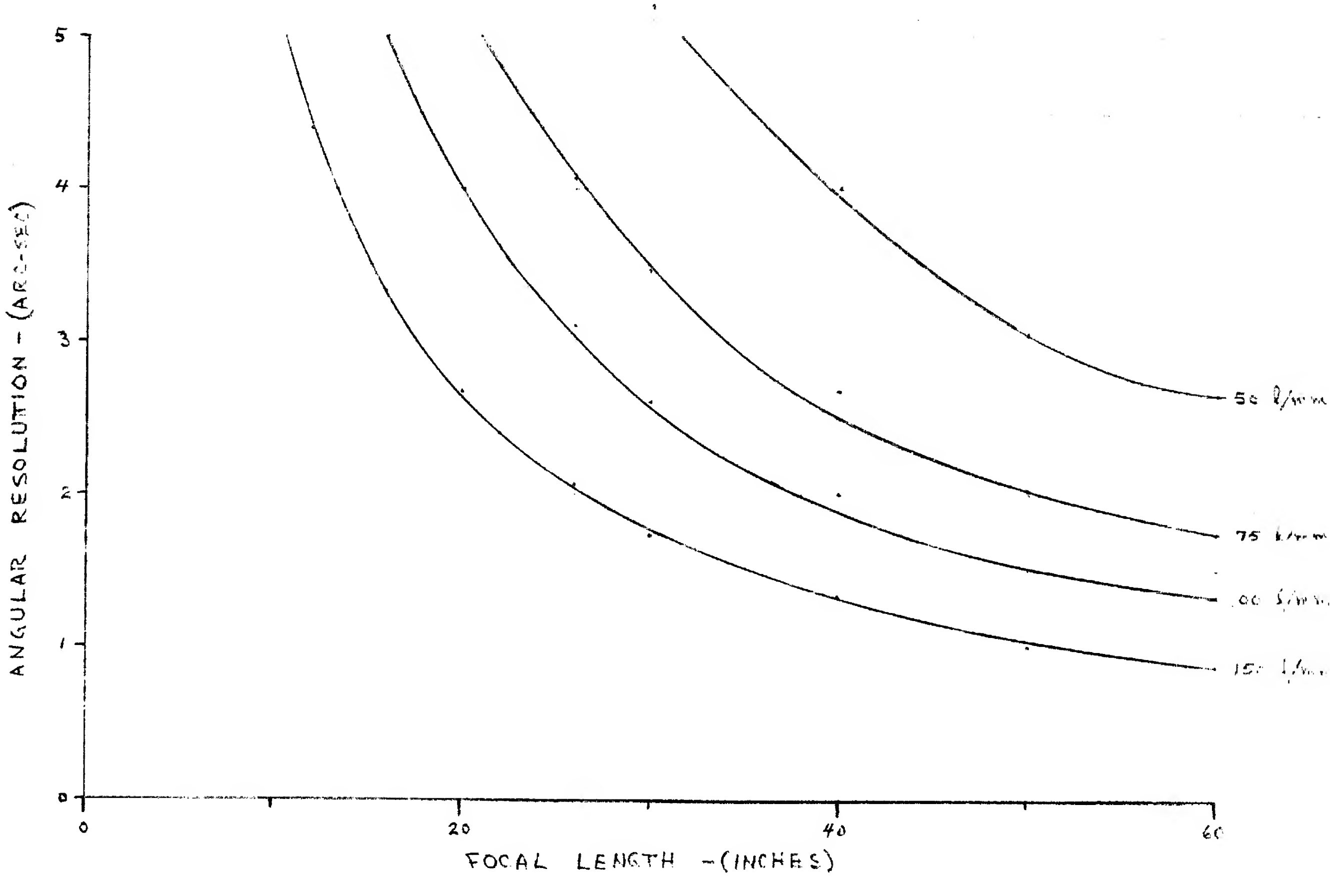

FIGURE C-5

SECRET LIMITED DISTRIBUTION

RESOLUTION, FIELD-OF-VIEW, AND DEPTH OF FOCUS

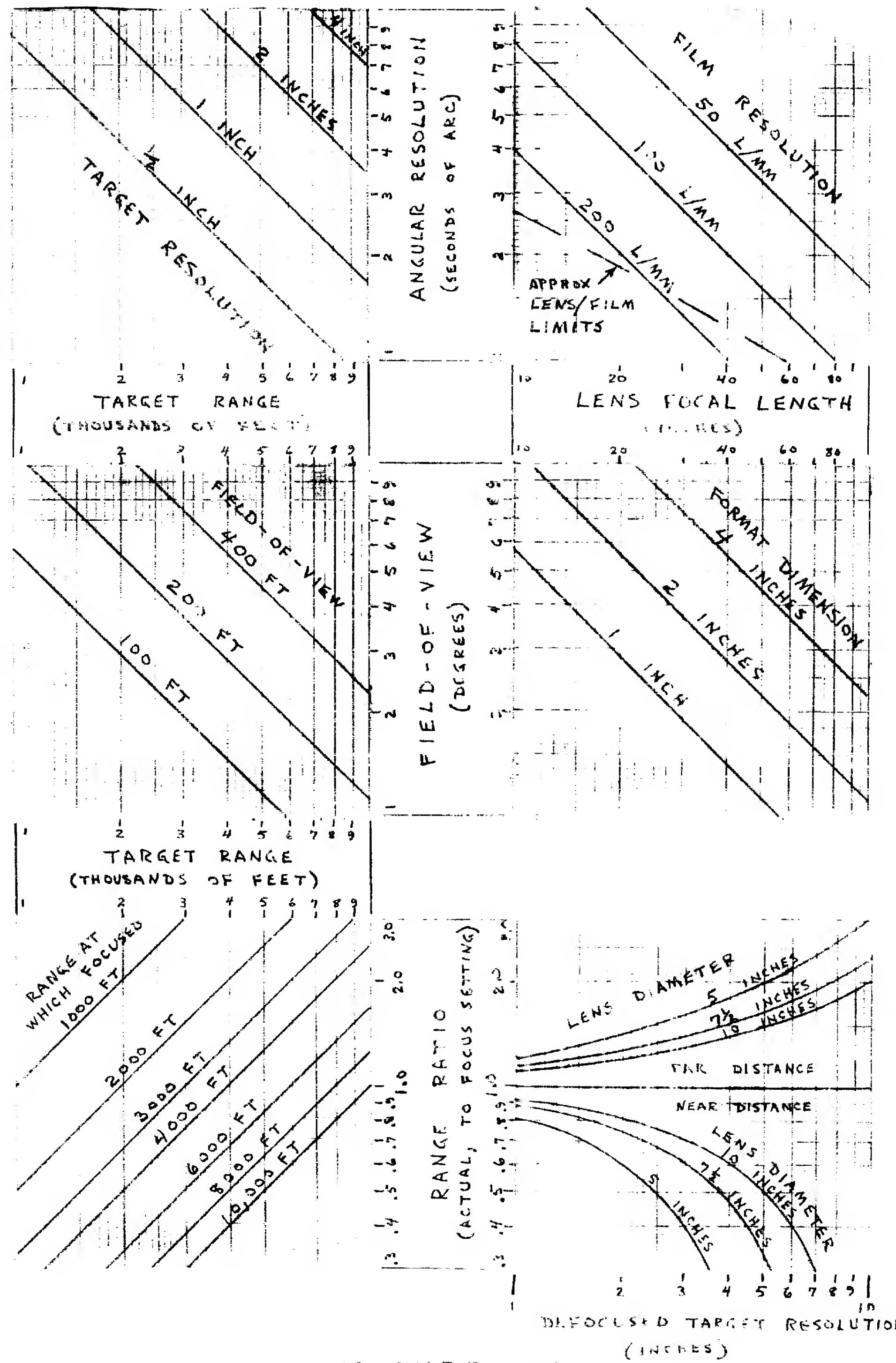

FIGURE C-6

SECRET LIMITED DISTRIBUTION

Approved For Release 2003/12/09 : CIA-RDP75B00157R000100110001-0

LENS FOCAL RATIO [illegible] SHUTTER SPEEDS

FOR INCIDENT ILLUMINANCE AT TARGET OF 13,600 F.C.

SHUTTER SPEEDS FOR MINIMUM RECORDABLE DENSITY
($E_o = 0.45\ E_m$)

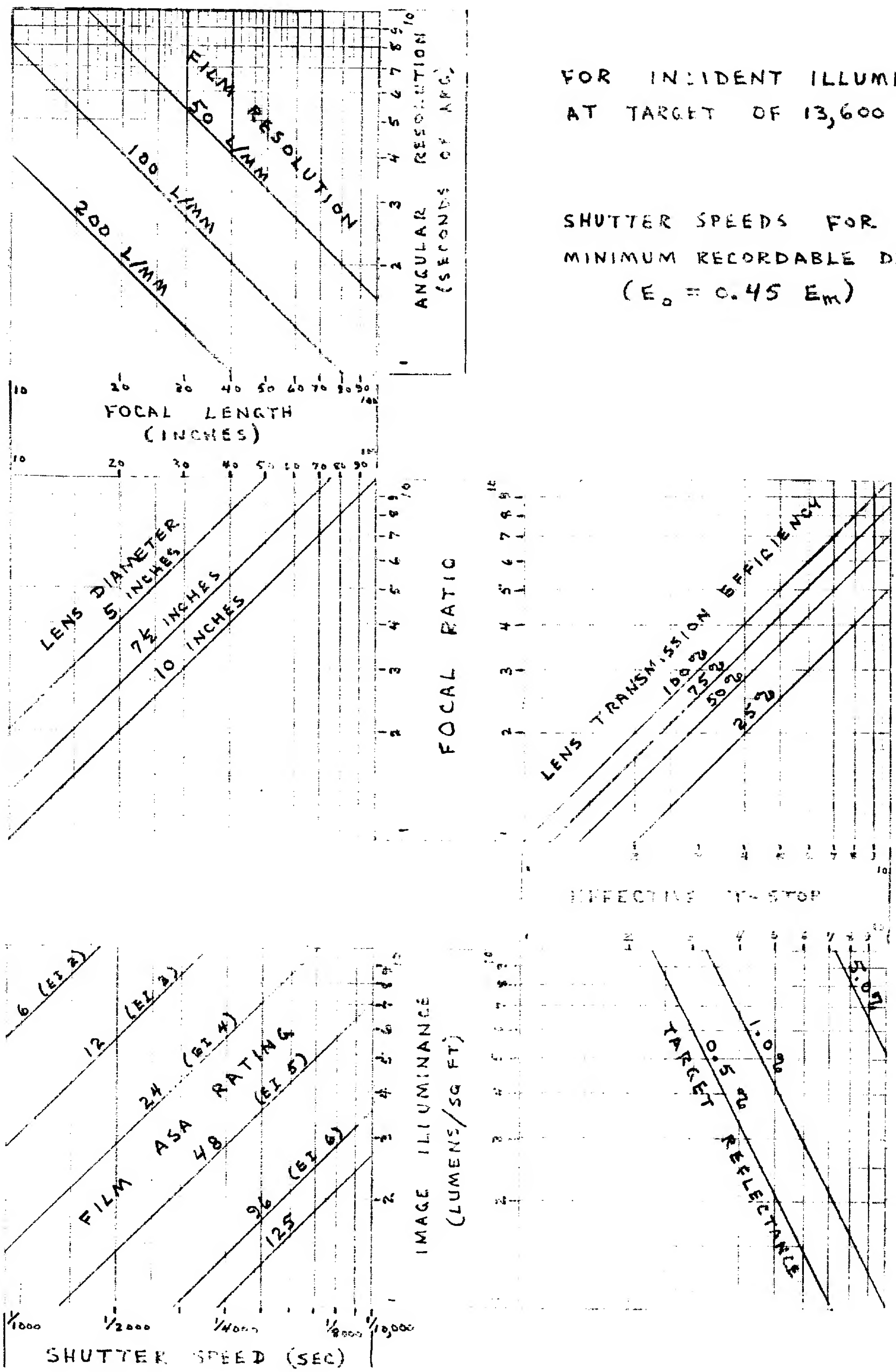

FIGURE C-7

IMAGE MOTION EFFECTS

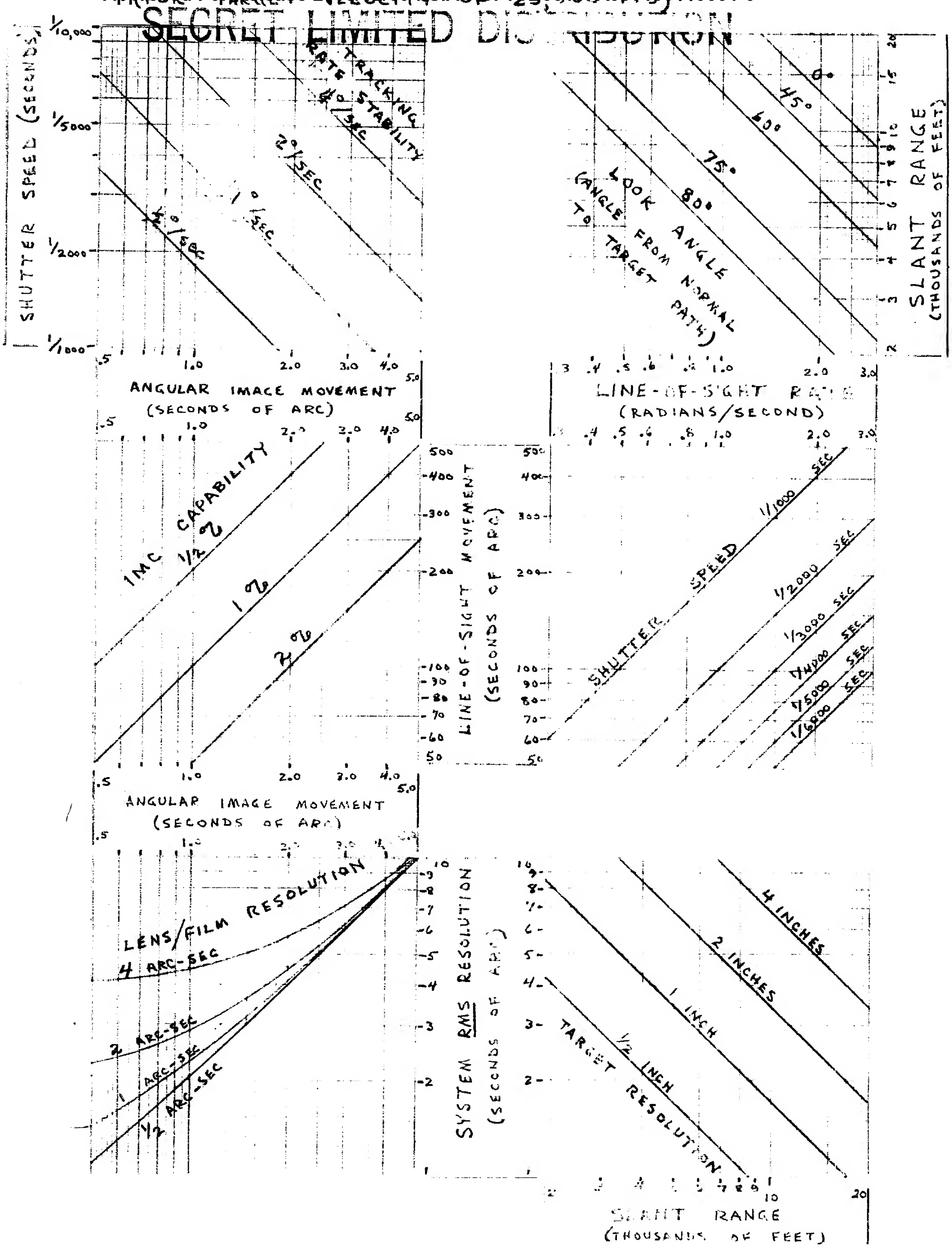

FIGURE C-8

SUMMARY OF APPROXIMATE LENS/FILM RESOLUTION LIMITS
(MINIMUM RECORDABLE DENSITY BASED ON 0.5% TARGET REFLECTANCE)

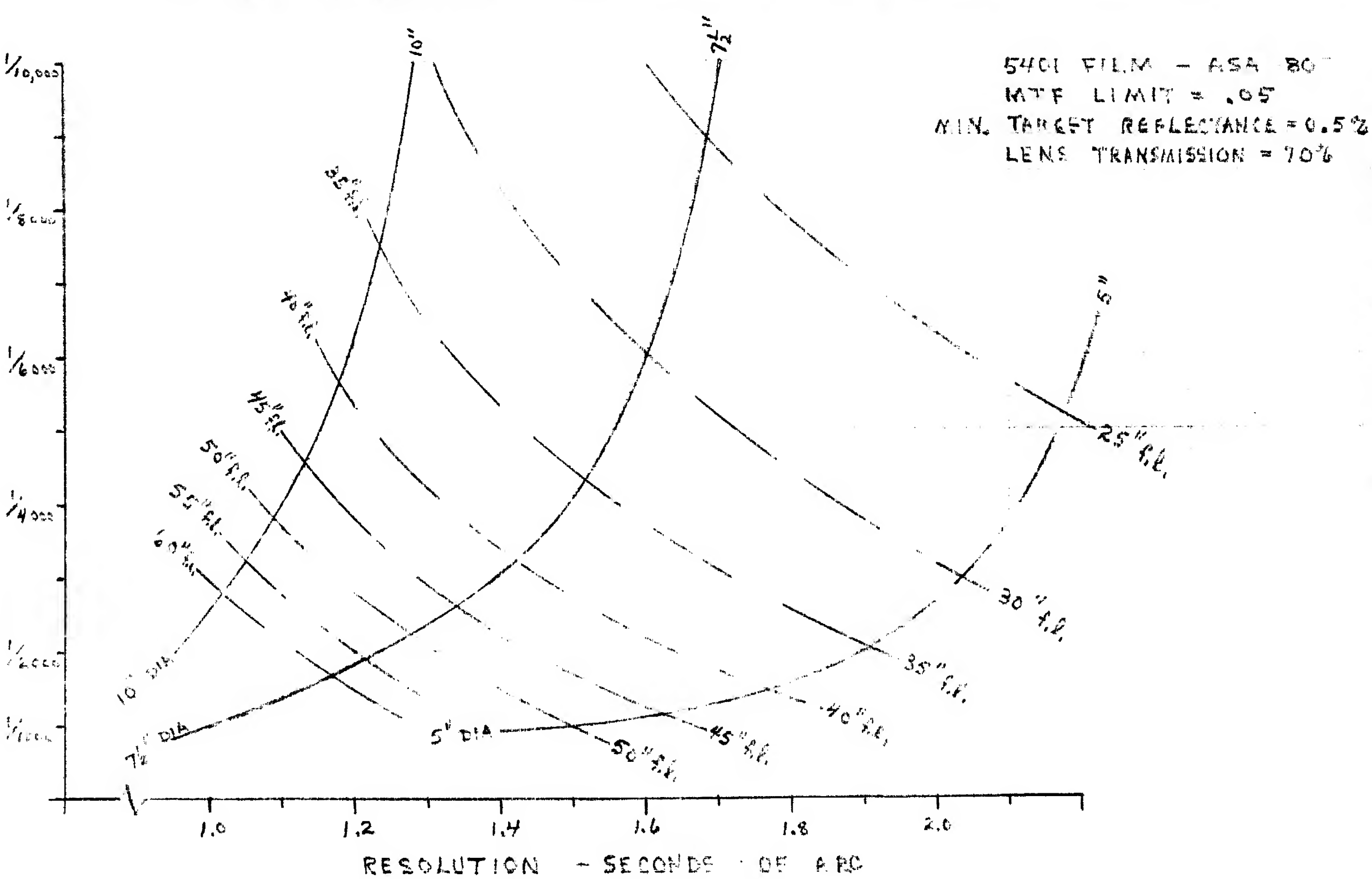

FIGURE C-9

PRELIMINARY SELECTION OF CAMERA SYSTEM PARAMETERS
1% IMC ERROR — TYPE 5401 FILM

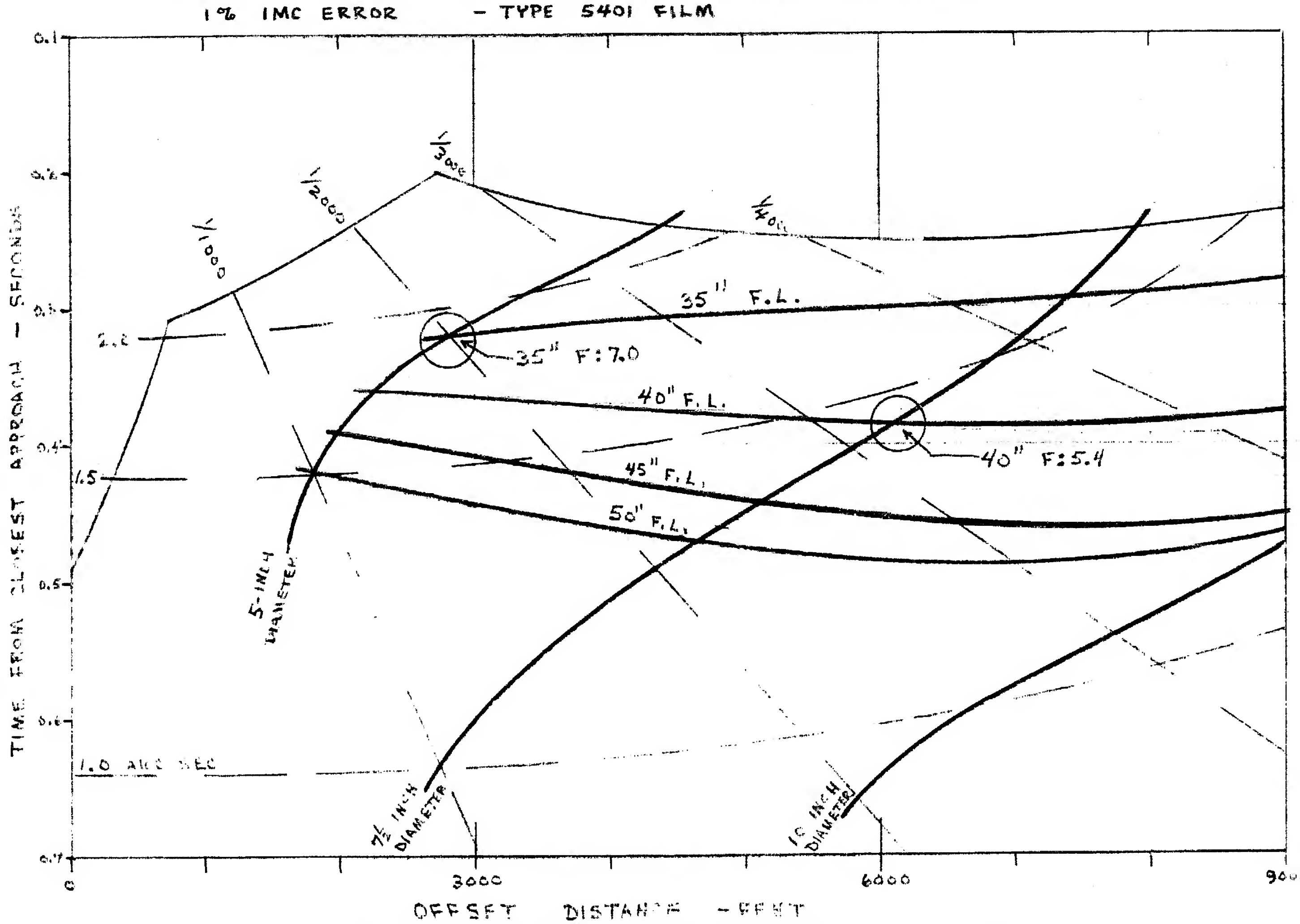

FIGURE C-10

Estimated performance limits of a system, selected qualitatively as being near optimum for the various tradeoffs considered, is presented in Figure C-11. For this summary chart system performance limits are considered to be the root-mean-square (RMS) values of the combined resolution factors. A system meeting these general requirements would have approximately the following characteristics:

Lens Diameter	- $8\frac{1}{2}$ inches
Focal Length	- 40 inches
Shutter Speed	- 1/4000 second
Film Type	- 5401
Format	- 1 x 1, to $1\frac{1}{2}$ x 2 inches
Frame Rate	- 50-100 FPS
Tracking Mirror	- Approx. $8\frac{1}{2}$ x 17 inches
	- Wedge Angle - Approx. 15 degrees
	- (Type 1, mounted in front of lens)
Trajectory Offset	- 3000 ft (1500 ft CEP)
Resolution	- 20 to 60 frames 1 inch or better
	- 60 to 140 frames 2 inches or better
	- 100 to 350 frames 4 inches or better

A more "Austere" system of perhaps 6 inches diameter and 33 inch focal length, with mirror size of 12 inches, and shutter speed of 1/3000 second, would provide about 75% as good resolution (i.e. minimum dimension larger by a factor of 1.33 than those quoted above, all other factors being equal).

ESTIMATED SYSTEM PERFORMANCE LIMITS

1.4 ARC SECONDS ANGULAR RESOLUTION
1% IMC ERROR
1/4000 SECOND SHUTTER SPEED

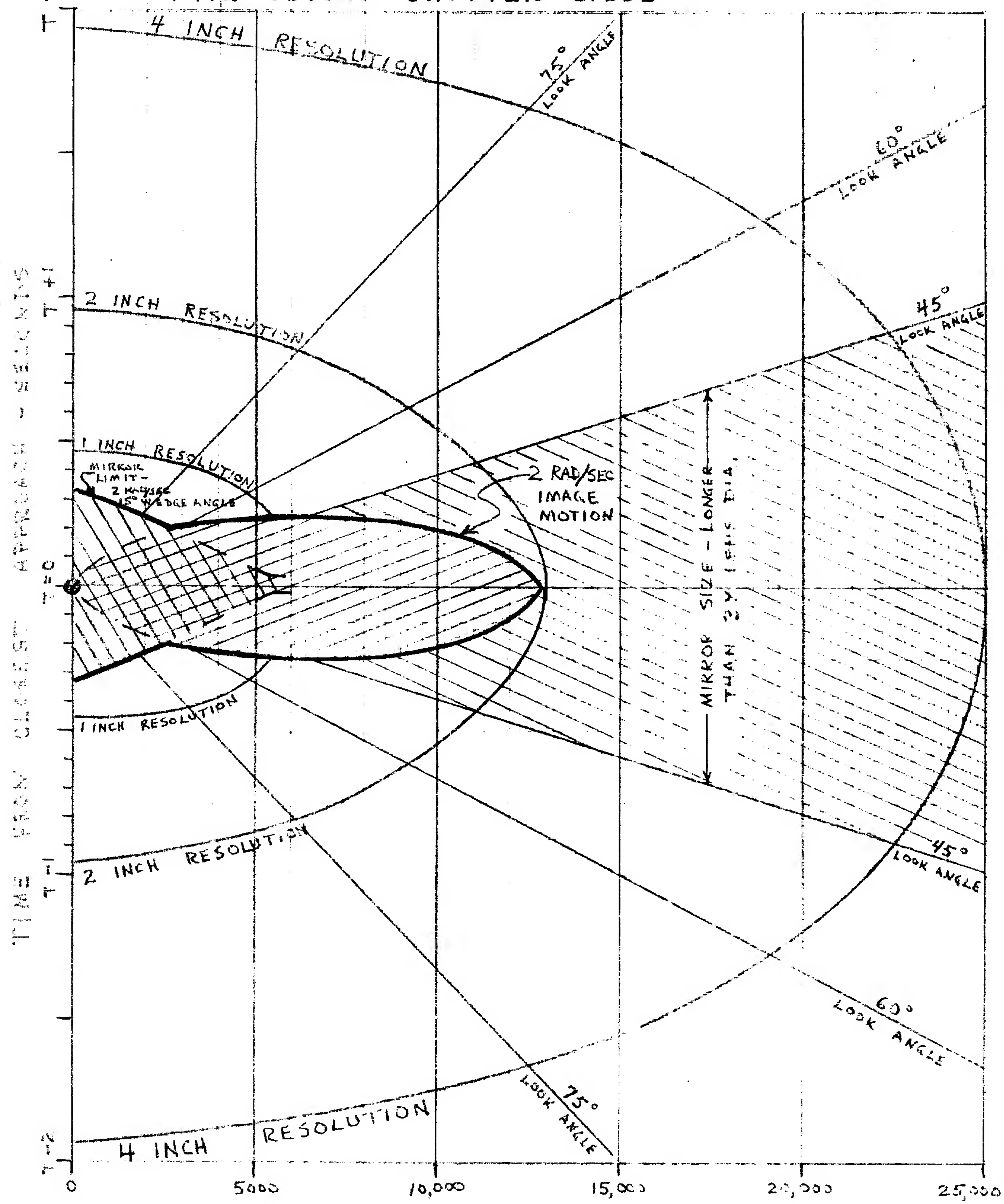

FIGURE C-11

4. Parametric Analysis - In order to quickly establish performance criteria by which system feasibility could be assessed, a detailed analysis of geometric optical parameters was made for the general case of limiting resolving power. Similarly, the general case of limiting exposure was assessed for exposure time limits of various photographic films at various target luminance values. The effects of (random) image motion on resolving power were also solved for the general case, to provide correlation of film sensitivity (shutter speed-vs-image illuminance) with resolving power. These factors are discussed in paragraphs a, b, and c, below, and illustrated in Figures C-12 through C-28.

The information content of target imagery is a complex combination of film density differences across varying spatial regions. Treated in a method analogous to a noisy communications channel, the information content for various spatial frequencies can be expressed in terms of Modulation Transfer Functions (MTF) equivalent to communications system bandwidth response. In order to provide a more meaningful assessment of ALIAS system information gathering capability, analyses of the Modulation Transfer Functions for various sensor elements has also been made for the general case of state-of-the-art lenses and films. These factors are carried to the limiting case of minimum practical detectability for application to the ALIAS system feasibility study. These factors are discussed in paragraph d, below, and illustrated in Figures C-29 through C-43.

The specific restrictions of the ALIAS mission are further correlated and specific ALIAS performance factors assessed in Figures C-44 through C-50.

A summary of terms used in deriving the parametric relationships is presented in Table C-1.

a. Resolving Power and Field of View - The angular resolution (θ) required at range (R_t) to resolve a given dimension (x_t) at the target is:

$$\theta = \tan^{-1} \frac{x_t}{R_t}$$

or for small angles: $\theta_{(arc\text{-}sec)} = \frac{(2.06)\ (10^5)\ x_{(ft)}}{R_{(ft)}}$ Figure C-12

The film resolution (r) in line pairs/mm required to resolve the angle (θ) at the focal plane, with lens focal length (f) is:

$$\theta = \tan^{-1} \frac{x_i}{f} = \tan^{-1} \frac{1}{rf}$$

or for small angles: $r = \frac{(2.06)\ (10^5)}{25.4\ \theta f} = \frac{(8.13)\ (10^4)}{\theta_{(arc\ sec)} f_{(in)}}$ Figure C-13

The threshold of film resolution is dependent upon the contrast (luminance ratio) of the image, (i.e. density difference between the resolution element and the background). As a rule-of-thumb the resolution limit at reduced contrast can be expressed approximately in terms of the percent of maximum resolution (high contrast) as a function of the reciprocal of luminance ratio for any resolution element. This approximate function is shown in Figure C-14, together with an empirical plot of a typical film emulsion. The nominal resolving power of various current aerial films are also listed in Figure C-14 for comparative purposes. Much of the detail of the ALIAS target is expected to be of relatively high contrast due to the anisotropic nature of the illumination from the sun; (reflected light from the earth, the atmosphere, and other surfaces of the target will normally constitute less than 10% of the total illumination).

The lens focal length required for a given target resolution at any given range can be found from the charts discussed above. The field-of-view (2ϕ) of a lens of focal length (f) with film format dimension (Y') is:

$$2\phi = 2 \tan^{-1} \frac{Y'}{2f}$$ Figure C-15

where:

2ϕ = Field-of-view (degrees)

Y' = linear dimension of format (inches)

f = focal length (inches)

TABLE C-1

SUMMARY OF TERMS USED IN DERIVING PHOTOGRAPHIC PARAMETERS

θ = Angular Resolution (seconds of arc)

x = Dimension of Resolution Element at Target (inches, normal to line-of-sight

r = Resolution (line pairs/mm at focal plane)

R_t = Range from Camera to Target (feet)

f = Focal Length (inches)

d = Lens Diameter (inches)

F = Lens Focal Ratio

ϕ = Lens half-angle (degrees)

y = Dimension of Field-of-View (feet)

y' = Dimension of Format (inches, at focal plane)

Δf = Shift of Back-Focal-Distance (inches, from primary focal point)

e = Error in Accuracy of Positioning Focal Plane (inches)

u = Range at which Focused

P = Ratio of Target Range to Range of Best Focus

x_n Target Linear Resolution (inches, at near distance)

x_f = Target Linear Resolution (inches, at far distance)

I_i = Image Illumination (lumens/sq. ft)

I_t = Illuminance at Target (i.e. solar illuminance of 13,600 foot-lamberts above atmosphere)

TABLE C-1 (Cont'd)

ρ = Reflectance (percent, based on assumption that target will have combination of specular and diffuse reflecting surfaces)

E_m = Film Exposure Level (footcandle-seconds for density of 0.1 above fog)

S = Film Speed (ASA rating for E_m)

T-stop = Effective Focal Aperture (including effects of lens transmission losses and lens occlusion)

μ = Angular Image Motion (during exposure period)

m = Linear Image Motion (during exposure period)

ANGULAR RESOLUTION REQUIREMENTS

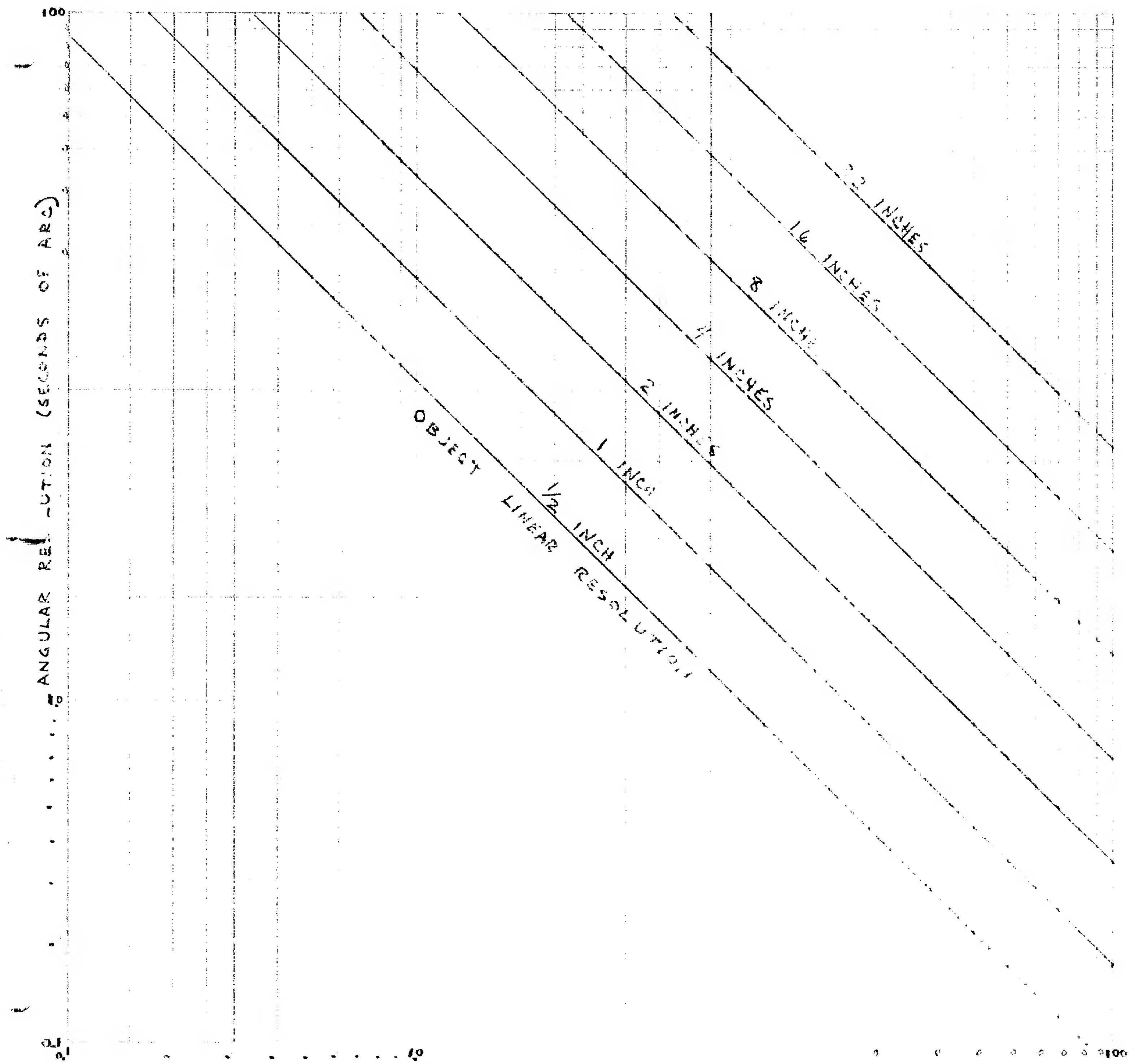

$$\theta = \frac{(2.06)(10^5)\chi}{12 R_t} = \frac{(1.72)(10^4)\chi}{R_t}$$

FIGURE C-12

ANGULAR RESOLUTION CAPABILITY (LENS/FILM COMBINATIONS)

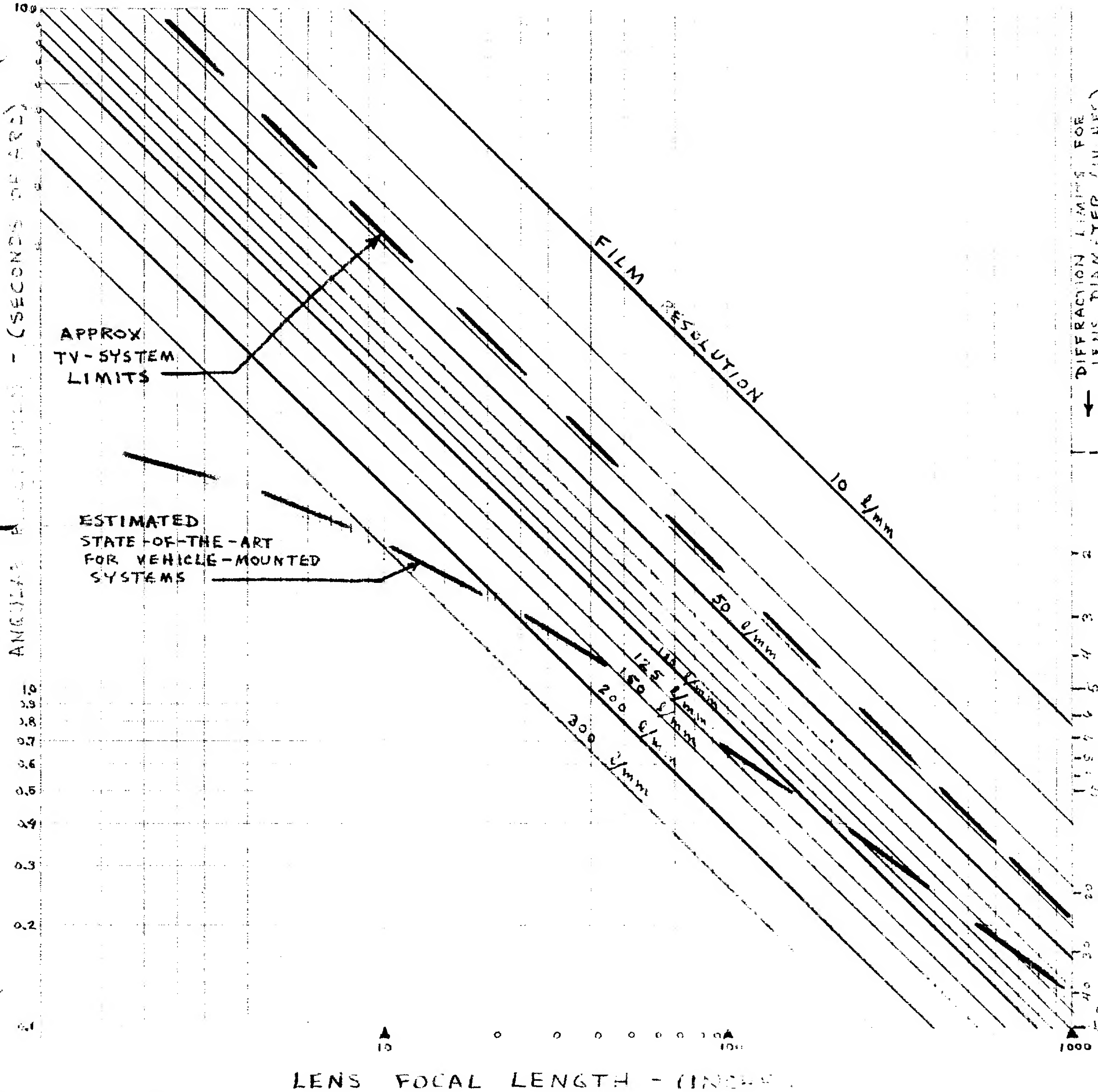

$$r = \frac{(8.13)(10^4)}{\theta f}$$

FIGURE C-13

VARIATION OF FILM RESOLVING POWER WITH CONTRAST

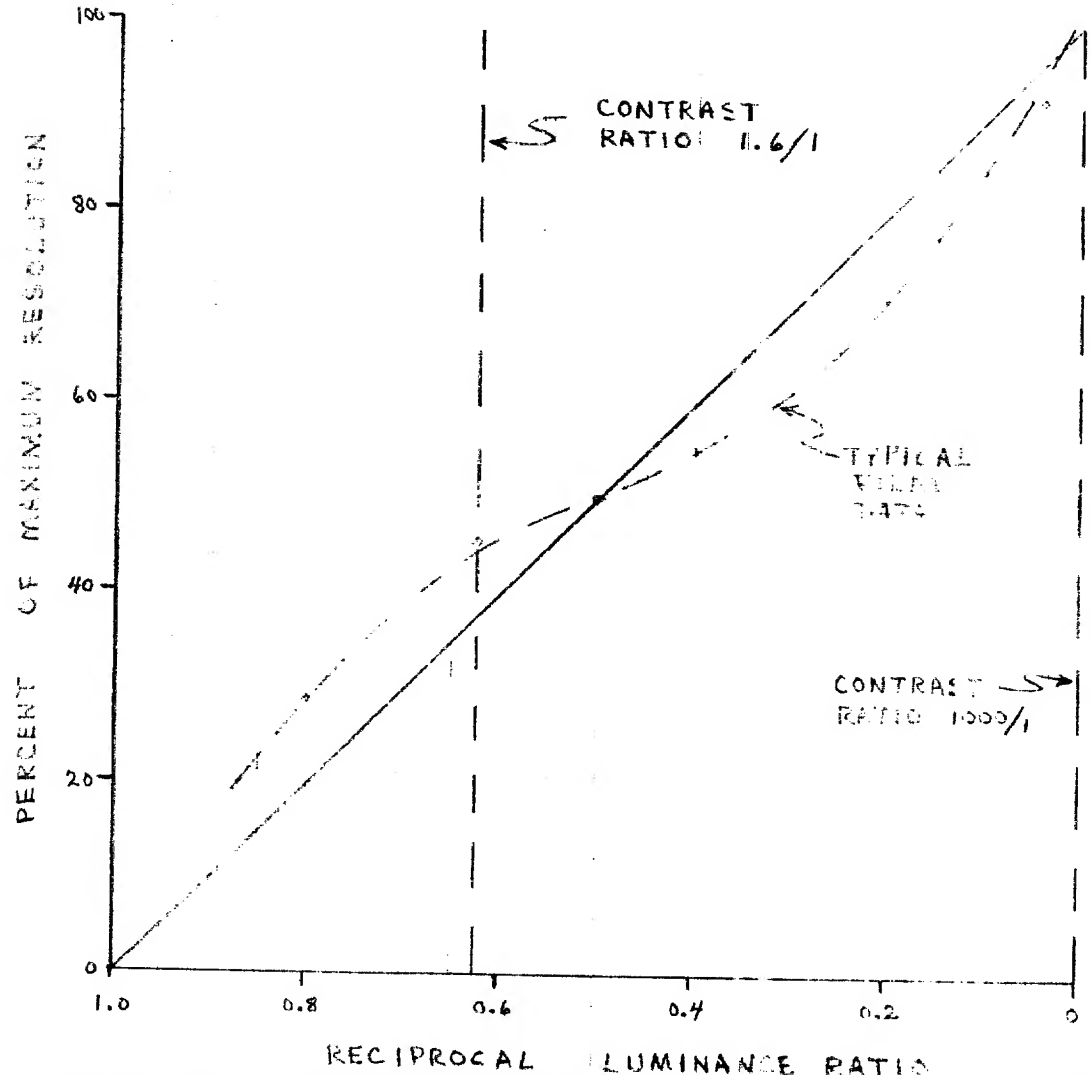

RESOLVING POWER OF TYPICAL FILMS (3-BAR TARGETS)

EXPOSURE INDEX	FILM TYPE	RESOLVING POWER (LINES/MM) CONTRAST 1000/1	CONTRAST 1.6/1
125	2405	85	38
80	5401	115	40
100	5425	75	30
80	8401	112	40
200	8403	71	28
80	2401	112	43
20	3400	170	65
64	3401 - 4401	105	40
1.6	3404 - 4404	475	200
20	SO-136	186	65
6	SO-206	336	112
6	SO-226	336	112
1.6	SO-243	465	205

FIGURE C-14

ANGULAR COVERAGE OF FORMAT

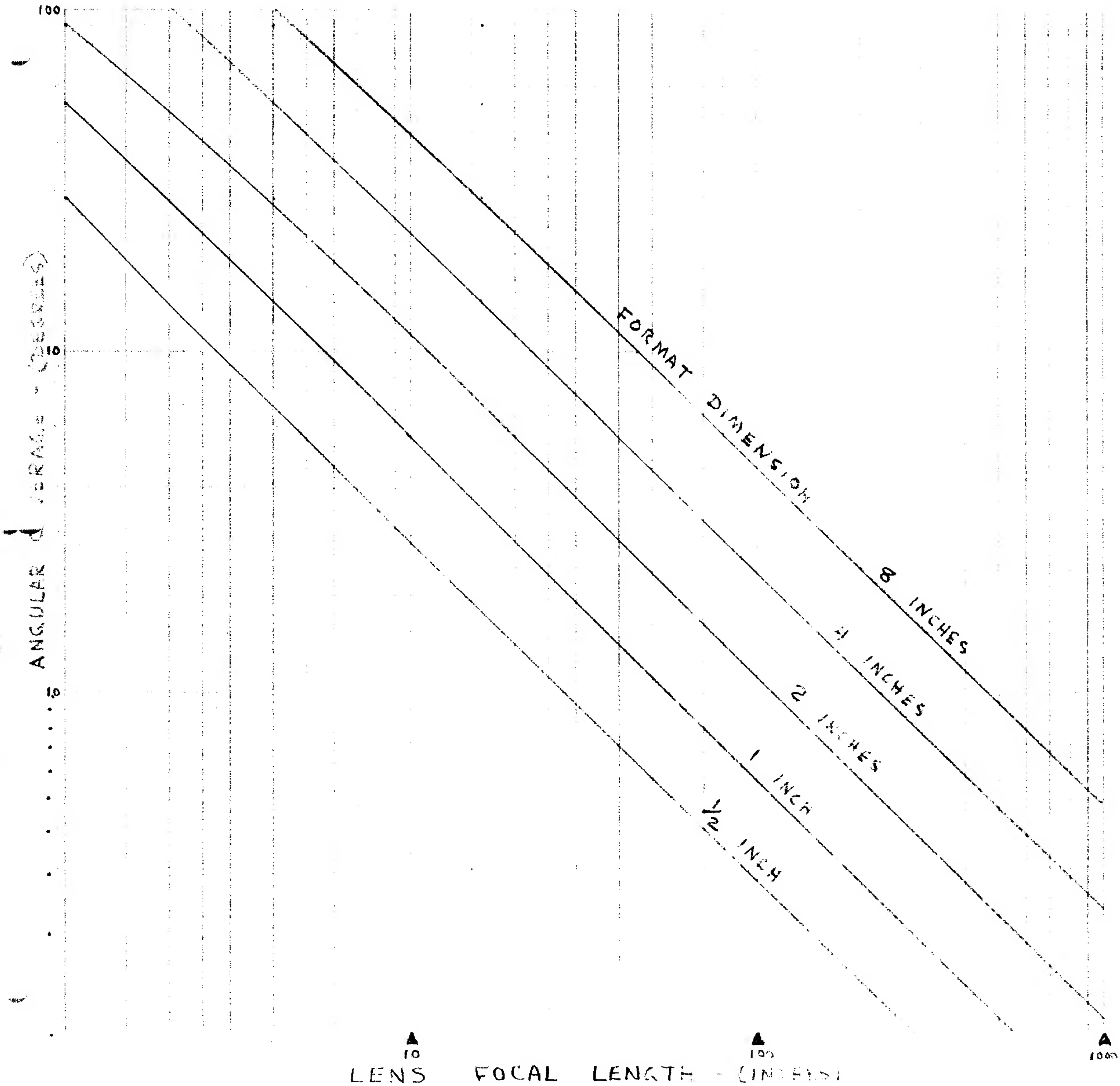

$2\phi = 2 \tan^{-1} \frac{y'}{2f}$

FIGURE C-15

The dimension (Y) of the optical field-of-view (2ϕ) at range (R) is:

$$Y = 2 R_t \tan \phi$$ Figure C-16

where: Y = dimension of field-of-view (feet)

R_t = range (feet)

ϕ = lens half-angle

Photographic line-of-sight ranges for the ALIAS mission will vary from a minimum of about 6000 ft to a maximum of over 50000 ft. To resolve one-inch, an angular resolution of less than one second of arc is desirable, through some usable photographs might be obtained at resolution of 8-10 arc-seconds (including all system degrading effects). With today's film emulsions of high sensitivity a practical limit of roughly 150 l/mm resolution will dictate an optical system approaching 40 inches focal length. A film format of $1\frac{1}{2}$ inches will provide about 2-degrees field-of-view which will encompass 150 feet at the anticipated minimum target photographic range of 6000 ft.

b. Effects of Focus Shift - The purpose of the photographic lens is to gather all the light encompassed within the solid angle (ω_t) of the target pupil for each resolution element of the target, and to focus all such light rays on the image resolution element. The geometry of the limiting ray elements is shown in Figure C-17. At infinite target range the light rays converge at the lens primary focal point (F'). At target range (R_t), with a well-corrected lens, the axial rays from a point on the target will converge at a distance ($f + \Delta f$) from the rear lens nodal point. The required shift (Δf) in position of the focal plane for lens of focal length (f) as a function of target distance (R_t) is approximately:

$$\Delta f_{(in)} = \frac{(6.95)\ (10^{-3})\ f^2\ (in)}{R_{t\,(ft)}}$$ Figure C-18

FIELD-OF-VIEW AT TARGET RANGE

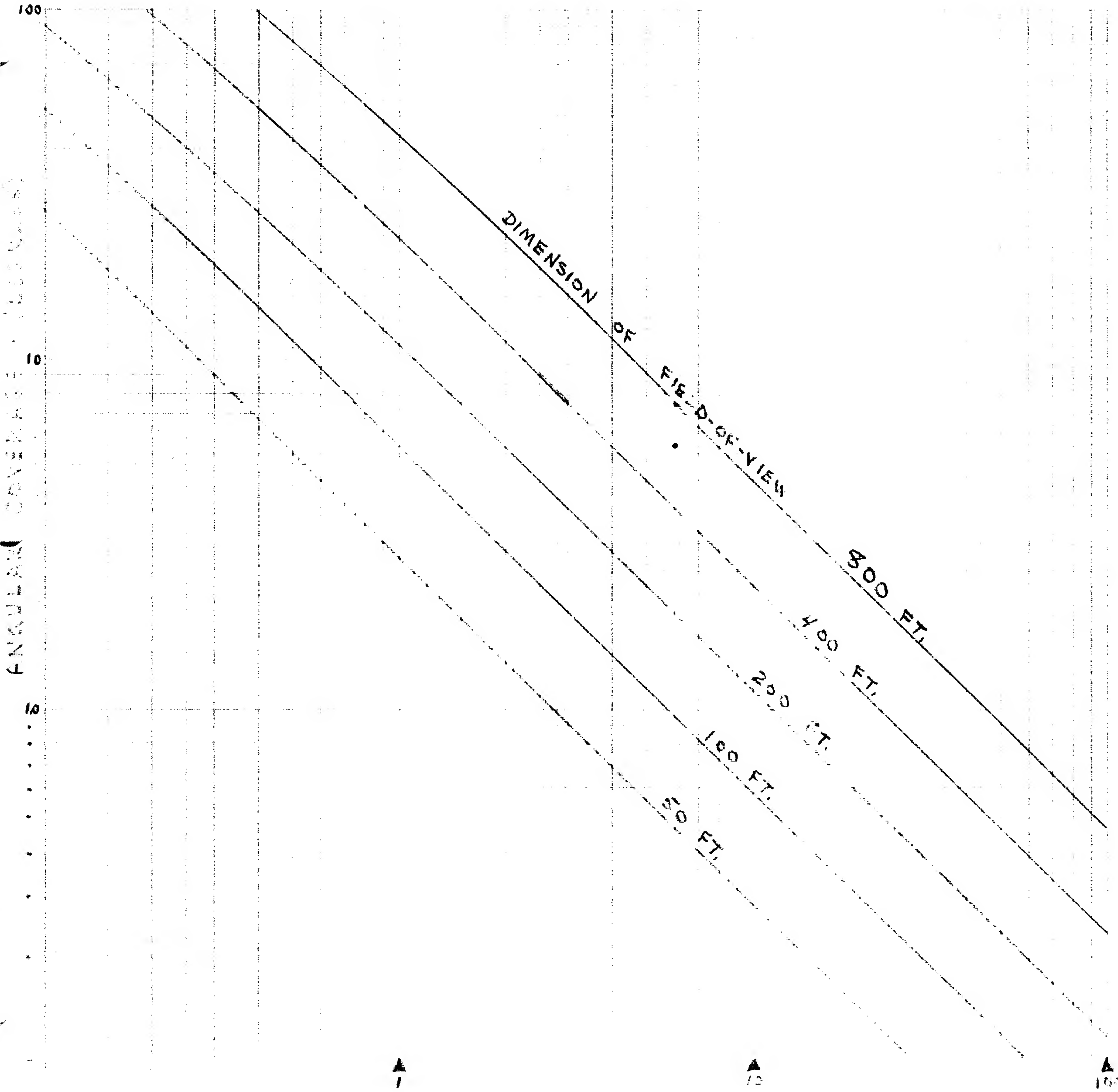

$y = 2 R_t \tan \phi$

FIGURE C-16

EFFECTS OF FOCUS SHIFT

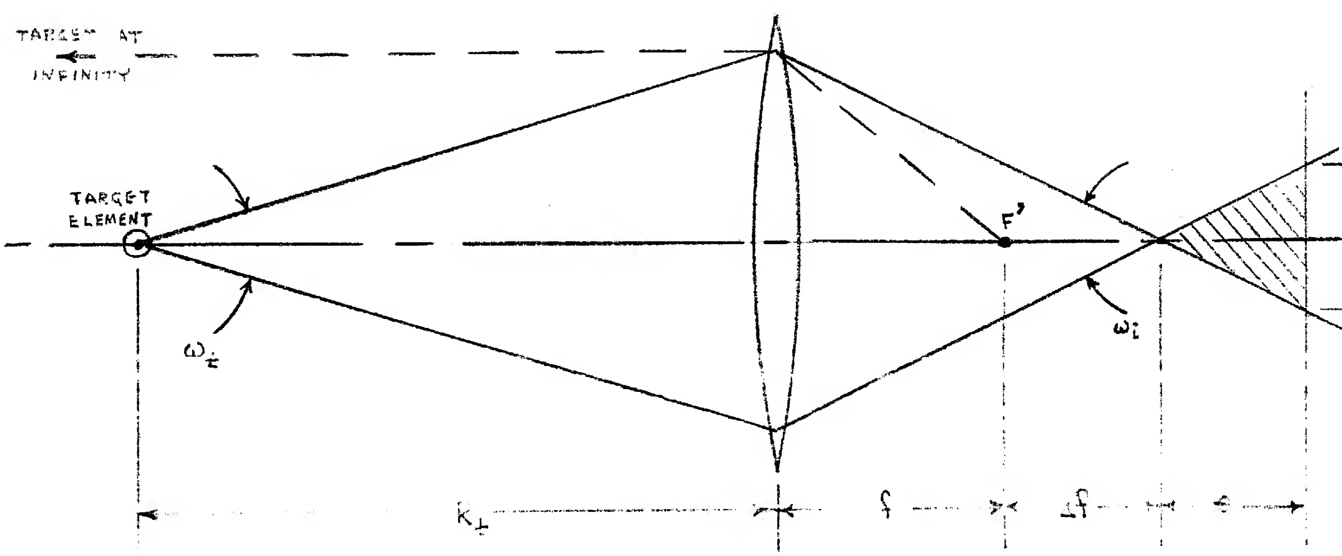

FIGURE C-7

REQUIRED SHIFT OF FOCAL PLANE FROM PLANE OF FOCUS WITH TARGET RANGE AT INFINITY

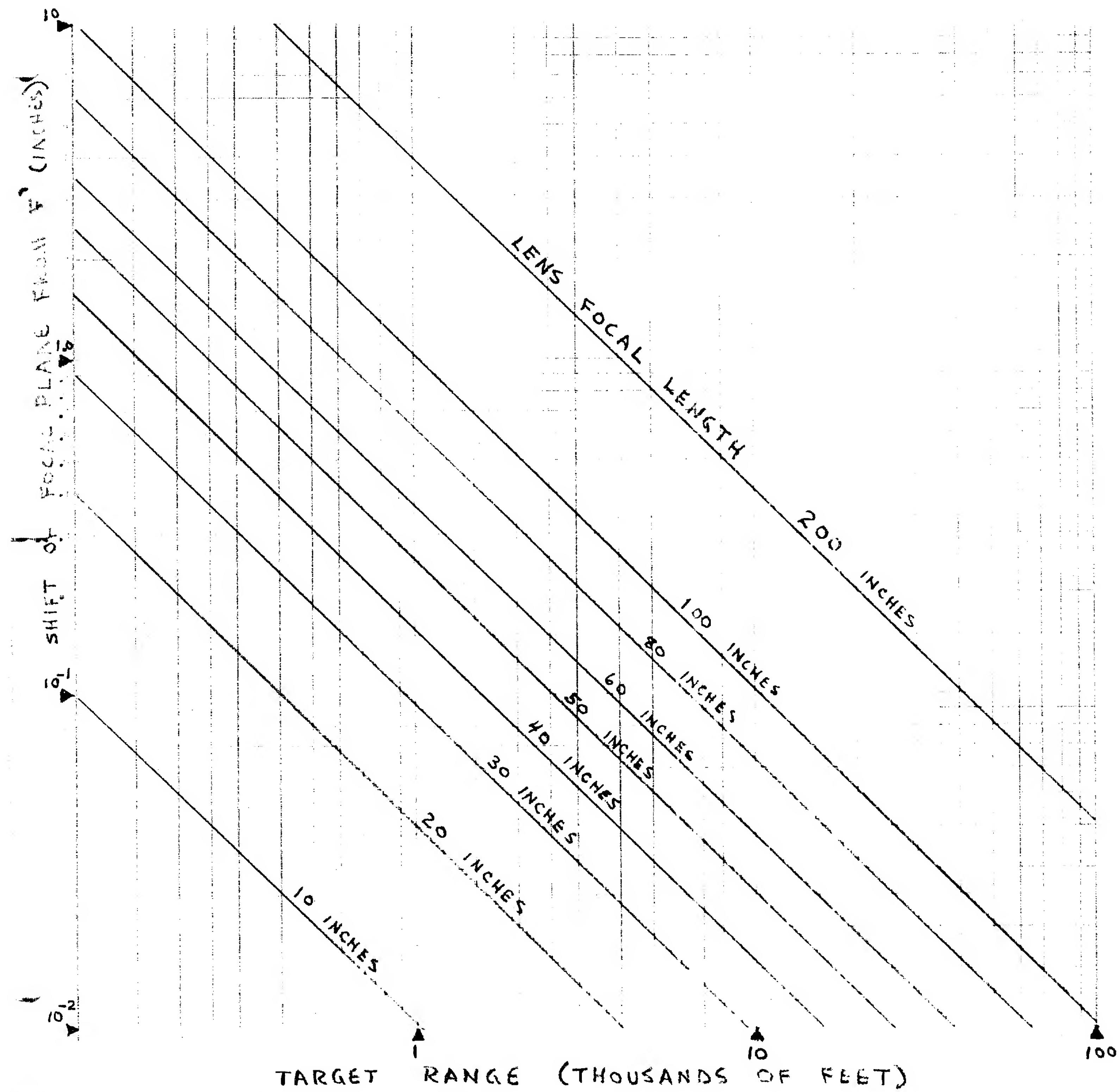

$$\Delta f \approx \frac{(6.95)(10^{-3})\, f^2}{R_t}$$

FIGURE C-18

Any error (ϵ) in placement of the focal plane will result in spreading (Δr) of the light rays from points on the target. Expressed in terms of limiting resolution, this becomes:

$$\Delta r\ (\ell/_{mm}) = \frac{2F}{25.4\epsilon} = \frac{(7.9)\ (10^{-2})\ F}{\epsilon\ (in)}$$ Figure C-19

When target range is much larger than lens focal length, the defocusing can be expressed approximately in terms of the ratio (ψ) of actual target range (R_t) to the range (u) at which the lens is adjusted for optimum focus. Figure C-20

The defocusing effects on linear resolution of target elements can be expressed in terms of the range ratio (ratio of actual range, to the range at which focussed) by:

Resolution at near distance, $\chi_{n(in)} = \dfrac{d\ (u - R_t)}{u}$ Figure C-21 (a)

and, Resolution at far distance, $\chi_{f(in)} = \dfrac{d\ (u - R_t)}{u}$ Figure C-21 (b)

The maximum shift in back focal distance required for anticipated ALIAS range variations will be approximately 0.07 inches. For lens diameter of from 4 to 8 inches the back focal length error cannot exceed about 0.004 inches; however, target range measurement error of about 10 percent can be tolerated without adversely affecting resolution as limited by focus error.

c. Image Illumination and Exposure Limits - The total solar illuminance incident on a target above the atmosphere is approximately 13,600 foot-lamberts within the spectrum of film sensitivity. The reflected illumination (radiant exitance) from the target is the product of the illuminance and the relative reflectance (ρ) of the target surface. A diffuse reflecting surface will obey Lambert's Cosine Law, whereas a specular reflecting surface will not. Maximum specular reflectance can approach 100%, while maximum diffuse reflectance will be $1/\pi$, or about 32%. Assuming that the satellite target has both diffuse and specular reflecting surfaces, the ALIAS system

LIMITING RESOLUTION AS A FUNCTION OF ERROR IN POSITION OF FOCAL PLANE

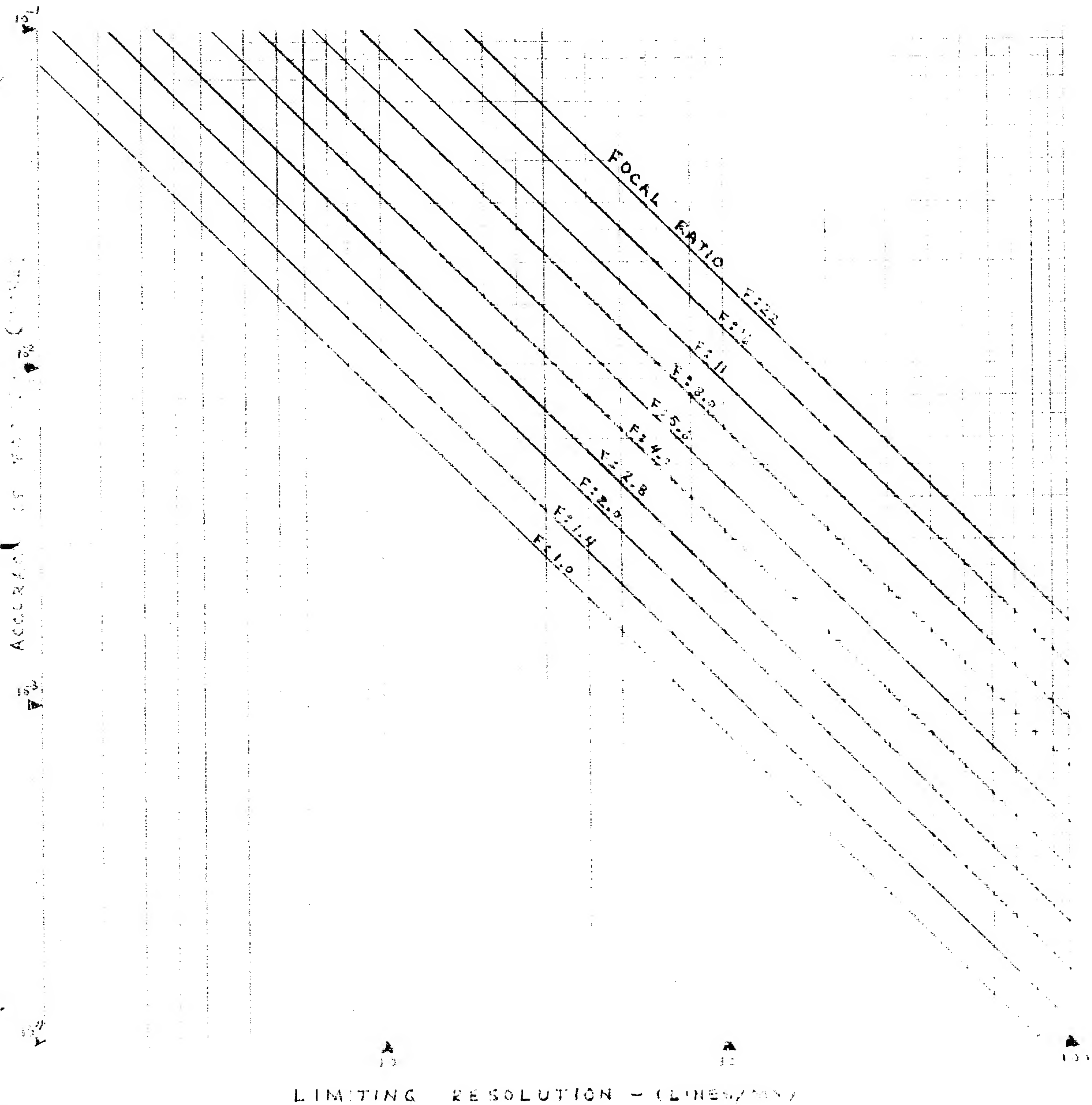

$$r = \frac{(7.9)(10^{-2})\,F}{\delta}$$

FIGURE C-19

RATIO OF TARGET RANGE
TO RANGE AT WHICH FOCUSED

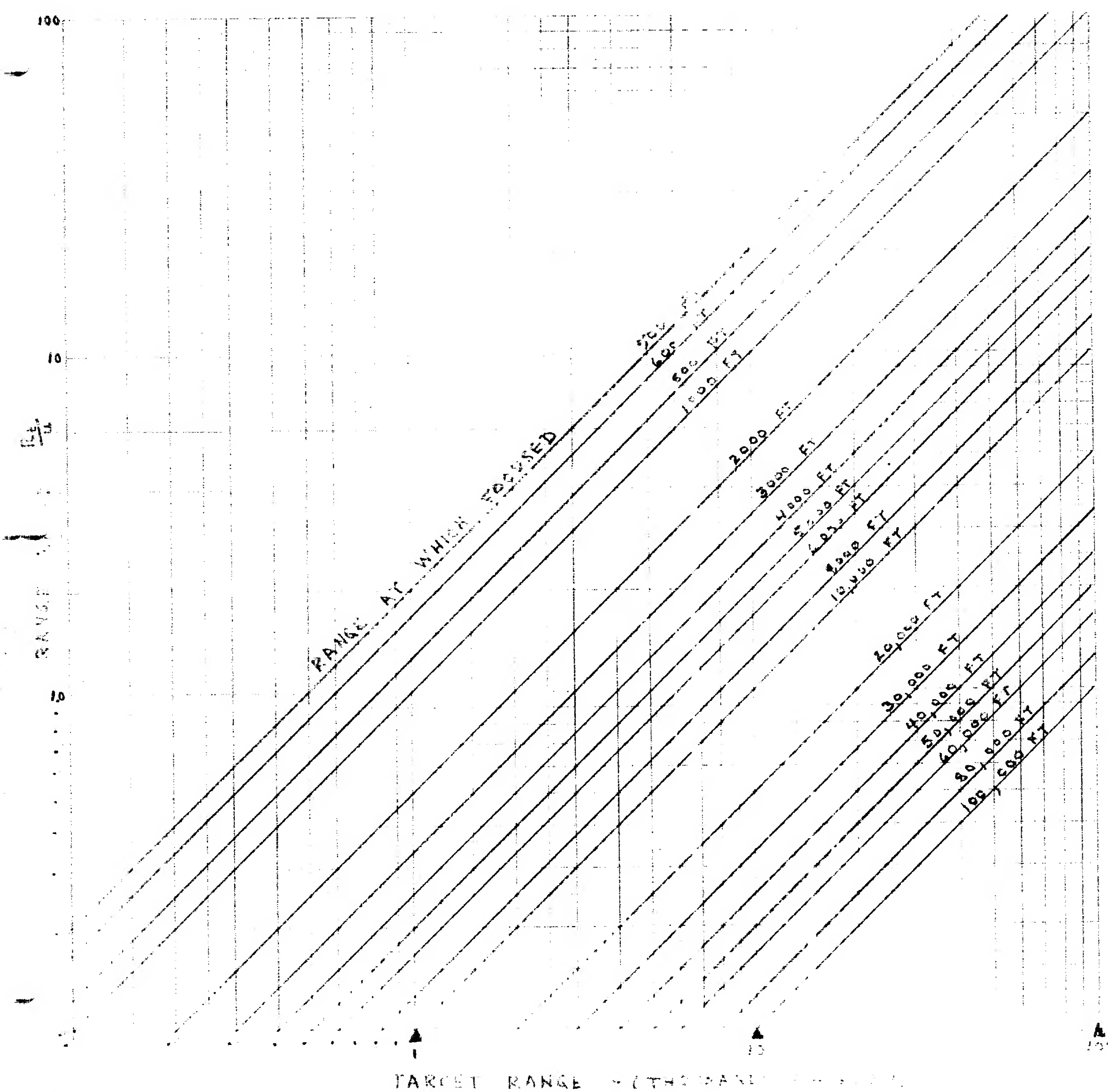

$P = \frac{R_t}{u}$

FIGURE C-20

DEFOCUSED TARGET RESOLUTION

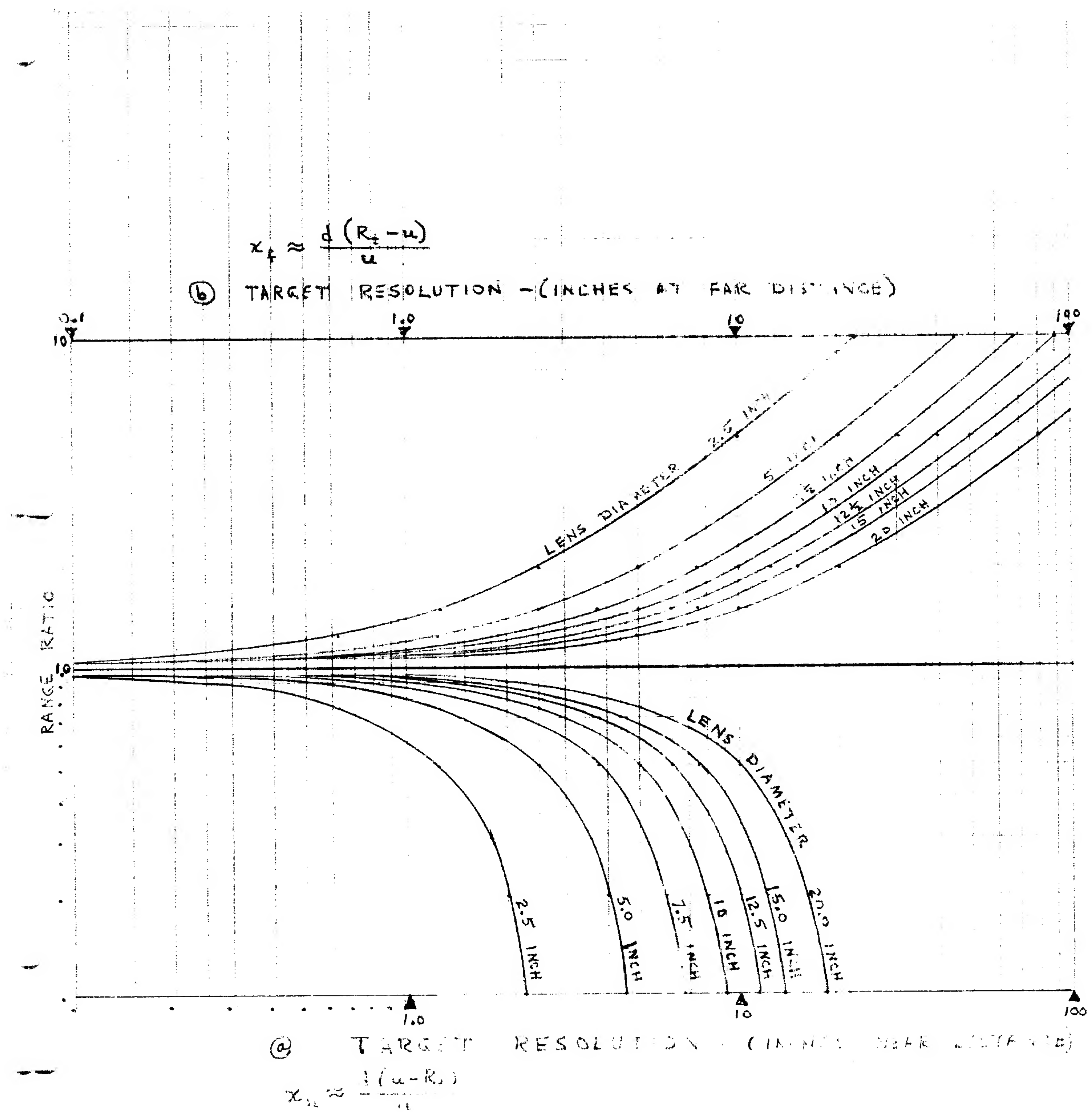

FIGURE C-21

should have a dynamic range capable of recording a full range of target luminance; however, the maximum intelligence information can be expected to fall within the range of zero to 32% reflectance. The illumination of the image is:

$$Ii = \frac{I_t \ \omega_i}{\omega_t}$$

where: I_i = image illumination

I_t = illuminance of target

ω_i = solid angle of image pupil

ω_t = solid angle of target pupil

The lens solid angle is determined by the diameter (d) of the lens and the focal length (f). Assuming 100% lens transmission efficiency the image illuminance becomes:

$$I_i \simeq \frac{\pi I_s \rho (d/2)^2}{f^2}$$

where: I_s = Source illuminance = 13,600 f.l.

The lens focal ratio (F) is:

$$F = \frac{f}{d}$$ Figure C-22

The effective lens aperture (T-stop), including lens transmission efficiency is:

$$(\text{T-stop}) = \frac{F}{(\text{eff})^{1/2}}$$ Figure C-23

$T_{STOP} = \frac{F}{(EFF)^{1/2}}$

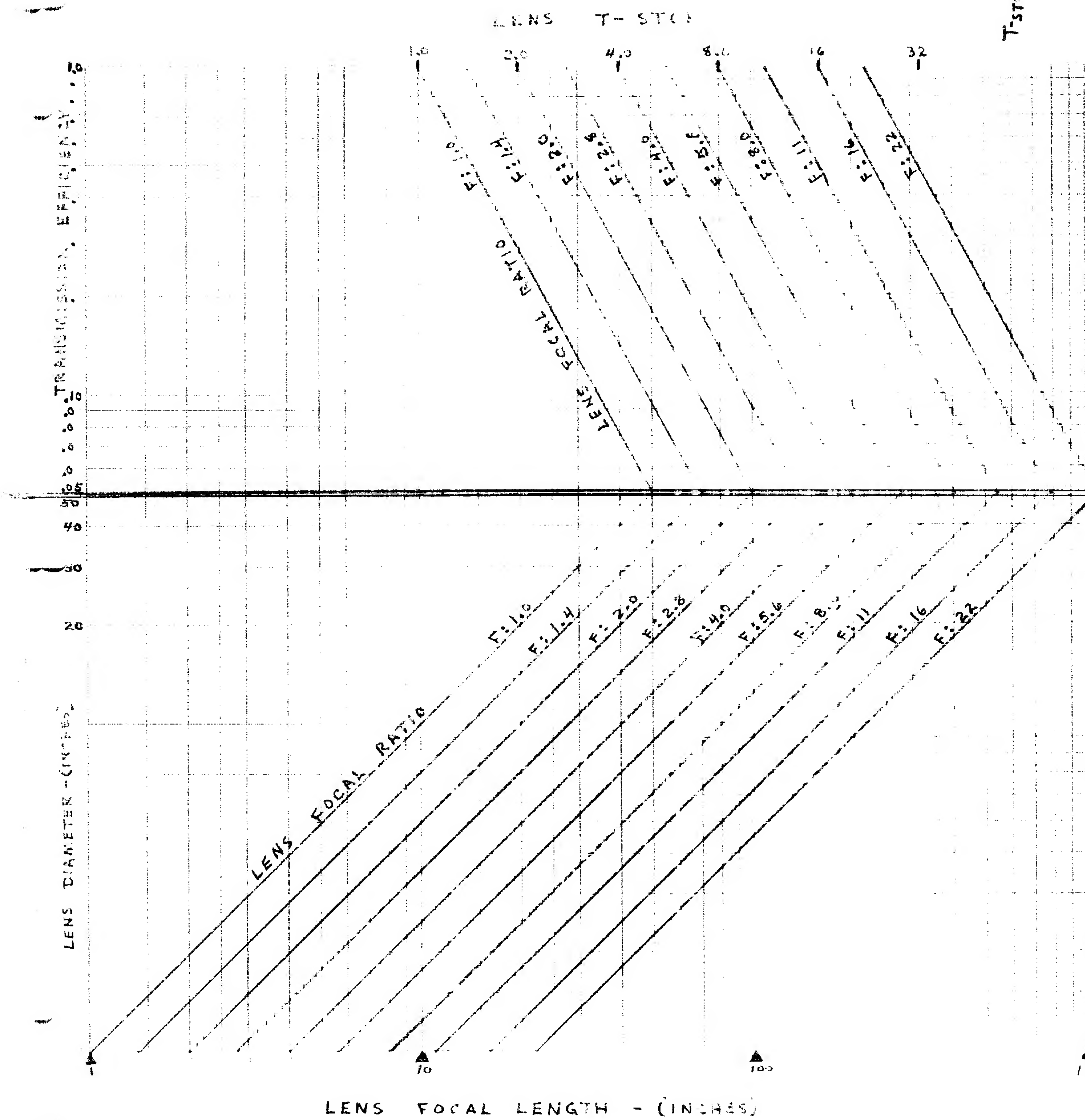

FIGURE C-23 - LENS T-STOP

FIGURE C-22 - LENS FOCAL RATIO

$F = \frac{f}{d}$

The effective image illuminance therefore becomes:

$$I_i \simeq \frac{\pi I_s \rho}{4\ (\text{T-stop})^2} \simeq \frac{(1.07\ (10^4)\rho}{(\text{T-stop})^2} \qquad \text{Figure C-24}$$

Specification of film sensitivities is based on a wide range of exposure conditions, film development methods and target parameters. All existing specification methods are, however, based on the familiar film characteristic curve, (Figure C-25), comparing total film exposure to resulting film density. The film exposure indexes, (Figure C-14), are defined as the reciprocal of twice the exposure at the point on the toe of the characteristic curve where the slope is 0.6 times the slope of the straight-line portion of the curve (for "Standard" development). The ASA index is based on the minimum exposure (E_m) for obtaining film density of 0.1 above base fog. Although these methods of specifying sensitivity are not equivalent, relative sensitivity of various films can be compared adequately to determine minimum detectable exposures with some confidence. Exposure time for minimum recordable density, in terms of film ASA ratings, can be expressed as:

$$T \approx \frac{0.45}{13.5\ S\ I_i} \approx \frac{(3.34)\ 10^{-2})}{S\ I_i} \qquad \text{Figure C-26}$$

where: S = Film ASA rating

I_i = Image illuminance (from Figure C-24)

The typical film characteristic curves vary considerably with different developers and times of development. The slope (gamma) of the characteristic curve for typical films can be controlled, within limits, from less than 1.0 to about 3.0. Optimization for any given conditions is best obtained experimentally. At extremely high shutter speeds, the total exposure effect suffers slightly due to failure of the Reciprocity Law (time-vs-light level); however, the reciprocity limits on the highly sensitive films currently under consideration are negligible at shutter speeds slower than 1/5000 second.

IMAGE ILLUMINANCE

FOR INCIDENT ILLUMINANCE AT TARGET OF 13,600 FOOT-CANDLES

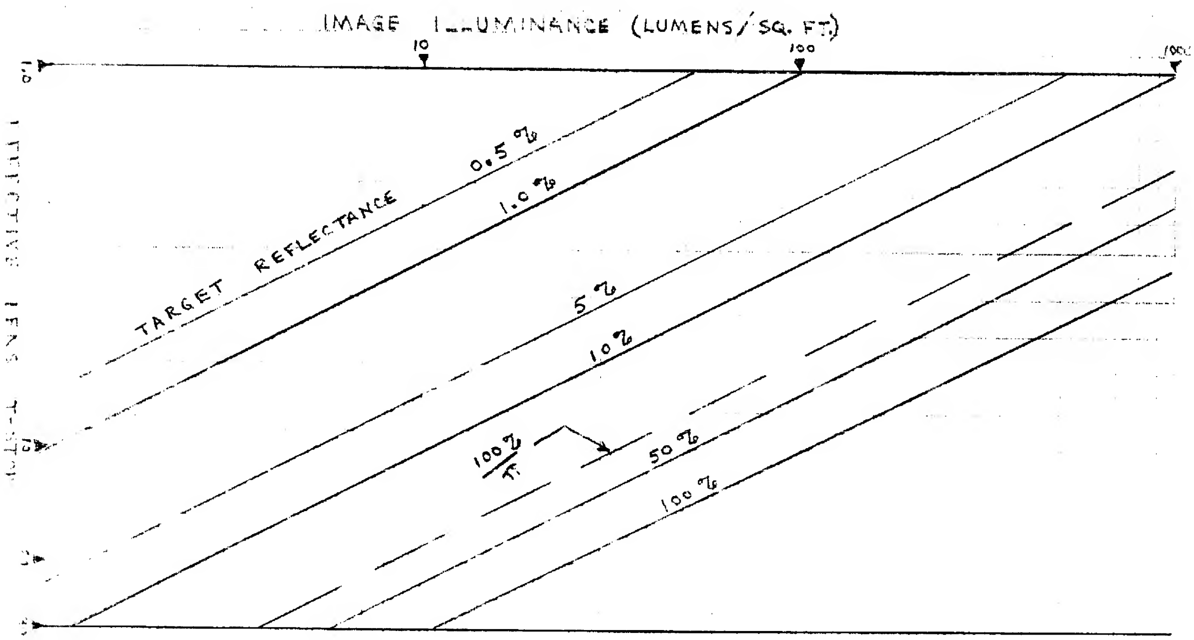

$$I_i \approx \frac{(1.07)(10^4)\,\rho}{(T\text{-stop})^2}$$

FIGURE C-24

TYPICAL FILM CHARACTERISTIC CURVE

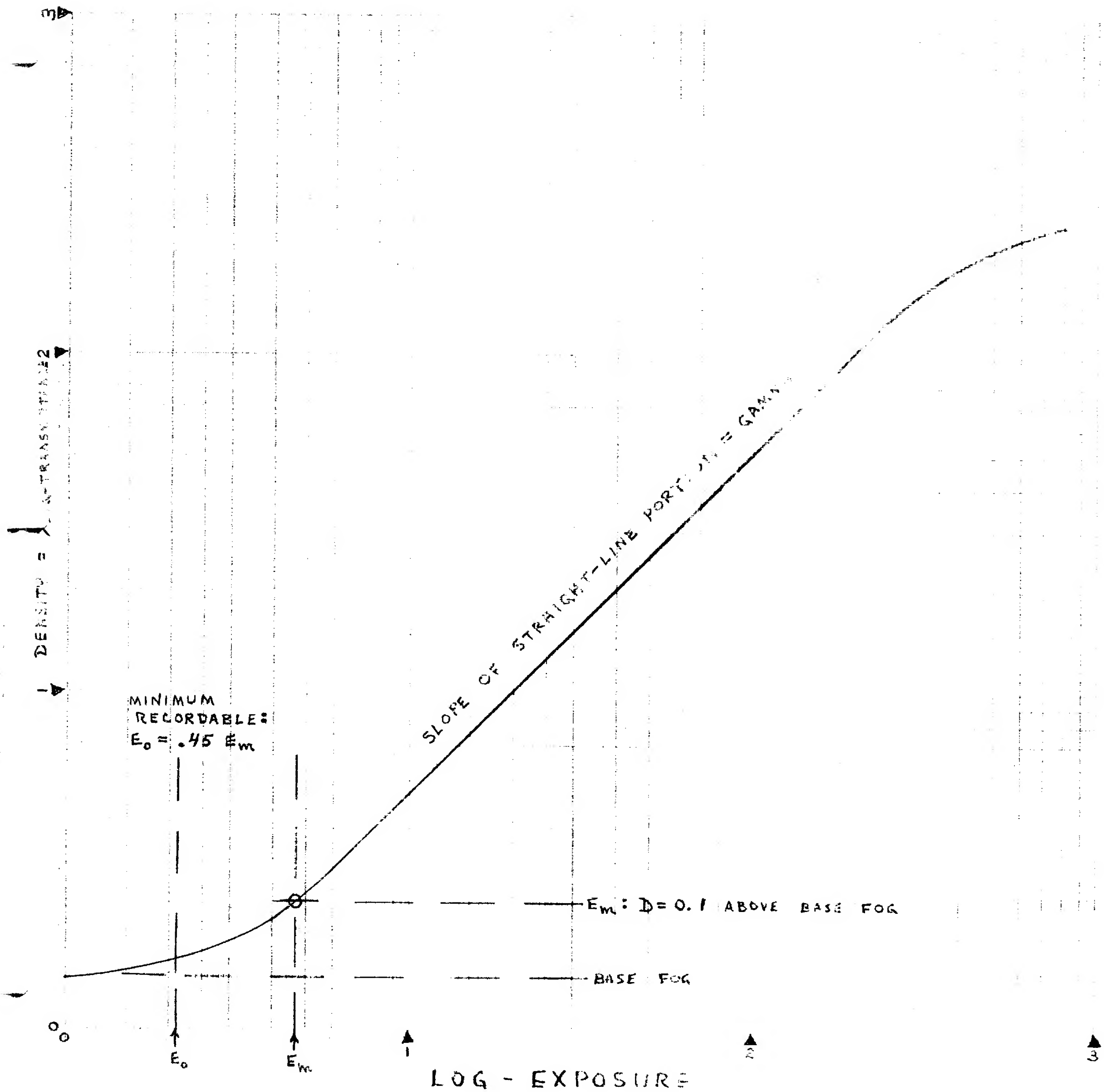

FIGURE C-25

FILM EXPOSURE TIME

(FOR MINIMUM RECORDABLE IMAGE: $E_o = .45\, E_m$)

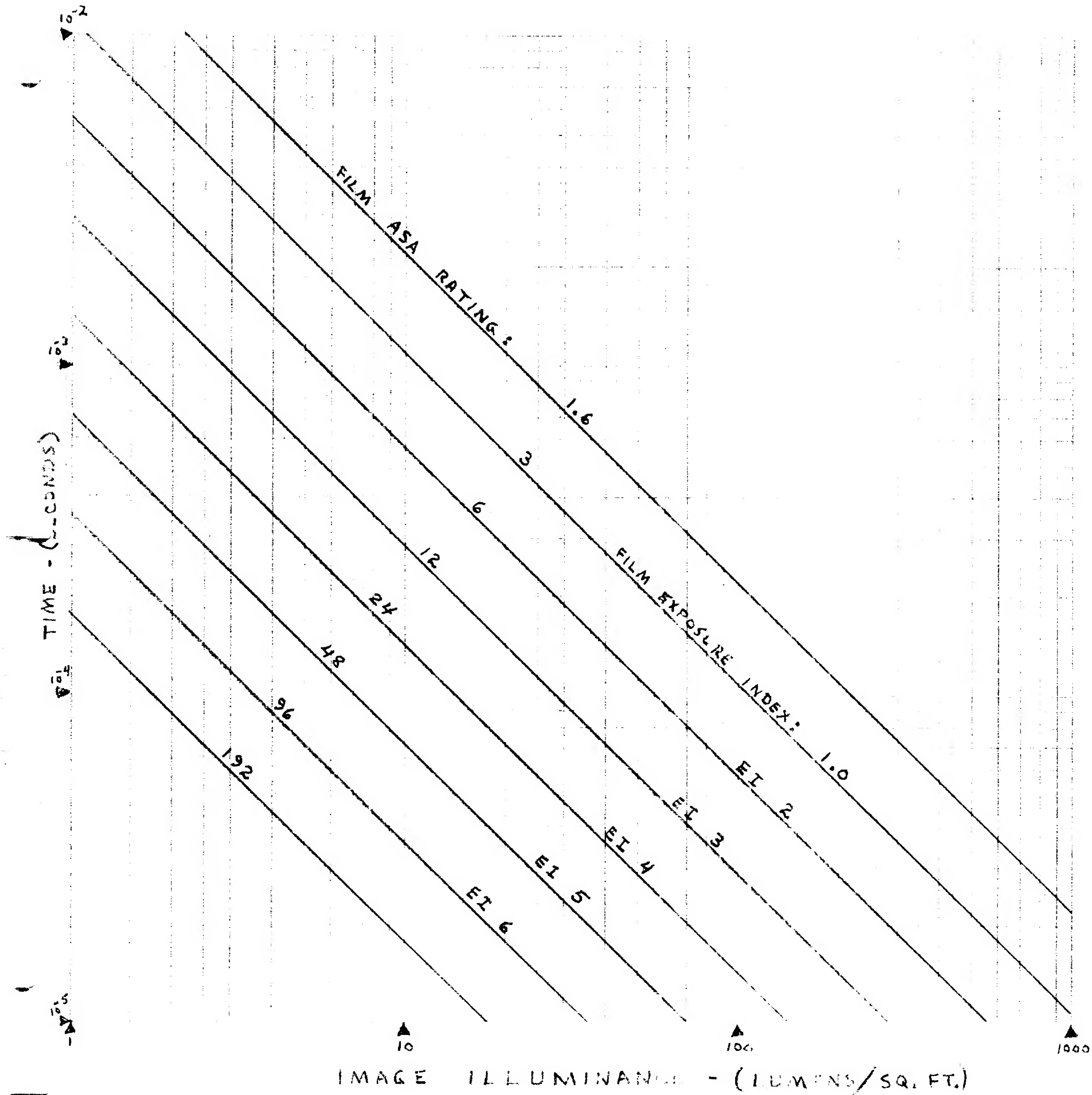

$$T \approx \frac{(3.34)(10^{-2})}{S\, I_i}$$

FIGURE C-26

At the high target crossing rates encountered during the ALIAS picture-taking sequence, accurate optical target tracking (image motion compensation) is required to reduce image motion to maintain the camera lens/film resolution capability. Image motion of one-half cycle, (i.e. one half the angle of one resolution element) will normally degrade the resolution by one full cycle. Motion-derived limits on angular resolution is shown in Figure C-27 as a function of IMC tracking rate stability and shutter speed.

Tracking rate stability required for 1% IMC during the ALIAS intercept is shown in Figure C-28 as a function of offset distance and time from closest approach.

Major image motion effects will generally be evidenced as a linear smear for the ALIAS system. The effect of such unidirectional motion upon the total information content of the ALIAS imagery cannot be readily assessed inasmuch as resolution is an area effect. As a conservative estimate of image motion effects, the root-mean-square (RMS) values of contributing resolution factors can be used to determine the limiting resolution of the system, including the assumption that maximum image motion is random in nature. The RMS value of contributing resolution factors takes the form:

$$\vartheta = \sqrt{\vartheta_1^2 + \vartheta_2^2 \; \ldots \; \vartheta_n^2}$$

The RMS value of ALIAS system resolution as a function of lens/film angular resolution and motion-derived limits on angular resolution during each exposure is shown in Figure C-29.

Using currently available film rated at ASA-80 with a system optical T-stop of 6.0, a shutter speed of about 1/4000 second will allow adequate dynamic range to record all normal target detail. IMC tracking stability of one degree/second will hold image motion to about 0.9 seconds of arc during this exposure period. With a lens/film resolution capability of about 1.4 arc-sec, the ALIAS system resolution capability would approach 1.9 arc-second. At 9000 ft target slant range, this system would resolve better than one-inch detail on the target.

d. Modulation Transfer Functions of System Parameters- Although convenient, the use of the above limiting system parameters is not completely satisfactory for evaluating the information content of a photographic system. The actual information transfer capability of various lenses and films will vary widely under different conditions;

MOTION-DERIVED LIMITS ON ANGULAR RESOLUTION
AS A FUNCTION OF TRACKING ERROR
(MOTION LIMITED TO 1/2 OF ANGLE RESOLVED)

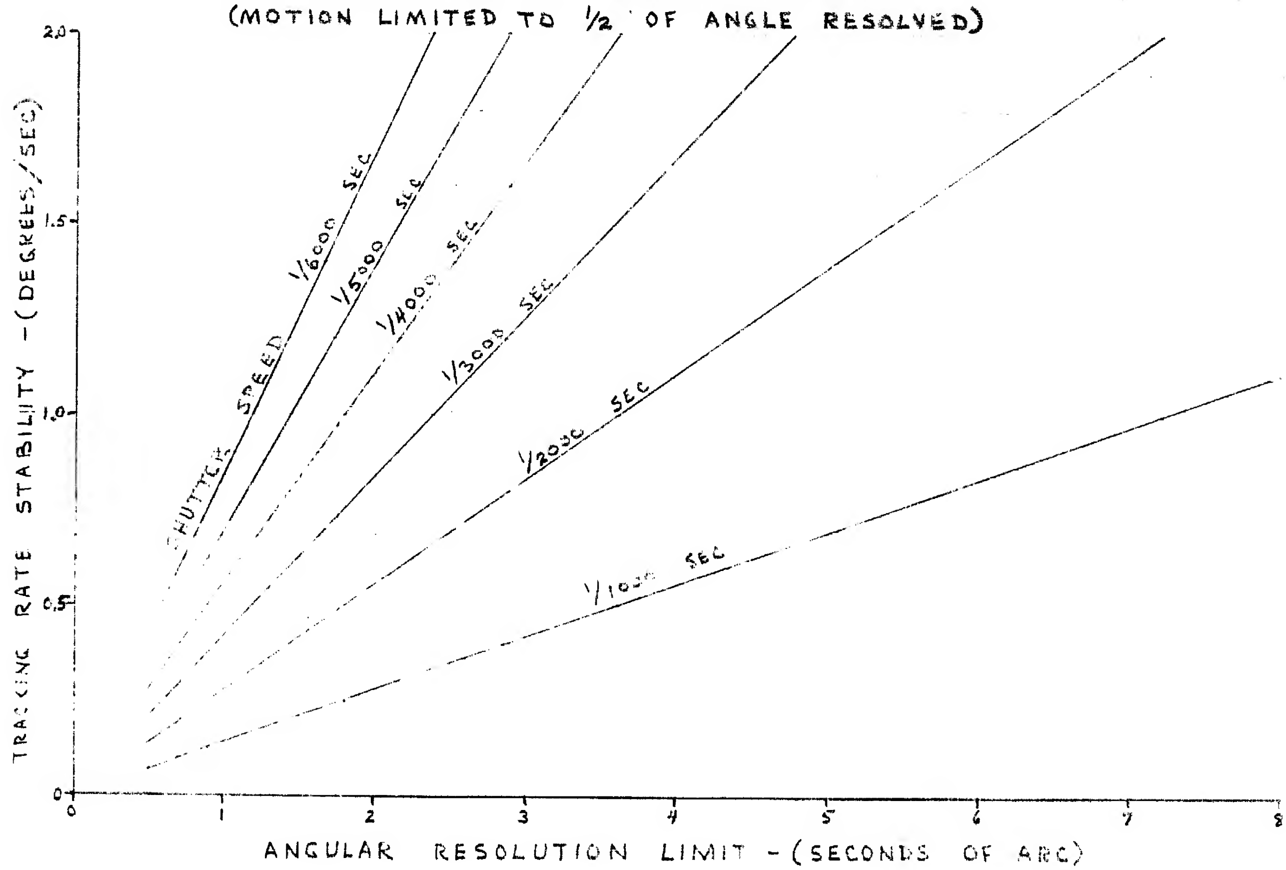

FIGURE C-27

APPROXIMATE ALIAS TRACKING STABILITY REQUIREMENTS

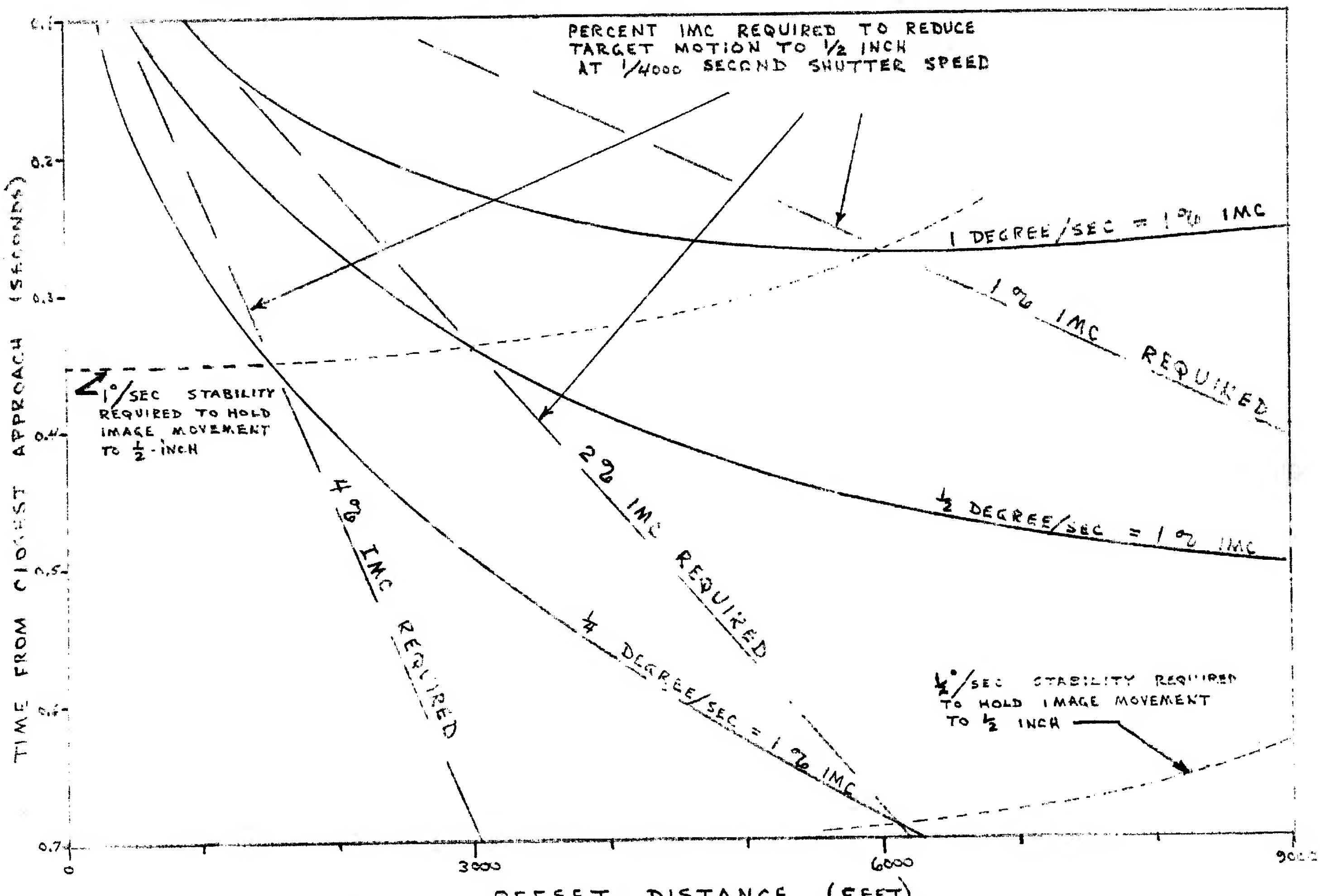

FIGURE C-28

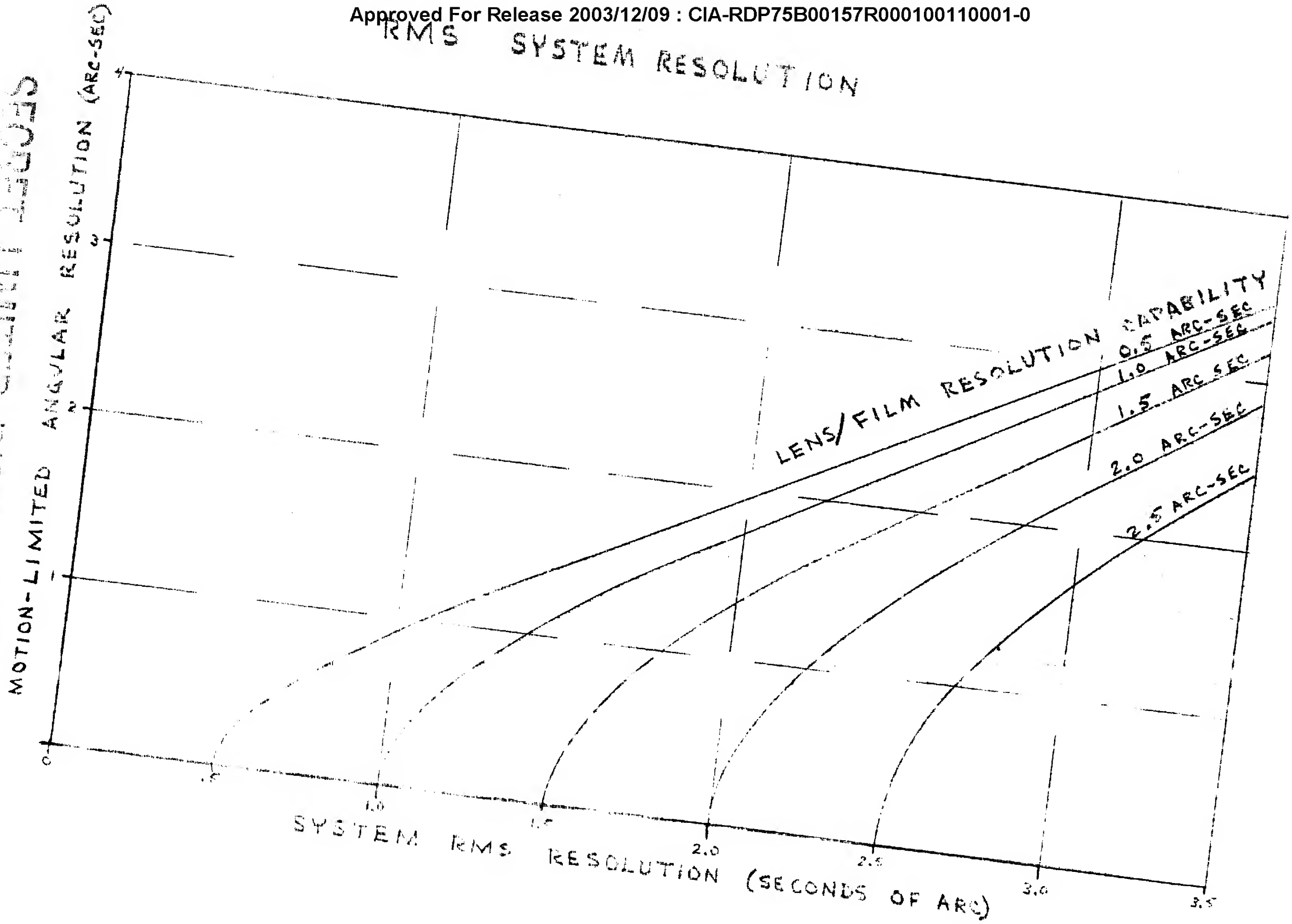
RMS SYSTEM RESOLUTION
MOTION-LIMITED ANGULAR RESOLUTION (ARC-SEC)
LENS/FILM RESOLUTION CAPABILITY
0.5 ARC-SEC
1.0 ARC-SEC
1.5 ARC-SEC
2.0 ARC-SEC
2.5 ARC-SEC
0
1
2
3
4
1.0
2.0
2.5
3.0
3.5
SYSTEM RMS RESOLUTION (SECONDS OF ARC)

FIGURE C-29

therefore, the actual system operational performance must be determined through simulation and through experimentally developed analogs of the contributing factors for each portion of the photographic system. The use of fourier transforms of image information content in terms of spatial frequencies and relative modulation (density range) provides a means of combining system performance factors. Graphically approximating the Modulation Transfer Functions (MTF) of various contributing parameters provides a ready means for estimating the product of the MTF effects on system performance.

Optical image transfer functions appropriate to typical state-of-the-art lens designs are shown in Figure C-30. Within the regions actually drawn on this chart, the transfer functions closely approximate the performance of existing lens capability. Modulation transforms for typical films which have been considered for the ALIAS system are shown in Figures C-31 and C-32. It should be noted that use of different developers and different processing techniques can vary the MTF considerably. For instance, Type 5401 film given standard development in D-19, falls somewhat below the curve shown. The use of D-19, however, provides a rather wide latitude for development to different degrees of contrast (gamma) and for varying the effective film sensitivity by shifting of the characteristic curve. Wide variations in film MTF also occur with exposure to light of varying wavelengths. Typical changes are shown in Figure C-33. The use of filters or emulsion dye to restrict exposure to the shorter wavelengths could increase film MTF for the ALIAS mission if sufficient sensitivity were available to compensate for the loss of light energy at the longer wavelengths.

A logical limiting modulation threshold is the minimum recordable film density which can be accurately measured by currently available film read-out devices. Density resolution of .02 to .03 (equivalent to MTF of .02 - .03) is possible with commercially available microdensitometers. The threshold of discrimination of the human eye, when accomodated to local densities within the visual field, is roughly .025 density units (MTF = .025). A threshold MTF of .05 was selected as a practical value. The MTF threshold requirements for several films are shown in Figures C-34 and C-35 together with the nominal MTF capability of existing lens designs. The lens/film intersections represent the threshold limits in lines/mm for a density threshold of MTF = .05.

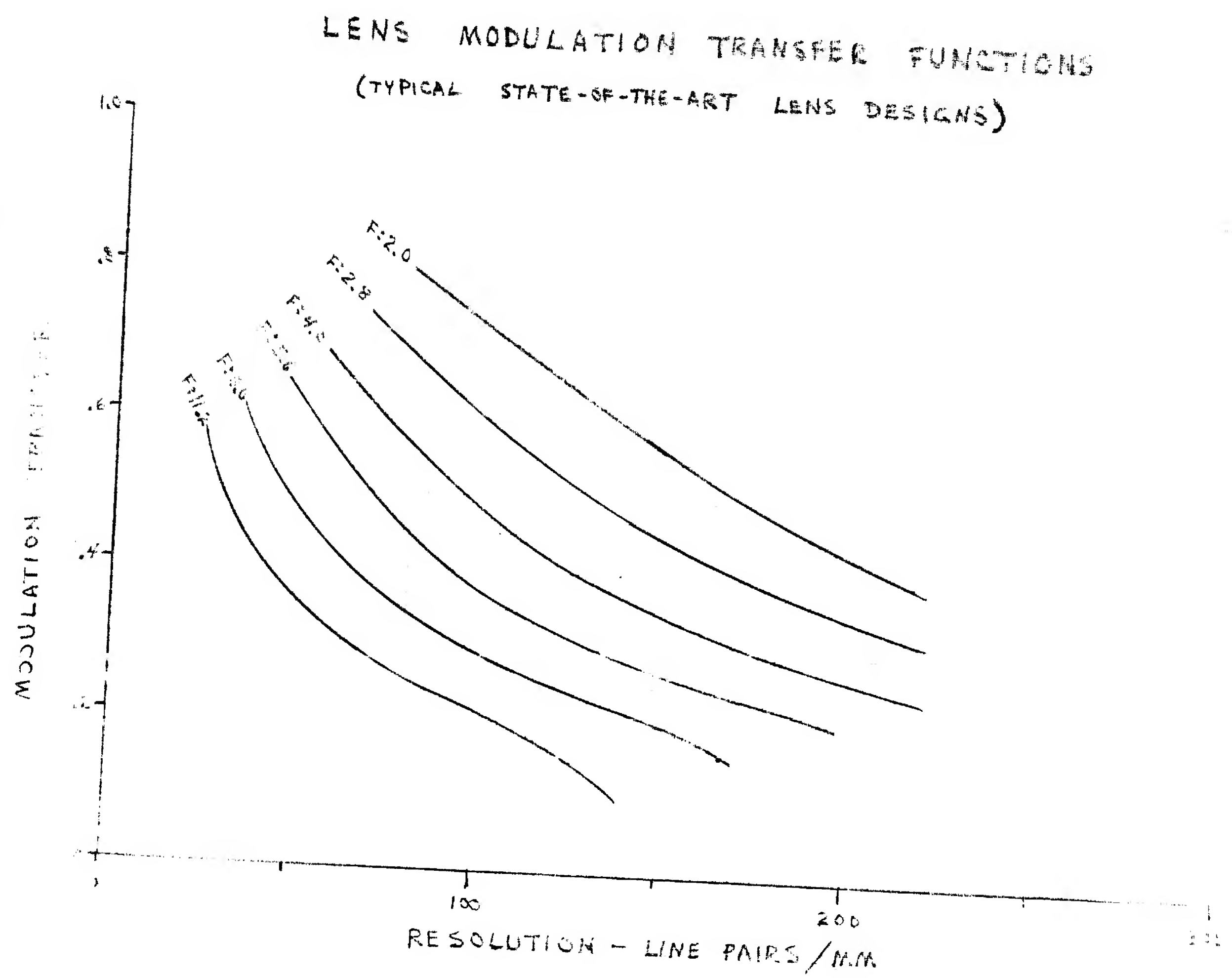
LENS MODULATION TRANSFER FUNCTIONS
(TYPICAL STATE-OF-THE-ART LENS DESIGNS)
F:2.0
F:2.8
F:4.5
F:5.6
F:8.0
F:11.0
MODULATION
RESOLUTION - LINE PAIRS/MM
100
200

FIGURE C-30

FILM MODULATION TRANSFER FUNCTIONS

GREEN LIGHT – AVERAGE EXPOSURE – HIGH CONTRAST TARGET

D-76 DEVELOPER

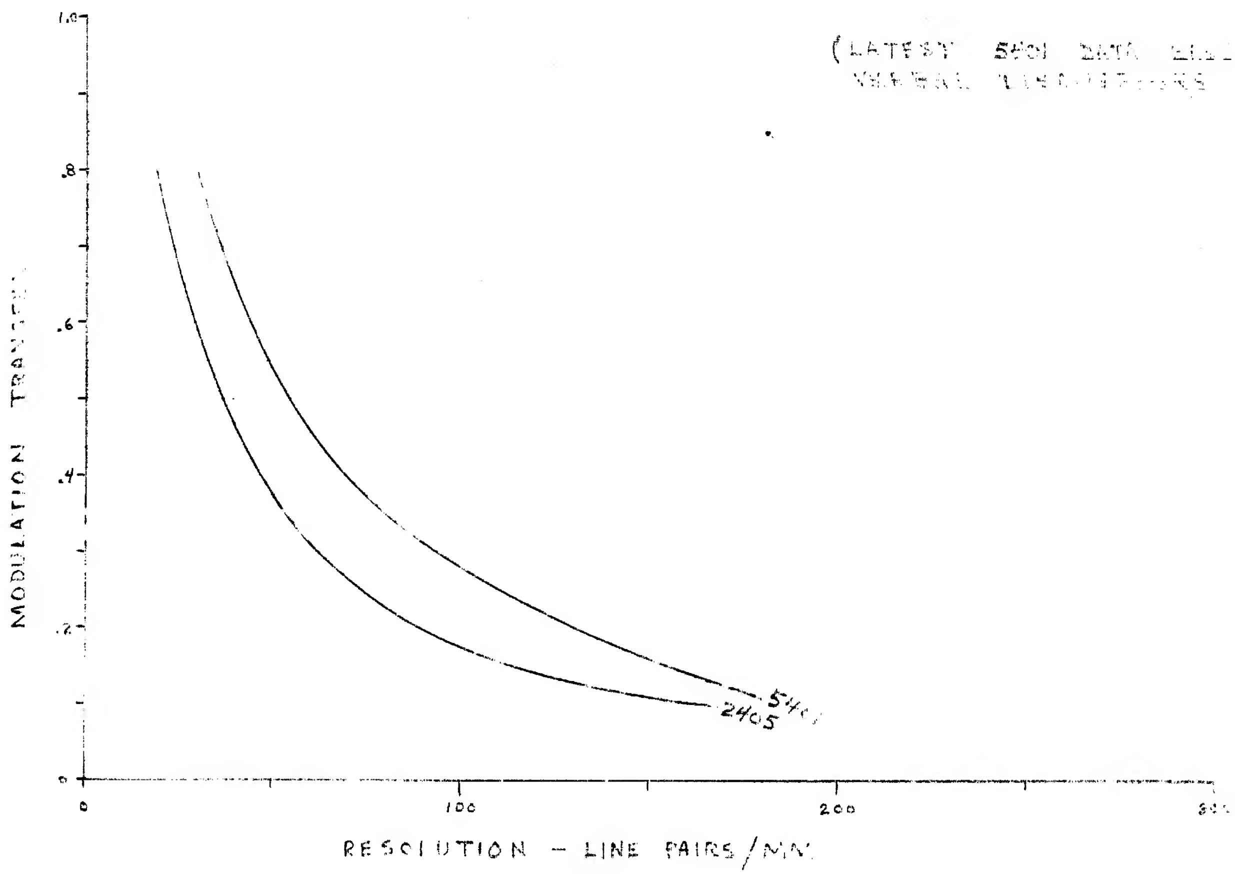

FIGURE C-51

FILM MODULATION TRANSFER FUNCTIONS

GREEN LIGHT - AVERAGE EXPOSURE - (GAMMA = 1?)

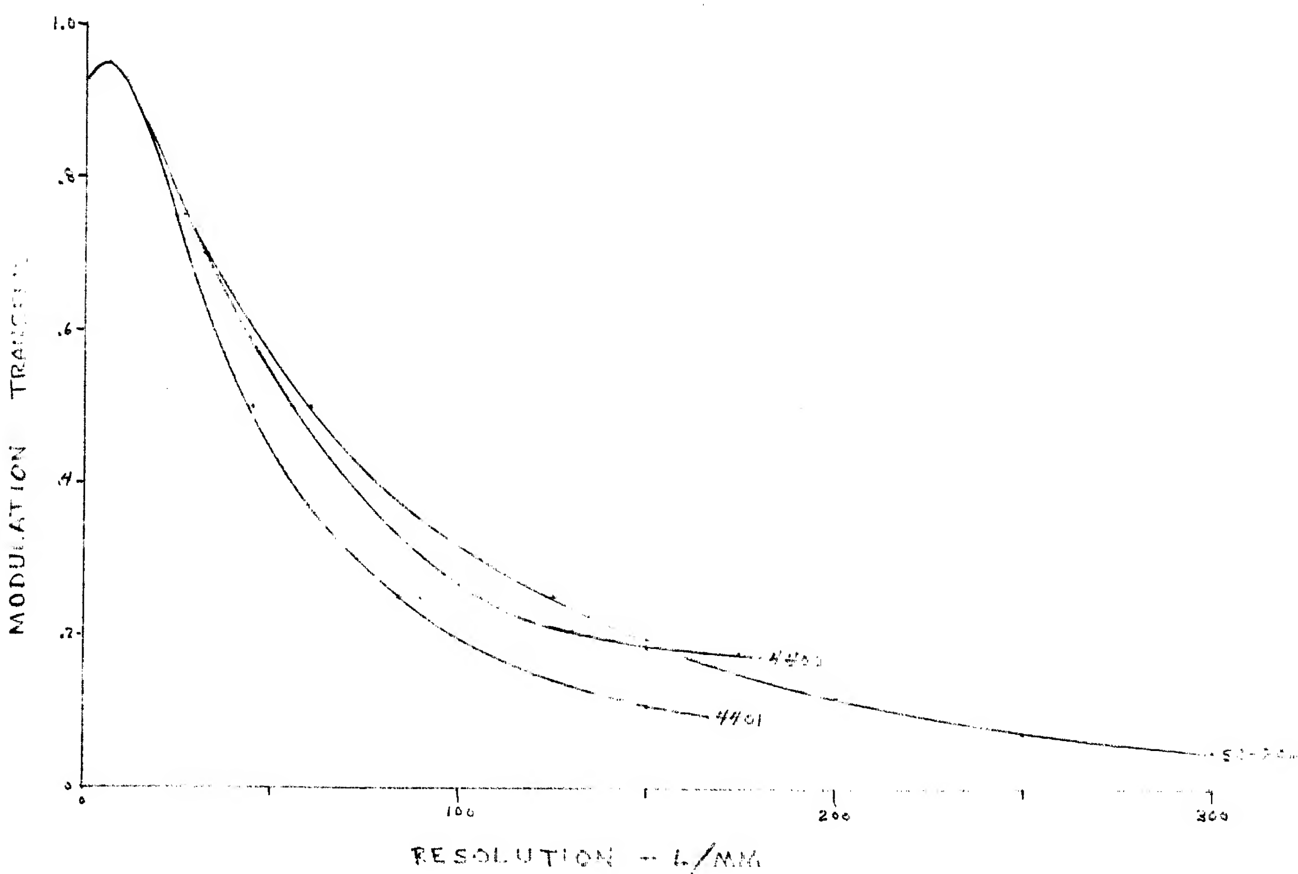

FIGURE C-9A

SECRET LIMITED DISTRIBUTION

TYPICAL CHANGES OF MTF AT DIFFERENT WAVELENGTH REGIONS

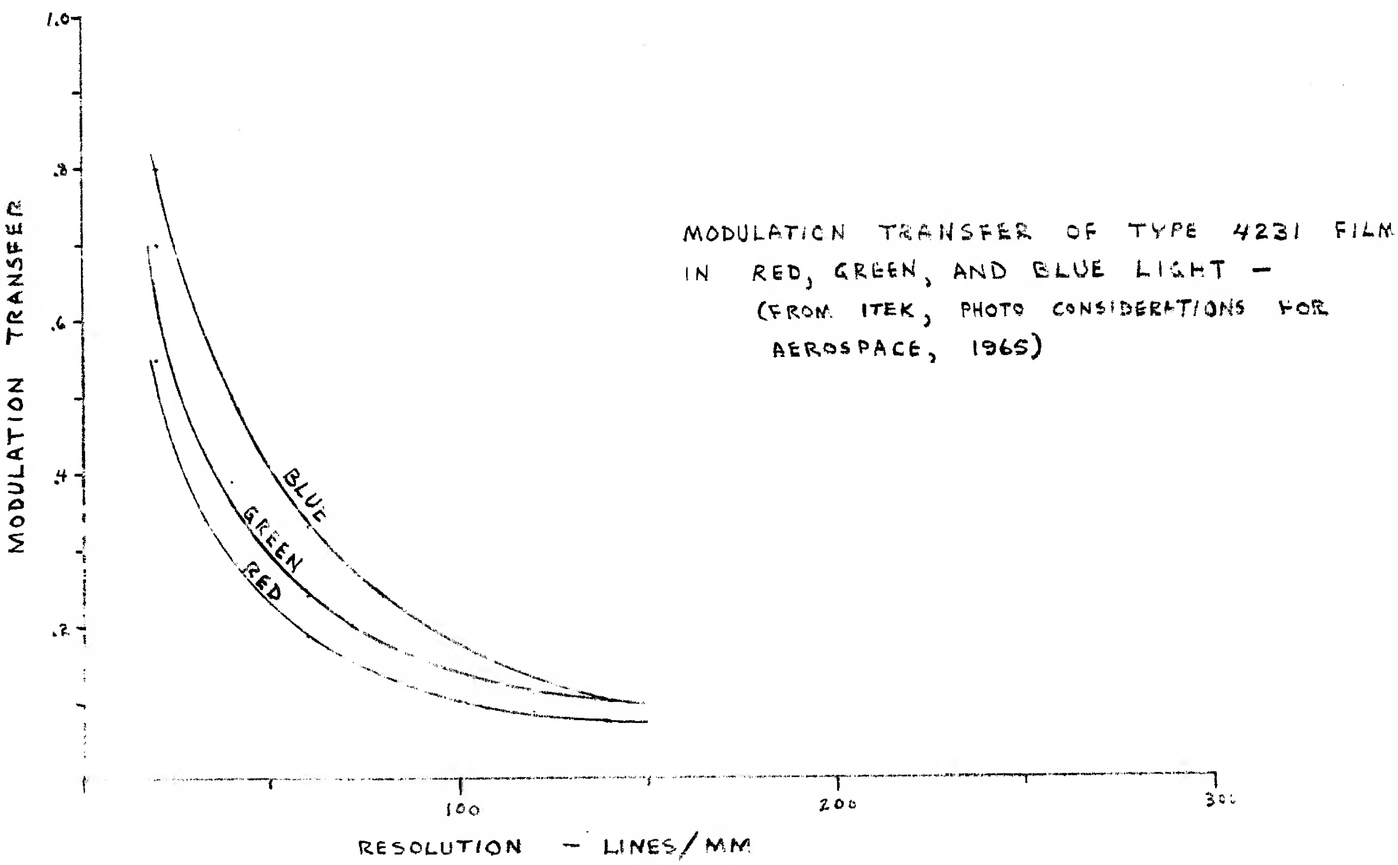

FIGURE C-3B

LENS/FILM MODULATION THRESHOLDS
FOR LIMITING RESOLUTION: MTF = .05

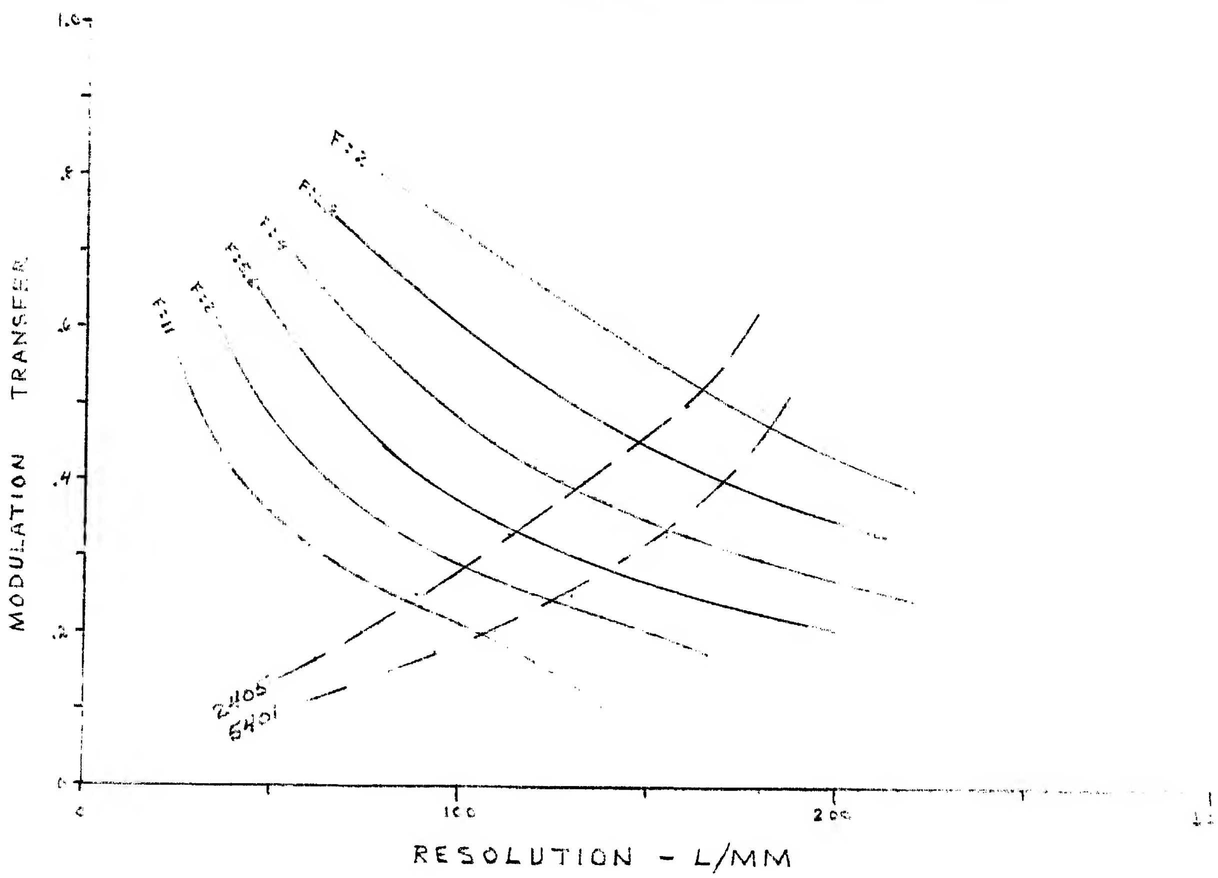

FIGURE C-34

LENS/FILM MODULATION THRESHOLDS

FOR LIMITING RESOLUTION: MTF = .05

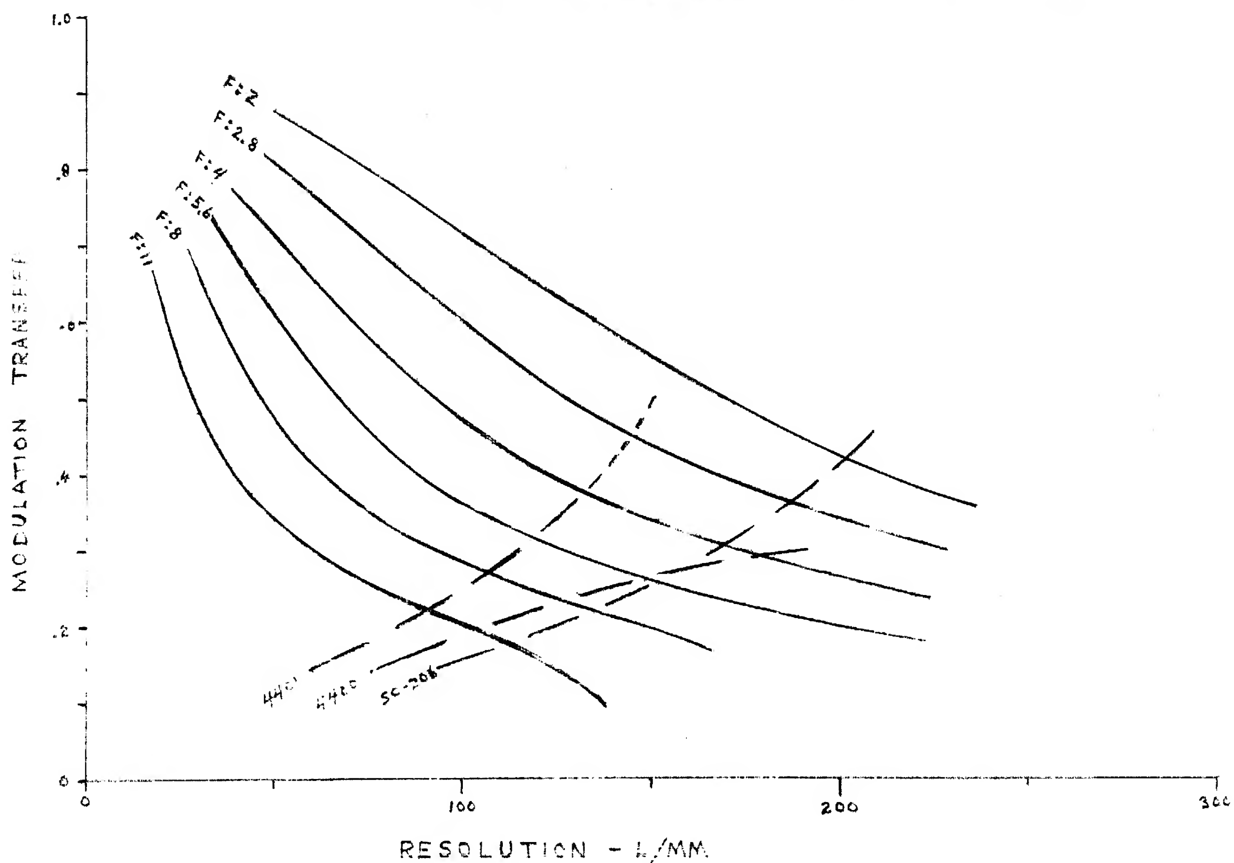

FIGURE C-35

The lens/film MTF resolution thresholds are plotted in Figure C-36, C-37 and C-38 for the two film types considered most suitable for the ALIAS mission. By computing lens focal length and angular resolution as a function of lens diameter, the limiting angular resolution as a function of lens focal ratio was cross-plotted in these figures. These show the resolution advantages which accrue to the larger lens apertures.

Computation of film sensitivities versus available image illuminance yields limiting shutter speeds for various lens focal ratios. These are shown in Figure C-39. Correlation of data from Figures C-36, C-37 and C-38 with those of Figure C-39 provides an expression of limiting angular resolution as a function of shutter speed and lens diameter. This relationship is shown in Figures C-40, C-41 and C-42, and is summarized for the two prime candidate film types in Figure C-43.

When the actual amount of image movement during exposure is known, the modulation transform of image motion takes the form:

$$\text{MTF} = \pi \theta \mu \sin (\pi \theta \mu) \qquad \text{Figure C-44}$$

where: θ = angular resolution

μ = angular image movement

Expressed in terms of linear resolution at the format, this becomes:[5]

$$\text{MTF} = \frac{\sin \pi r m}{\pi r m}$$

where: r = spatial frequency (1/mm)

m = image movement (mm)

This transform is shown for several representative values of image motion in Figure C-44. For specific conditions, the product of image motion MTF and other lens/film/shutter speed MTF can be computed to determine the overall system performance.

The image motion transforms for two specific candidate systems, under conditions of a specified image motion rate, are plotted in Figure C-45. The lens/film MTF for the two specified systems are also plotted on this chart. A summary of combined system transfer functions is given in figure C-46 for a specific condition, typical of what would be encountered at about mid-point of an ALIAS intercept under average anticipated conditions.

5/ Brock, G.C., et al, Photographic Considerations for Aerospace, The Itek Corporation, Lexington, Mass., 1965

LIMITING ANGULAR RESOLUTION (SECONDS OF ARC)
5 INCH LENS DIAMETER

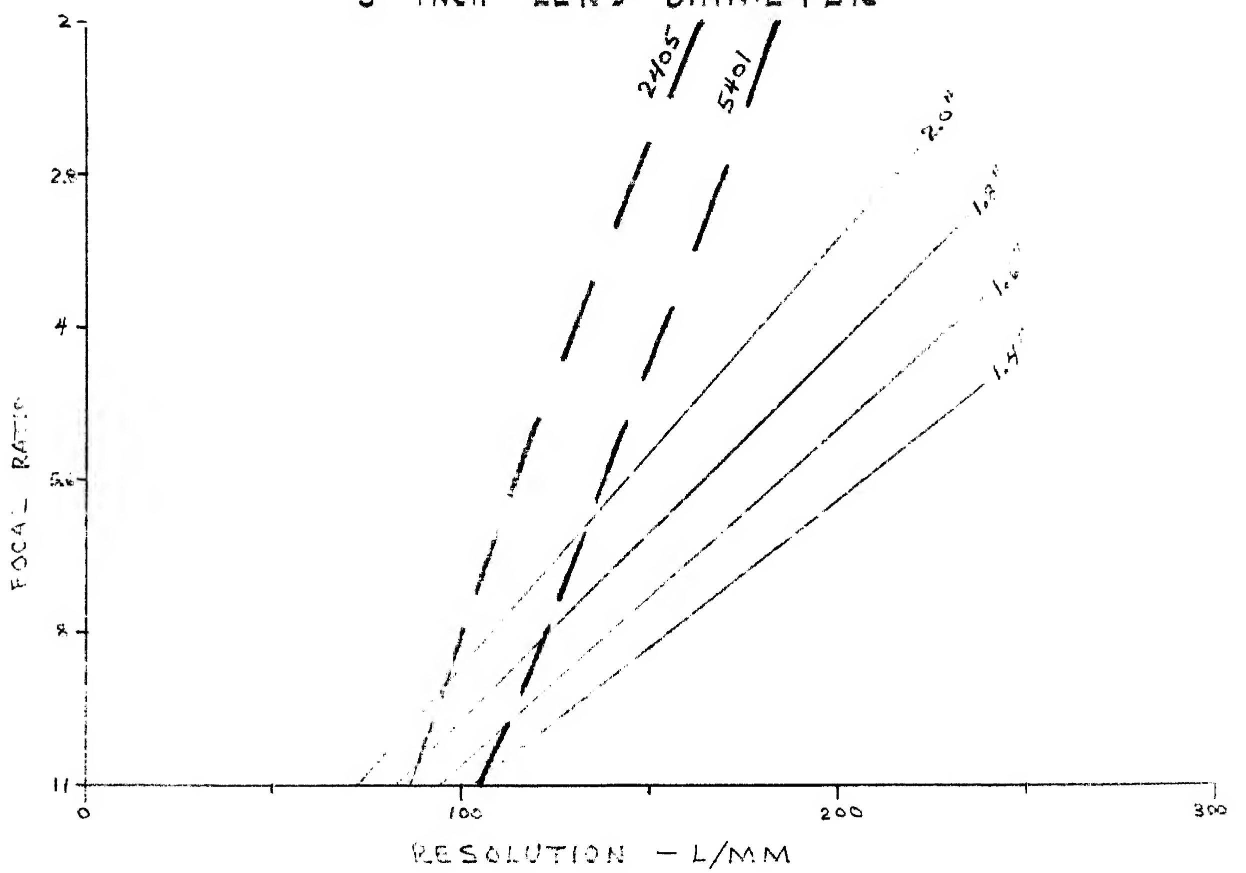

FIGURE C-56

LIMITING ANGULAR RESOLUTION (SECONDS OF ARC)
7½ INCH LENS DIAMETER

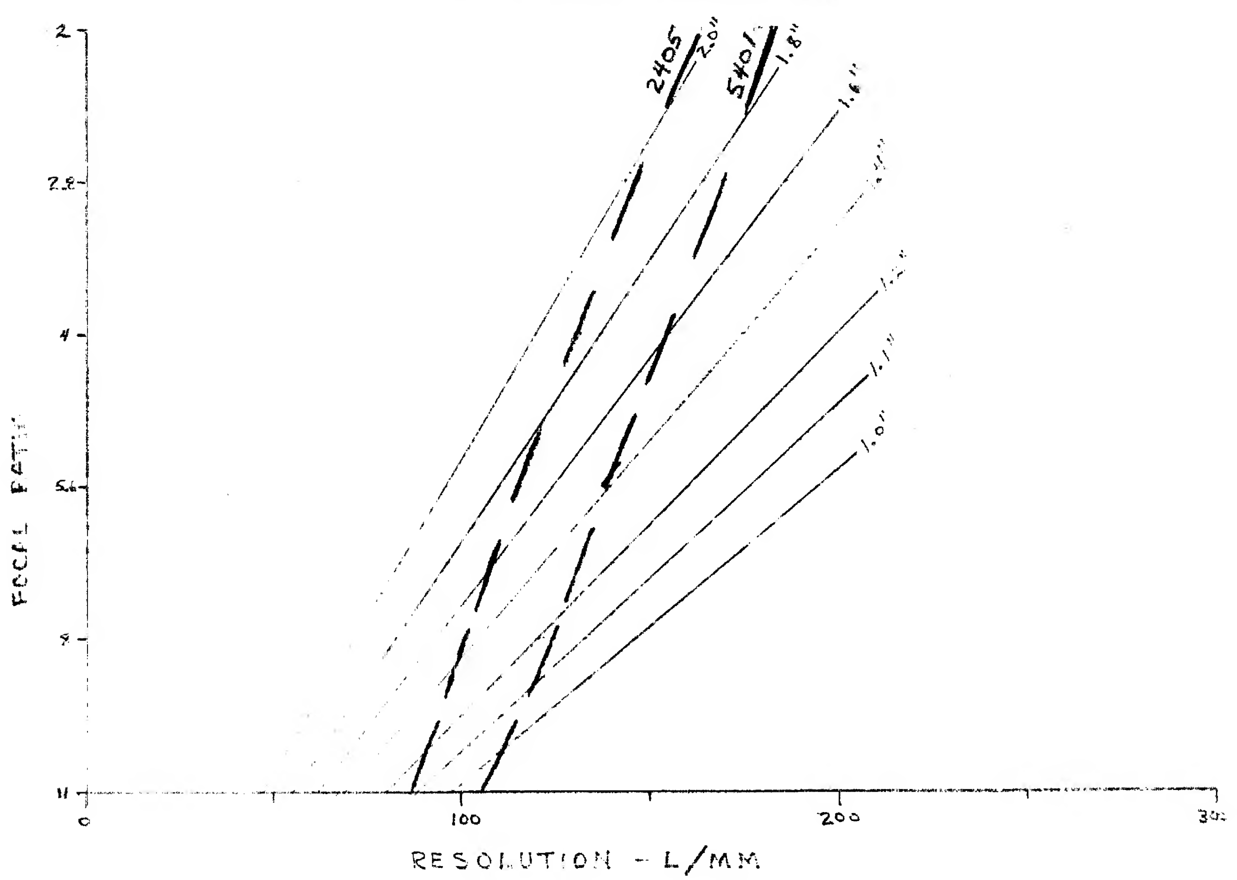

FIGURE C-57

LIMITING ANGULAR RESOLUTION (SECONDS OF ARC)
10 INCH LENS DIAMETER

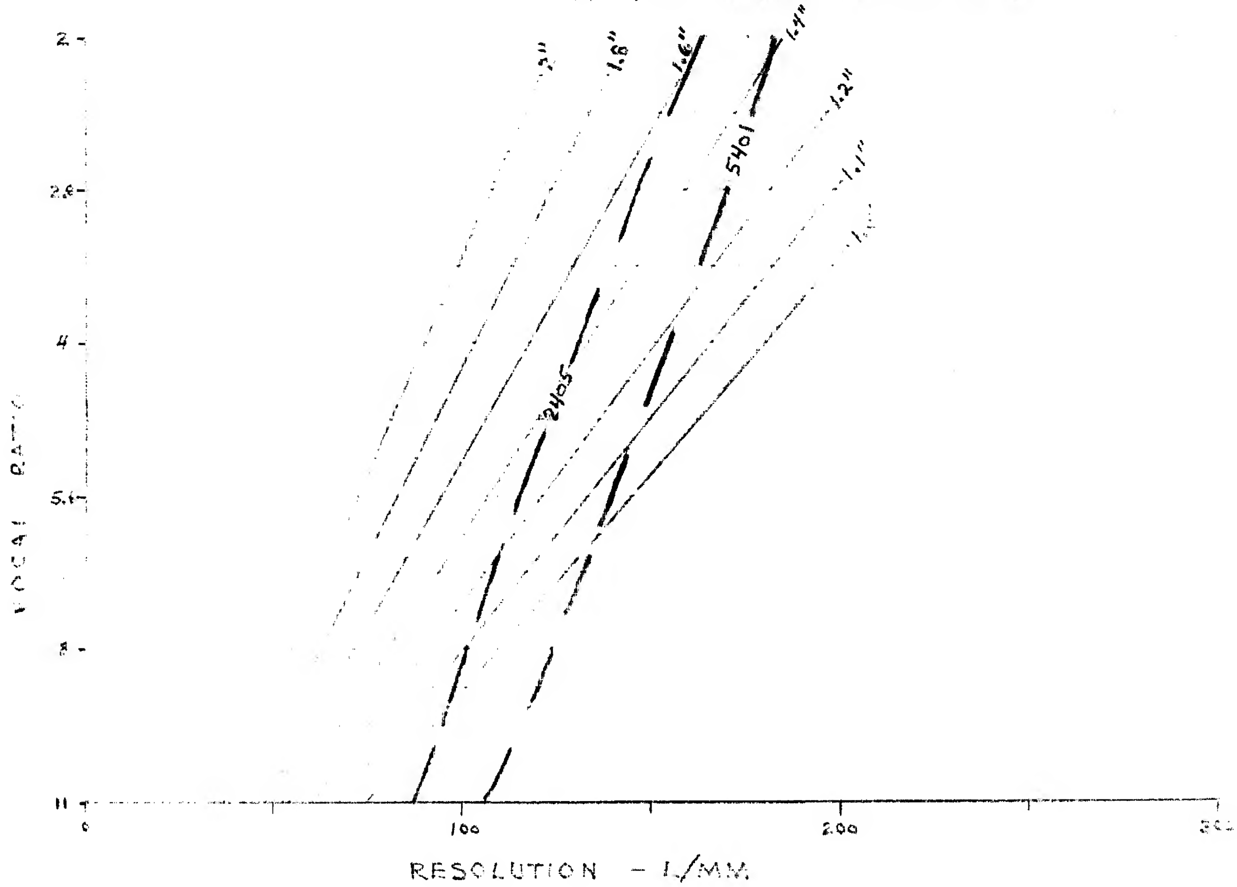

FIGURE C-58

SHUTTER SPEED LIMITS FOR MINIMUM RECORDABLE EXPOSURE

- 0.5% TARGET REFLECTANCE
- 70% LENS TRANSMISSION
- (INCLUDES ESTIMATED RECIPROCITY LIMITS)

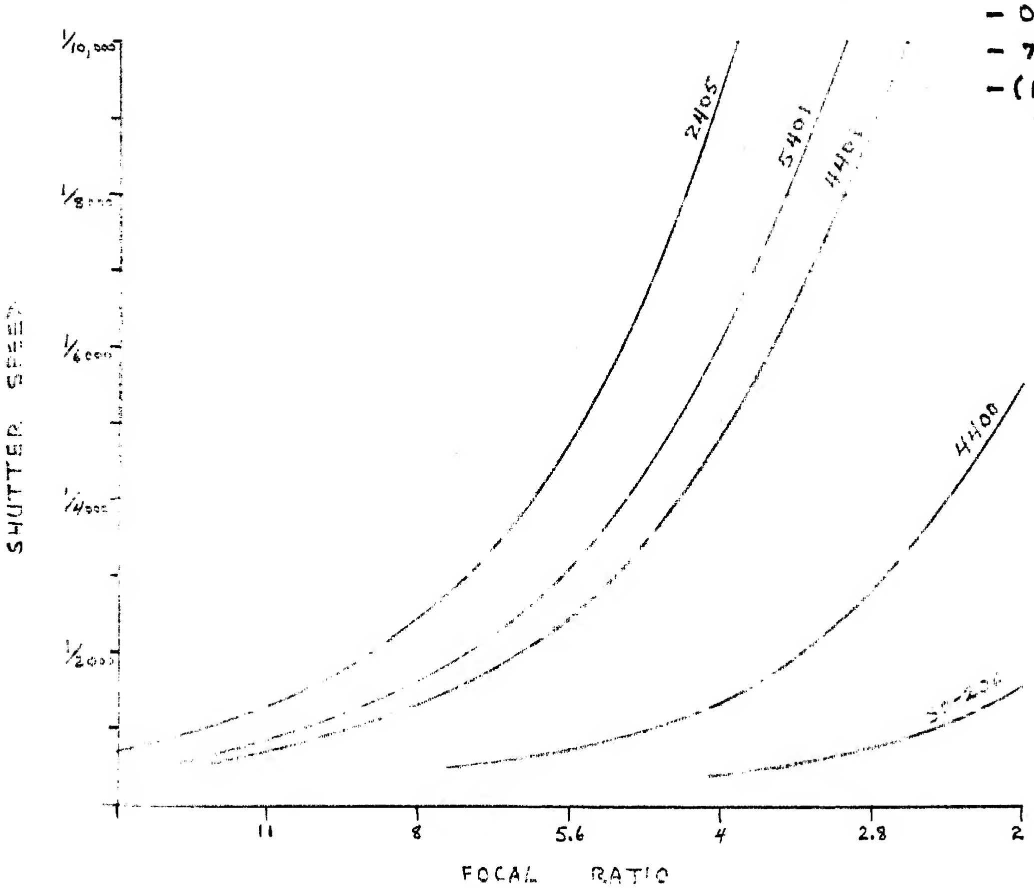

FIGURE C-39

LIMITING ANGULAR RESOLUTION

5 INCH LENS DIAMETER

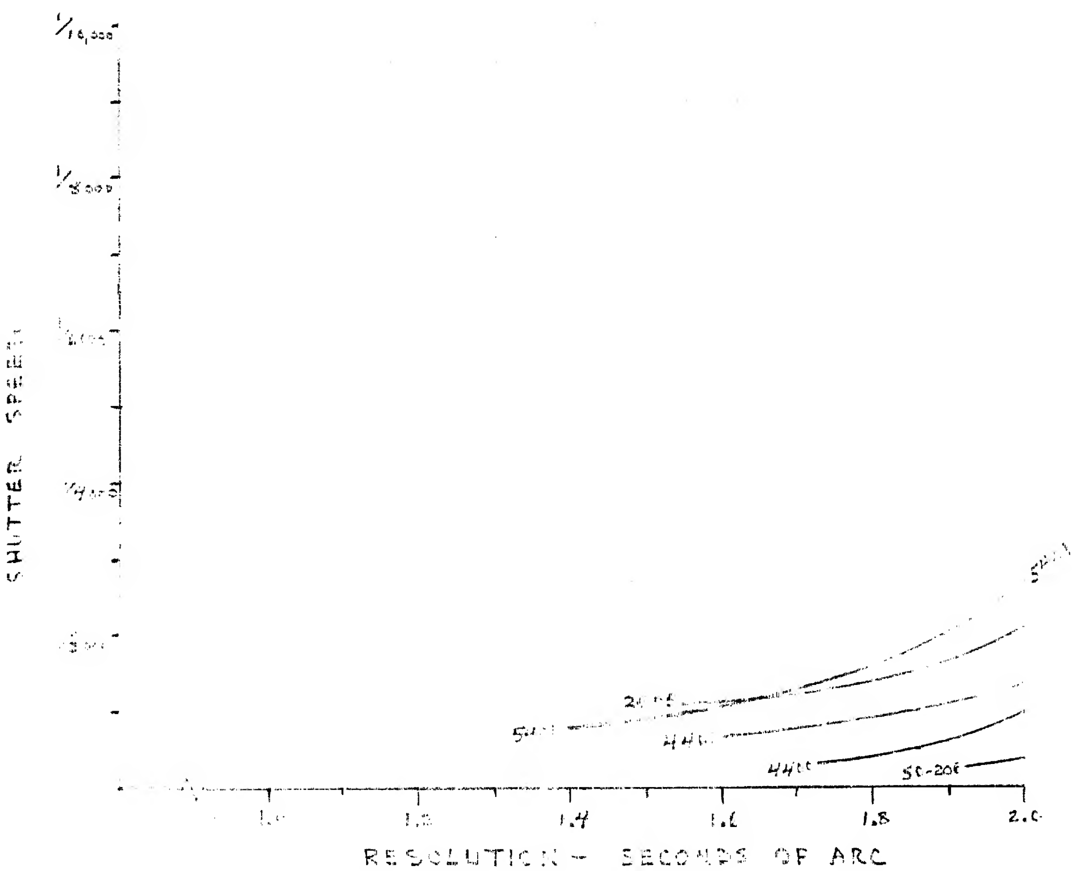

SECRET LIMITED DISTRIBUTION

FIGURE C-48

LIMITING ANGULAR RESOLUTION

7½ INCH LENS DIAMETER

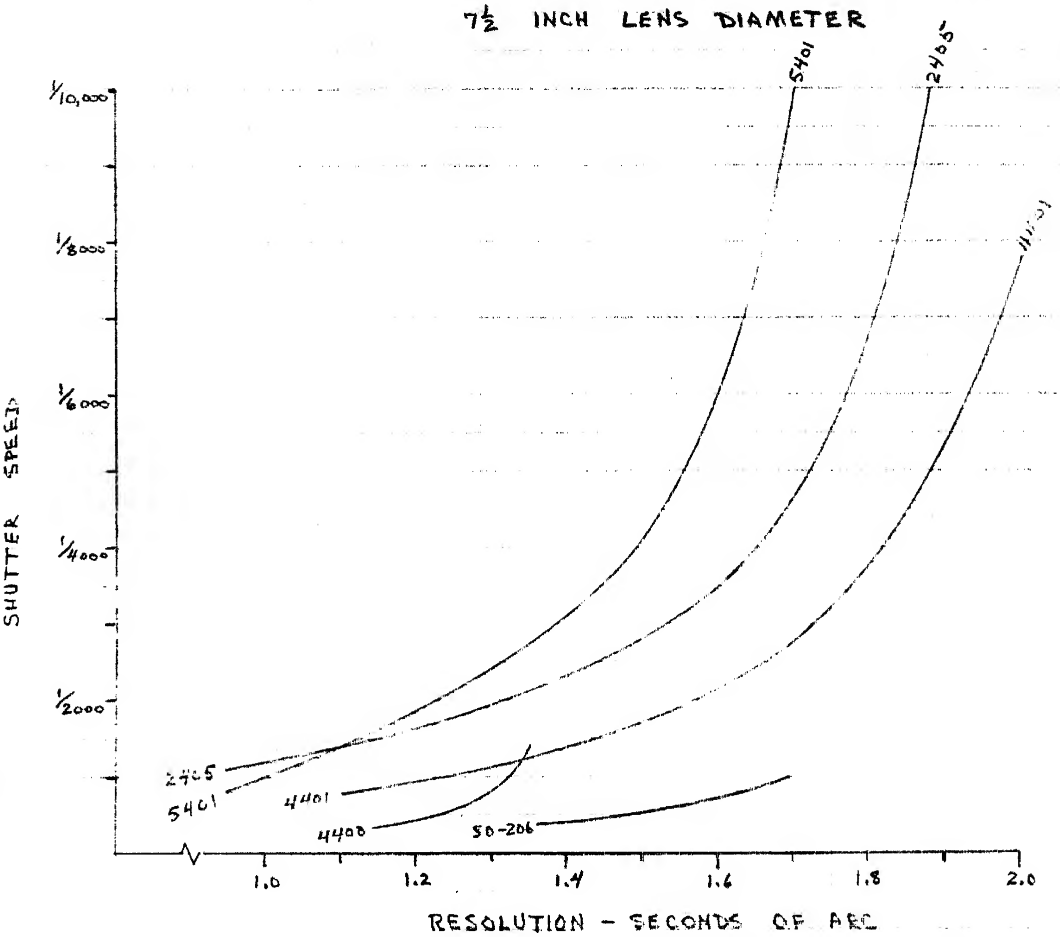

FIGURE C-41

SECRET LIMITED DISTRIBUTION

Approved For Release 2003/12/09 : CIA-RDP75B00157R000100110001-0

LIMITING ANGULAR RESOLUTION

10 INCH LENS DIAMETER

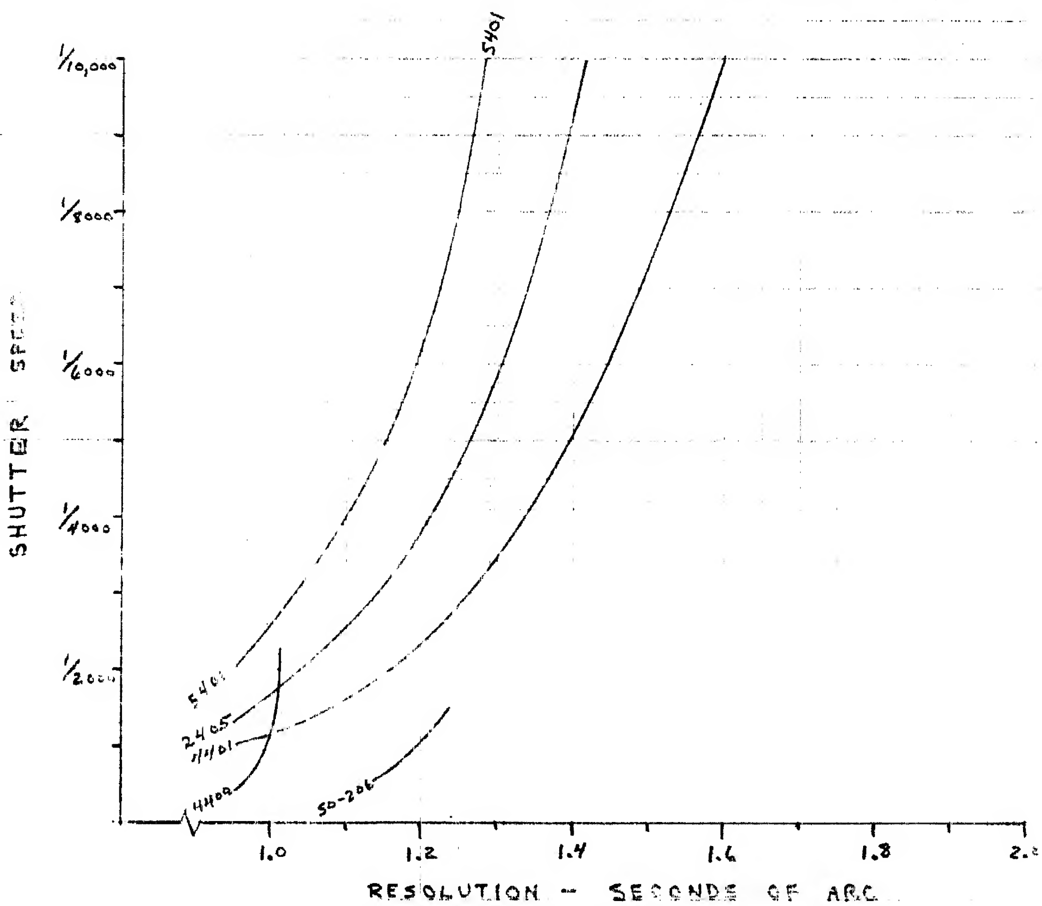

FIGURE C-42

LIMITING ANGULAR RESOLUTION

AS A FUNCTION OF SHUTTER SPEED AND LENS DIAMETER

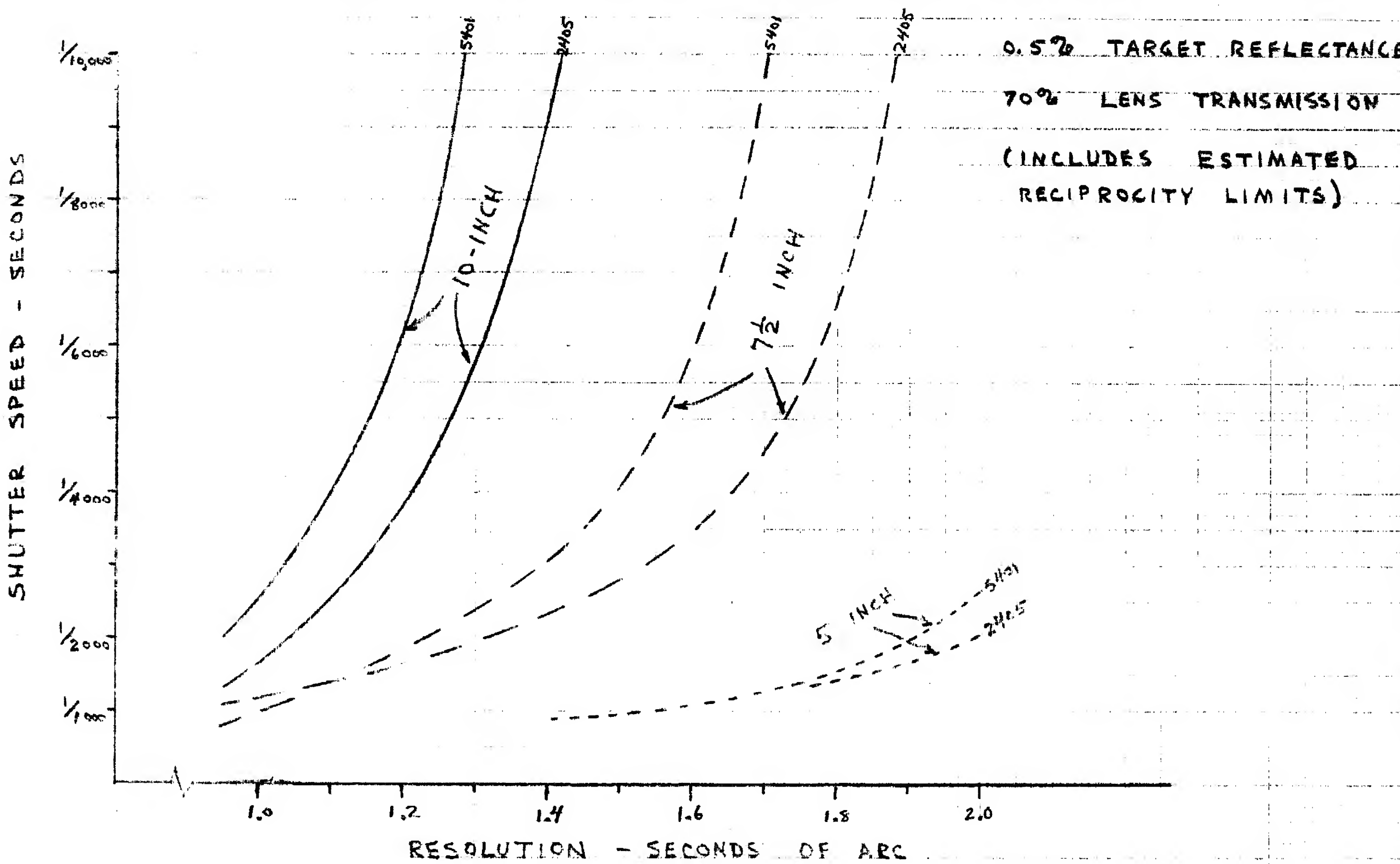

SECRET LIMITED DISTRIBUTION

FIGURE C-43

EFFECT OF IMAGE MOTION ON MODULATION TRANSFER FUNCTION

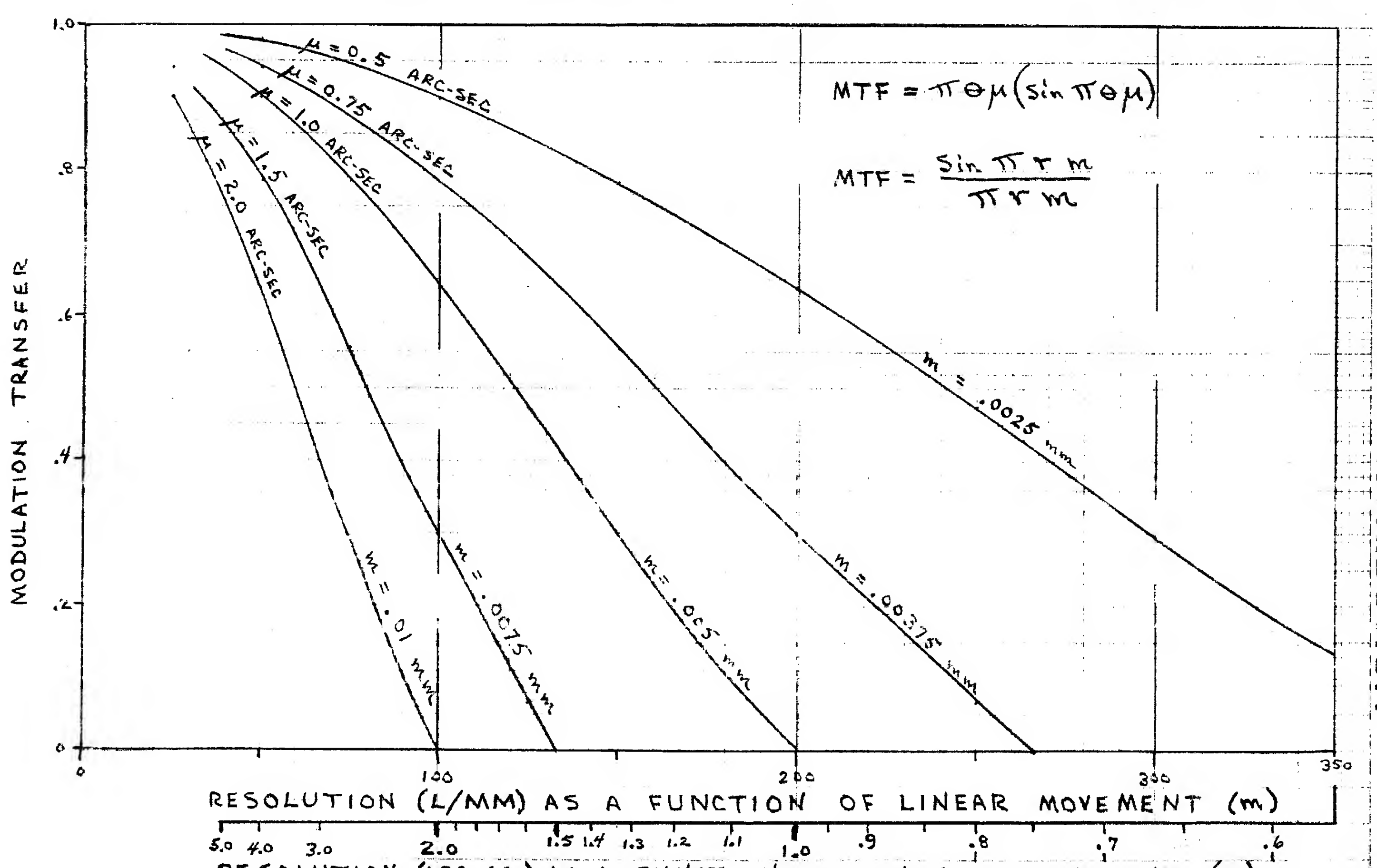

FIGURE C-44

TRANSFER FUNCTIONS FOR TWO REPRESENTATIVE SYSTEMS
(EFFECTS OF LENS/FILM TRANSFER FUNCTIONS -VS- EFFECTS OF TYPICAL IMAGE MOTION)

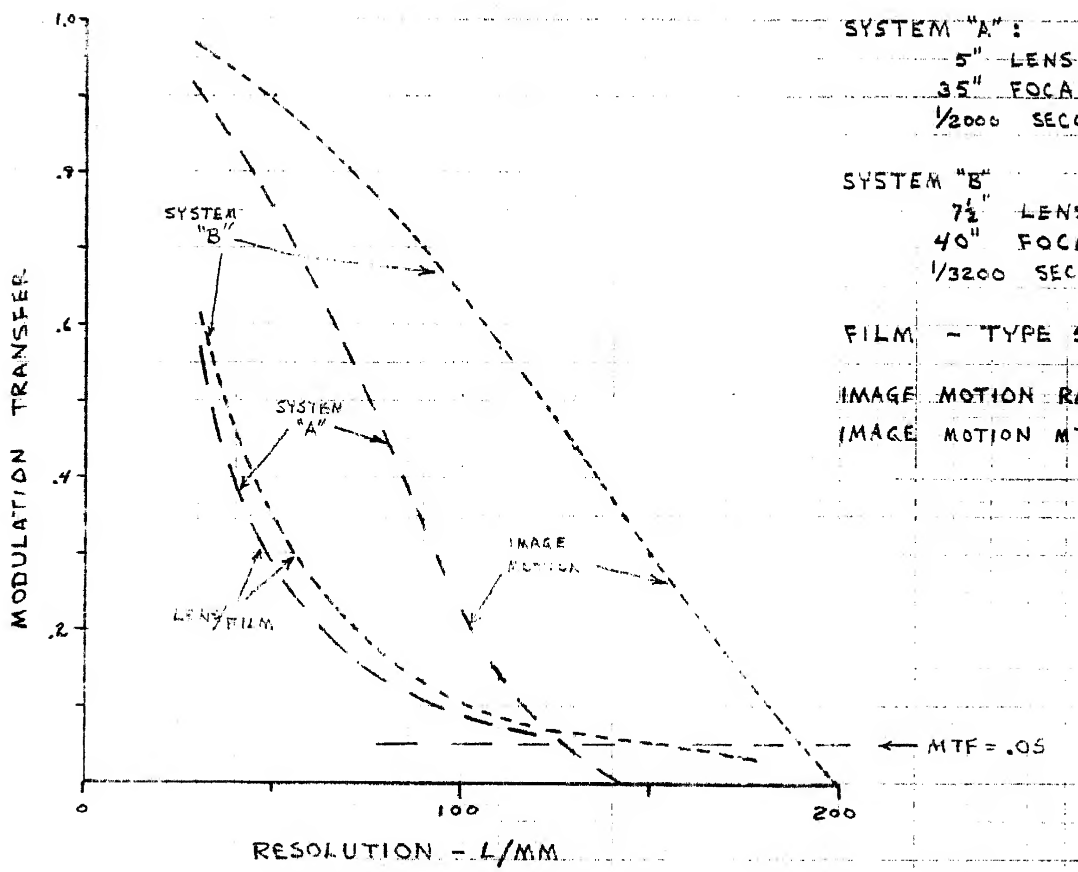

SYSTEM "A":
5" LENS DIAMETER
35" FOCAL LENGTH
1/2000 SECOND SHUTTER SPEED

SYSTEM "B"
7½" LENS DIAMETER
40" FOCAL LENGTH
1/3200 SECOND SHUTTER SPEED

FILM - TYPE 5401, ASA 80

IMAGE MOTION RATE - 16 MM/SECOND
IMAGE MOTION MTF = $\sin \pi n x / \pi n x$
where: n = L/mm
x = movement

FIGURE C-45

COMBINED SYSTEM TRANSFER FUNCTIONS — ANGULAR RESOLUTION

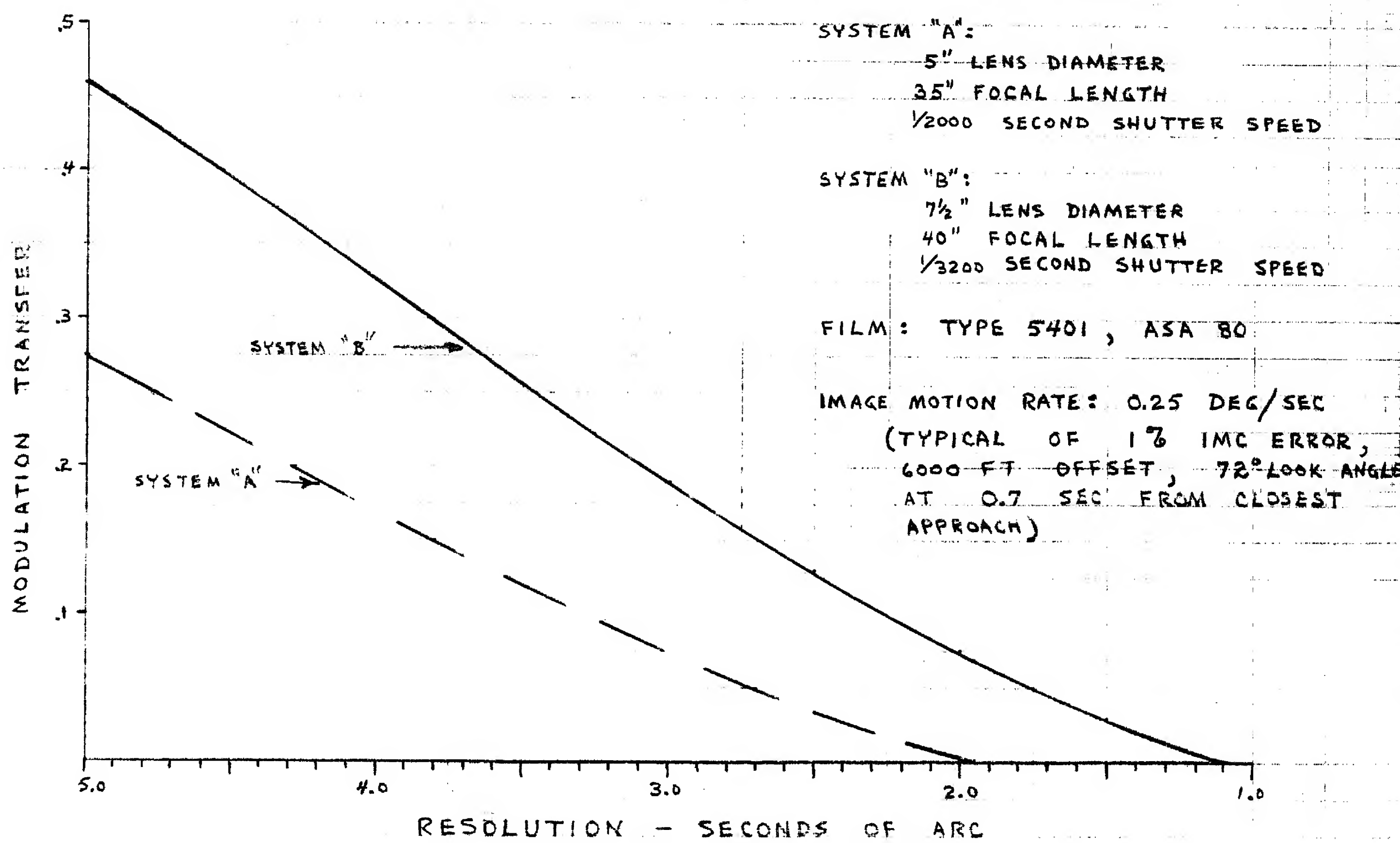

FIGURE C-46

For purposes of preliminary ALIAS system selection and evaluation, the RMS value of angular resolution versus image motion effects was more readily assessed for widely varying conditions, and was therefore used for evaluating system performance for various intercept parameters. The intercept problem; with angular resolution and shutter speed requirements for obtaining one-inch resolution, each considered separately; is shown in Figure C-47. One percent IMC accuracy is assumed for the shutter speed plots on this chart. Estimated RMS resolution values resulting from the combined lens/film/ motion effects for two candidate camera systems are shown in Figure C-48. Effects of variations in IMC error for these two systems, (as required to resolve $1\frac{1}{2}$ inch), are shown in Figures C-49 and C-50. The effects are much more pronounced at the larger missile offset distances, (smaller look angles) indicating a system performance trade-off between missile CEP and IMC tracking accuracy. A summary of anticipated ALIAS system intelligence collection capability (at 1.4 arc-sec resolution, 1/4000 sec shutter speed, and 1% IMC error) as a function of missile offset distance, is shown in Figure C-51. The shaded central limiting zone surrounding T=0 does not represent absolute limits of photography; but rather, indicates the time at which the quality of the photographic coverage would begin to deteriorate rapidly.

e. Summary - The use of modulation transfer functions to describe the general case of system resolution capability under widely varying intercept conditions becomes too complex for manual computation;however, the use of modulation transfer functions as point-checks of the limiting factors shown in paragraphs a, b, and c, above, provides reasonable confirmation of the system performance capability derived from the analysis of geometric limits. In any case, accurate prediction of operational system performance will require laboratory tests and simulation of the many photographic parameters. System design optimization must be derived, at least partially, by empirical techniques.

5. System Interface Design Factors

The design of the ALIAS sensor system is based on straight-forward optical and mechanical concepts; however, the stringent performance requirements will dictate optimal design of all camera parameters, and use of very precise control inputs from other ALIAS subsystems. Figure C-52 is a preliminary sketch of the suggested ALIAS camera configuration.

a. Time-Shared Tracking Functions. Since the primary sensor system (which is actually in operation for less than 4 seconds) is a very precise instrument, operating in the space environment, it is logical to share functions with the target tracking subsystem in order to exploit every possible advantage for accurate pointing and camera adjustment during the picture-taking sequence. In addition, the homing guidance technique selected for correction of initial ALIAS trajectory errors, (caused by ephemeris inaccuracies at time of launch), will require long range target acquisition and tracking for guidance purposes. Fortunately the selected sensor primary optics are ideally suited to both the guidance and tracking requirements.

COMPARISON OF ANGULAR RESOLUTION AND SHUTTER SPEED LIMITS FOR 1-INCH RESOLUTION
ONE PERCENT IMC ERROR – 3000 FPS VEHICLE VELOCITY

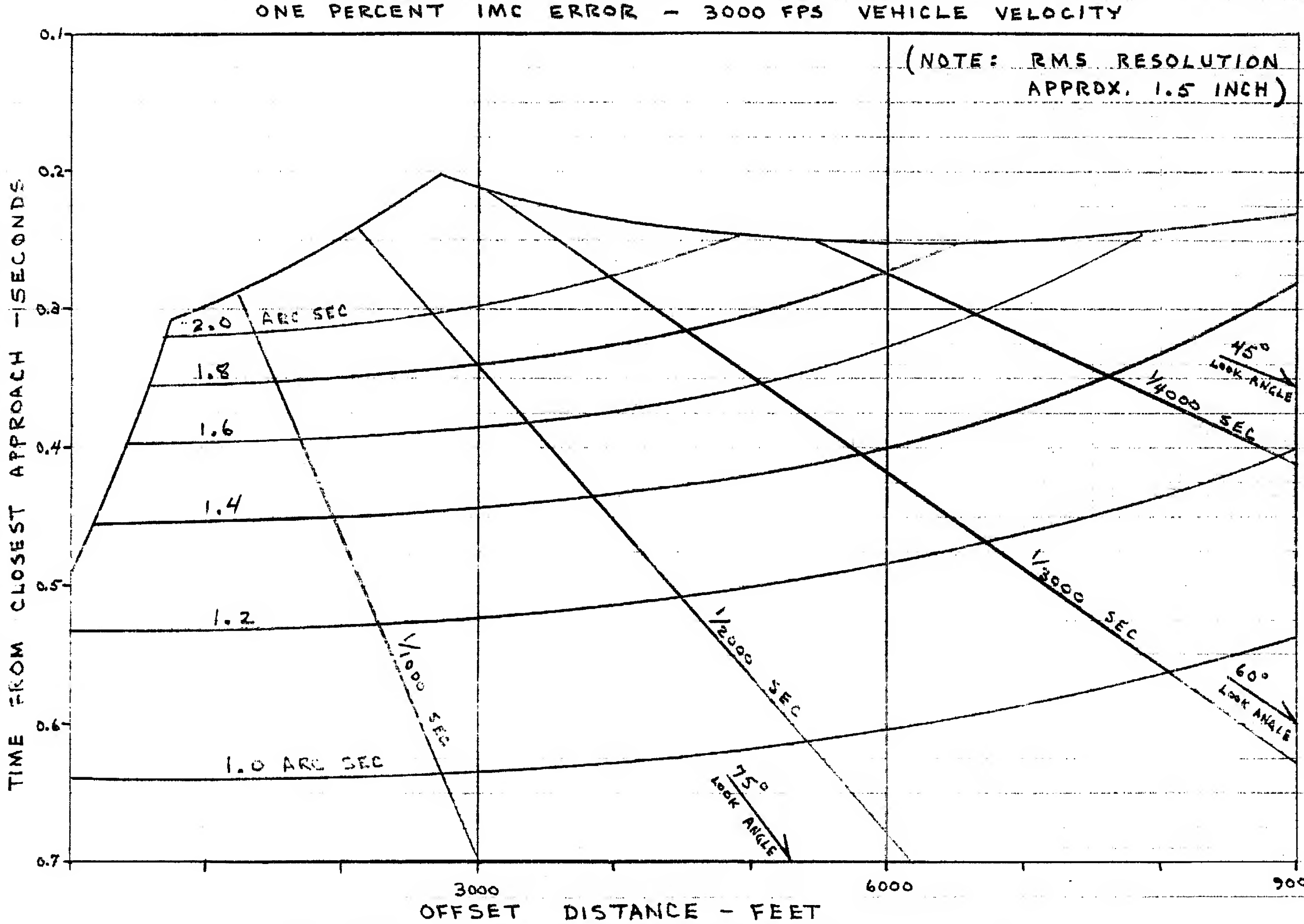

SECRET LIMITED DISTRIBUTION

FIGURE C-47

PERFORMANCE COMPARISON OF TWO CANDIDATE SENSOR SYSTEMS: (RMS RESOLUTION)
(ASSUMING 1% IMC ERROR)

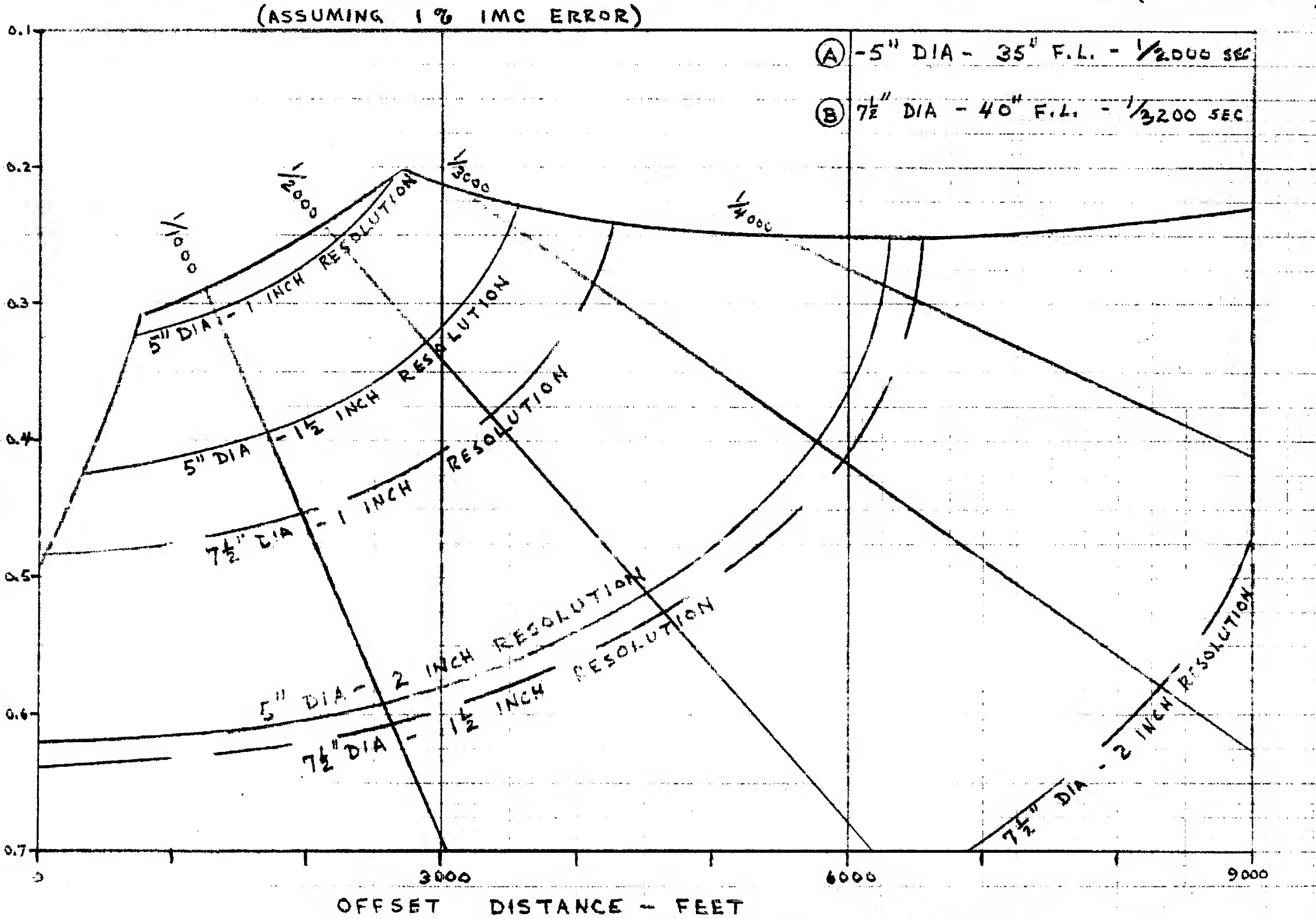

FIGURE C-48

SECRET LIMITED DISTRIBUTION

ESTIMATED EFFECTS OF VARIATIONS IN IMC ERROR: FOR RESOLUTION OF 1½ INCH

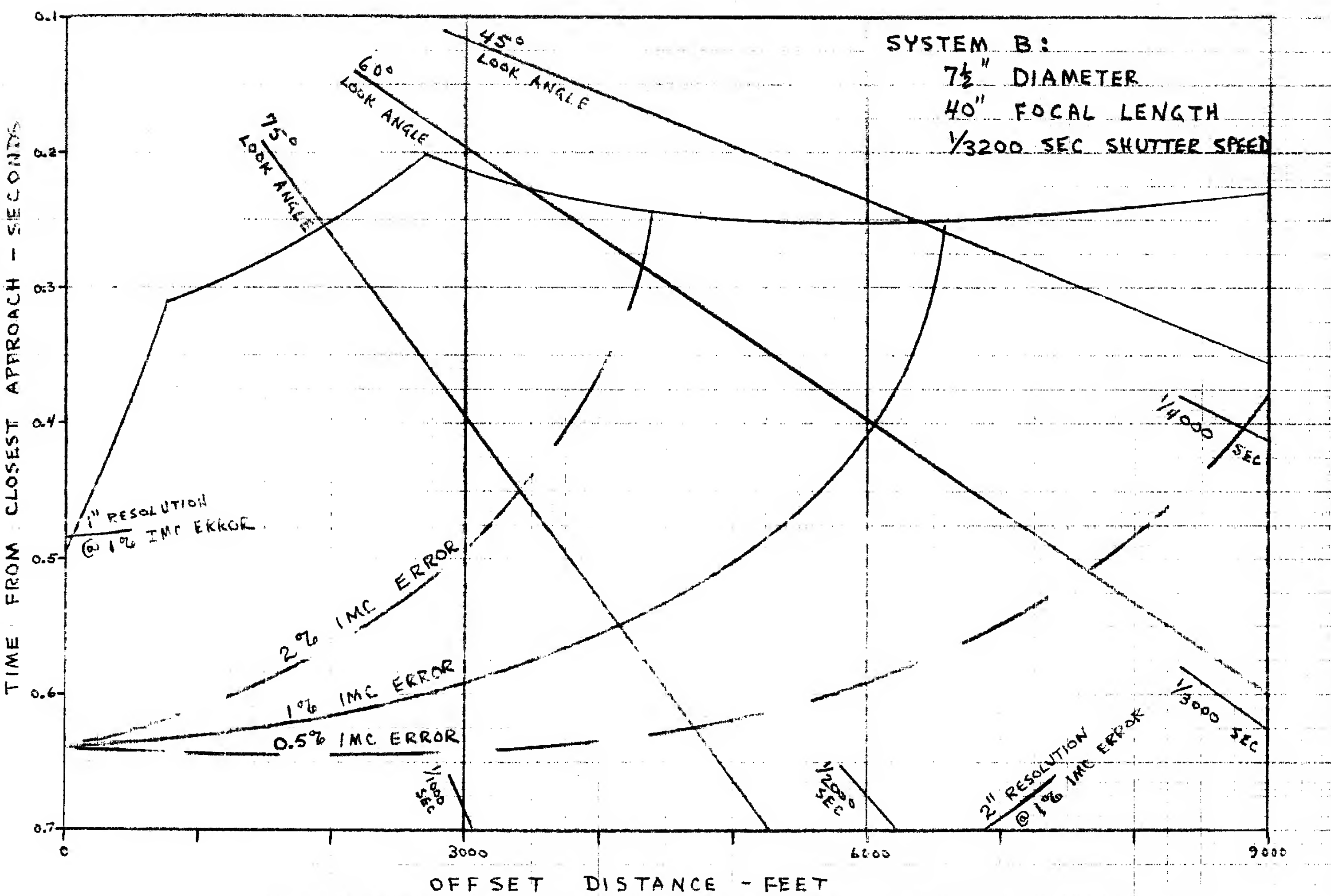

FIGURE C-49

ESTIMATED EFFECTS OF VARIATIONS IN IMC ERROR: FOR RESOLUTION OF 1½ INCH

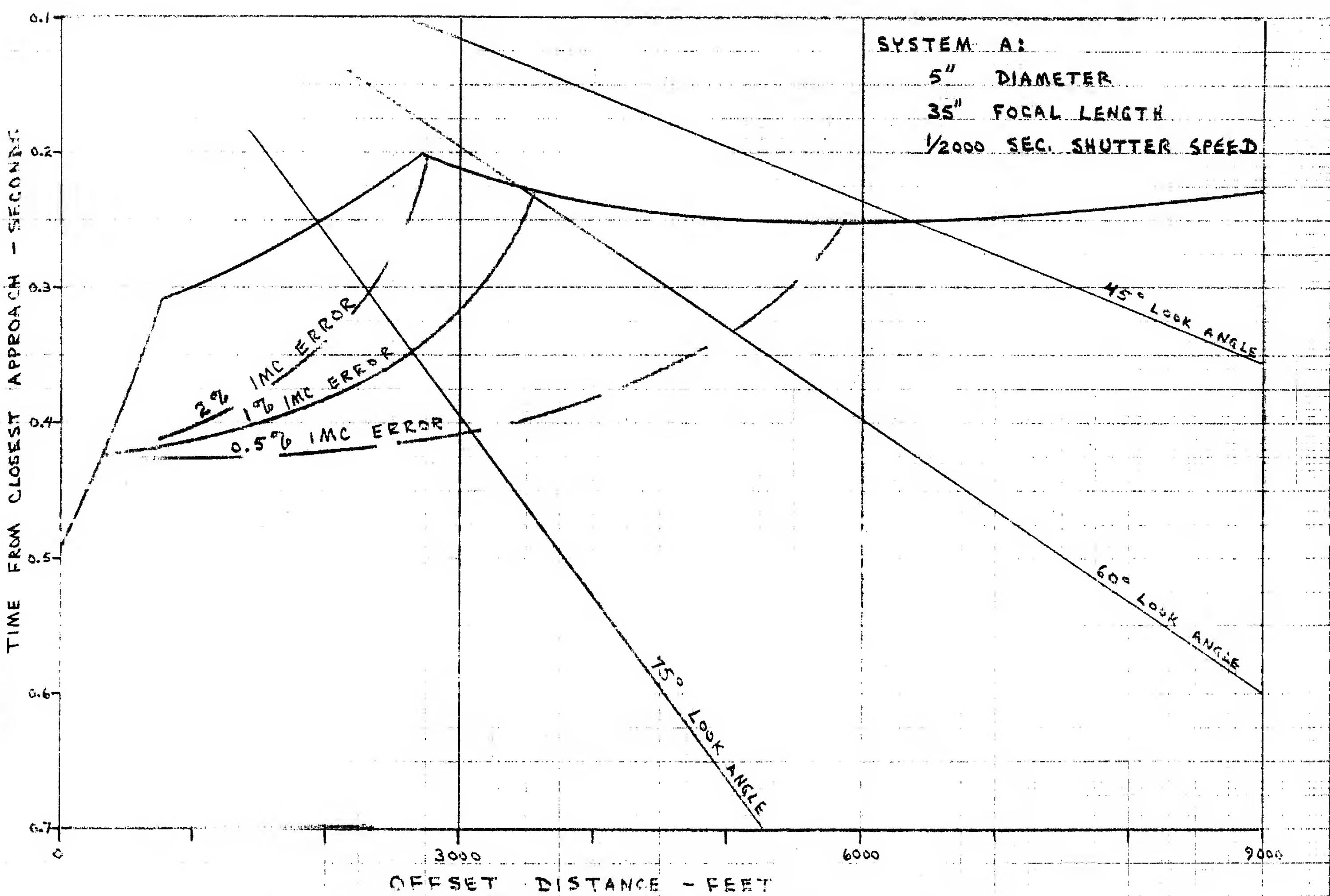

FIGURE C-50

SECRET LIMITED DISTRIBUTION

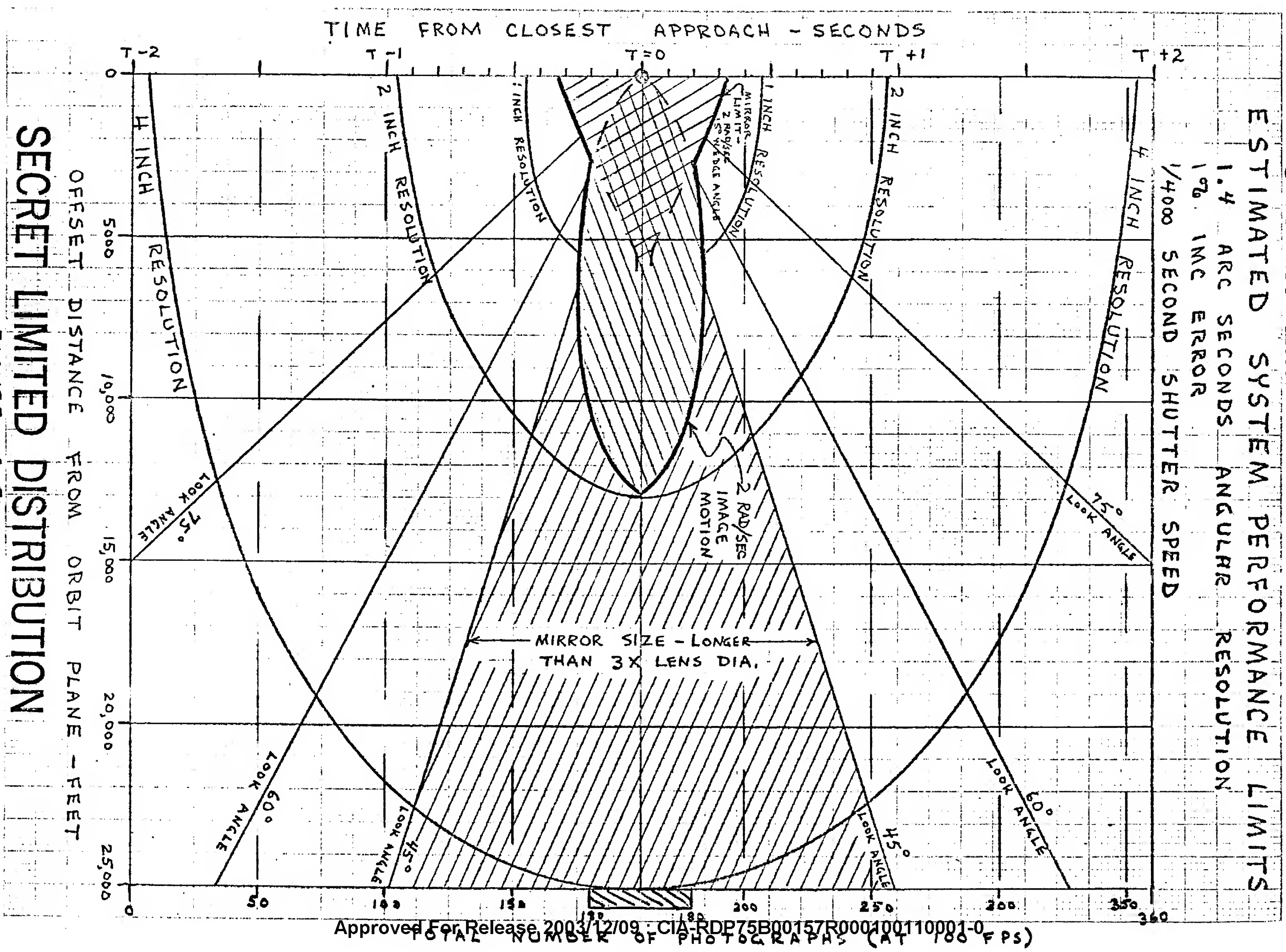

SECRET LIMITED DISTRIBUTION

FIGURE C-51

C-72

GENERAL LAYOUT OF CAMERA SYSTEM

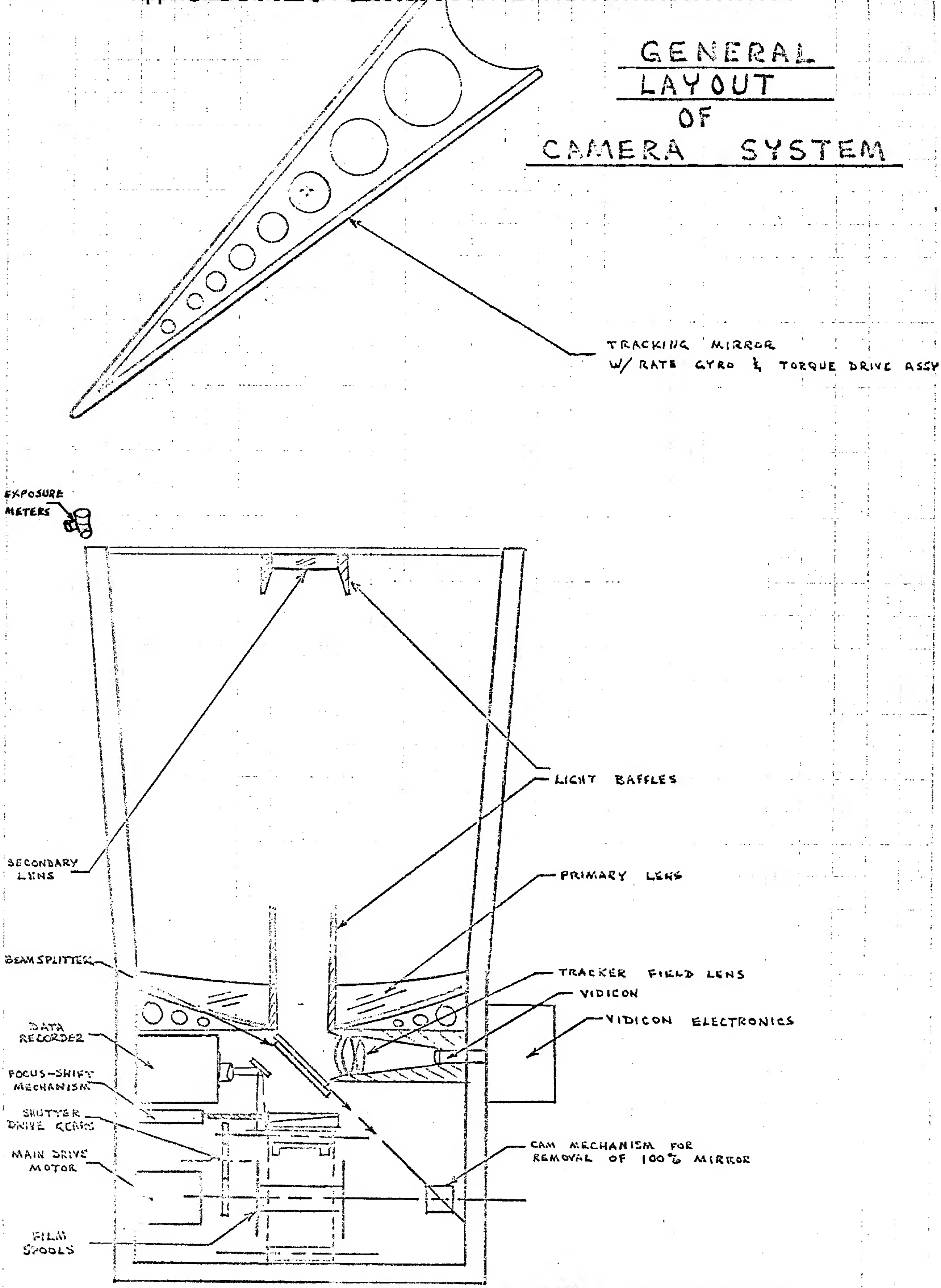

Sharing of the optical path will be accomplished for initial target acquisition and tracking by use of a 100 percent reflecting mirror and field lens for focusing the incoming target/background illumination on the guidance-tracker vidicon (or orthicon) face. At acquisition ranges, the target will represent a point-source. Just prior to the picture-taking sequence the target angular subtense will be large enough to be imaged on the tracker face. At this time, a beamsplitter reflecting 5 to 10 percent of the target image illuminance will replace the 100 percent mirror, and appropriate adjustments will be made to the tracker for subsequent image motion compensation. The remaining 90-95 percent of the available illuminance will be transmitted to the film format for the photographic sequence.

b. Control of Resolution Factors. Three significant factors affect the quality of camera resolution. These are: 1) image motion compensation, 2) adjustment of camera back focal distance, and 3) elimination of random vibrations.

(1) Image Motion Compensation - Tracking stability during the picture-taking sequence should be one degree-per-second or better. A feedback control loop will be required for controlling tracking mirror rotation to this rate accuracy. The rapid angular acceleration of the line-of-sight during the most important portion of the photographic sequence presents the most significant constraint on system performance. Figures C-53, C-54 and C-55 show acceleration histories for three offset distances, and for both early and late ALIAS vehicle arrival times.

Theoretically the IMC tracking error signal could be derived by sensing the angle rate mismatch between the mirror and the actual target line-of-sight; however, the error-sensing time-constant of a full-frame vidicon tracker (50 cps) will not allow time resolution feedback of error signals to correct for the the rapid angle rate changes occurring during the most critical part of the photographic sequence. Since target image excursions will normally be restricted to a narrow line normal to the mirror axis, it should be possible to decrease the vidicon scanned area and thus increase the frame rate by perhaps a factor of 10. Assuming maximum vidicon resolution, (.012 degrees with 6 degree field), and the shortest error sensing time-constant,(about .002 second), the problem of correcting the line-of-sight rate by error sensing alone is still marginal. For instance, with ALIAS offset distance of 3,000 ft.

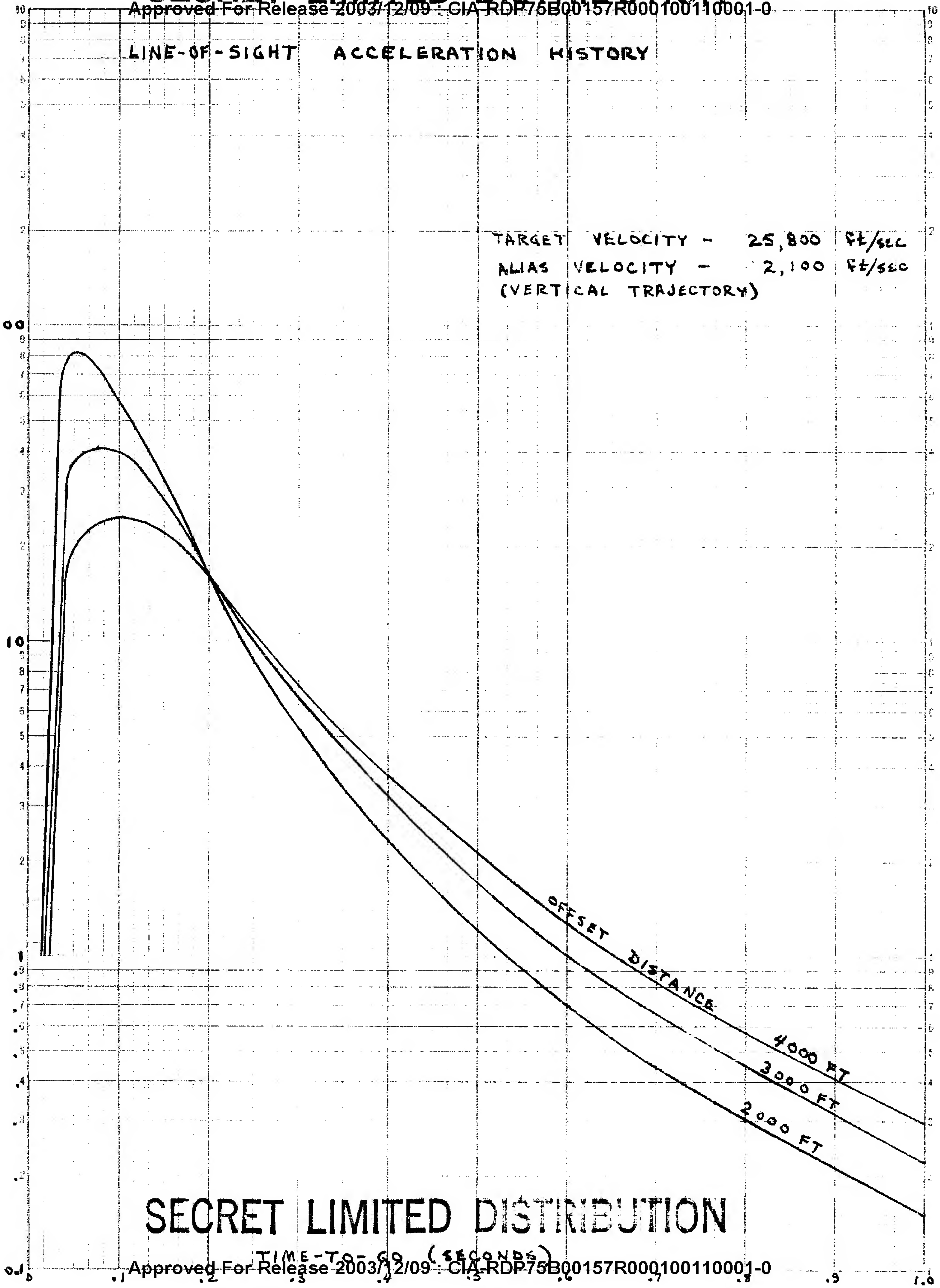
LINE-OF-SIGHT ACCELERATION HISTORY
TARGET VELOCITY - 25,800 ft/sec
ALIAS VELOCITY - 2,100 ft/sec
(VERTICAL TRAJECTORY)
OFFSET DISTANCE
4000 FT
3000 FT
2000 FT
$\dot{\omega}$ (RADIANS/SEC^2)
TIME-TO-GO (SECONDS)

FIGURE C-53

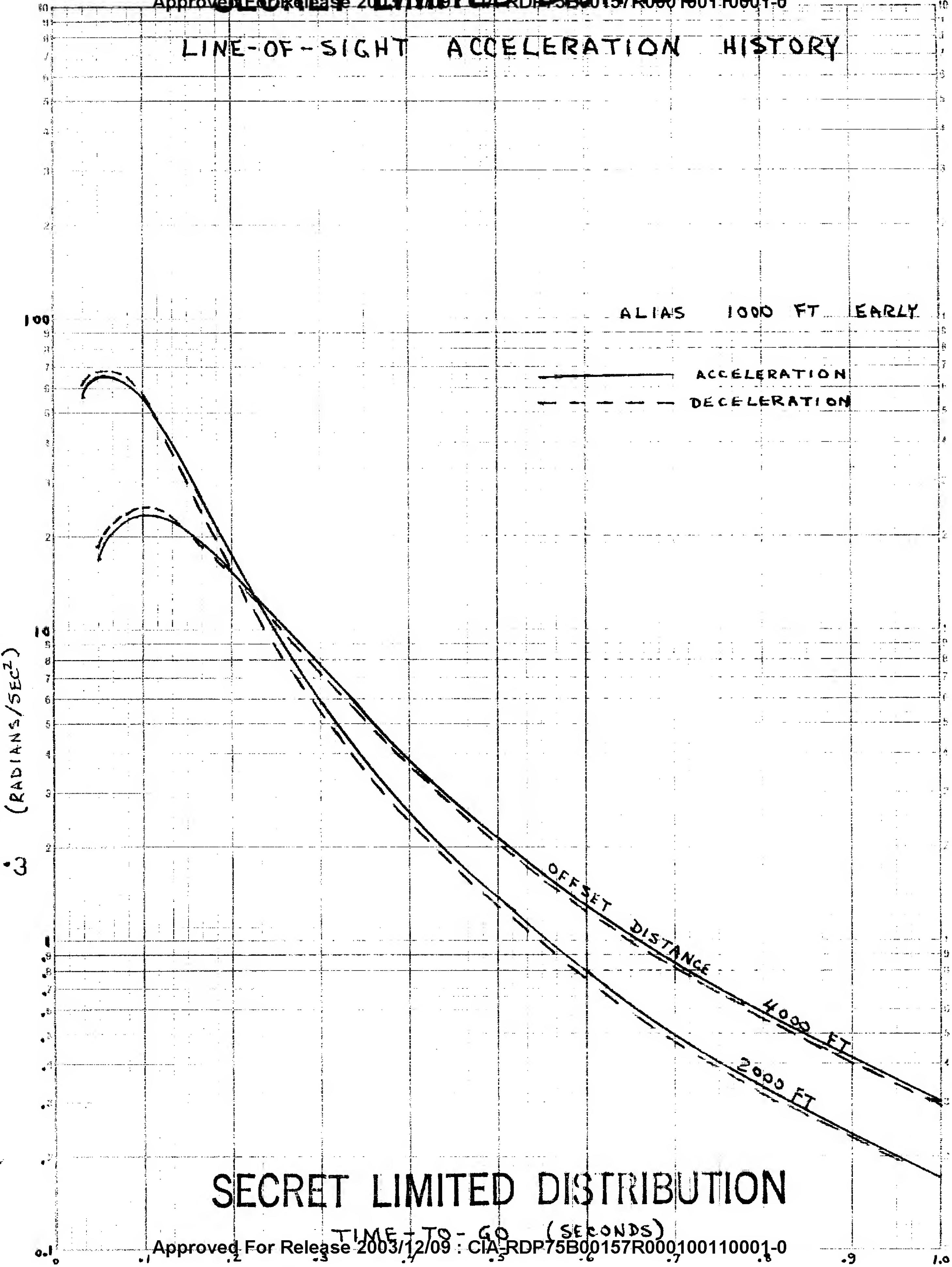
LINE-OF-SIGHT ACCELERATION HISTORY
ALIAS 1000 FT EARLY
ACCELERATION
DECELERATION
OFFSET DISTANCE
4000 FT
2000 FT
$\dot{\omega}$ (RADIANS/SEC^2)
TIME-TO-GO (SECONDS)
100
10
1
0.1
0
.1
.2
.3
.4
.5
.6
.7
.8
.9
1.0

FIGURE C-54

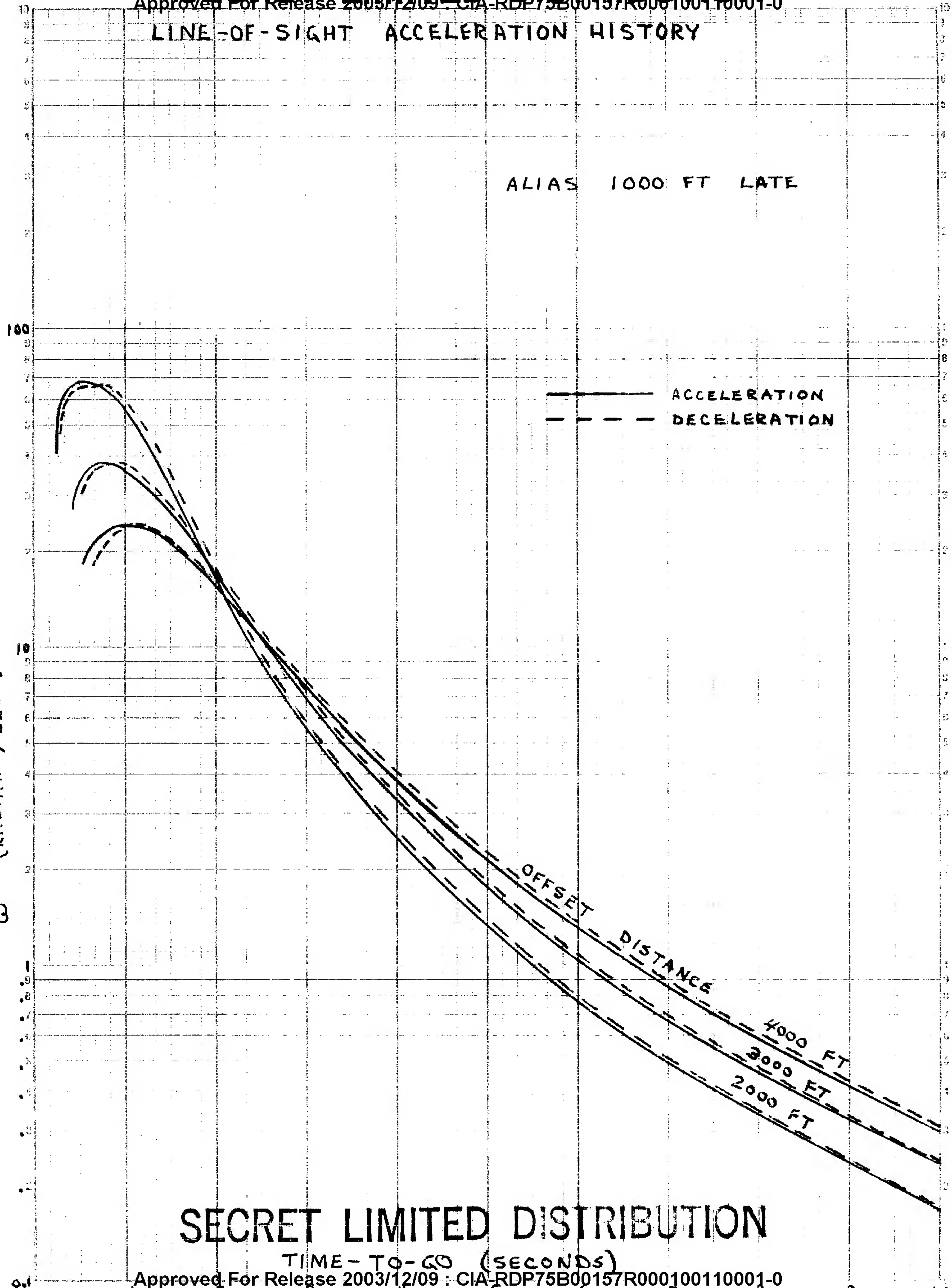
LINE-OF-SIGHT ACCELERATION HISTORY
ALIAS 1000 FT LATE
ACCELERATION
DECELERATION
OFFSET DISTANCE
4000 FT
3000 FT
2000 FT
(RADIANS/SEC^2)
100
10
1
0.1
0
.1
.2
.3
.4
.5
.6
.7
.8
.9
1.0
TIME-TO-GO (SECONDS)

FIGURE C-55

at .4 seconds from closest approach, the line-of-sight acceleration is 3 radians/sec^2, which constitutes an angle rate change of over .3 degrees/second/frame. Angular rate readout errors also accrue from vidicon electronic scanning beam resolution limits, from scanning beam linear time-base errors, and from tracking different points on the target during successive scans. Use of either target centroid or target image leading edge tracking will be necessary in order to reduce the latter error.

Matching of the line-of-sight error sensing to predicted line-of-sight angular acceleration characteristics should greatly improve the angle rate readout accuracy, particularly during the critical period of rapid acceleration change. This third-derivative matching solution is necessarily iterative, since the computed angular rate at the time each line-of-sight angle is measured is dependent upon the acceleration predicted during the previous vidicon scan; which in turn is dependent upon the predicted time-to-go and the predicted final offset distance. The iterative solution is first initiated when the aircraft/target range measurements provide the first prediction of time-to-go. By iteration, the angular rate error will converge to decreasing level as time-to-go approaches zero. With perfect acceleration prediction, the angular velocity error may be reduced to 15-20% of the value produced by error sensing alone.

The derived torque command signals will be supplied to the mirror drive at more frequent intervals than the vidicon frame rate. The torque command will be based on predicted LOS acceleration, on predicted rate of change of LOS acceleration, and the difference between the predicted LOS rate and twice the actual rate of the half-speed mirror. A rate gyro mounted within the mirror will provide for measurement of actual mirror rate. The desired angular rates can be generated from the vidicon-measured angles and estimated time to go. Typical values are shown in Figure C-56.

The rotational moment of inertia for a mirror of $7\frac{1}{2}$ inch width is estimated to be about .03 slug-ft^2. Maximum mirror acceleration, (at 2000 ft. offset distance), is less than 9 radians/sec^2. With one ft-lb of torque available, rate errors of 2 degrees/sec could be corrected in about .005 second.

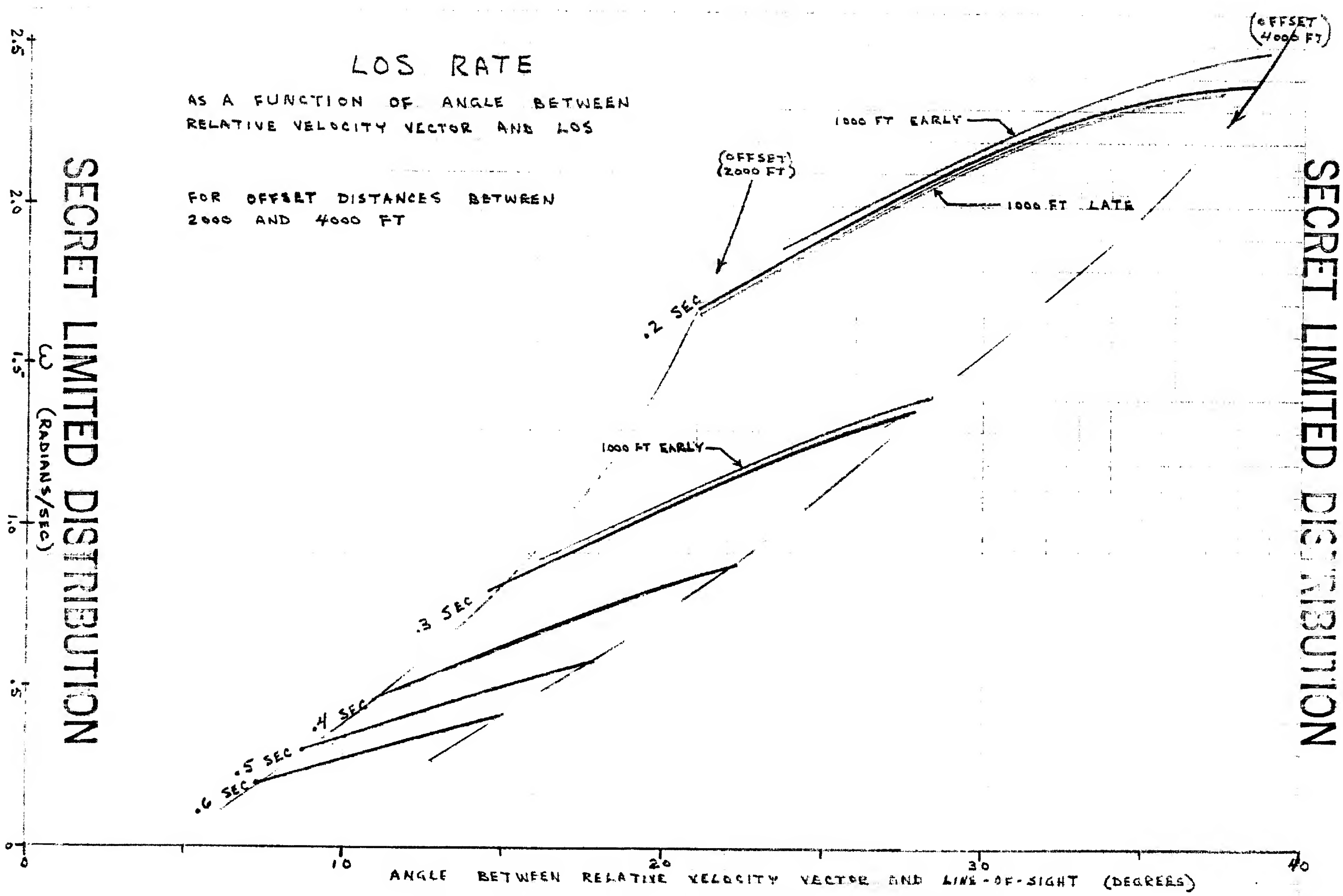

SECRET LIMITED DISTRIBUTION

FIGURE C-56

Roll-position errors in positioning the mirror rotational axis would induce sizable image motion errors. Attitude misalignment of $\frac{1}{2}$ degree will induce an error roughly 1/180 of the line-of-sight rate; at 3000 ft. off-set and .2 second to go, this alignment error alone would induce LOS rate errors exceeding IMC accuracy limits. Roll-position corrections must therefore be derived from the vidicon error signal and updated continuously throughout the entire photo sequence.

(2) Focus Adjustments - The effect of focus blur on image modulation functions has not been quantitatively assessed; however, from Figure C-21 target range measurement errors of over 10 percent are seen to be within the geometric limits specified (for first minima of a point image circle of confusion). A 5 percent range error would produce virtually no resolution loss for a system with $7\frac{1}{2}$ inch aperture diameter. The tracking accuracy required for image motion compensation provides precise angle and angle rate data for range derivation which can be readily predicted to considerably better than one percent during the critical portion of the photo sequence. Range accuracy within one percent will be obtained throughout the entire photo sequence. Focus adjustment will be accomplished by an optical wedge pair, controlled by the derived target range signal.

Some focus shift may occur due to thermal gradients during missile flight. Although thermal stabilization may not be reached prior to the photo sequence, there should be no measurable change during the short picture-taking period. Focus adjustments for the predicted optical (structural) dimensions at time of photography will be pre-set. No continuous focus adjustments other than range variations will be required.

(3) Random Vibrations - The high shutter speeds required for the ALIAS sensor system will greatly reduce effects of internal vibration; however, all structural members and all moving parts should be designed for minimum vibration and for high frequency damping. The small mass of those mechanisms required for camera operation should present no problem. Payload attitude control forces will be quite small and are expected to be adequately damped by the payload structure and camera mounts.

c. Sensor Data Recording. An internal data recording strip will be exposed along the edge of each film frame to provide additional (binary-coded) data for assistance in analysis of the imagery. The data block need not be exposed through the focal plane shutter; hence, may use such techniques as neon bulb "light pipes" for exposure at about 1/250 second. The resolution of the recorded time should, however, be better than 1/1000 second, and should present on each frame the time at midpoint of the focal plane shutter travel. It is desirable that the data recording block provide the following information:

Frame number
Exposure meter readings, (see paragraph d, below)
Time at midpoint of shutter travel, (time from T=0)
Target range
X-Y angle
X-Z angle
Predicted LOS rate
Actual tracking angle rate

A data recording block capacity of about 50 bits should provide adequate resolution of those recorded values within the range of values required for frame-by-frame analysis. Correlation with information recorded aboard the ALIAS aircraft could serve to resolve any amibguities resulting from camera data record values falling outside the limits established by the capacity of the camera data block.

d. Camera Controls and Mechanical Functions. Camera control will be straightforward, based primarily on pre-set functions operating against a time-base (from T=0, the predicted time of closest approach).

Focus adjustments will be made by derived target range outputs obtained from the on-board computer.

Exposure control will be pre-set before launch, based on anticipated light values. It may be desirable to provide for varying exposure for the approaching and departing sequences, because of the different sun aspect angles. This could be accomplished by programming a change in shutter slit-width, or alternatively by splicing films of varied sensitivity (and resolution) to obtain the desired variation. In order to assure wide dynamic range, it may also be desirable to vary the exposure time (or film sensitivity) between alternate frames during the entire photo sequence. In order to provide further flexibility, it is recommended that exposure meters be installed (oriented on three axes) to record incident light readings from selected aspect angles. In practice, a short strip of film would be processed normally to obtain the initial recorded values. From sensitometric analysis of the few initial film frames, the ALIAS payload attitude, the solar aspect angles, and the incident light readings, it will then be possible to optimize the film development process for the remaining footage, so that the maximum information content can be extracted from the film.

A focal plane shutter, either rotating disc-type or linear belt-type, is recommended. Continuous operation during the photo sequence is desirable to reduce reactive effects of intermittent operation. A linear slit movement would simplify image rectification in the event of so-called focal-plane-distortion caused by image motion during the shutter travel time. Slit movement normal to the tracking direction, (i.e. across the small dimension of the format), would minimize the shutter travel time during each cycle.

Film cycling rate will be 50-100 fps, with 1-1½ inches forward movement per frame. Standard perforated 70 mm film should provide trouble-free cycling with semi-standard precision film handling mechanisms. Mechanical film flattening will be accomplished by an intermittent pressure plate. The film compartment and cycling mechanism will be pressurized to retain required film flexibility and humidity. It is anticipated that the pressure seal between the film chamber and the optics can be accomplished by the focusing wedge assembly without the need for an optical flat window. Some pressure bleed can be tolerated, and may even be desirable to increase flow of the pressurizing gas (N_2).

The additional mechanical motions required are:

(1) Removal of the 100 percent reflecting mirror used for tracking prior to the photo sequence. This is a simple hinged or sliding motion, as shown graphically in Figure C-52.

(2) Rotation of the slotted shield for the tracking mirror. This is accomplished during the dead time between T, minus .2 and T, plus .2 seconds to expose the reverse side of the tracking mirror for photographic coverage of the departing target aspect.

(3) Tie-down of the tracking mirror after termination of the photo sequence. This will be accomplished to avoid mirror damage from shock loads encountered during payload recovery.

e. Sensor Structure and Environment. No unusual problems are anticipated in fabrication and environmental control of the sensor package. The camera system will not be pressurized, with the exception of the film chamber as discussed above. Thermal conditioning will be accomplished by radiation and conduction. The only design problem foreseen will be that of providing dimensional stability during the final tracking and photo sequences. Reduction of flare light will be accomplished by standard internal baffling.

APPENDIX D

TERMINAL VEHICLE ANALYSIS

APPENDIX D

TERMINAL VEHICLE

1. Introduction

There is little question that the design of an ALIAS terminal vehicle is feasible given the adequacy of the sensor package and guidance subsystem as described in Appendicies B and C respectively. There is little in the vehicle performance requirements which demands a unique solution to technical problems that have not been faced in similar applications before. The design of the vehicle's primary structure, aerodynamic heating protection, aerodynamic stability and control elements and, recovery equipment therefore may draw heavily on existing documented experience to effect an efficient solution. The only potentially stringent design problem that could arise in the ALIAS terminal vehicle development is in meeting the requirements for precise attitude control during the photographic sequence.

The true significance of this analysis of the terminal vehicle therefore is not with regard to its own feasibility but rather with its interaction on other total ALIAS system components. Of major importance here is the effect of the terminal vehicle configuration and weight upon the sizing of the booster vehicle. These data are undoubtably the most sensitive inputs to the booster vehicle analysis. This analysis of the ALIAS terminal vehicle therefore has necessarily taken the form of a rather detailed preliminary design effort in its attempt to yield data for assessing terminal vehicle effects on boost vehicle requirements and in turn on the total ALIAS concept.

2. Sizing Analysis

The terminal stage vehicle is sized primarily by the trajectory correction requirements as well as the payload weights and dimensional restrictions. Payload weights have been estimated with a reasonable degree of confidence to approximate 154 lbs. and to be packageable within an 18 inch diameter which is consistant with the anticipated boost stage dimensions. Since these values would not be expected to vary more that $\pm$ 10% they were assumed as constant to simplify the terminal vehicle sizing analysis. Primary performance requirements of the terminal vehicle are: its need to provide an incremental velocity correction capability, (ΔV); its need to control its attitude and its need for internal temperature control in the payload section. These factors can readily be seen to be more or less dependent upon the gross weight of the vehicle and its overall configuration. Another size and configuration dependent factor is the weight of the vehicle primary structure. The structure is also a weak function of the maximum load factor experienced by the system which on the basis of payload considerations has been constrained to less than 20 g's throughout the entire flight sequence.

SECRET LIMITED DISTRIBUTION

A generalized expression for the terminal vehicle weight estimate may be written:

$$W_g = W_{pl} + W_v \qquad (1)$$

where: W_g = gross stage weight

W_{pl} = payload (fixed) weight

W_v = size & performance dependent (variable) weight

Payload fixed weights may be grouped as:

$$W_{pl} = W_c + W_g + W_j + W_r \qquad (2)$$

where: W_c = camera sensor weights

W_g = guidance component weights

W_j = special structure weights

W_r = recovery system weights

A detailed weight estimate of the fixed payload components was made on the basis of known weights of candidate or similar components as follows:

Group	Component	Weight - lbs
Sensor	tracking mirror	10.0
	torquemotors	4.0
	rate gyro	0.5
	angle pickoff	.8
	secondary mirror	4.0
	primary mirror	18.0
	image splitter	0.5
	vidicon	0.2
	vidicon control electronics	9.0
	glass plate	2.0
	film	2.0
	film cannister	3.0
	film transfer mechanism	5.0
	data recorder	3.0
	shutter	3.0
	Sub-total sensor group	65.0

Group	Component	Weight - lbs
Guidance [1]	UHF antennas	1.0
	power supply	7.0
	transmitter/receiver	5.0
	encoder/decoder	3.0
	computer [2]	20.0
	inertial platform [3]	27.0
	sub-total guidance group	63.0
Special structure	Nose fairing	6.0
	plastic foam	3.0
	slotted mirror shields	6.0
	sub-total special structure	15.0
Recovery components	21 ft. diam. silvered parachute [4]	6.0
	reflective mylar balloon & 50 ft tether line [5,6]	2.0
	dye marker	1.5
	strobe light	1.5
	sub-total recovery components	11.0
W_{pl} = total fixed payload weight		154.0

1. Guidance System for the Large Payload Test Vehicle Program, February 1965, Nortronics 65-25

2. NIS-105 Suitcase Navigator, Nortronics 65-67

3. NDC-1050 Data Processor, Technical Description, Nortronics 64-339

4. United States Air Force Parachute Handbook, Wright Air Development Center Report WADC 55-265, December 1956.

5. Aerial Recovery and Cargo Delivery Systems, F. Highley & R. Parker, SAE Report 915A, October 1964

6. Drogue Parachute Weight, K.E. French, Astronautics & Aerospace Engineering, June 1963

SECRET LIMITED DISTRIBUTION

The sum of the system dependent weights may be expressed as:

$$W_v = W_s + W_t + W_a + W_m \tag{3}$$

where the size & performance dependant component weights are:

W_s = primary structure

W_t = thermal control

$W_{a/c}$ = attitude control system

W_m = velocity correction motor

Three relationships for preliminary estimates of the size dependent component weights were obtained from an STL study 7/ and are reproduced on Figure D-1. The second of these figure K_s vs W_g was adjusted to our assumed vehicle diameter of 18.0 inches. An initial estimate of gross vehicle weight, W_{gi} = 300 lb was obtained from the first figure assuming ΔV = 1000 ft/sec for a mean thrust to weight ratio $(\overline{F}/\overline{W}_g) = 5.0$ and W_{pl} = 154 lbs. This value was then used to obtain estimates of $W_s + W_t$ = 33 lbs and $W_{a/c}$ = 17 lbs from the second and third charts of Figure D-1. Substituting the estimated values obtained for equations 2 & 3 into equation 1 we now obtain:

$$W_g = 204 + W_m \tag{4}$$

where W_m may be written:

$$W_m = 1/\lambda \, W_p \tag{5}$$

and where:

W_p = propellant weight

λ = propellant mass fraction = W_p/W_m

7. Space Technology Laboratories: Vol II Final Report "Satellite Interception System Feasibility Study" for ARPA STL 8424-6018-RS000, 6 November 1963

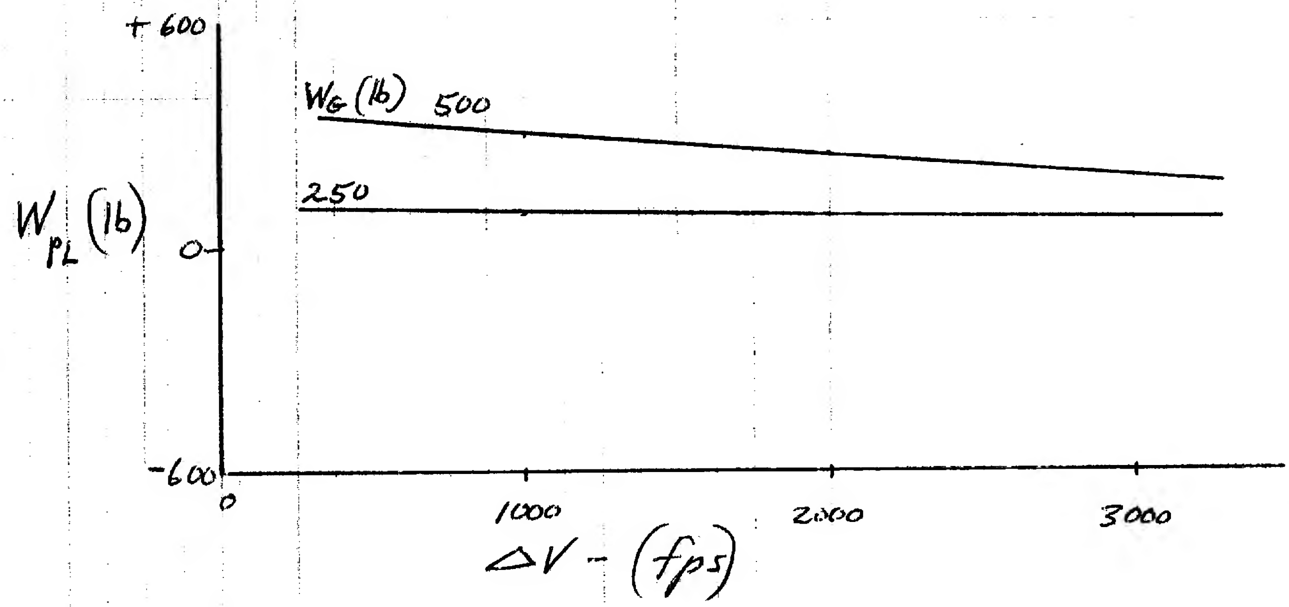

W_{PL} vs ΔV & W_G for $\bar{F}/\bar{W}$ = 5.0 Upper Stage

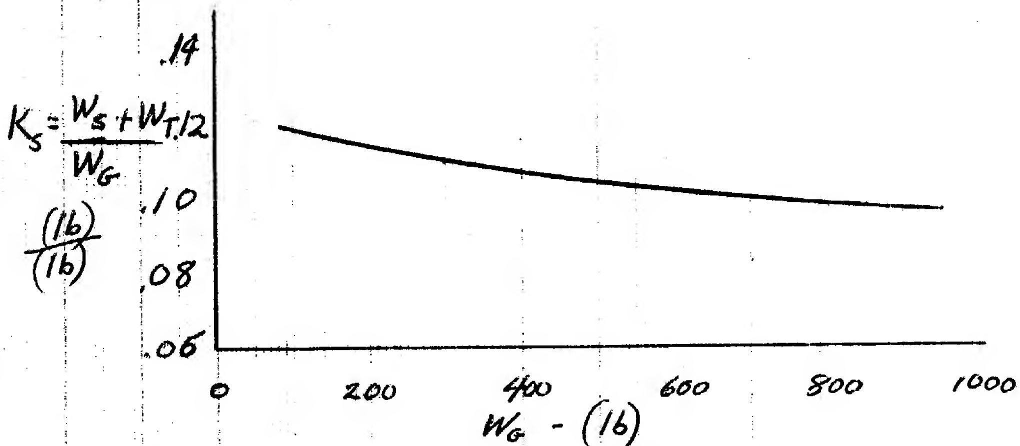

K_S vs W_G for 18" Diam Upper Stage

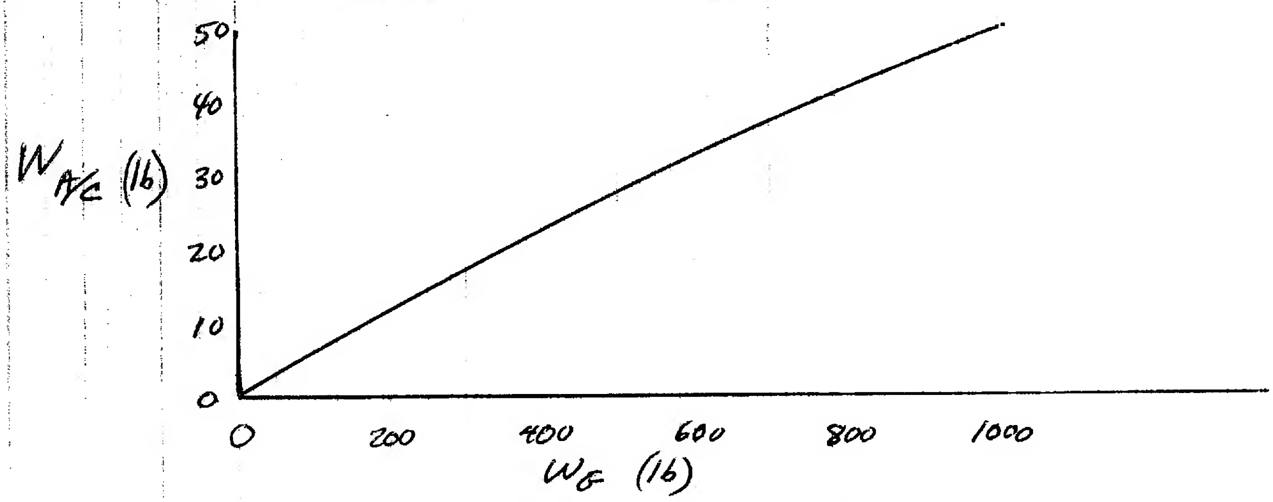

$W_{A/C}$ vs W_G for Upper Stage

Vau
2 Aug 65

The following rocket relationship may then be used to obtain an estimate of W_p:

$$W_p = W_g \left(1-e^{\frac{-\Delta V}{32.2\, I_{sp}}} \right) \tag{6}$$

Analysing equation 6 we find that W_p is far more sensitive to the normal range of values of ΔV than to I_{sp} as seen in the charts of Figure D-2. With this in mind we will fix I_{sp} at a near state of the art value for solid propellant vacuum performance.

Examining the data from six recently developed upper stage spherical solid propellant motors of our approximate requirements, we obtain:

I_{sp} range: 256 to 288

mean value I_{sp} = 275

λ range: = .875 to .920

mean value λ = .895

Using the above mean values and substituting equations 5 and 6 into equation 4, we thus obtain:

$$W_g = 204 + 1/\lambda \; W_{gi} \left(1-e^{\frac{-\Delta V}{8860}} \right) \tag{7}$$

Taking our previously obtained preliminary estimate of W_{gi} = 300, we may thus obtain an approximate solution for W_g as a function of Δ V, the most sensitive weight governing parameter, over the velocity range of interest. The solution to a double iteration estimate of W_g using equation 7 is presented in the first chart of Figure D-3.

Maintaining the $\overline{F}/\overline{W}_g$ = 5.0 for the correction motor we may now estimate the burning time of the motor from:

$$t_b = I_{t}/\overline{F} = \frac{W_p \times I_{sp}}{\overline{W}_g \times \overline{F}/\overline{W}_g} \tag{8}$$

FIGURE D-2

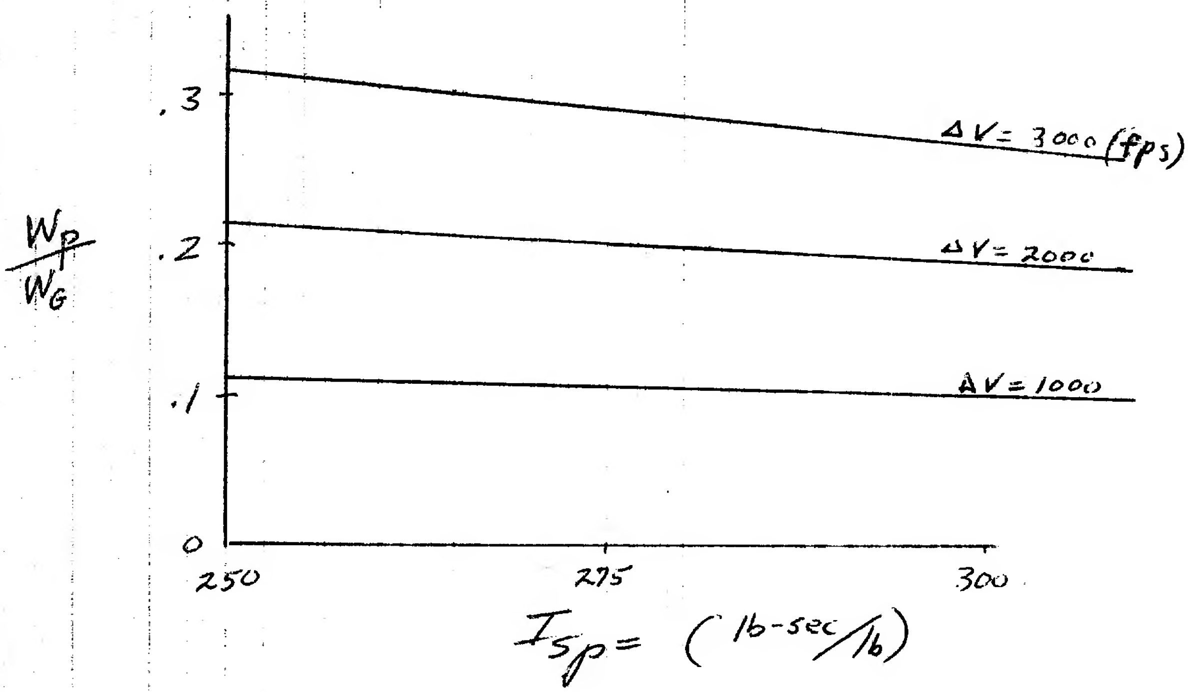

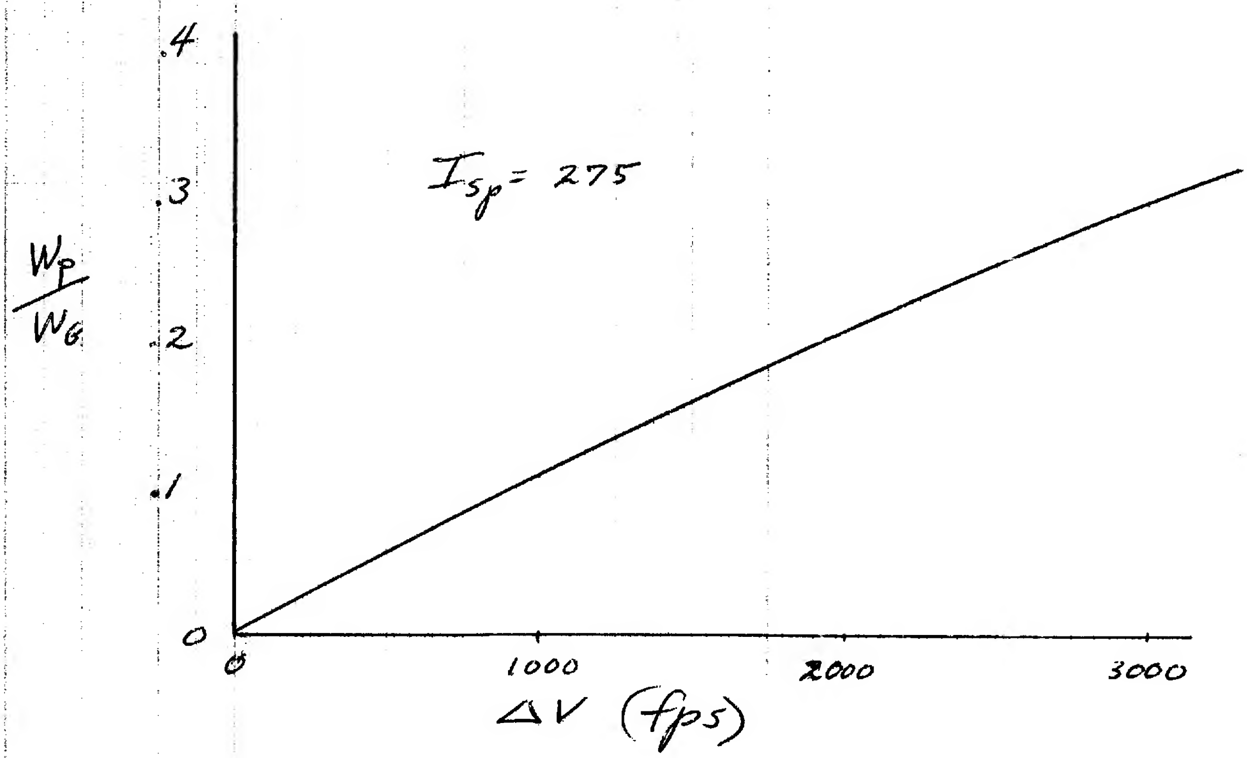

tn
2 Aug 65

FIGURE D-3

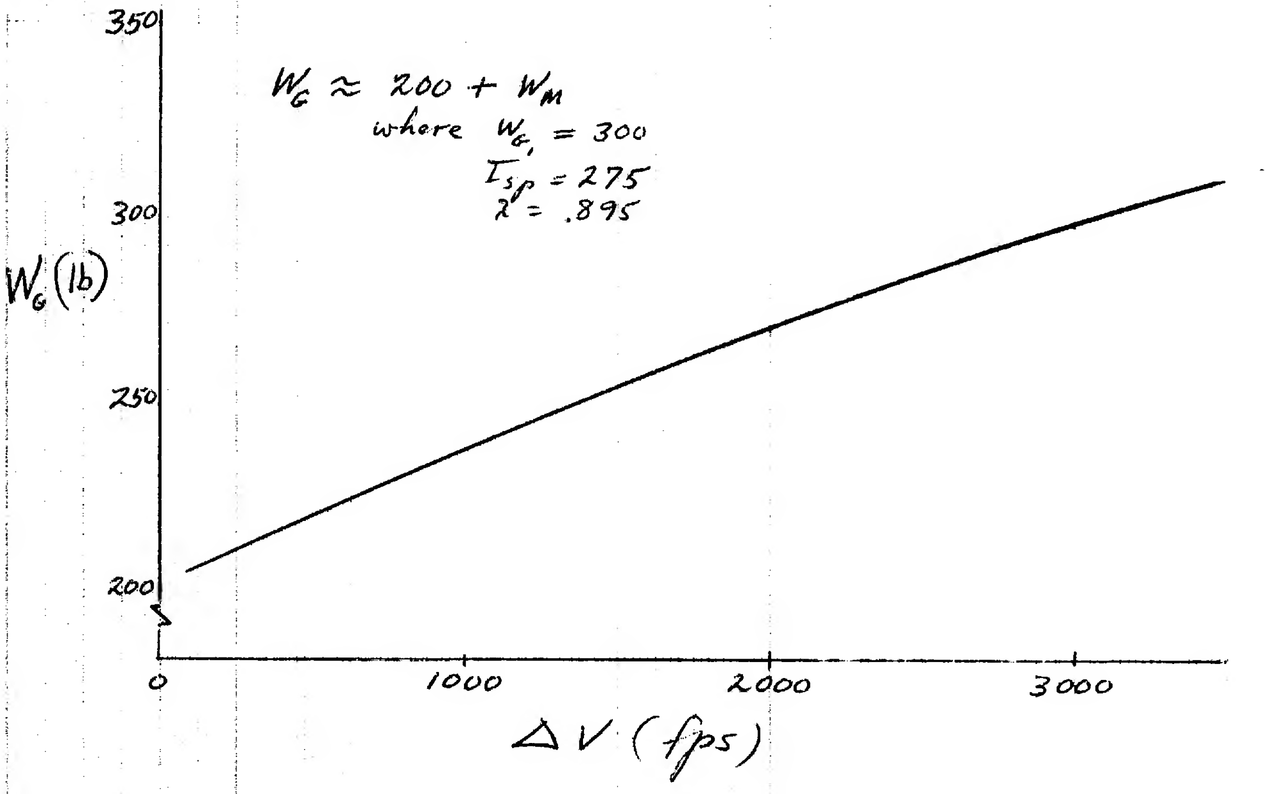

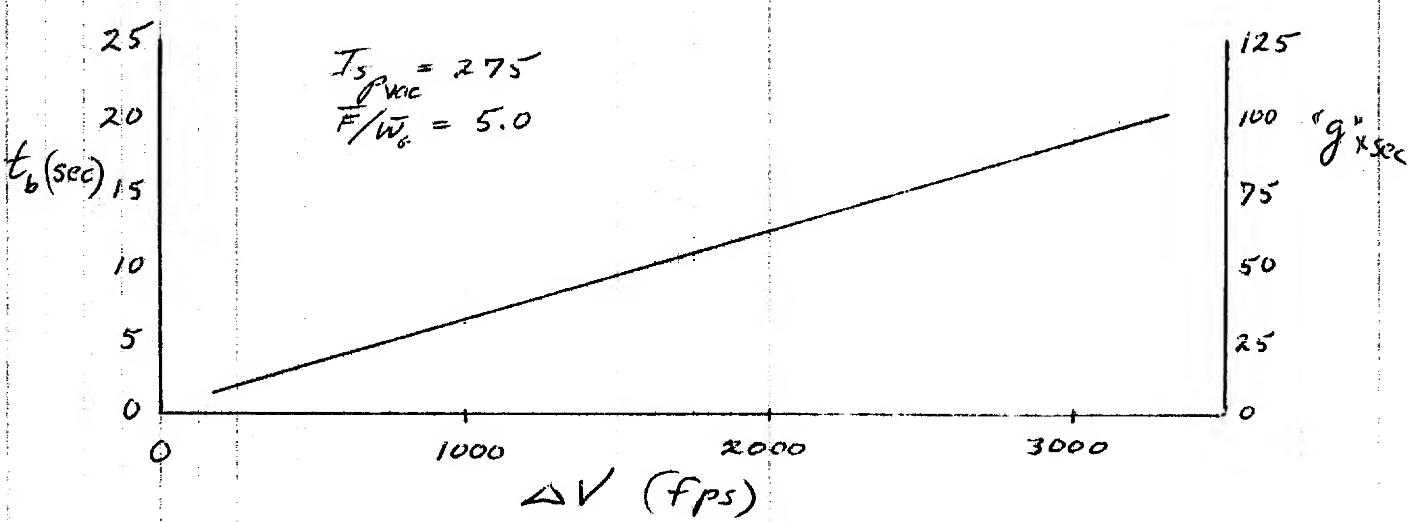

Tam
4 Aug 65

where:

t_b = motor burn time

I_t = total impulse of rocket

$\overline{F}$ = average thrust required

$\overline{W}_g$ = mean vehicle weight = $W_g - W_p / 2$

and since W_p & W_g are functions of ΔV, we may also express t_b as an approximate function of ΔV. Further, we may multiply t_b by the constant $\overline{F}/\overline{W}_g = 5.0$ to obtain a "g" sec product as a function of ΔV as an indication of the contribution of the second stage motor's burning to the drift rate errors of the payload's gyro platform. These two relationships are shown graphically in the second chart of Figure D-3.

3. Selected ALIAS Configuration

The configuration of the selected concept for an ALIAS terminal vehicle is presented in Figure D-4. Significant in this configuration is the choice of the terminal correction motor. The motor selected was a TE-385 unit produced by Thiokol Chemical Corporation as the NASA Gemini spacecraft retrograde motor. This unit offers an incremental velocity capability of approximately 1650 fps rather than the 1000.0 fps used as the basis for the sizing estimate previously discussed. This additional capability although desirable does add additional weight to the terminal vehicle over the minimum required for the derived ALIAS performance. The selection of this motor however is based on the fact that it is the minimum rocket motor currently available which will meet the requirement. The penalty of approximately + 10% of total terminal vehicle weight would appear to be worth the savings in cost of designing, developing and testing a motor specifically tailored to the ALIAS need. Indeed it is encouraging within the feasibility purview to note that an off-the-shelf motor can be adapted to the ALIAS mission without exceeding a 10% penalty over an optimized design. A by-product of the use of this motor of course is the fact that it provides some growth capability to the basic ALIAS scheme as now envisioned.

The final launch and recovery weight estimates for the selected ALIAS concept are presented in Chart D-1.

ALIAS Terminal Vehicle Layout

(Several Components Out of Place for Clarity)

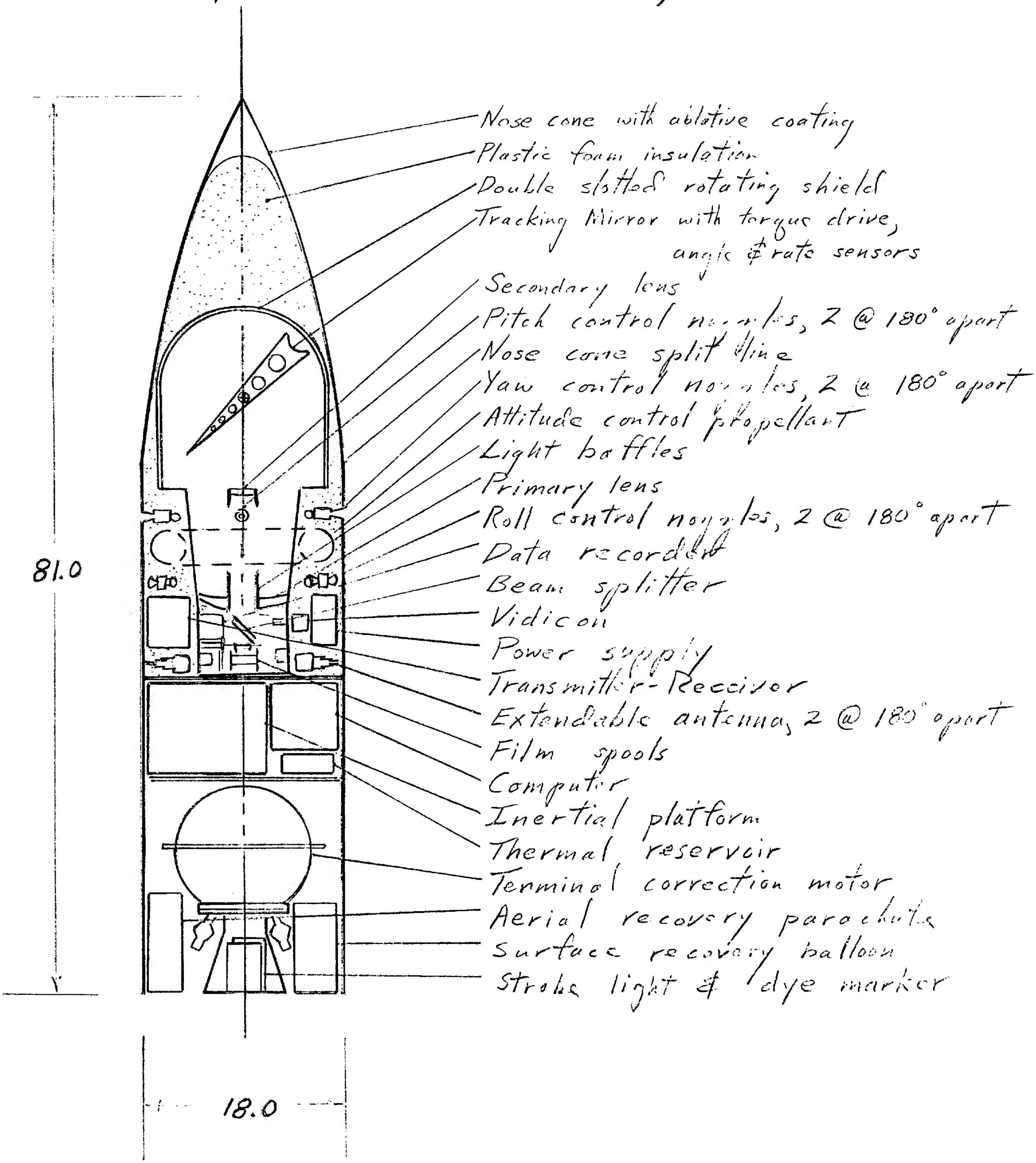

Chart D-1

Terminal Vehicle Weight Statement

Group	Item	Launch Wt-(lb)	Recovery Wt-(lb)
Sensor	tracking mirror	10.0	
	torque motors	4.0	
	rate gyro & angle pick-off	1.3	
	secondary mirror	4.0	
	primary mirror	18.0	
	image splitter	0.5	
	vidicon & vidicon electronics	9.2	
	glass plate	2.0	
	film, cannister, mech., recorder	13.0	
	shutter	3.0	
		65.0	65.0
Guidance	UHF antennas	1.0	
	power supply	7.0	
	transmitter/receiver & encoder	8.0	
	computer	20.0	
	inertial platform	27.0	
		63.0	63.0
Special Structure	nose fairing	6.0	0.0
	insulation	3.0	3.0
	mirror shields	6.0	6.0
		15.0	9.0
Recovery Components	parachute	6.0	
	balloon	2.0	
	dye marker & strobe	3.0	
		11.0	11.0
Control	pitch & yaw jets	4.0	4.0
	roll jets	3.0	3.0
	attitude control fuel (65% mean use)	8.0	2.8
	correction motor (Gemini Retro)	65.6	10.2
Other	thermal reservoirs	2.0	2.0
	primary structure	30.0	30.0
		112.6	52.0
		266.6	203.0

APPENDIX E

BOOSTER SYSTEM ANALYSIS

APPENDIX E

BOOSTER VEHICLE

1. Introduction

Several criteria were established for the selection of boost vehicle candidates in the feasibility analysis of an ALIAS concept. They were:

a) Maintain maximum sustained longitudinal accelerations, of the total system, of less than 10.0 g's.

b) Maintain levels of peak acceleration loads (duration less than 100 milliseconds) imparted to the system of less than 20.0 g's.

c) Minimize handling and flight safety considerations.

d) Total vehicle dimensions and weight to be reasonably compatible with the concept of aircraft transport and air launch.

e) Provide 2000 $\pm$ 75% fps crossing velocity at intercept altitude.

f) Vehicle diameter to be reasonably compatible with payload packaging (minimum diam. = 18") while avoiding problems of inherent instability (bulbous nose).

g) Vehicle to possess positive or near neutral negative aerodynamic stability.

h) Propulsion system to be an existing or minor modification of a proven system rather than a new development.

i) Possess the ability to meet both the low (90 n mi) and high (150 n mi) orbit as well as intermediate intercept altitude requirements of ALIAS.

Although the desire for thrust termination capability, controllable thrust levels and maximum propulsive efficiency would (for maximum acceleration limits) suggest liquid propellant systems, the safety and handling criteria as well as the desirability of adopting available and proven propulsion components dictated the use of a solid propellant system.

On the basis of these criteria it was decided that a search of the current inventory of solid rocket motors would be made to determine what solid propellant rockets were available to meet the ALIAS requirements.

The design of a rocket vehicle involves the analysis of several interacting parameters which must be traded off within the constraints of the basic vehicle criteria to approach an efficient design. Thus the process of vehicle selection for the feasibility investigation for ALIAS was necessarily an iterative process. Primary interactions are summarized in chart E-1.

Chart E-1

Vehicle Design Parameters	Primary Influencing Variables
Booster total impulse	desired trajectory type, initial launch conditions, propellant specific impulse, stage fraction, propellant mass fraction, intercept altitude, intercept crossing velocity
Thrust level	axial acceleration limit, gross weight variation with time, drag losses, gravity losses, thrust coefficient variation with altitude, nozzle expansion efficiency
Burning time	total impulse requirement, thrust scheduling
Flight weight	Motor inert weight, propellant mass loss rate, attitude control system gross weight and mass losses, aerodynamic stabilizing surface weight, thrust reversal system weight, terminal vehicle weight, acceleration of gravity variation with radius from earth center.
Thrust reversal system weight	retro rocket parameters, structure, booster motor thrust level
Attitude control system weight	stability parameters variations with Mach number and dynamic pressure
Terminal vehicle weight	Sensor, attitude control performance requirement, terminal correction motor performance requirement, structure
Drag losses	Drag reference area, variation of drag coefficients with Mach number, velocity, atmospheric density
Gravity losses	vehicle attitude along trajectory path, variation of acceleration of gravity with radius from earth center.
Aerodynamic stability	center of gravity variation with propellant burning, center of aerodynamic moment variation with Mach number, angle of attack, moment coefficients, reference area, dynamic pressure

2. Booster Analysis

The iterative process was aided by the use of a computerized point mass trajectory program and as well as by some limiting of the design choices on the basis of experienced judgment. Thus although the following discussion of the evolution of the selected ALIAS vehicle design is presented as a sequence of considerations it should be realized that the process actually involved inherent feedback and iterative estimates.

First choice, in selection of actual booster units, would be given to a single proven motor that could meet the high orbit requirement (150 n mi) and whose thrust could be terminated for lesser orbit altitude requirements. This precluded the need for selecting various booster motor units matched to various orbit altitudes in the requirements spectrum from 90 to 150 n mi. Although there would be a recognized excess propulsion capability thus built into the ALIAS system it is believed that the expense associated with this excess would be far less than those expenses associated with the design, development, testing, crew training and operation of several or even a few booster systems each optimized to a chosen orbit altitude.

Since there are not now available any solid rocket propulsion units in the total impulse range required which incorporate an integral thrust termination system, a retro-thrust scheme utilizing a cluster of small size, short duration retro rockets as thrust reversers was considered appropriate for the ALIAS application. The SR11-HP-1 retro-rockets developed by Hercules Powder Co. have been fully qualified and produced in large quantities for use on Wing II and Wing VI Minuteman Missiles for 3rd stage thrust reversal. These motors, each producing 860 lbs of thrust, weigh only 4.8 pounds with a maximum envelope dimension of 5.75 inches. These motors thus appear ideally suited to the task of ALIAS thrust reversal when clustered in an appropriate arrangement to match ALIAS main booster thrust level. A companion motor also developed and fully qualified for Minuteman is the 1.0 lb SR11-MP-1 tumble motor. This motor or a similarly qualified unit is desirable for applying a lateral tumbling moment to the retarded booster motor to insure that the booster is directed off the trajectory path of the terminal stage following stage separation to preclude a later collision of the still thrusting booster motor with the coasting terminal stage.

A scheme for maintaining flight attitude was required for the ALIAS booster concept. For this purpose an analysis of the center of gravity and center of pressure travel for a range of small angles of attack as a function of Mach number was made for a number of likely vehicle candidates. This data was correlated with estimates of dynamic pressure obtained as a function of Mach from the simulated trajectory runs. Peak dynamic pressure values were used to estimate the maximum destabilizing moments. A maximum allowable angle of attack of 10° at maximum dynamic pressure was assumed. From the general relationship:

$$M = \alpha \times C_{n_\alpha} \times q \cdot S \cdot (cp - cg)$$

where

M	= destabilizing moment (ft-lb)
α	= angle of attack (deg)
C_{n_α}	= slope of pitching moment coefficient curve (per degree)
q	= dynamic pressure (lb/ft^2)
S	= reference area (ft^2)
$(cp - cg)$	= distance between center of gravity and center of pressure (ft)

On the basis of the above, it was found that the maximum destabilizing moment occurred at approximately M = 3.0 which corresponds to t + 20.0 from launch for the selected ALIAS vehicle concept. Figure E-1 presents the relationships between static stability margin and q as functions of Mach which establishes this point. As seen from this figure the vehicles without an aft stabilizing surface posses a large degree of inherent instability at maximum q. Thus, an aft flare surface was incorporated on the booster motor to produce near neutral stability throughout the Mach range. The near neutral stability might enable the pitch, roll and yaw control jets of the terminal stage to provide up to the 10° angle of attack correction with a thrust level that is within the thrust level established for terminal vehicle attitude control requirements. A more straight forward design approach would employ two separate control systems. In either case the combination of neutral stability and low thrust attitude control jets is believed to be more efficient from a weight and size standpoint than use of larger control jets without augmented aerodynamic stability.

A stability flare was chosen since the magnitude of the increase in drag over a finned vehicle with a boattail can easily be tolerated for the flight trajectory when launched from 35,000 feet in exchange for the benefits of:

(1) less possibility of misalignment due to poor fabrication or rough handling

(2) it can provide equal stability at a significantly lesser span than fins

FIGURE E-1

ALIAS VEHICLE STATIC STABILITY

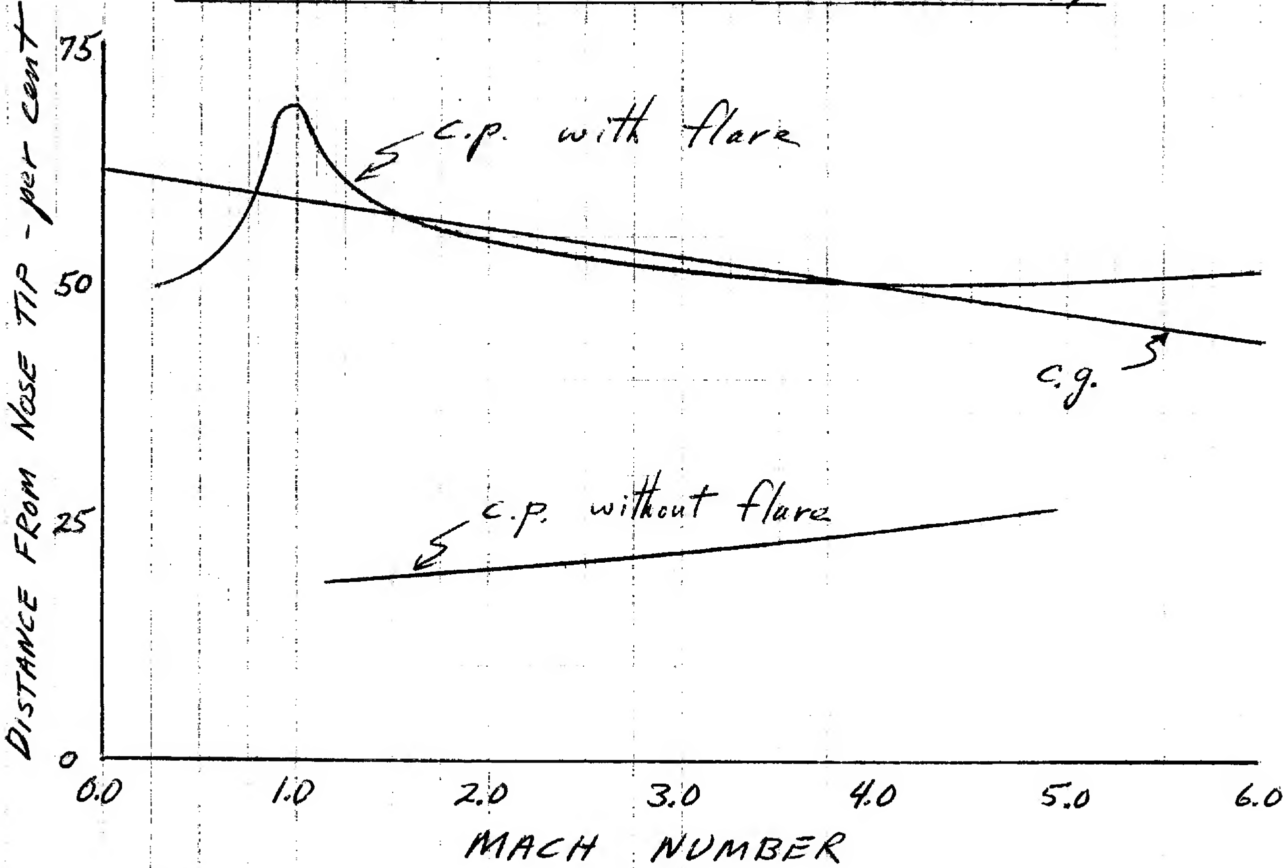

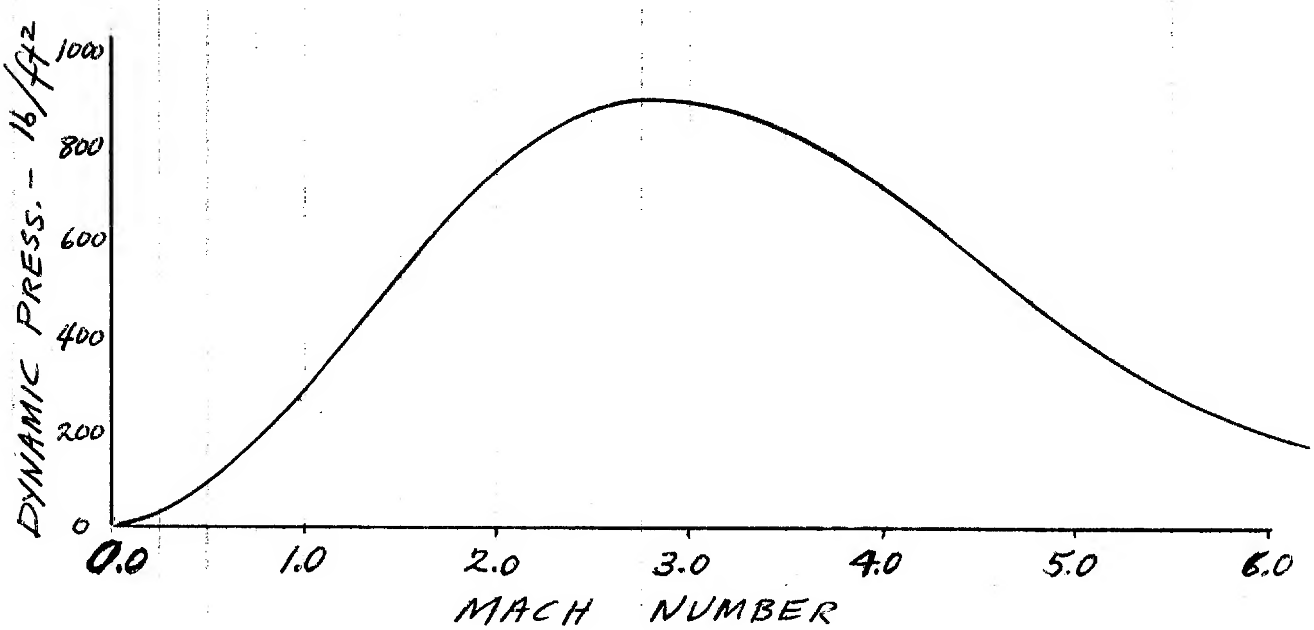

10/8/65

(3) it can double as a piston and guide in the launcher tube.

For the selected design a flare span of 27" (1.50 x vehicle diam) insures a reasonable launch tube diameter compatible with the air launch concept envisioned for ALIAS.

An analysis of the flight performance of a number of selected propulsion systems chosen from the latest published information[1/] available on solid rocket motors was made, using a point mass, non-rotating earth, computerized, trajectory program. Few units were found available to meet the ALIAS requirement within the several constraints imposed on the system. One motor however comes very close to being ideally designed for the ALIAS mission. It is the United Technology Center's FW-3 unit rated as 38KS 5600. This motor is a high mass ratio motor originally designed for Scout or Delta upper stage application. It has an E-glass filament wound chamber with a 30 to 1 expansion ratio nozzle. Propellant is an aluminized composite with ammonium perchlorate oxidizer. Other significant parameters are:

Principal Data

Length	74.7 inches
Maximum diameter	18.2 inches
Temperature limits	60 to 100° F
Acceleration limits at 70° F	
Axial	30 g
lateral	12 g
Nominal operating altitude greater than 50,000	
Propellant weight	760 lb
Total weight	827 lb

1/ SPIA/MI Rocket Motor Manual (U), compiled by Chemical Propulsion Information Agency, May 1965

Performance Data (vacuum, 70° F)

Ave. burning time	37.8 seconds
Ave. chamber pressure	593. psia
Ave. thrust	5760 lbf
Total impulse	218,000 lbf-sec
Specific impulse	288 lbf-sec/lbm

Although this motor has not been qualified to MIL specification and is not in quantity production, considerable company sponsored testing has been accomplished on the unit. It is believed however that a rocket unit displaying a reliable operation in a reasonable number of tests as exemplified by this motor would be sufficient qualification to meet the ALIAS requirement.

A full program of MIL specification PFRT & Qualification testing would be an undue expense for the ALIAS system use since the system would be expected to be used within a controlled environment by well-trained and qualified personnel and on missions whose individual success is not overly critical.

Chart E-2 is a reproduction of the simulated computer trajectory output for the selected ALIAS vehicle using the FW-3 booster motor on a programmed true vertical flight path. Time histories of vehicle acceleration, velocity, altitude, mach number, dynamic pressure and flight weight are among the outputs listed. Also shown is the cumulative acceleration-time product (CATP) in g-seconds.

The primary sizing parameter for the ALIAS/booster was the gross vehicle weight. This weight for the selected concept was derived as follows for launch and burnout:

	Launch	Burnout
Terminal vehicle	267. lb	267
Thrust termination	49	49
Stabilizing flare	10	10
Booster	827	67
	1153	393

Since terminal vehicle represents 68% of total inert weight, the terminal vehicle weight estimate is a most sensitive determiner of booster requirements and/or performance. Appendix D of this report describes the basis for the terminal vehicle weight estimate in detail. Figure E-2 shows the variation in the ALIAS selected vehicle (FW-3 booster) performance as a function of changes in terminal vehicle (payload) weight.

FIGURE E-2

ALIAS VEHICLE PERFORMANCE

90° trajectory
launch at -66 fps, 35,000 ft. alt.

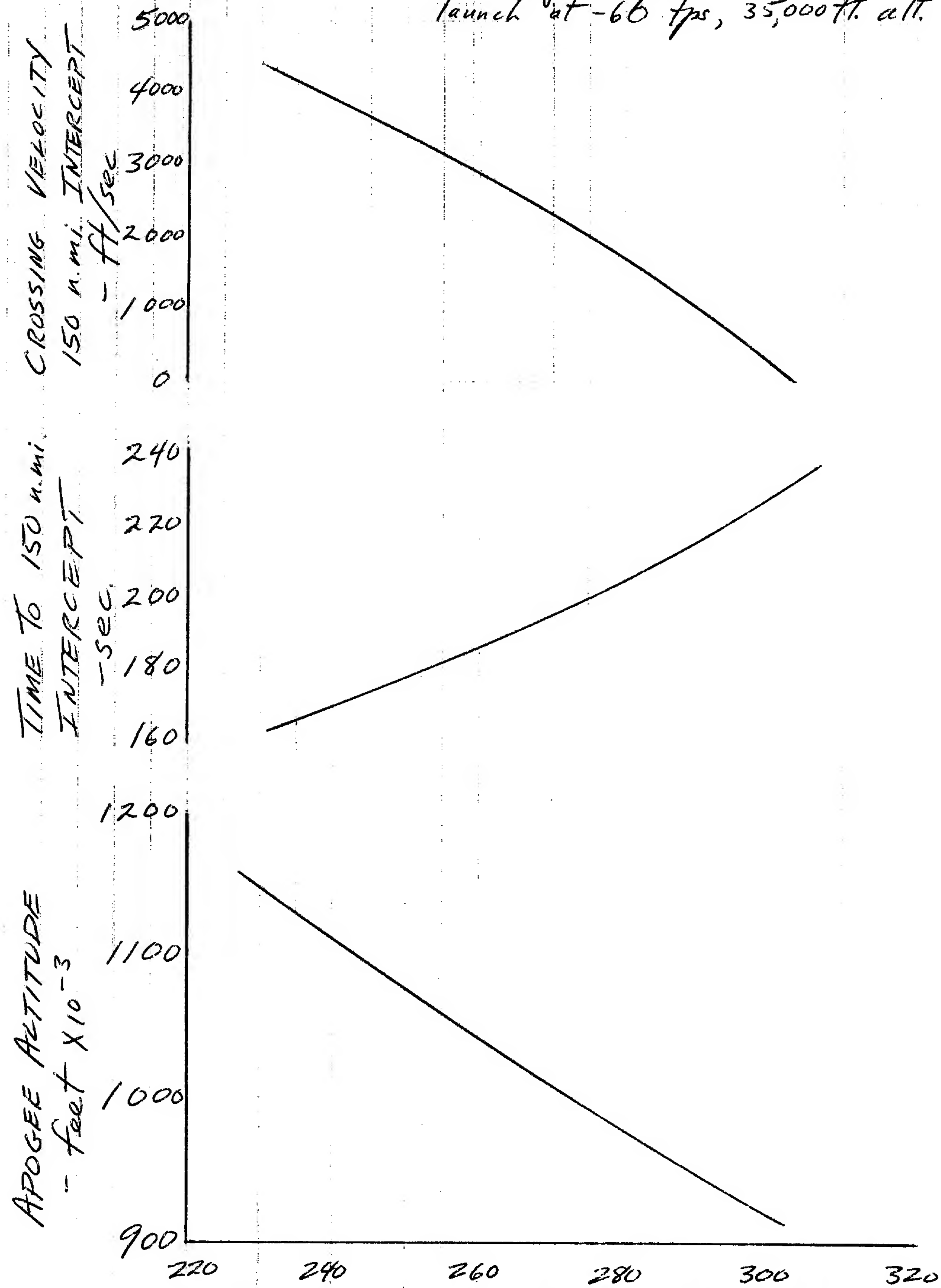

TM
10/8/65

Figure E-3 provides a diagram of the selected total vehicle envisioned for the ALIAS concept. Size, weight and performance values are indeed reasonable and compatible with other ALIAS system requirements. The vehicle concept has been limited to adapting existing components and proven techniques and thus is readily producible with economy of time and expense. Development and testing should prove relatively straight forward and no major problem areas requiring special effort are foreseen. It is thus concluded that the concept of an air launched ALIAS vehicle is highly feasible.

FIGURE E-3

ALIAS VEHICLE - SELECTED CONCEPT

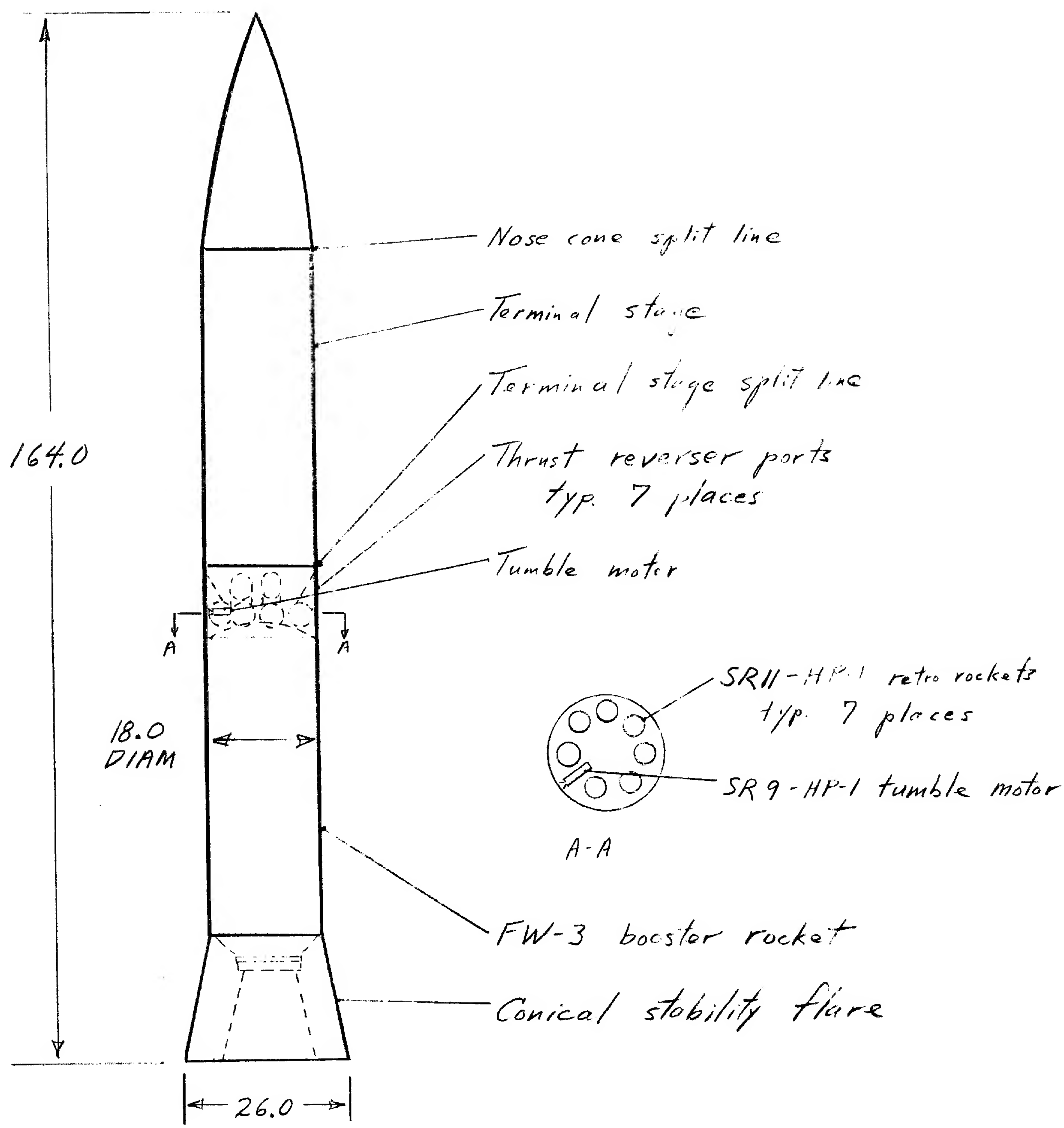

CHART E-2

23 F W - 3 OCTOBER 5, 1965 101365

INITIAL TRAJECTORY PARAMETER VALUES

RAIL LENGTH	ANGLE	VELOCITY	ALTITUDE	PAYLOAD	TIME
0.	90.000	-60.00	35000.00	267.000	0.

STAGE 1 OF 1 STAGES

WEIGHT	THROAT AREA	EXIT AREA	DESIGN ATMOS. PRESSURE	DESIGN THRUST COEFF.	DRAG REF. AREA	STAGE TIME	INTEG. INTVL.	PRINT INTVL.	MASS	CONSTANTS OF PRINT	INTEG.	THRUST
886.000	6.660	198.500	1.2300	1.735	3.000	360.00	0.500	3.000	0.003400	1.000	1.000	0.

TIME	ACCEL	VELOCITY	ALTITUDE	THETA	RANGE	THRUST	DRAG	MACH	Q	F GAIN	D LOSS	G LOSS	FLT WGT	CATP
3.00	3.42	247.29	35278.26	90.00	0.00	4862.38	25.97	0.25	22.33	142.49	0.76	32.07	1094.21	10.26
6.00	4.11	614.24	36552.95	90.00	0.00	5447.68	158.30	0.63	130.62	168.84	4.91	32.06	1034.49	22.60
9.00	4.29	1024.65	39006.19	90.00	0.00	5722.32	582.80	1.06	323.32	188.71	19.22	32.05	972.01	35.46
12.00	4.61	1449.66	42709.80	90.00	0.00	6005.19	914.19	1.50	542.14	211.91	32.26	32.04	908.05	49.28
15.00	5.13	1915.67	47745.40	90.00	0.00	6275.64	1110.69	1.98	743.96	238.54	42.22	32.03	842.61	64.67
18.00	5.59	2429.24	54251.36	90.00	0.00	6287.77	1168.04	2.51	876.41	258.97	48.11	32.01	777.15	81.43
21.00	5.86	2980.10	62359.50	90.00	0.00	5968.73	1072.99	3.08	895.25	267.35	48.06	31.98	714.04	99.00
24.00	6.17	3556.10	72156.15	90.00	0.00	5558.03	865.42	3.67	798.37	271.32	42.25	31.95	654.56	117.51
27.00	6.69	4168.33	83730.04	90.00	0.00	5222.20	616.89	4.29	628.07	278.45	32.89	31.92	598.60	137.59
30.00	7.52	4847.47	97233.51	90.00	0.00	5027.15	384.64	4.86	431.57	294.25	22.51	31.88	544.61	160.16
33.00	8.51	5611.79	112899.17	90.00	0.00	4889.45	221.35	5.46	276.28	317.00	14.35	31.83	490.94	185.69
36.00	9.72	6479.57	131007.61	90.00	0.00	4808.75	117.76	6.10	164.95	349.26	8.55	31.77	437.49	214.86
39.00	-1.16	7311.84	151870.52	90.00	0.00	0.	61.05	6.65	88.54	0.	4.94	31.71	391.56	218.32
42.00	-1.07	7206.79	173646.37	90.00	0.00	0.	26.62	6.52	38.58	0.	2.16	31.65	390.75	221.53
45.00	-1.03	7107.38	195116.74	90.00	0.00	0.	12.65	6.75	18.36	0.	1.02	31.58	389.95	224.63
48.00	-1.01	7010.59	216293.23	90.00	0.00	0.	5.73	7.07	8.33	0.	0.46	31.52	389.17	227.67
51.00	-1.01	6915.20	237181.66	90.00	0.00	0.	2.35	7.44	3.41	0.	0.19	31.46	388.40	230.69
54.00	-1.00	6820.56	257785.17	90.00	0.00	0.	0.86	7.91	1.25	0.	0.07	31.40	387.65	233.70
57.00	-1.00	6726.34	278105.43	90.00	0.00	0.	0.25	7.95	0.37	0.	0.02	31.34	386.91	236.70
60.00	-1.00	6632.39	298143.46	90.00	0.00	0.	0.07	7.82	0.10	0.	0.01	31.28	386.18	239.70
63.00	-1.00	6538.64	317899.93	90.00	0.00	0.	0.02	7.26	0.03	0.	0.00	31.22	385.46	242.70

TIME	ACCEL	VELOCITY	ALTITUDE	THETA	RANGE	THRUST	DRAG	MACH	Q	F GAIN	D LOSS	G LOSS	FLT WGT	CATP
66.00	-1.00	6445.07	337375.43	90.00	0.00	0.	0.01	6.76	0.01	0.	0.00	31.16	384.75	245.70
69.00	-1.00	6351.67	356570.48	90.00	0.00	0.	0.00	5.96	0.00	0.	0.00	31.10	384.06	248.70
72.00	-1.00	6258.43	375485.57	90.00	0.00	0.	0.00	4.92	0.00	0.	0.00	31.05	383.38	251.70
75.00	-1.00	6165.37	394121.21	90.00	0.00	0.	0.00	4.26	0.00	0.	0.00	31.00	382.71	254.70
78.00	-1.00	6072.46	412477.90	90.00	0.00	0.	0.00	3.80	0.00	0.	0.00	30.94	382.05	257.70
81.00	-1.00	5979.71	430556.11	90.00	0.00	0.	0.00	3.44	0.00	0.	0.00	30.89	381.40	260.70
84.00	-1.00	5887.12	448356.30	90.00	0.00	0.	0.00	3.16	0.00	0.	0.00	30.84	380.77	263.70
87.00	-1.00	5794.68	465878.95	90.00	0.00	0.	0.00	2.93	0.00	0.	0.00	30.79	380.14	266.70
90.00	-1.00	5702.39	483124.50	90.00	0.00	0.	0.00	2.74	0.00	0.	0.00	30.74	379.53	269.70
93.00	-1.00	5610.25	500093.41	90.00	0.00	0.	0.00	2.57	0.00	0.	0.00	30.69	378.93	272.70
96.00	-1.00	5518.25	516786.11	90.00	0.00	0.	0.00	2.42	0.00	0.	0.00	30.64	378.34	275.70
99.00	-1.00	5426.40	533203.03	90.00	0.00	0.	0.00	2.29	0.00	0.	0.00	30.59	377.76	278.70
102.00	-1.00	5334.68	549344.59	90.00	0.00	0.	0.00	2.20	0.00	0.	0.00	30.55	377.20	281.70
105.00	-1.00	5243.10	565211.20	90.00	0.00	0.	0.00	2.13	0.00	0.	0.00	30.50	376.64	284.70
108.00	-1.00	5151.66	580803.28	90.00	0.00	0.	0.00	2.07	0.00	0.	0.00	30.46	376.09	287.70
111.00	-1.00	5060.34	596121.22	90.00	0.00	0.	0.00	2.01	0.00	0.	0.00	30.42	375.56	290.70
114.00	-1.00	4969.16	611165.41	90.00	0.00	0.	0.00	1.96	0.00	0.	0.00	30.37	375.03	293.70
117.00	-1.00	4878.10	625936.24	90.00	0.00	0.	0.00	1.91	0.00	0.	0.00	30.33	374.52	296.70
120.00	-1.00	4787.16	640434.08	90.00	0.00	0.	0.00	1.87	0.00	0.	0.00	30.29	374.02	299.70
123.00	-1.00	4696.35	654659.28	90.00	0.00	0.	0.00	1.82	0.00	0.	0.00	30.25	373.52	302.70
126.00	-1.00	4605.65	668612.23	90.00	0.00	0.	0.00	1.77	0.00	0.	0.00	30.21	373.04	305.70
129.00	-1.00	4515.07	682293.27	90.00	0.00	0.	0.00	1.73	0.00	0.	0.00	30.17	372.57	308.70
132.00	-1.00	4424.60	695702.73	90.00	0.00	0.	0.00	1.69	0.00	0.	0.00	30.14	372.11	311.70
135.00	-1.00	4334.25	708840.96	90.00	0.00	0.	0.00	1.64	0.00	0.	0.00	30.10	371.65	314.70
138.00	-1.00	4244.00	721708.29	90.00	0.00	0.	0.00	1.60	0.00	0.	0.00	30.06	371.21	317.70
141.00	-1.00	4153.86	734305.03	90.00	0.00	0.	0.00	1.56	0.00	0.	0.00	30.03	370.78	320.70
144.00	-1.00	4063.82	746631.50	90.00	0.00	0.	0.00	1.52	0.00	0.	0.00	30.00	370.36	323.70

TIME	ACCEL	VELOCITY	ALTITUDE	THETA	RANGE	THRUST	DRAG	MACH	Q	F GAIN	D LOSS	G LOSS	FLT WGT	CATP
147.00	-1.00	3973.89	758688.02	90.00	0.00	0.	0.00	1.48	0.00	0.	0.00	29.96	369.95	326.70
150.00	-1.00	3884.05	770474.88	90.00	0.00	0.	0.00	1.45	0.00	0.	0.00	29.93	369.55	329.70
153.00	-1.00	3794.31	781992.38	90.00	0.00	0.	0.00	1.41	0.00	0.	0.00	29.90	369.15	332.70
156.00	-1.00	3704.66	793240.80	90.00	0.00	0.	0.00	1.37	0.00	0.	0.00	29.87	368.77	335.70
159.00	-1.00	3615.11	804220.41	90.00	0.00	0.	0.00	1.33	0.00	0.	0.00	29.84	368.40	338.70
162.00	-1.00	3525.64	814931.48	90.00	0.00	0.	0.00	1.30	0.00	0.	0.00	29.81	368.04	341.70
165.00	-1.00	3436.26	825374.30	90.00	0.00	0.	0.00	1.26	0.00	0.	0.00	29.78	367.68	344.70
168.00	-1.00	3346.97	835549.11	90.00	0.00	0.	0.00	1.22	0.00	0.	0.00	29.75	367.34	347.70
171.00	-1.00	3257.76	845456.16	90.00	0.00	0.	0.00	1.19	0.00	0.	0.00	29.72	367.00	350.70
174.00	-1.00	3168.63	855095.70	90.00	0.00	0.	0.00	1.15	0.00	0.	0.00	29.70	366.68	353.70
177.00	-1.00	3079.57	864467.95	90.00	0.00	0.	0.00	1.12	0.00	0.	0.00	29.67	366.36	356.70
180.00	-1.00	2990.59	873573.16	90.00	0.00	0.	0.00	1.08	0.00	0.	0.00	29.65	366.06	359.70
183.00	-1.00	2901.69	882411.55	90.00	0.00	0.	0.00	1.05	0.00	0.	0.00	29.62	365.76	362.70
186.00	-1.00	2812.86	890983.33	90.00	0.00	0.	0.00	1.01	0.00	0.	0.00	29.60	365.47	365.70
189.00	-1.00	2724.09	899288.72	90.00	0.00	0.	0.00	0.98	0.00	0.	0.00	29.58	365.20	368.70
192.00	-1.00	2635.39	907327.89	90.00	0.00	0.	0.00	0.94	0.00	0.	0.00	29.56	364.93	371.70
195.00	-1.00	2546.76	915101.07	90.00	0.00	0.	0.00	0.91	0.00	0.	0.00	29.53	364.67	374.70
198.00	-1.00	2458.18	922608.43	90.00	0.00	0.	0.00	0.88	0.00	0.	0.00	29.51	364.42	377.70
201.00	-1.00	2369.67	929850.16	90.00	0.00	0.	0.00	0.84	0.00	0.	0.00	29.49	364.18	380.70
204.00	-1.00	2281.22	936826.46	90.00	0.00	0.	0.00	0.81	0.00	0.	0.00	29.48	363.94	383.70
207.00	-1.00	2192.82	943537.48	90.00	0.00	0.	0.00	0.78	0.00	0.	0.00	29.46	363.72	386.70
210.00	-1.00	2104.47	949983.37	90.00	0.00	0.	0.00	0.74	0.00	0.	0.00	29.44	363.51	389.70
213.00	-1.00	2016.17	956164.30	90.00	0.00	0.	0.00	0.71	0.00	0.	0.00	29.42	363.30	392.70
216.00	-1.00	1927.93	962080.41	90.00	0.00	0.	0.00	0.68	0.00	0.	0.00	29.41	363.10	395.70
219.00	-1.00	1839.72	967731.84	90.00	0.00	0.	0.00	0.65	0.00	0.	0.00	29.39	362.92	398.70
222.00	-1.00	1751.57	973118.75	90.00	0.00	0.	0.00	0.62	0.00	0.	0.00	29.38	362.74	401.70
225.00	-1.00	1663.46	978241.25	90.00	0.00	0.	0.00	0.58	0.00	0.	0.00	29.36	362.57	404.70

TIME	ACCEL	VELOCITY	ALTITUDE	THETA	RANGE	THRUST	DRAG	MACH	Q	F GAIN	D LOSS	G LOSS	FLT WGT	CATP
228.00	-1.00	1575.38	983099.48	90.00	0.00	0.	0.00	0.55	0.00	0.	0.00	29.35	362.41	407.70
231.00	-1.00	1487.35	987693.53	90.00	0.00	0.	0.00	0.52	0.00	0.	0.00	29.34	362.26	410.70
234.00	-1.00	1399.35	992023.53	90.00	0.00	0.	0.00	0.49	0.00	0.	0.00	29.33	362.11	413.70
237.00	-1.00	1311.38	996089.59	90.00	0.00	0.	0.00	0.46	0.00	0.	0.00	29.32	361.98	416.70
240.00	-1.00	1223.45	999891.80	90.00	0.00	0.	0.00	0.43	0.00	0.	0.00	29.31	361.85	419.70
243.00	-1.00	1135.54	1003430.25	90.00	0.00	0.	0.00	0.40	0.00	0.	0.00	29.30	361.74	422.70
246.00	-1.00	1047.66	1006705.03	90.00	0.00	0.	0.00	0.37	0.00	0.	0.00	29.29	361.63	425.70
249.00	-1.00	959.81	1009716.21	90.00	0.00	0.	0.00	0.33	0.00	0.	0.00	29.28	361.53	428.70
252.00	-1.00	871.98	1012463.87	90.00	0.00	0.	0.00	0.30	0.00	0.	0.00	29.27	361.44	431.70
255.00	-1.00	784.17	1014948.07	90.00	0.00	0.	0.00	0.27	0.00	0.	0.00	29.27	361.36	434.70
258.00	-1.00	696.38	1017168.87	90.00	0.00	0.	0.00	0.24	0.00	0.	0.00	29.26	361.28	437.70
261.00	-1.00	608.61	1019126.34	90.00	0.00	0.	0.00	0.21	0.00	0.	0.00	29.26	361.22	440.70
264.00	-1.00	520.85	1020820.50	90.00	0.00	0.	0.00	0.18	0.00	0.	0.00	29.25	361.16	443.70
267.00	-1.00	433.11	1022251.41	90.00	0.00	0.	0.00	0.15	0.00	0.	0.00	29.25	361.12	446.70
270.00	-1.00	345.37	1023419.09	90.00	0.00	0.	0.00	0.12	0.00	0.	0.00	29.24	361.08	449.70
273.00	-1.00	257.64	1024323.59	90.00	0.00	0.	0.00	0.09	0.00	0.	0.00	29.24	361.05	452.70
276.00	-1.00	169.92	1024964.91	89.99	0.00	0.	0.00	0.06	0.00	0.	0.00	29.24	361.03	455.70
279.00	-1.00	82.21	1025343.09	89.98	0.00	0.	0.00	0.03	0.00	0.	0.00	29.24	361.01	458.70
282.00	-1.00	-5.47	1025458.12	90.21	0.00	0.	0.00	0.00	0.00	0.	0.00	29.24	361.01	461.70
	APOGEE													

APPENDIX F

RECOVERY SYSTEM ANALYSIS

APPENDIX F

RECOVERY

1. Introduction

This section will deal primarily with the problem of recovery of the data package and reusable payload components. Also of interest however is a brief look at the potential problems associated with the surface impact of all descending system components in the event that the ALIAS intercept should be attempted over populated areas.

The ALIAS system component separation events are recounted here in their order of occurrence with comments on their impact potential as follows:

a. Vehicle Launched from Stabilizing Parachute & Launch Guide Tube. The extraction & stabilizing parachute together with the launch guide tube will be designed for a descent velocity of approximately 50 fps at 35,000 feet altitude. Following the launch of the vehicle from the parachute the remaining gear will weigh approximately 600 lbs and at sea level altitude could be expected to have a final descent velocity of about 17 fps. Thus, this system component could be expected to produce an impact energy level of between 250 to 300 ft-lbs. Location of the impact area in the presence of an average 20 kt. wind in one direction in the altitude range between 35,000 ft and sea level is estimated to be approximately 8.0 nautical miles, from a point below the air launch point in the direction of the wind. Time of descent would be about 25 minutes.

b. Booster Motor Separation and Burnout. Booster motor burnout follows closely the thrust reversal motor ignition & separation from the terminal vehicle. The spent booster hardware could be expected to weigh anywhere from approximately 100 to 400 lbs depending upon the particular choice of booster motors and the intercept altitude requirements. If it is desired to limit the impact energy of the falling burned out booster motor we could use as a guide the long established Army Ballistic Missile Agency criteria that impact energy must be less than or equal to 57.0 ft-lbs to be considered non-lethal. If we then assume a booster inert weight of 250 lbs we may calculate an allowable impact velocity of 4 fps. To accomplish this, would require a parachute of approximately 150 ft. diameter, weighing a minimum of 40 lbs. In as much as this would offer a significant penalty to the vehicle performance it appears that the best approach to the booster impact safety problem is to provide only sufficient deceleration to the spent motor to provide assurance that its descent would be observable from the ground in time to initiate evacuation of the immediate impact area. Thus, we might conceive of a sea level descent velocity of 25 fps as being sufficient

for this purpose. Such a scheme would require a parachute of only 15 feet diameter weighing approximately 3.5 lbs. It is also conceivable that a whistle type audio warning and/or a flashing warning light could be incorporated on the descending booster at a negligible penalty in weight or performance.

Impact energy of the falling booster with the 15 foot parachute would be approximately 2500 ft-lbs.

c. Nose Cone Fairing Ejection. The nose cone fairing weighing about 6.0 lbs would be ejected shortly after separation of the booster stage. The nose cone will experience a stable attitude descent trajectory with a terminal velocity at sea level estimated to be between 80 and 90 fps. Thus impact energy will be on the order of 670 ft-lbs.

2. Payload Recovery

In addition to the exposed film it is desired to recover intact all of the reusable components of the terminal vehicle. These include the camera, inertial platform and computer. It is estimated that the dollar value of the reusable element would be in the neighborhood of $100,000. The payload recovery method planned for the selected ALIAS concept utilizes an air-to-air technique for primary recovery with a surface-to-air technique as back up. Both recovery methods may be accomplished with the same aircraft (assumes use of a C-130) that is used to launch the ALIAS vehicle. A description and analysis of the candidate recovery scheme follows.

a. Figure F-1 presents a sequence of events of the terminal stage descent. Closing of the mirror shield protects the mirror surface from particle impingement during the descent and seals the forward section of the terminal vehicle to protect the optics and camera in event of surface impact due to a missed aerial recovery. The attitude control system is used to place the terminal vehicle into a horizontal attitude and to initiate a flat spin limited to approximately 10.0 radians/sec. maximum. The horizontal attitude imparts an initial deceleration to the vehicle as it re-enters the atmosphere by presenting the high drag of the vehicle side area in cross flow while maintaining a near neutral stability. The spinning action imparts an additional stabilizing moment due to gyroscopic effect. The final decelerator is a parachute which is deployed when the ballistic coefficient (W/C_D S, lbs/ft^2) of the descending body is matched as a function of Mach Number to the design opening ballistic coefficient of the parachute. This consideration prevents extreme shock loading due to mismatch. The parachute deployment is expected to take place at approximately 200,000 ft altitude and may require a positive action canopy spreader to insure inflation in the rarified atmosphere existing at this altitude. An altitude-velocity history of a typical descent trajectory is presented in Figure F-2.

ALIAS DESCENT & RECOVERY SEQUENCE

ALTITUDE – feet X10⁻³ | EVENT

Apogee

1,000 — Rotate mirror shield closed

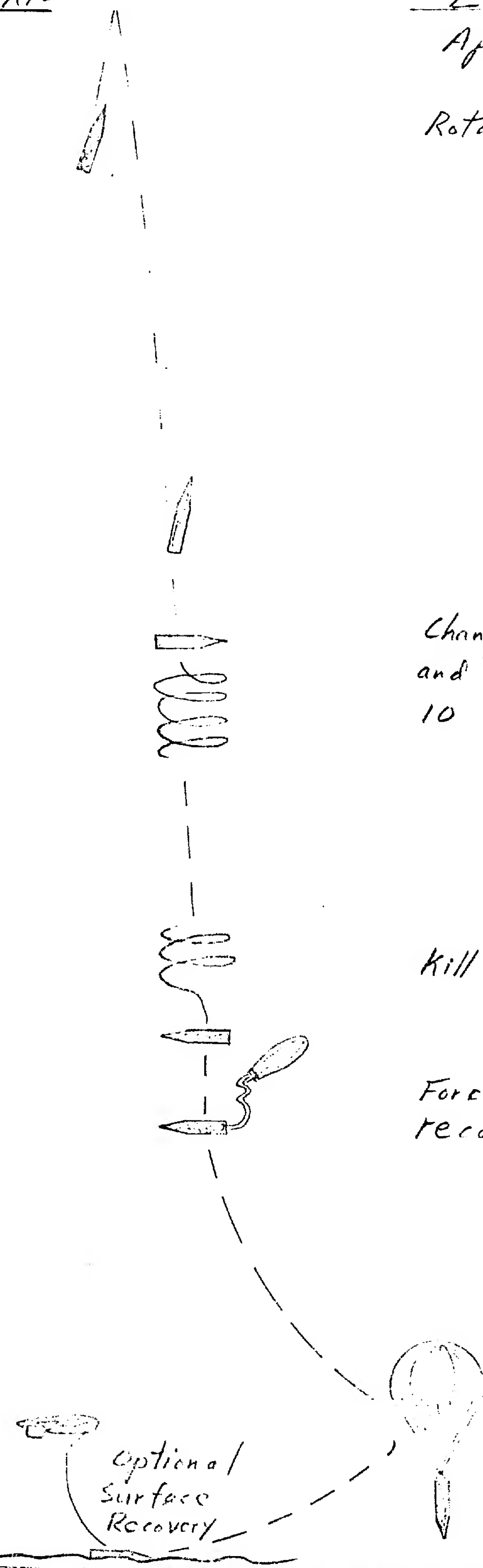

500 — Change attitude to horizontal and begin flat spin at 10 radians/second

Kill spin but hold attitude

200

Forcibly deploy silvered recovery parachute

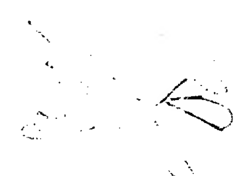

10

S.L.

10/11/65

FIGURE F-2

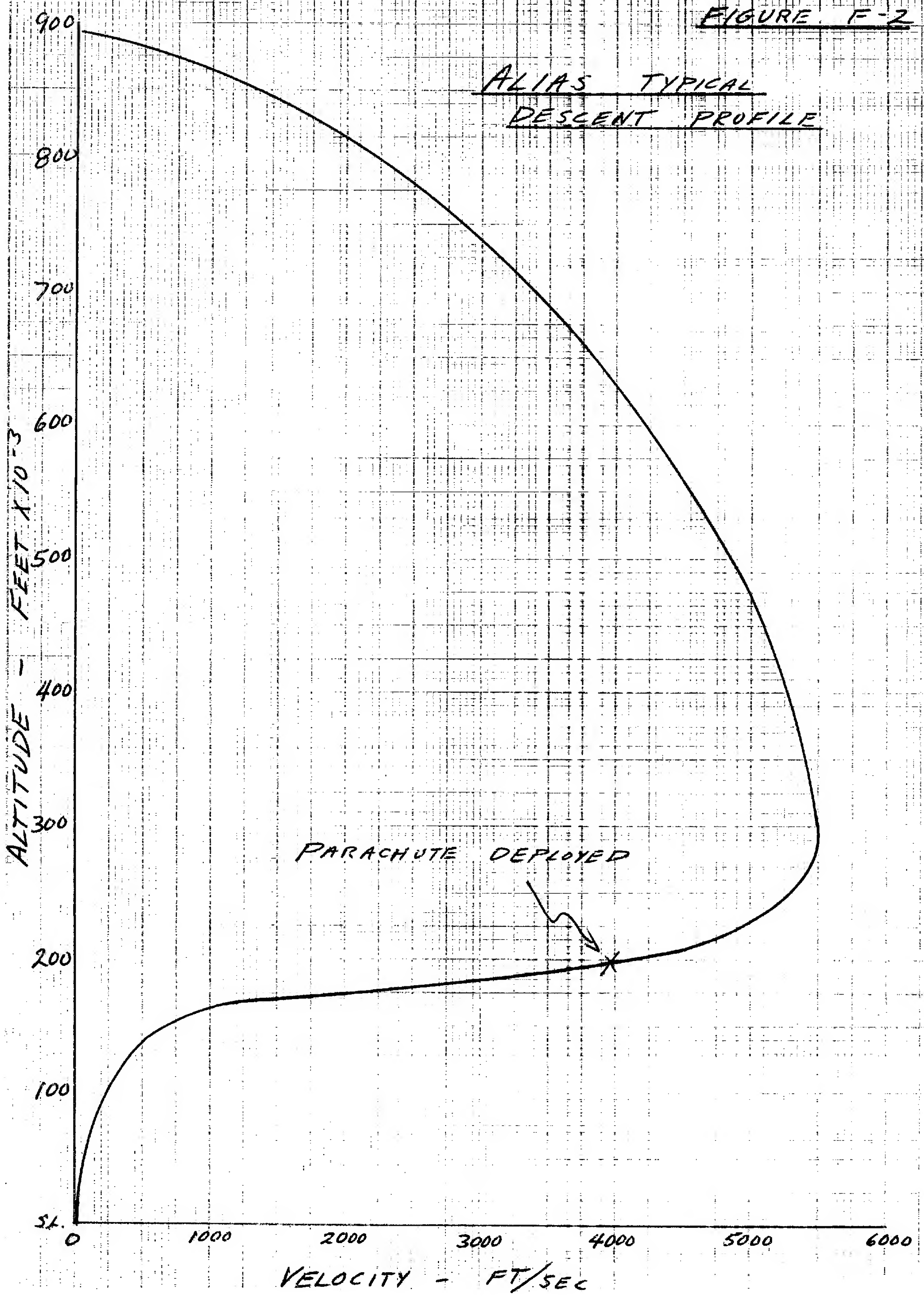
ALIAS TYPICAL DESCENT PROFILE
900
800
700
600
500
400
300
200
100
S.L.
ALTITUDE - FEET X 10^-3
PARACHUTE DEPLOYED
0
1000
2000
3000
4000
5000
6000
VELOCITY - FT/SEC

b. Ground range position of the descending ALIAS payload is primarily determined by the orientation of the final correction motor velocity vector. A final correction of 1500 fps in a horizontal direction at 150 n. mi. altitude could yield a maximum range contribution, including allowance for unfavorable wind drift of the deployed parachute of approximately 80.0 n. mi. Time associated with the descent to aerial recovery altitude is on the order of 30.0 minutes. Assuming an average speed of the launching aircraft of 200 knots, it is thus seen that this same aircraft could be on station in the recovery area 6.0 minutes before the payload descended to the 10,000 ft. recovery altitude. Since this example is a worst case situation, there appears to be no constraint to the feasible use of the launch aircraft for recovery operations.

c. ALIAS guidance system outputs to insure air-to-air intercept in the recovery phase are easily available as a bonus use of basic system equipment. Thus velocity and position data may be transmitted from the payloads inertial reference to the recovery aircraft. These data together with aircraft velocity and position data could be used as inputs to an intercept computation to provide a velocity, heading, rate-of-descent and time-to-go display to the recovery aircraft pilot.

This system could be further refined by use of the aircraft weather radar to provide speed and direction data as well as radar range. The sideward orientation of the descending payload should present a good radar target and parachute deployment sensing can be enhanced by increasing the radar reflective cross section through the use of a silvered canopy.

Dusk recovery would be further aided by the use of a payload on-board strobe light to insure pilot visual tracking. Air Force experience with this technique[1] has shown that illuminated balloons or parachutes may be located from a distance of 5.0 n. mi. and that there is little problem with respect to depth perception or determination of target attitude relative to the recovery aircraft.

d. Actual air-to-air and surface-to-air recovery operations utilizing C-130 aircraft have exceeded 9000 attempts to date with a demonstrated reliability of 99% in air-to-air and 95% for surface-to-air. Either mode of recovery can be accomplished with the same on-board equipment. The recommended equipment for use in the ALIAS application would consist of two flexible recovery poles, extending rearward and downward from the aircraft's open rear fuselage cargo ramp. The poles (approximately 30 ft) support attached hooks to engage the parachute. The hooks are stripped from the poles upon engagement bringing with them the attached recovery line which extends forward into the aircraft.

---

1. Aerial Recovery & Cargo Delivery Systems, F.M. Highly Jr & R.V. Parker, SAE Paper 915A. Cotober 1964

At engagement a differential velocity of approximately 130 knots exists between the aircraft and the parachute supported payload. This velocity difference is reduced by reeling out the recovery line which is attached to an energy absorbing winch. A pre-set line load is thus used to control the winch brake and hence the maximum acceleration force imparted to the payload. When the payload is accelerated to aircraft velocity, the payload is reeled up to bring the payload close to the aircraft. A small boom is then used to engage the payload and lift it onto the cargo ramp.

e. The only significant difference in surface-to-air recovery over air to air recovery is flight operational consideration given to wind direction. Wind direction in air-to-air recovery is not a significant factor. In surface-to-air recovery however the line inclination away from the wind above the object should be utilized to reduce the pickup acceleration loads and to insure a near vertical initial pickup trajectory. Thus the surface-to-air pickup is generally made in a direction into the surface wind.

Location aides for surface pickup are provided in the ALIAS selected concept by utilizing the payload transmitter as a radio beacon. Also included in the recovery kit are a strobe light and dye marker. The aerial recovery engagement device consists of a non-rigid blimp-shaped balloon supporting a nylon recovery line of about a 50 ft. length.

APPENDIX G

SUMMARY OF SUBSYSTEM FUNCTIONS AND PERFORMANCE CRITERIA

ALIAS MISSION SEQUENCE

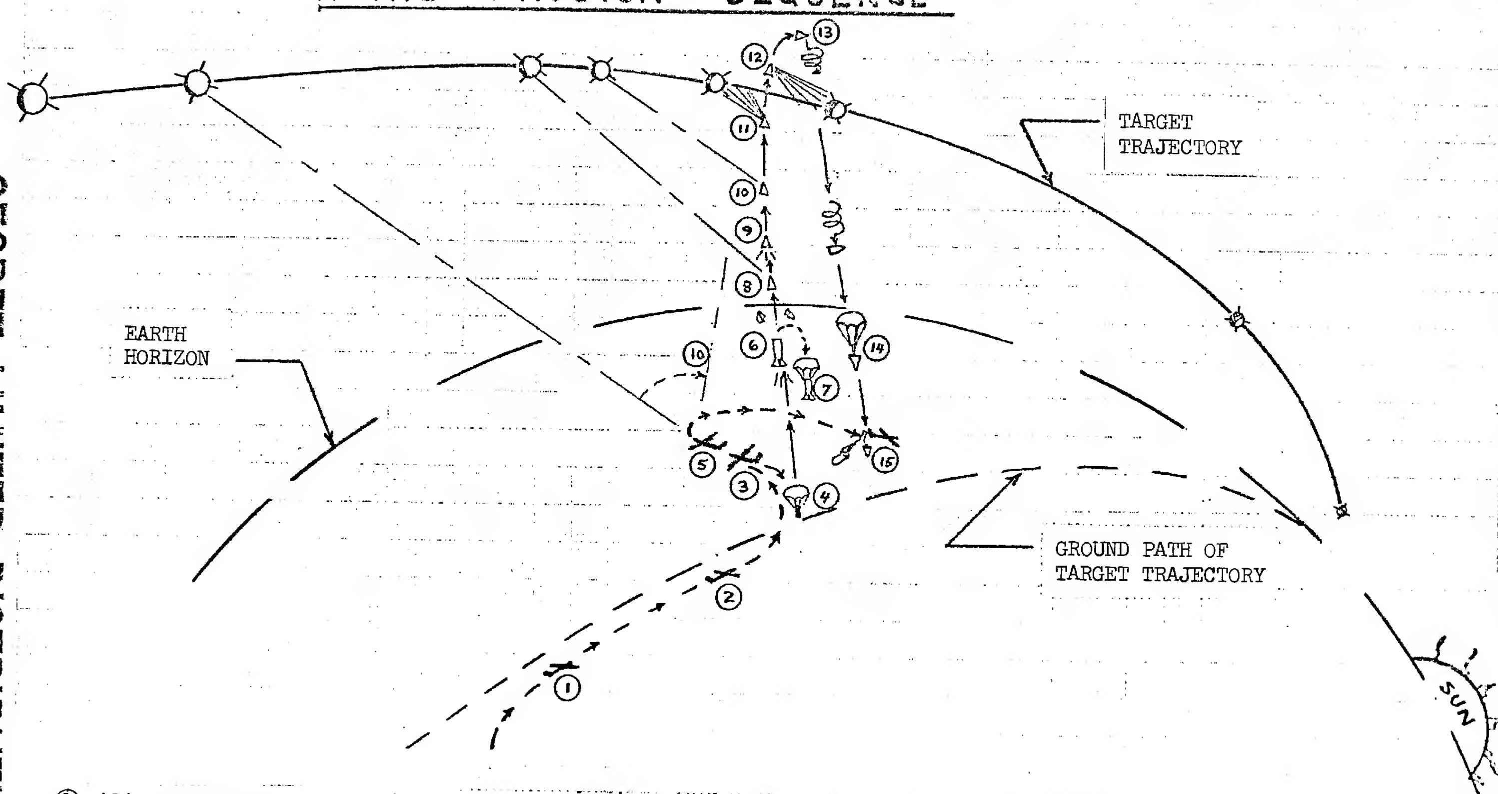

(1) Align platforms.
(2) Update ephemeris.
(3) Turn across orbit plane. Eject missile.
(4) Fire missile.
(5) Aircraft acquires target.
(6) First-stage & fairings separate.
(7) First-stage soft lands.
(8) ALIAS vehicle acquires target.
(9) Vehicle attitude adjusted. Terminal correction motor fires.
(10) Vehicle re-acquires target.
(11-12) Photographic sequence.
(13) Apogee. Flat-spin initiated.
(14) Flat-spin stopped. Recovery chute deployed.
(15) Aircraft recovers ALIAS vehicle.

FIGURE G-1

SECRET LIMITED DISTRIBUTION

SECRET LIMITED DISTRIBUTION

Aircraft System

Functions	Performance Requirements	Candidate Component
1. Transport ALIAS vehicle to launch point and return recovered payload. Updated ephemeris data for launch point selection	Maximum mission radius capability to 1500 n mi. Total mission response cycle less than 12 hrs. at 1500 n mi radius	C-130 modified as below. HF radio for latest SPADATS 66 data.
2. Navigate to point below predicted intercept point in plane of the satellite trajectory	3000 ft CEP; 0.5 minutes of arc in vertical & azimuth	AN/ASN-59 Litton Stellar inertial navigation system aboard aircraft, (or Nortronics NAS-14).
3. Determine satellite position along track with respect to aircraft	one n. mi. error (1σ)	Prime: AN-APS-96 airborne radar modified to match satellite tracking and C-130 aircraft installation requirements Secondary: Northrop - ALOTS optical tracking system, (modified).
4. Transmit satellite relative range data from the aircraft to the missile	High reliability of transmission and accurate reception	Commercially available UHF transmitter equipment low data rate.
5. Air launch ALIAS vehicle using rearward parachute extraction technique	Minimum air speed at service ceiling less than 180 kts. Rear fuselage extraction capability	C-130 with sealed launch duct for rearward extraction at 35,000 ft altitude.
6. Aerial and/or surface recovery of payload	110 to 140 kt speed capability from sea level to 10,000 ft.	All American Engineering model 90 recovery equipment installed for rear door pickup from C-130. Recovery intercept computer (see Recovery System.)

SECRET LIMITED DISTRIBUTION

Launch System

Functions	Performance Required	Candidate
1. Rearward horizontal extraction of air launched ALIAS package with subsequent deceleration and 90° altitude change.	Peak shock loads less than 15 g's smooth trajectory to stable 90° attitude with descent velocity less than 50 fps accomplished within 8 sec and 300 ft altitude loss	Standard 50 ft. diam. ribbed guide surface single stage parachute with snatch load mitigation devices
2. Provide smooth operation aircraft extraction of ALIAS package from the aircraft	Limit lateral shock loading to less than 10 g's peak amplitude during extraction	Close-tolerance guide rail or duct with forward dolly & release brakes for track within the aircraft (to be developed)
3. Provide aerodynamically stable launch package and vehicle launch guide	Minimum of one caliber stability of the launched package over the launch phase trajectory. Guide ignited rocket through the crown of the parachute to preclude fouling of vehicle stabilization skirt with risers, etc.	Launch tube encloses the ALIAS vehicle, ballasted nose fairing & rear aerodynamic drag cone (to be developed)

Boost Vehicle

Functions	Performance Requirements	Candidate Components
1. Boost terminal vehicle to intercept area	Max. load factor less than 10.0 g's Intercept altitude selectable to 1 or more increments between 90 and 150 n. mi. with max. low pt. crossing velocity not exceeding 3000 fps. Accumulated acceleration time product to intercept less than 400 g-secs.	Possible candidates rocket motors pending confirmation by simulated trajectory program runs: a) 2 stage 2 cluster Terrier I sustainer b) Iris plus M8 Aircraft Jato c) UTC FW-3 with 7 Hercules retro motors
2. Augment damping of prelaunch oscillations & limit vehicle roll rate and trajectory dispersion	Capable of overcoming aerodynamic moments at most aft center of gravity. Pitch, roll & yaw control to accuracy consistent with the inertial guidance and thrust reversal sub-systems	Low thrust, low pressure hot gas multi nozzle system from forward tanks for pitch & yaw. Cold gas very low thrust roll control jets. Systems to be built up from commercially available components.
3. Guide Booster Vehicle to within ephemeris error volume.	.5 n.m. probable spherical error	Inertial guidance system using: NIP 105 Platform with high quality components; constant time of flight guidance equations as in Wing VI Minuteman; NDC 1050 computer; inertial angle reference from stellar inertial aircraft system by acceleration matching. Initial position and velocity from aircraft navigation system; Boost termination with retro rockets.

Terminal Correction

Function	Performance Criteria	Candidate Sub-System
1. Attitude Position Terminal Stage at 40 seconds to go	$1/2^{\circ}$ accuracy in azimuth and elevation 90° pitch and stop in 2 seconds	a) Hypergolic or cold gas attitude control system b) Inertial platform angle reference and computer derived pointing angles
2. Acquire Target in Star Background	.2 milliradian angle resolution; 6° field of view; 5 frames per second; .5 mr/sec star discrimination threshold; expected number of target equivalent stars is 6 for discrimination logics with most unfavorable target lighting conditions expected	a) Westinghouse 7290 or RCA 7263 Vidicon and vidicon control electronics b) Optics shared with photo system c) 100% mirror in optical path to vidicon. (5% during picture taking sequence. d) Angle pickoff on mirror e) Angle reference from Vidicon to stable platform f) NDC 1050 computer will also do star discrimination computations.

Terminal Correction (Continued)

Function	Performance Criteria	Candidate Sub-System
3. Track Satellite and Compute Terminal Guidance Correction	a) .05 mr/sec smoothed angle rate accuracy	a) NIP 105 platform with g sensitive drift of .5° hr/g. Accelerometers bias of 10^{-5} g's. Max Level 20 g's. Inertial angle reference after booster burnout, within 3 minutes of arc.
	b) 6 minutes of arc angle error between observed line of sight and computed relative velocity vector direction	b) NDC 1050 guidance computer using aircraft supplied range data or vidicon angles and angular rates. Satellite velocity data to 30 ft/sec accuracy cross track.
	c) .5 seconds arrival time accuracy (5% of time to go, without aircraft supplied range data.)	c) Two second smoother length for vidicon angle rate estimate with angle rate acceleration keyed to time-to-go and measured offset angle (Also NDC 1050)
	d) Angular rotation rate direction to one degree accuracy.	d) Rotating mirror angle pickoff and Vidicon angle reference resolving 1 minute of arc
	e) 1500 feet one sigma guidance correction accuracy. (2 dimensional distribution in plane normal to relative velocity vector at closest approach) when correcting 18,000 feet lateral error.	e) Receiver and decoder for aircraft transmitted relative range data

Terminal Correction (Continued)

Function	Performance Criteria	Candidate Sub-system
		f) Computer logics to determine direction and time of firing the correction motor (Also NDC 1050 computer using stored motor characteristics)
4. Implement Computed Guidance Correction	a) Attitude position correction motor to within 1°; 90° pitch, and stop in 2 seconds.	a) Attitude control system of terminal stage as discussed above.
	b) A velocity correction capability of greater than 1000 ft/sec at a level greater than 5 g's.	b) Angle reference from NIP 105
		c) Gemini retro motor (TE-385)
5. Locate Recovery Zone for Aircraft	a) 40 ft/sec all-axis one-sigma velocity error. 6000 ft position error.	a) Read-out of inertial computed value, decoding, and transmission after correction motor burnout. Small low data rate low power UHF transmitter.

Sensor

Function	Performance Requirements	Candidate Components
1. Angle track target just prior to photographic sequence (T, minus 4 seconds).	Adjust payload attitude for tracking mirror axis normal to tilted plane traced by missile/target intercept vector. Attitude accurate to 0.5° or better. Measure range to 1%. Establish tracking rate at error not to exceed 1° sec.	Wedge-shaped 2-sided mirror mounted in front of lens and rotated on axis normal to optical axis. This mirror arrangement will allow tracking of target in both approach and departure phases, without necessity of extremely high mirror angular accelerations as point of closest approach is passed. Mirror may be cast beryllium, machined, coated and polished; or Corning foam glass with solid face, also coated and polished. Supporting cradle may be used to maintain mirror flatness. Tie-downs may also be used for protection from shock loading during launch and recovery. Mirror drive and control loop not yet evaluated. Anticipate either electric motor or pneumatic drive system.

Function	Performance Requirements	Candidate Components
2. Maintain tracking rate (image motion compensation) and target framing during photographic sequence, (T, minus 2 to T, minus 0.2 and T, plus 0.2 to T, plus 2).	Mirror should provide full coverage for look angles from 90° to 60° either side of closest approach. Total mirror area occlusion at 45° look angle should not exceed 33%. Synchronized mirror tracking rate stability $\frac{1}{2}^\circ$/sec to maximum mirror rate of 1 radian/sec. Maximum mirror angular rate while slewing through "dead" area (T, minus 0.2 to T, plus 0.2) should be at least 2 radians/sec with deceleration to match target motion to $\pm 1^\circ$/sec at T, plus 0.2. Energy-sharing beam-splitter used during photo sequence to transmit 95% of light to film format and 5% of light to tracking sensor. Injection of beam-splitter should not degrade film resolution nor affect tracker accuracy.	Primary optics used with full transmission to tracker prior to initiation of photo sequence.
3. Maintain high angular resolution capability at high shutter speeds	Mirror flatness maintained to $\frac{1}{4}$ wavelength during photo sequence. Center of rotation placed at center of mass to avoid additional counter-balance weight. F:4.5 to F:6.0 system at 33-40 inch focal length required, with at least 70% transmission efficiency (including secondary lens occlusion and light transmission losses). Structural components must provide mechanical and thermal stability during photo sequence.	Cassegrainian optics. Beryllium primary mirror may save weight and improve thermal stability. Spacers for secondary mirror may be Invar, though quartz may be more desirable if mechanical and thermal shock is not a problem. Internal lens baffles of black resin impregnated fiberglass would be lightweight and flexible to survive high-g's during launch & recovery

Function	Performance Requirements	Candidate Components
	Vibration amplitude must be less than 0.7 arc-sec at 2000 cps, and higher. Dimensional stability of back focal length, .003 inches or better, (.001 inch desirable).	
4. Adjust optics for optimum focus	Maximum shift of back focal distance, approx. 0.1 inch. Focal plane accuracy of .003 inch or better required at all times. Actual target range setting, $\pm$ 10%	Derived range outputs available in digital form from on-board computer. Focus shift accomplished by means of optical wedges.
5. Adjust shutter speed for best exposure (maximum information content). (Exposure control pre-computed for expected target characteristics and lighting conditions during anticipated photo sequence).	Pre-programmed shutter speeds adjustable during photo sequence for any value from 1/1500 second to 1/5000 second. shutter motion must be continuous to reduce unwanted vibration.	Shutter may be either rotating disc or moving belt, focal plane type. High shutter efficiency required, with primary goal being high angular resolution. Adjust slit width with twin shutters; or, adequate variation may be possible by pre-programmed acceleration or deceleration of shutter mechanism.
6. Provide film cycling rate of 50-100 fps for high rate of information gathering	Total film capacity, 200-400 frames. film handling mechanism to provide forward movement (of perforated 70mm film) of 1 to $1\frac{1}{2}$ inches per frame, with pin registration. (Without pin registration, fiducial marks would be desirable to mark optical center-line). Mechanical film flattening required to .001 inch or better. Film supply, takeup, and framing actions should not induce vibration during exposure cycle.	Alternatively, films of varying sensitivity (and resolution capability may be spliced to match anticipated exposure variations. Semi-standard film handling mechanisms. Acme-type or new developments by D.B. Milliken or Flight Research, Inc. , chosen for reliability and minimum vibration.

Function	Performance Requirements	Candidate Components
7. Utilize film with optimum compromise of resolution and sensitivity.	High-contrast resolution of 100 lines/mm or higher, required at ASA rating of 80, or over.	Most logical film choice appears to be type 5401 or 2405.
8. Provide internal data recording block on each film frame.	Self-illuminated binary recording of frame number, time, target range, x-y angle, and X-Z angle required at resolution sufficient to support subsequent image analysis.	Internal digital pickoffs from on-board computer. Encoding and recording must be supplied as part of camera subsystem. Data must be recorded on appropriate film frame.
9. Provide camera environmental control	Film handling must include either pressurized area between hold-down and platen, or must provide unpressurized film handling during exposure cycle without incurring film damage or degrading resolution.	Camera system not pressurized, with exception of film storage. Thermal conditioning by radiation and conduction, to stabilize prior to photo-sequence. Some pre-conditioning prior to launch.

Recovery System

Function	Performance Requirements	Candidate Components
1. Locate payload for aerial recovery	Minimum time delay in location & recovery Max shock on reusable components 10.0 "g"s	Payload equipped with altitude deployable reefed parachute to provide approx. 25 fps descent rate at 10,000 ft. altitude Terminal vehicle inertial platform velocity and position data is transmitted to aircraft. Weather radar is also used to' provide range data input. Inputs are supplied to a recovery computer which displays heading descent rate, speed and time to go information to the recovery aircraft pilot. C-130 aircraft with All American Engineering Model 90 aerial recovery equipment or equivalent prime candidate recovery unit.
2. Provide for payload survival & backup recovery scheme in lieu of aerial recovery	Max. impact shock on reusable components 20.0 "g"s. Film & reusable components sealed from salt water and sunlight. Internal heat not to exceed 200°F for short period, 100°F sustained.	1. Plastic Foam encased a canister for thermal insulation, flotation & impact shock absorption. 2. Radio beacon 3. Dye marker 4. Strobe light 5. Self inflating balloon & 50 ft nylon line for surface-to-air pick-up by C-130 (All above to be assembled from commercially available components)

Function	Performance Criteria	Candidate Components
3. Decelerate spent booster motor hardware to provide warning of and to mitigate impact effects on possible personnel or facilities in the impact area.	Limit sea level descent velocity to less than 25 fps. Limit sea level impact energy to less than 2500 ft-lbs.	A self-deployable parachute of approx. 15 ft. dia. will be used to decelerate the spent booster motor hardware.